UNIVERSITY OF SOUTHAMPTON

EVALUATION OF P-GLYCOPROTEIN ACTIVITY AND EXPRESSION IN PRIMARY CULTURED HUMAN RENAL TUBULAR CELLS: EFFECT OF LONGER-TERM EXPOSURE TO CYCLOSPORIN

TIMOTHY DAVID LEACH
BM MRCP

DOCTOR OF MEDICINE

FACULTY OF MEDICINE, HEALTH AND BIOLOGICAL SCIENCES, DEPARTMENT OF MEDICINE

Submitted: December 2004

UNIVERSITY OF SOUTHAMPTON

ABSTRACT

FACULTY OF MEDICINE, HEALTH AND BIOLOGICAL SCIENCES

MEDICINE

Doctor of Medicine

EVALUATION OF P-GLYCOPROTEIN ACTIVITY AND EXPRESSION IN PRIMARY CULTURED HUMAN RENAL TUBULAR CELLS: EFFECT OF LONGER-TERM EXPOSURE TO CYCLOSPORIN

by Timothy David Leach

Renal failure causes significant morbidity and mortality and renal dialysis is a drain on resources. Transplantation is the treatment of choice, but to prevent rejection medications to suppress the immune system must be taken. Cyclosporin A has had the greatest effect on renal transplant survival, by reducing the incidence of acute rejection. There is still a significant long-term attrition rate, presumed to be a result of cyclosporin toxicity. The mechanisms of this are not fully understood, but seem to relate to intra-renal cellular accumulation of cyclosporin.

To investigate this chronic accumulation in vitro, human cells in culture need to be exposed to cyclosporin over a period of weeks. Stable (non-proliferating) cell culture would be the most appropriate for this, but such methods are currently unavailable. The first part of this thesis describes a model for quiescent culture of primary human renal tubular epithelial cells, which maintain viability and phenotype as close to normal as possible for at least 6 weeks. Characterisation by light and electron microscopy, enzyme activity and epitope expression by immunofluorescence and flow cytometry are described.

Renal tubular cells, among others, possess a transmembrane protein called P-glycoprotein, whose physiological role is not fully understood, but which is involved in effluxing (potentially toxic) hydrophobic macromolecules from the cell cytoplasm. One such macromolecule is cyclosporin.

The second part of the thesis describes the function of P-glycoprotein in human primary cultured renal tubular epithelial cells in normal fully defined growth medium, the retention of normal function in quiescent cells for up to 6 weeks in culture, and then investigates the effects of co-incubation with cyclosporin for at least 3 weeks.

Incubation of quiescent cells with higher pharmacological cyclosporin doses impairs the cellular character. Incubation with lower pharmacological concentrations of cyclosporin increases the efflux activity of P-glycoprotein, as measured by a fluorescent substrate, but does not affect the membrane expression of the protein.

This is the first time that (i) such a quiescence model has been described, (ii) P-glycoprotein has been investigated in primary cultured human renal epithelial cells, and (iii) the effect of prolonged exposure to cyclosporin in culture has been studied.

Contents

ABSTRACT 2

Contents 3

Dedication 7

List of Figures 8

List of Tables 14

Acknowledgements 15

Abbreviations 16

Chapter 1 General Introduction 24

Summary 24

Cyclosporin A toxicity 25

Renal Cell Culture 28

Renal Cell Culture 28

Chapter 2 General Methods 30

Preparation of main material 30

Subjects *30*

Tissue Preparation *31*

Culture methods 32

First passage *32*

Cell detachment *33*

Second passage *35*

Morphology techniques 35

Phase-contrast light microscopy *35*

Cell viability *35*

Transmission electron microscopy (TEM) *36*

Scanning electron microscopy (SEM) *36*

Biochemistry techniques 36

Microprotein estimation *36*

Alkaline phosphatase activity estimation *36*

Gamma-glutamyl transferase activity estimation *38*

Immunofluorescence techniques 38

Flow cytometry techniques 38

Chapter 3 Quiescent Cell culture 39

Summary 39

Introduction 41

Culture Medium Composition *41*

Quiescence *42*

Proliferation *43*

Characterisation *45*

Cell Populations *47*

Methods 48

Cell Culture – Preparation for Characterisation *48*

Light microscopy 49
Immunostaining 50
Enzyme activity 51
Cell viability 52
Cell cycle 53
Transmission electron microscopy (TEM) 53
Regrowth 53
Results 54
General Culture 54
Culture success 54
BrdU incorporation in "quiescing" media 55
Quiescence success 55
Characterisation 60
Discussion 72
Conclusion 75

Chapter 4 Later work on HTECs in quiescence 76
Summary 76
Introduction 77
General Methods 79
Method for cytoskeletal appearance 80
Method for hormonally stimulated adenylate cyclase activity 81
Method for transepithelial resistance 81
Method for dextrans 82
Method for glucose transport 82
Results 84
Discussion 90
Conclusions 91

Chapter 5 P-glycoprotein and Cyclosporin A 92
Summary 92
Introduction 93
P-glycoprotein 93
P-glycoprotein and Cyclosporin A 103
Methods 111
Cell Culture 111
P-gp activity and expression 112
Results 114
Cell culture success 114
Characterisation 114
P-gp expression experiments 132
P-gp activity experiments 145
Simultaneous measurement of P-gp activity and expression in the same cells . 161
Discussion 187
Appropriateness of Model 187
Exposure to CsA 189
Measurement of P-gp activity 189
Measurement of P-gp expression 191
Potential Limitations of Expression Studies 194
Conclusions 197

Chapter 6 Presentations 198
Preservation of phenotype in longer-term culture of primary renal tubular epithelial cells *198*
Functional P-glycoprotein is expressed on cultured primary renal tubular epithelial cells in longer-term culture *201*
Cyclosporin A exposure upregulates P-glycoprotein activity, but not expression, in longer-term cultured primary renal tubular epithelial cells *202*
Primary human renal tubular epithelial cells after six weeks of quiescent culture retain F-actin cytoskeleton and maintain cAMP response to renal hormones . *203*

Appendix 1 Southampton Ethical Application 205

Appendix 2 Portsmouth Ethical Application 206

Appendix 3 Laser Confocal Microscopy 207
Fluorescence 207
Fluorescence microscopy 207
Confocality 208
Laser confocal microscopy 208
Advantage of using a confocal microscope 209

Appendix 4 Flow cytometry 212
Introduction 212
Background 212
The machinery 213
Fluidics 213
Optics 213
Filters 214
Computer 214

Appendix 5 Experimental Protocols 217
General procedures 217
Preparation of Phosphate Buffered Saline *217*
Preparation of Tris Buffered Saline *219*
Preparation of Bovine Serum Albumin *220*
Preparation of Paraformaldehyde *221*
Preparation of Antifade *222*
Preparation of Media *223*
Specific procedures 225
Protocol 1 Cell counting and viability estimation *225*
Protocol 2 Transmission Electron Microscopy *228*
Protocol 3 Scanning Electron Microscopy *230*
Protocol 4 Microprotein Measurement *231*
Protocol 5 Alkaline Phosphatase Activity Measurement *235*
Protocol 6 γ-Glutamyltransferase Activity Measurement *239*
Protocol 7 Indirect Immunofluorescence Staining *243*
Protocol 8 Immunofluorescence microscopy *245*
Protocol 9 Laser confocal microscopy *247*
Protocol 10 Flow Cytometry: General Protocol *249*
Protocol 11 Indirect Epitope Detection by Flow Cytometry *254*
Protocol 12 BrdU incorporation by immunofluorescence *256*
Protocol 13 Cytocentrifugation *258*

Protocol 14 *Cell Cycle Determination by Flow Cytometry* 261
Protocol 15 *Measurement of Cyclosporin A* 264
Protocol 16 *Measurement of Lactate Dehydrogenase Activity* 266
Protocol 17 *Transcellular passage of Cyclosporin A* 267
Protocol 18 *P-gp activity and expression by flow cytometry 1* 270
Protocol 19 *P-gp activity and expression by flow cytometry 2* 274
Protocol 20 *Quantification of Immunofluorescence* 278

Glossary 279

References 283

Dedication

This thesis is dedicated to my wife, Zillah. Without her help and forbearance none of the work presented here would have been possible and the writing-up would never have happened.

List of Figures

Figure 1. Molecular schematic of Cyclosporin A 27

Figure 2. Characteristic striped fibrosis of Cyclosporin A toxicity 27

Figure 3. Phase-contract light photomicrographs of primary human renal cortical cell homogenates on uncoated plastic culture flasks 34

Figure 4. Equipment for culture of polarised cell monolayers 37

Figure 5. Protein content of identical aliquots of cell suspension subjected to increasing periods of sonication 37

Figure 6. Cell cycle – a schematic overview 44

Figure 7. Cell distribution through the Cell Cycle by DNA content 44

Figure 8. BrdU accumulation immunofluorescence micrographs in different quiescent media at three time points 56

Figure 9. Viability counts of cells remaining adherent to the culture surface: effect of quiescent medium and DMSO 58

Figure 10. Viability counts of cells removed in supernatant medium (corrected to daily means) 59

Figure 11. Light microscopic characterisation of cell monolayers 63

Figure 12. Phase-contrast light micrographs of cell monolayers at confluence, kept in QM (refreshed weekly) for 150 days 63

Figure 13. Effect of medium composition on light microscopic character of confluent passage 1 cell monolayers 64

Figure 14. Transmission electron micrographs of confluent cells in quiescence 65

Figure 15. Flow cytometry histograms of characterisation epitopes on cells in confluence in DM 66

Figure 16. Effect of quiescence for six weeks on characterisation epitopes on confluent cells in $25cm^2$ flasks 66

Figure 17. Confocal laser scanning micrographs of indirect immunofluorescence on cytocentrifuge preparations of cells at confluence in $25cm^2$ culture flasks in DM 67

Figure 18. Effect of quiescence for more than 6 weeks on characterisation epitope expression on cytocentrifuge preparations of confluent cells in QM from $25cm^2$ flasks 68

Figure 19. Confocal laser scanning micrograph of indirect immunofluorescence with ZO-1 monoclonal antibody on an intact monolayer of cells in QM for six weeks 69

Figure 20. Effect of medium composition on proportions of cells in each cell cycle phase 70

Figure 21. Effect of reintroduction of growth factors and trace elements on cells in quiescence 70

Figure 22. Effect of re-exposure of quiesced cells to growth medium on the proportions of cells in each cell cycle phase 71

Figure 23. Effect of regrowth from quiescence on characterisation epitopes in confluent cells in 25cm^2 flasks 71

Figure 24. Laser confocal micrographic appearance of cytoskeleton of cells in defined medium at confluence 85

Figure 25. Laser confocal micrographic appearance of cytoskeleton of cells in quiescence medium after 6 weeks 85

Figure 26. Reno-active hormone-stimulated cAMP release from cells in defined and quiescent medium 86

Figure 27. Transepithelial resistance across confluent monolayers of cells in defined and quiescence medium 87

Figure 28. Fluorescence of standard dextran concentrations 88

Figure 29. Permeability to dextrans of confluent monolayers of cells after 1 and 7 weeks in culture 88

Figure 30. Effect of quiescence on Na^+-dependent αMG uptake 89

Figure 31 Time courses of aMG release in quiescent culture 89

Figure 32. Diagrams of P-gp structure 95

Figure 33. Diagrammatic representation of fluorescent substrate efflux experiments 97

Figure 34. Effect of 23 day CsA-exposure on confluent monolayers of passage 1 cells on 6-well culture membranes 115

Figure 35. Effect of 24 day CsA-exposure on confluent monolayers of passage 1 cells on uncoated plastic culture 24-well plates 118

Figure 36. Effect of different concentrations of CsA on cells quiesced on 6-well culture membranes for 45-48 days, medium exchanged weekly 119

Figure 37. Effect of exposure to CsA with thrice-weekly medium change on confluent monolayers of cells on 6-well culture membranes over 23 to 25 days 120

Figure 38. Transmission electron micrograph of control cells (without CsA exposure) quiesced for 26 days with medium change thrice weekly ... 121

Figure 39. Effect of CsA exposure on surface ultrastructure of confluent cells on 6-well culture membranes 122

Figure 40. Effect of CsA exposure on immunofluorescence characterisation of cell monolayers in passage 1 on 6-well culture membranes kept in QM for 43 days 123

Figure 41. Effect of CsA exposure on confocal laser fluorescence characterisation of confluent monolayers of passage 1 cells kept quiesced on 6-well culture membranes for 21-23 days 124

Figure 42. Effect of incubation with CsA on flow cytometric characterisation of passage 1 cells on 6-well culture membranes in QM for > 21 days 127

Figure 43. Effect of CsA exposure on cell cycle 128
Figure 44. Brush border enzyme activities 128
Figure 45. CsA concentrations in medium from passage 1 cells in confluent monolayers grown on 6-well culture membranes in medium with 300ng/ml CsA initially placed in the well (basal) medium 130
Figure 46. Bar charts showing CsA transport results 131
Figure 47. LDH concentration in refreshed medium from passage 1 cells in confluent monolayers on culture membranes in 6-well plates 133
Figure 48. Extrapolated total LDH content of medium from passage 1 cells in confluent monolayers on culture membranes in 6-well plates 133
Figure 49. Streptavidin-Biotin immunoperoxidase staining of frozen sections of human renal cortical tissue 136
Figure 50. Diagrammatic representation of the Streptavidin-Biotin indirect immunohistochemistry technique 137
Figure 51. Immunofluorescence micrograph of frozen section with no primary or secondary antibodies, counterstained with PI 138
Figure 52. Laser confocal micrograph of frozen section, stained with MRK16 and TRITC-conjugated secondary antibody, without counterstaining 138
Figure 53. Laser confocal micrograph of frozen section with MRK16 and α1-antitrypsin 139
Figure 54. Streptavidin-Biotin immunoperoxidase light micrographs of confluent cells in DM on 8-well glass chamber slides 139
Figure 55. Laser confocal micrograph "sections through" a confluent monolayer of cells on 6-well culture membrane, stained with FITC-secondary and MRK16 141
Figure 56. Representative flow cytometry histograms of confluent cells disrupted from DM and stained with JSB-1 using differing fixation techniques. 143
Figure 57. Representative flow cytometry histograms of confluent cells disrupted from DM and stained with JSB-1 using differing permeabilisation techniques 144
Figure 58. Representative flow cytometry histograms of confluent cells disrupted from DM and stained with MRK16 using differing fixation techniques 146
Figure 59. Representative flow cytometry histograms of confluent cells disrupted from DM and stained with Neomarkers' Anti-P-gp monoclonal antibody 2.5μg/ml using differing fixation techniques, and effect of Ab concentration 147
Figure 60. Flow cytometric investigation of cells incubated with R123 149
Figure 61. Effect of R123 incubation period on flow cytometry results 149
Figure 62. The effect of variation of sample cell number on the accumulation of R123 150

Figure 63. The effect of R123 concentration on FL-1 flow cytometric fluorescence signal 150
Figure 64. Effect of efflux time on flow cytometry histograms of cells pre-incubated with R123 153
Figure 65. Comparison of R123 efflux between a commercial porcine cell line and primary cultured human renal tubular epithelial cells 153
Figure 66. Effect of different concentrations of known inhibitors of P-gp activity on R123 efflux 154
Figure 67. Comparison of effects of known inhibitors of P-gp activity between transformed porcine cell line and primary human cells 154
Figure 68. Effect of different Mg-ATP concentrations with sodium orthovanadate on R123 efflux 155
Figure 69. Effects of the vehicles of cyclosporin A and sodium orthovanadate on the efflux of R123 155
Figure 70. Effect of cimetidine on R123 efflux 156
Figure 72. The effect of P-gp inhibition (and cimetidine) on R123 accumulation in primary human cells and transformed porcine cells 158
Figure 73. Schematic diagram of van der Kolk *et al*'s [265] experiments 159
Figure 74. Flow cytometric determination of the "Efflux Blocking Factors" of CsA on renal cells 159
Figure 75. The effect of changing FL-1 photomultiplier amplification on R123 signal and Efflux Blocking Factors 162
Figure 76. Flow cytometry histograms of R123 and TRITC-MRK16 signals, and dot plot of simultaneous detection 162
Figure 77. Flow cytometry histograms and density plot of R123 and TRITC-MRK16 on double-stained cells 163
Figure 78. Emission spectra of fluorochromes 163
Figure 79. Flow cytometry histograms and density plots of simultaneous R123 fluorescence and MRK16 staining with Cy5-conjugated secondary antibody 166
Figure 80. Effects of incubation on ice, and fixation on ice with 2% Paraformaldehyde, on R123 retention 166
Figure 81. Flow cytometry histograms of R123 accumulation and efflux and the effect of fixation and staining with MRK16 167
Figure 82. Effect of duration of CsA incubation of confluent passage 1 cells in defined medium 169
Figure 83. Effect of cell passage in defined medium without CsA on P-gp expression and activity 169
Figure 84. Effect of cell passage in defined medium with CsA 500ng/ml on P-gp expression and activity 170

Figure 85. Effect of time in quiescent medium without CsA on P-gp expression and activity in passage 0 cells in 25cm2 culture flasks 171
Figure 86. Effect of time in quiescent medium without CsA on P-gp expression and activity in passage 1 cells in 24-well culture wells 171
Figure 87. Effect of time in quiescent medium without CsA on P-gp expression and activity in passage 1 cells on 6-well culture membranes 172
Figure 88. Effect on P-gp expression of incubation of confluent passage 1 cells on 6-well permeable culture membranes in quiescence medium for 43-48 days with different CsA concentrations 175
Figure 89. Effect of incubation with different CsA concentrations in quiescence medium for 43-48 days on P-gp expression in confluent passage 1 cells on 6-well permeable culture membranes 176
Figure 90. Effect on P-gp activity of incubation of confluent passage 1 cells on 6-well permeable culture membranes in quiescence medium for 43-48 days with different CsA concentrations 177
Figure 91. Effect of CsA exposure on confluent cell monolayers in quiescence medium for 21 days – Subject 4 181
Figure 92. Effect of CsA exposure on confluent cell monolayers in quiescence medium for 22 days – Subject 5 182
Figure 93. Effect of CsA exposure on confluent cell monolayers in quiescence medium for 23 days – Subject 6 183
Figure 94. Effect of CsA-exposure on P-gp expression in confluent cells on 6-well culture membranes in quiescent medium for 21 to 23 days 184
Figure 95. Measurement of antigen expression by flow cytometry 185
Figure 96. Effect on P-gp activity of incubation of confluent passage 1 cells on 6-well permeable culture membranes in quiescence medium for 21-23 days with different CsA concentrations 186
Figure 97. Effects of CsA and PKC on P-gp activity 192
Figure 98. Schematic of epi-fluorescence microscope 210
Figure 99. Focusing objective with pinhole screen 210
Figure 100. Schematic of scanning laser confocal microscope 211
Figure 101. Schematic of cell flow within a flow cytometer 215
Figure 102. Schematic of dichroic filter 215
Figure 103. Schematic of a band pass filter 215
Figure 104. Schematic of flow cytometer 216
Figure 105. Counting grid on Improved Neubauer Haemacytometer 227
Figure 106. Microprotein 96-well microtitre plate layout 233
Figure 107. Sample standard curve for microprotein assay 233
Figure 108. Absorbance of standard protein solutions for different light wavelengths. 234

Figure 109. Absorbance of higher protein concentrations 234
Figure 110. Alkaline phosphatase 96-well microtitre plate layout 238
Figure 111. Sample standard curve for alkaline phosphatase activity assay 238
Figure 112. Gamma-glutamyltransferase 96-well microtitre plate layout 242
Figure 113. Sample standard curve for gamma-glutamyltransferase activity assay 242
Figure 114. Flow cytometric scattergram of Forward Scatter (FSC) versus Side Scatter (SSC) 252
Figure 115. Flow cytometer set-up of FL-1 (to include positive control peak while keeping negative control signal less than 10^1) 253
Figure 116. Cytocentrifuge 260
Figure 117. Flow cytometer set-up for cell cycle 263
Figure 118. 24-well set-up for transcellular CsA movement protocol 269
Figure 119. Schematic of experimental protocol for simultaneous P-gp activity / expression measurement 273
Figure 120. Flow cytometer set-up for P-gp double-staining 273
Figure 121. Schematic of experimental protocol for parallel P-gp activity / expression measurement 277

List of Tables

Table 1. Culture medium composition, Basal medium plus supplements 33

Table 2. Culture medium composition, Basal medium plus supplements: Comparison of quiescence medium with defined medium 48

Table 3. BrdU incorporation experiment medium composition, basal medium plus supplements 49

Table 4. Characterising Antibodies 50

Table 5. Flow Cytometry Characterising Antibodies 51

Table 6. Brush-border enzyme activities 62

Table 7. Medium composition: basal medium, antibiotics, hormones and trace elements 80

Table 8. αMG transport medium composition 83

Table 9. Anti-P-gp monoclonal antibodies 100

Table 10. P-gp expression up-regulators, tissues affected and references 102

Table 11. Flow cytometry / immunofluorescence fixatives and permeabilisation 112

Table 12. Microprotein assay calibration samples: 231

Table 13. Alkaline phosphatase calibration samples 236

Table 14. Gamma-glutamyltransferase calibration samples 240

Table 15. Tube contents / treatment for P-gp activity / expression flow cytometry... 271

Table 16. Tube contents / treatment for P-gp activity / expression flow cytometry... 275

Acknowledgements

My thanks are extended to my supervisors Janet Albano, Juan Mason and Paul Bass. Without their expertise, enthusiasm, encouragement and persistence this work would not have been possible, or completed. Janet also carried out the Cyclosporin A assay work, as I was not in possession of an ionising radiation certificate.

Special thanks are for Sara Campbell and Tony Carr, whose education and assistance in the art of laboratory work was invaluable, whose optimism kept me sane when things did not work and who kept the cells alive when I was on holiday. Sara also completed the lactate dehydrogenase assay while performing this for her own experiments and continued the characterisation protocols once I had completed my research placement.

Thanks too to Anton Page and Roger Alston from Biomedical Imaging for their education and guidance in fluorescence microscopy.

I wish to express my gratitude to Jude Holloway for her training and advice in the use of the flow cytometer.

Thanks to Professor Tom McDonald in whose department I was able to perform this work, and to the Renal Research Committee for funding the research.

Thanks particularly to Ann Farrer for her performance of the electron microscopy and the fantastic photomicrographs she produced.

I would also like to take this opportunity to state that the ideas behind this work were seeded by Janet Albano and Sara Campbell, but that the conception of the study, the design of the protocols and all the laboratory work including the imaging and flow cytometry (except electron microscopy, lactate dehydrogenase measurement, Cyclosporin A assays and further characterisation work as above) were my own work.

Abbreviations

Abbreviation	Full name
7AAD	7-amino-actinomycin D: a DNA-binding, fluorescent dye which is efficiently excited by the 488 nm laser line commonly used in flow cytometry, but yields fluorescence emission further into the red spectrum than alternative DNA-specific fluorochromes
^{14}C αMG	Radiolabelled αMG
Ab	Antibody
ADP	Adenosine diphosphate: substance produced when adenosine triphosphate is phosphatased, releasing energy
ALP	Alkaline phosphatase: an enzyme of the hydrolase class that catalyses the cleavage of orthophosphate from orthophosphoric monoesters under alkaline conditions – present on the brush border of proximal renal tubular cells
αMG	α-methyl-D-glucopyranoside – methylated glucose analogue used to measure Na^+-dependent glucose uptake into epithelial cells
APES	3-aminopropyltriethoxysilone: coating for glass microscope slides which promotes tissue adhesion
AT2	Angiotensin II: potent vasoconstricting hormone formed as a result of renal renin secretion
AUC	Area under the curve: quantification of drug exposure as product of blood concentration and time
AVP	Arginine vasopressin: antidiuretic and vasoconstricting hormone secreted from the posterior pituitary, acting on distal convoluted renal tubular epithelial cells through cAMP production
BM	Basal medium: DMEM:Ham's-F12 and 2mM glutamine
BrdU	5-Bromo-2'-deoxyuridine: fluorescent thymidine analogue which is taken up by the nuclei of proliferating cells
BSA	Bovine serum albumin
$CaCl_2$	Calcium chloride

Abbreviation	Full name
cAMP	Adenosine 3',5'-cyclic monophosphate: a cyclic nucleotide that serves as an intracellular and, in some cases, extracellular "second messenger" mediating the action of many peptide or amine hormones. The nucleotide binds to cAMP-dependent kinases and releases free (catalytically active) subunits.
COX-2	Cyclo-oxygenase 2: enzyme of prostaglandin synthesis pathway
CQ	CsA-containing quiescent medium
CsA	Cyclosporin A (see Glossary)
DABCO	1,4-Diazabicyclo (2,2,2) Octane: prolongs fluorescence of fluorochromes
DM	Defined medium: Culture medium with half antibiotics (see Glossary), with full concentrations of trace elements and hormones. See Table 1
DMEM	Dulbecco's Modified Eagles Medium: contains most nutrients (excluding Glutamine) for mammalian cell culture
DMSO	Dimethyl sulphoxide: has the unique capability to penetrate living tissues without causing significant damage, resulting in the ability to replace some of the water molecules associated with the cellular constituents, or to affect the structure of the omnipresent water
DNA	Deoxyribonucleic acid: chromosomal genetic material
EBF	Efflux blocking factor
EDTA	Ethylenediaminetetraacetic acid: a chelating agent, forming coordination compounds with most divalent (or trivalent) metal ions such as calcium (Ca2+) and magnesium (Mg2+), used to scavenge metal ions, for metal ion titrations, and in buffers
EGF	Epidermal growth factor: signalling cytokine growth factor which regulates cell proliferation, differentiates specific cells and is a mitogenic factor for cells of ectodermal and mesodermal origin
EIA	Enzyme immunoassay

Abbreviation	Full name
ELISA	Enzyme-linked immunosorbant assay: method to visually quantify antigenic components of solutions
EMA	Epithelial membrane antigen: present in glandular organs; breast and skin are strongly positive, a lesser degree is seen in endometrium, kidney, thyroid, stomach, pancreas, lung, colon, ovary, prostate and cervix
ET	Endothelin: the most potent vasoconstrictor substance known. The endothelins are produced by a variety of tissues in vivo, including lung, kidney, brain, pituitary, peripheral endocrine tissues and placenta
$F(ab')_2$	Antibody molecule with two identical antigen binding sites and no constant region (Fc)
FACS	Flow activated cell sorting: sorting of individual cells depending on flow cytometry signals (see Appendix 4)
FBS	Foetal Bovine Serum
Fc	Antibody constant region: the component of an antibody which is species-specific
FDGM	Fully Defined Growth Medium: see DM
FITC	Fluorescine isothiocyanate: fluorochrome which emits light of ~530nm wavelength (green) when excited at 488nm
FL-×	Fluorescence detector in flow cytometer – × from 1 to 4 = different wavelengths of emitted light (see Appendix 4)
FSC	Forward scatter – channel of data from flow cytometer measures cell size (see Appendix 4)
$G_0/_1$	Cell cycle phase – non-dividing cells with one copy of DNA
G_2/M	Cell cycle phase – dividing cells with two copies of DNA
GaM	Goat-anti-Mouse: an antibody raised in a goat, directed against mouse Fc
GaR	Goat-anti-Rabbit: an antibody raised in a goat, directed against rabbit Fc

Abbreviation	Full name
GGT	γ-glutamyltransferase: enzyme of renal brush border membrane (among others) which enables cell detoxification by cycling of the cellular antioxidant glutathione
GM	Geometric mean: average of logarithmic samples – used to compare (log scale) flow cytometry fluorescence results
HBSS	Hanks' Balanced Salt Solution
HC	Hydrocortisone: glucocorticoid hormone
HCl	Hydrochloric acid
HEPES	N-2-Hydroxyethylpiperazine-N'-2-ethanesulphonic acid: organic buffer commonly used to maintain physiological pH in cell culture
HM	Half-defined medium: Culture medium with half antibiotics (see Glossary), with half-concentrations of trace elements and hormones, and half maximal USG – weaning cells from UM to DM. See Table 1
HTEC	Human tubular epithelial cell
IAAP	[^{125}I]-iodoaryl azidoprazosin: [radiolabelled] azide dye with affinity for P-gp
IBMX	Isobutyl methylxanthine: a potent cyclic nucleotide phosphodiesterase inhibitor, increases cAMP and cyclic GMP in tissue, activating cyclic nucleotide-regulated protein kinases
IgG_x	Immunoglobulin G: monomeric class of antibody, with subclasses (×) 1, 2a and 2b
IL-×	Interleukin-×: any of a family of immunological mediators
KCl	Potassium chloride
KOH	Potassium hydroxide
MAb	Monoclonal antibody
MDCK	Madin-Darby canine kidney cell: renal tumour cell line
MDR	Multi-drug resistance: usually followed by a number, denoting a protein product of a member of the MDR gene family
MgADP	Magnesium salt of ADP

Abbreviation	Full name
$MgSO_4$	Magnesium sulphate
MHC	Major histocompatibility complex: membrane-spanning protein present on the surface of all mammalian cells; involved in immune surveillance
MMF	Mycophenolate mofetil (see Glossary)
mRNA	Messenger ribonucleic acid: cellular messenger between nucleus and ribosome, which contains the code for protein synthesis
Na^+-K^+-ATPase	Sodium/potassium exchanger, which metabolises ATP for active transport: the fundamental mechanism for maintaining the normal physiological state of intracellular high potassium and low sodium concentrations (active transport against concentration gradients)
NaCl	Sodium chloride
Necr	Necrosis / necrosed
NF-κB	One of the nuclear transcription factors: of major importance in the biology of pro-inflammatory cytokines, such as TNF-alpha and IL-1alpha, thereby intimately involved in the process of inflammation
NQ	Quiescent medium without CsA
PBS	Phosphate buffered saline
PCR	Polymerase chain reaction: method of identifying mRNA by amplification
PET	Polyethylene teraphthalate: a hard, stiff, strong, dimensionally stable material that absorbs very little water. It has good gas barrier properties and good chemical resistance except to alkalis (which hydrolyse it). It can be highly transparent and colourless but thicker sections are usually opaque and off-white
PGE_1	Prostaglandin E_1: required for optimal renal cell growth and maximal metanephric cell differentiation
P-gp	P-glycoprotein: transcellular transport protein – the human MDR1 gene product
PHTEC	Primary human tubular epithelial cell

Abbreviation	Full name
PI	Propidium iodide: small fluorescent molecule (red light emitting) which binds to DNA when it can penetrate the cellular membrane (in permeabilised or dead cells)
PIPES	Piperazine-N,N'-bis[2-ethanesulphonic acid]: used in physiological buffers of various pHs
PKC	Protein kinase-C: phosphorylates a variety of target proteins which control growth and cellular differentiation
PTH	Parathyroid hormone: secreted by the parathyroid glands to stimulate calcium re-absorption by proximal renal tubular epithelial cells (among others)
QM	Quiescence medium: Medium formulated from one previously reported to promote the nearest normal (i) brush border enzyme expression, (ii) biochemical properties and (iii) glucose transport in a transformed human renal tubular epithelial cell line [1] – see Table 2
R123	Rhodamine 123: a fluorescent cationic dye which is taken up by mitochondria of living cells; transport substrate of P-gp
R^2	Pearson correlation coefficient
RaM	Rabbit-anti-Mouse: antibody against mouse Fc raised in rabbit
RNA	Ribonucleic acid: cellular messenger between nucleus and ribosome, which contains the code for protein synthesis
RNAse	Enzyme to degrade RNA
RO	Reverse osmosed: (water) purified by movement across a semi-permeable membrane
RPMI	Culture medium synthesised at Roswell Park Memorial Institute, hence the acronym. RPMI-1640, when properly supplemented, has demonstrated wide applicability for supporting growth of many types of cultured cells
RT	Room temperature (air-conditioning-controlled to 22±1°C)
S	Phase of cell cycle – synthesis of DNA from one to two copies per cell

Abbreviation	Full name
SAB	Streptavidin-Biotin: staining method of indirect immunohistology (see Figure 50)
SEM	Scanning electron microscopy: exhibits surface detail at high resolutions
SSC	Side scatter: channel of data from flow cytometer measures cell surface roughness (see Appendix 4)
SMAD	Evolutionarily conserved protein(s) identified as mediators of the gene-transcriptional activation induced by the TGF-beta superfamily of cytokines
Sub G_0	Phase of cell cycle – cells with less than normal quantity of DNA implying apoptosis (normal cell size) or necrosis (cell fragments)
T3	Tri-iodothyronine: thyroid hormone which enhances renal tubule cell replication by stimulating EGF receptor expression
T43	Human convoluted tubule membrane antigen (67 and 83% proximal and distal specificity respectively)
TAC	Tacrolimus (see Glossary)
TBS	Tris-buffered saline
TEM	Transmission electron microscopy: exhibits intracellular detail at high resolution
TER	Transepithelial resistance: a measure of cell monolayer confluence (TER is exponentially proportional to confluence)
Tf	Transferrin: (with insulin) stimulates DNA synthesis in renal cell culture
TGFβ	Transforming growth factor-β: a growth factor synthesised in a wide variety of tissues, which acts synergistically with TGFα in inducing a profibrotic phenotype.
TM	Trans-membrane
TRIS	Trizma
TRITC	Tetramethyl rhodamine isothiocyanate: fluorochrome which emits light at 570nm (red) when excited at 550nm

Abbreviation	Full name
Trizma	Tris(Hydroxymethyl)aminomethane: physiological pH buffer
UM	UltroSerG medium: Culture medium with full antibiotics, with 2% USG. Used to promote initial cellular adhesion and growth. See Table 1
USG	UltroSerG: synthetic serum substitute
V_i	Vanadate: salt of vanadium, metal which blocks Na^+-K^+-ATPase activity with MgATP
ZO-1	Zonula occludens protein-1 fusion protein: component of human epithelial cell tight junctions

Chapter 1 General Introduction

Summary

Renal failure causes significant morbidity and mortality. The treatment, dialysis, is not without complications and is expensive. Renal transplantation improves patients' qualities of life, and the one-year survival of transplanted kidneys has been improved significantly by the administration of a fungally derived immunosuppressant, Cyclosporin A (CsA).

However, CsA treatment has not improved the steady, time-dependent, graft loss after the first few months after transplantation, suggesting that the immunological protection afforded by CsA is offset, outside the acute post-transplant period, by toxicity.

The mechanisms of chronic CsA toxicity are not fully understood, but the common cause appears to be the accumulation of CsA within the renal tubular epithelium.

In order to study this accumulation *in vitro* (especially in humans, as animals and animal cell lines behave differently to humans and human cells to toxic attack), primary renal tubular epithelial cells need to be kept exposed to therapeutic concentrations of CsA in culture for weeks if not months, while maintaining their viability and phenotype as close to normal as possible.

Cyclosporin A toxicity

Renal failure is a relatively common cause of morbidity in the developed world. Dialysis will prevent death from renal failure, but is itself associated with significant morbidity and mortality, and is a large drain on medical resources [2].

Renal transplantation improves the health, quality of life, and longevity of patients with renal failure [3]. However, the prevention of rejection of transplanted kidneys (and other organs) requires medication to decrease the immunity of the recipient. Before the late 1970s this was not fully effective and led to the loss of a significant proportion of renal grafts within the first year (33-47%) [4]. Major improvements followed the introduction of Cyclosporin A (CsA) in 1978.

CsA is a cyclic peptide (molecular weight 1202.64) consisting of 11 amino acids (see Figure 1), seven of which are N-methylated and include a novel amino acid, butenyl-dimethyl-L-threonine. Residues 1,2,3,10 and 11 are required for immunosuppressive activity [5]. The compound was originally isolated from the 7939/F strain of the fungus *Tolypocladium inflatum* [6], and found to possess antimicrobial, immunosuppressive and antiparasitic activity [7]. CsA is lipophilic, and its absorption from the gut is therefore facilitated by bile. It is metabolised by the hepatic cytochrome P450 system (P-450 3A4 [8]), which results in hydroxylation, demethylation and cyclisation of the compound. The major route of excretion is biliary, mostly as metabolites. Less than 6% of the total administered dose is eliminated via the kidneys [9].

After a single dose, CsA can be detected in all tissues, but the total amount of drug per weight of tissue can be up to 20-fold greater than in plasma and varies considerably between organs and between individuals: the highest levels are found in adipose tissue, pancreas, liver and kidney [10]. CsA enters T-lymphocytes by a membrane partition process [10], where its action to reduce cell-mediated immunity is well documented. It binds with cyclophillin, and then calcineurin, blocking the cellular production of and nuclear responses to IL-2, thus inhibiting the activation and proliferation reaction of the lymphocytes to presented antigen [11].

The introduction of CsA in 1978 was responsible for a significant decrease in the rate of acute renal transplant rejection within the first three months of transplantation (approximately three-fold reduction), with an improvement in first-year graft survival rates from 53-67% to well over 80% [4;12-14]. However, the chronic attrition rate (the rate of longer-term graft loss) remained remarkably constant throughout this period [15], suggesting either that chronic graft loss is purely non-immunological, or that the reduction in the immunological insult on the kidney afforded by CsA has been replaced by a toxic insult [16].

CsA nephrotoxicity is now well recognised. Its mechanisms, however, are not well understood. Renal CsA toxicity occurs in two forms: direct acute cellular damage – which is reversible on reduction or discontinuation of the drug [17] – and chronic irreversible damage, which may be due in part to microvascular ischaemia, and/or to perturbations of calcium metabolism within the renal tubular epithelial cells [18;19]. Certainly, chronic exposure to CsA *in vivo* causes characteristic striped renal interstitial fibrosis visible on light microscopy (loss of tubular cell height, interposition of fibrous tissue within parenchyma – see Figure 2), suggestive of microvascular ischaemia [20]. It is well reported that CsA induces the formation of the pro-fibrotic transforming growth factor (TGF)-β [21] among others [15]. On electron microscopy, rounded mitochondria and giant cytoplasmic vesicles are recognised features, which suggest an inhibition of calcium efflux from the cells [18;20;22;23]. A reduction in microsomal protein synthesis has also been reported [24].

A further possible detrimental effect of CsA on the renal tubular epithelium is the induction of apoptosis. The exposure of renal cortical cells to CsA *in vitro* increases the rate of apoptosis [25;26], the mechanism of which appears to be nitric oxide-related [27;28].

However, despite the lack of agreement on the mechanism of chronic CsA nephrotoxicity, the common finding within such literature is the discovery of the accumulation of CsA within tubular epithelial cells affected by CsA damage [29;30].

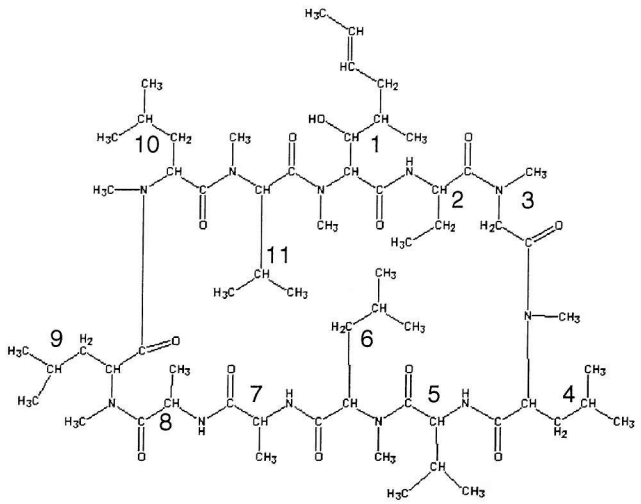

Figure 1 – Molecular schematic of Cyclosporin A: diagrammatic chemical formula, numbers = residues (constituent amino acids).

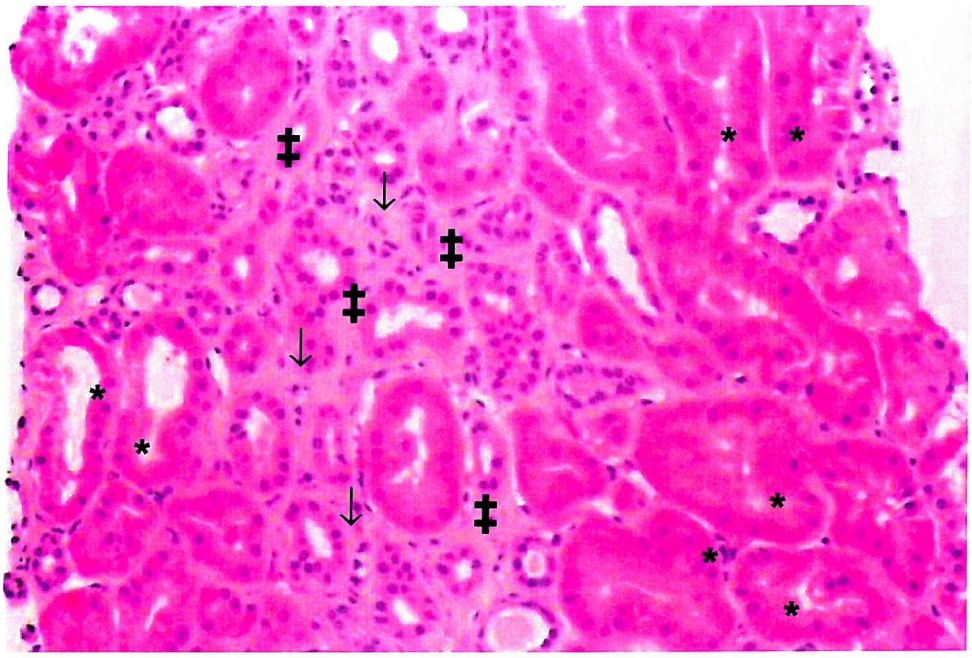

Figure 2 – Characteristic striped fibrosis of Cyclosporin A toxicity. The normal renal parenchyma (right and far left of picture) demonstrates "back-to-back" tubules (*) with good cell height and few intervening cells. The (vertically) central area shows interstitial fibrosis; characterised by loss of tubular cell height, interposition of fibrous tissue (‡) and presence of inflammatory cells (↓). (Haematoxylin and eosin stained section of human renal cortex, original maginification ×40.)

Renal Cell Culture

In order to investigate *in vitro* any mechanisms related to chronic CsA toxicity, and particularly to remove the influences of any potential perfusion defects, it would appear to be necessary to culture renal tubular epithelial cells, then expose them to pharmacological doses of CsA for a number of weeks, if not months.

There are a number of established animal cells lines in common use for *in vitro* studies of renal tubular epithelium, both of virally transformed "normal" cells (pig – $LLC\text{-}PK_1$ [31], American opossum – OK [32] and rabbit proximal tubular cells [33]) and of tumour cells (dog – MDCK [34]).

However, there are well-documental problems with these cell lines. They respond to insults, particularly toxic insults, differently to human renal cells [33;35](Abstract: Pearson AL et al, 2001. Contrasting responses of transformed versus primary proximal tubular epithelial cells to albumin and retinol binding protein. *The Renal Association Spring Meeting*: 2001).

Tumour and transformed cell lines also undergo slow, continued but inconsistent transdifferentiation from their *in vivo* phenotype during subsequent passages [36]. To extrapolate nephrotoxic effects on animal cells to the human condition would, therefore, appear not to be wholly appropriate. Cell lines also continually divide and proliferate: tumour cells have, at best, minimal contact growth inhibition [37], and virally transformed cells will lose contact inhibition if left at confluence for extended periods [37], and will ultimately overgrow. Continued growth is not found in normal renal tissue, where the proportion of cells proliferating in the tubular epithelium at any one time has been shown to be 0.2-0.3% [38].

Current established techniques for human renal tubular cell culture involve either virally transformed lines (HK-2 [39] or HK-5 [40]) or the growth, in hormonally and trace element defined culture medium, of primary cells from macroscopically normal renal tissue. Primary cells can be obtained: as direct outgrowths from

(i) explant tissue (1-2mm pieces of intact cortical tissue) [41],

(ii) biopsy specimens [42];

(iii) microdissected nephronal segments [43]; or

(iv) mechanically and enzymatically disaggregated isolated cell suspensions [36].

Although our group has successfully grown cells from biopsies and explants, (i) time constraints (such cultures take greater than twenty days to reach confluence [unpublished observations] and Detrisac (1984) [41]) and (ii) the achievement of reproducibly appropriate cell growth and phenotype in this department [44] have led to this group adopting mechanical and enzymatic disaggregation and plating out of isolated cell suspensions as the culture method of choice.

In order to detect effects of chronic pharmacological toxicity on cells in culture, the cells need to be exposed to the toxic insult for a period of time. Non-differentiating cells, which maintain their human phenotype while remaining in culture for a number of weeks to months, would therefore be ideal. Such culture conditions are not currently available.

Chapter 2 General Methods

Preparation of main material

Subjects

Ethical approval was already in place prior to the study commencing (see Appendix 1), and did not include extra informed consent, above that obtained for the surgery. The senior and junior surgical, theatre and pathology department staffs were informed of the study. Examination and consideration of the procedures for tissue retention was undertaken continuously by Professor M. Church, the medical adviser to the Southampton Local Research Ethical Committee (LREC), and pending redesign of the Trust's consent form the study remained within the LREC guidelines.

The study commenced on the 1st June 2000. All adult nephrectomies performed by the urological surgeons in Southampton University Hospitals NHS Trust were considered for the study. Through liaison with theatre staff, the normal procedure of placing nephrectomy specimens in formalin was delayed by minutes until a consultant pathologist examined the kidneys. The research team then dissected those deemed appropriate for the study. All kidneys reached formalin within the time considered appropriate for optimum preservation of histology by the consultant pathologists.

In August 2001, ethical approval was obtained for identical tissue harvesting from Portsmouth Hospitals NHS Trust (see Appendix 2), and the necessary procedures were put in place. All adult nephrectomies performed by the urological surgeons in this trust were considered for the study. Full informed consent of these patients was obtained prior to their inclusion in the study. Full agreement was obtained from the pathology department (stipulating that the tumour margins should remain intact, the adrenal glands should not be taken and the serosa should not be removed).

All samples were kept anonymous by a sequential numerical code. No histological diagnoses were subsequently sought, as the samples were anonymous as per ethical advice. Likewise no information was recorded of the patients' co-morbidity, previous

medical history or current/past medication. Only the patients' ages and genders were recorded with the numerical code.

Tissue Preparation

In Southampton, the kidneys were bisected by the pathologist and the depth of cortex, tumour size and spread were assessed visually: cortical tissue was taken if approximately $3cm^3$ of tissue could be taken while widely avoiding the tumour margins (cortices of less than 6-8mm rarely fulfilled this criterion). Tissue recovered after 4pm was stored in RPMI medium with 2× antibiotics at 4°C overnight [36], then processed as normal the next day.

In Portsmouth, the consultant urologist performing the nephrectomy removed approximately $3cm^3$ of macroscopically normal cortex from the kidney for the research project prior to fixation of the remainder in formalin. The research sample was stored in RPMI medium with 2× antibiotics at 4°C for at most overnight [36], prior to processing.

Under sterile Class II tissue culture conditions any visible adipose, serosal, medullary and vascular tissue was dissected away, and the resulting tissue was washed in cold RPMI to remove as much blood as possible.

Two approximately 2×2×10mm portions of tissue were removed longitudinally and transversely and snap-frozen in liquid nitrogen for subsequent frozen section. The remainder was minced with crossed scalpels in cold RPMI until in pieces of < 1mm. The resulting homogenate was twice washed in RPMI and sedimented by centrifugation at 250×*g* for 10mins, then resuspended in 20ml 0.1% collagenase (Type IV)/0.1% trypsin in PBS, and incubated for 1 hour at 37°C, agitating gently and refreshing the air within the tube every 15-20mins. The proteases were inhibited with 20ml 0.15% trypsin inhibitor in PBS, and the tissue was sedimented again, before washing twice more in RPMI, all at 250×*g* for 10mins.

The resulting pellet was then resuspended in 2-5ml RPMI and passed through cell strainers – first 70μm to remove glomeruli and other structural debris, then 40μm to remove larger cells. This filtrate was a suspension of isolated cells.

All subsequent culture methods were performed in sterile conditions. Cell growth occurred at 37°C in a temperature-controlled humidified atmosphere of 95% O_2 / 5% CO_2.

Culture methods

First passage

The number of flasks required to distribute the isolated cell suspension was estimated. Attempts were made to count the number of cells in the isolate and standardise the numbers of cells seeded into each flask, but this proved impossible owing to the large amount of debris still present in the solution. Therefore, after much trial and error, between 6 and 14 flasks were seeded depending on the size of the initial tissue sample and a visual assessment of the turbidity of the isolated cell suspension.

The flasks used for the first passage were Nalge Nunc Nunclon Delta 25cm^2 clear uncoated polystyrene culture flasks. The cell suspension was made up to 6ml for each flask, with UM (see Table 1), and then plated out.

Cells were observed by inverted phase contrast microscopy at least daily for infection and for cell growth and morphology. The medium was changed to HM (see Table 1) on day 1 or 2 when cells had stuck down (cells in the initial cell suspension are rolled-up [Figure 3a]: when they adhere to the culture surface, they unroll and spread slightly on the flask surface, which is visible down the microscope: Figure 3b) and had formed colonies of ~10 cells (Figure 3c).

Once the cells covered about half the culture surface (usually days 3-5: Figure 3d) the medium was changed again to DM (see Table 1).

At confluence (no gaps in the cell monolayer, assessed by phase-contrast light microscopy: Figure 3e), the medium was changed to the media under investigation, or the cells were detached from the flask for subculture or further examination.

Table 1. Culture medium composition, Basal medium[a] plus supplements

Medium	Antibiotics[b]	USG %v/v	DMSO mM	EGF[c] ng/ml	HC[d] ng/ml	Insulin ng/ml	PGE_1[e] ng/ml	PTH[f] ng/ml	Sel[g] ng/ml	Tf[h] mg/ml	T3[i] pg/ml
UM[j]	100/ml	2									
HM[k]	50/ml	1		5	18	2.5	5		2.5	2.5	2.5
DM[l]	50/ml			10	36	5	10		5	5	5
QM[m]	50/ml	0.2	140	25				0.5			

[a] DMEM:Ham's F-12 (1:1) with 2mM glutamine

[b] penicillin (iu) and streptomycin (μg)

[c] Long-epithelial growth factors: human EGF with an added peptide chain to prevent metabolism while retaining bioactivity [45] – allows medium change every 7 days

[d] hydrocortisone

[e] prostaglandin E_1

[f] whole human parathyroid hormone

[g] selenium

[h] apo-transferrin

[i] tri-iodothyronine

[j] USG medium: to promote cellular adhesion without the need for collagen coating of the culture surface

[k] Half-defined medium: weaning off USG while adding hormones and trace elements

[l] Defined medium: formulated to maintain the phenotype of explanted human tubular epithelial cells [41]

[m] Quiescence medium: based on a culture medium previously derived to promote maximal differentiation of a transformed human renal cell line [1]

Cell detachment

A well-recognised method was used [36;41]. Cells on the culture surface were removed by first decanting off the culture medium, and then incubation with 1×HBSS for 10mins at 37°C (10ml for a 25cm^2 flask, 2ml for a 6-well insert). The HBSS was

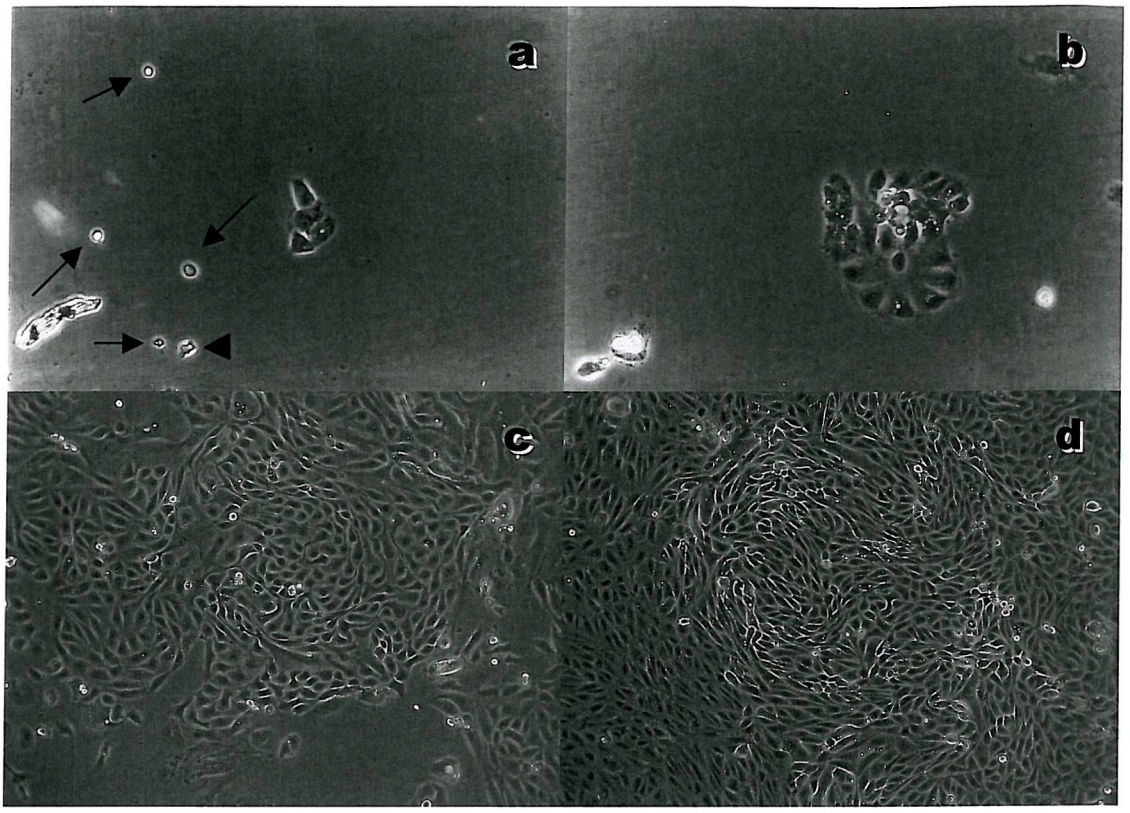

Figures 3: Phase-contract light photomicrographs of primary human renal cortical cell homogenates on uncoated plastic culture flasks. (a) cells rolled-up prior to adherence (arrowed), unrolling (arrow head) and sticking-down (centre group), **(b)** cells forming colonies of ~10 cells, **(c)** cells at approximately half flask coverage, and **(d)** cells in a confluent monolayer, showing the characteristic whirling pattern of renal tubular epithelial cells in culture. (Original magnification a,b ×40; c,d ×10).

tipped off and 0.05% trypsin / 0.02% EDTA solution was added (2ml for 25cm^2, 0.5ml for 6-wells), and kept at 37°C, for usually around 5 to never more than 10mins, with intermittent light tapping of the flask, until the cells were detached. 10 or 2ml of RPMI (no antibiotics) / 10% FBS was then added to inhibit the trypsin, and the cells were pelleted at 250×*g* for 5 mins, then washed in RPMI at 250×*g* twice for a further 5mins each time, to remove all FBS.

Second passage

Detached cells were plated out at a subculture ratio of 1:3 or 1:4, which would become confluent again in 2-3 days. Falcon Biocoat uncoated transparent PET 0.4µm-pore culture membrane inserts (see Figure 4) were pre-soaked for 30mins (as per manufacturer's instructions) in basal medium, which was then discarded. The cells were suspended in 1ml of HM per well, and added to the apical chamber. 2ml of HM was also added to the basal chamber. Cells were again inspected by inverted phase-contrast microscopy at least daily for infection, and cell number and morphology. The medium was changed to DM after 24 hours, then to QM at monolayer confluence.

Morphology techniques

Phase-contrast light microscopy

Performed on a Nikon Diaphot-TMD inverted microscope. Digital images were captured from this microscope with a Nikon Coolpix 990 camera, and printed unchanged via Adobe Photoshop software for PC.

Cell viability

Performed by trypan blue exclusion. Trypan blue is taken up immediately by dead, but not by viable cells, and hence can be used to differentiate these by light microscopy [46] – see Protocol 1.

Transmission electron microscopy (TEM)

Performed on cell monolayers on culture well inserts. The cells were washed in situ, and then cut from their mounts. Cells and inserts were fixed, post-fixed, dehydrated, infiltrated then embedded in resin. Polymerisation was performed, sections were cut and stained. Grids were examined by electron microscopy, from which photomicrographs were taken (Protocol 2).

Scanning electron microscopy (SEM)

Performed on cell monolayers on culture well inserts, initially prepared as for TEM (Protocol 3).

Biochemistry techniques

Cell suspensions produced by cell detachment were washed in PBS (to remove FBS which would interfere with the microprotein assay) at RT at 250×*g*. The pellet was resuspended in 250µl of PBS: 50µl was used for cell viability counting, 50µl for microprotein estimation, 50µl for alkaline phosphatase activity, and 100µl for gamma glutamyl transferase activity.

Microprotein estimation

Performed on disrupted cells. Using a Soniprep 150 (MSE) the cells were disrupted by sonication at 14µm for 10 seconds. This was shown to be sufficient to completely disrupt the cells (Figure 5). The cells' total protein content was then assayed using Brilliant blue G (according to the method by Bradford [47]) using the Sigma 610-A kit (Protocol 4).

Alkaline phosphatase activity estimation

Performed using the Sigma 104-LS kit. This utilises the phosphatase-dependent liberation of p-nitrophenol, which turns yellow on alkalinisation, to spectrophotometrically determine the alkaline phosphatase activity of whole cells (Protocol 5).

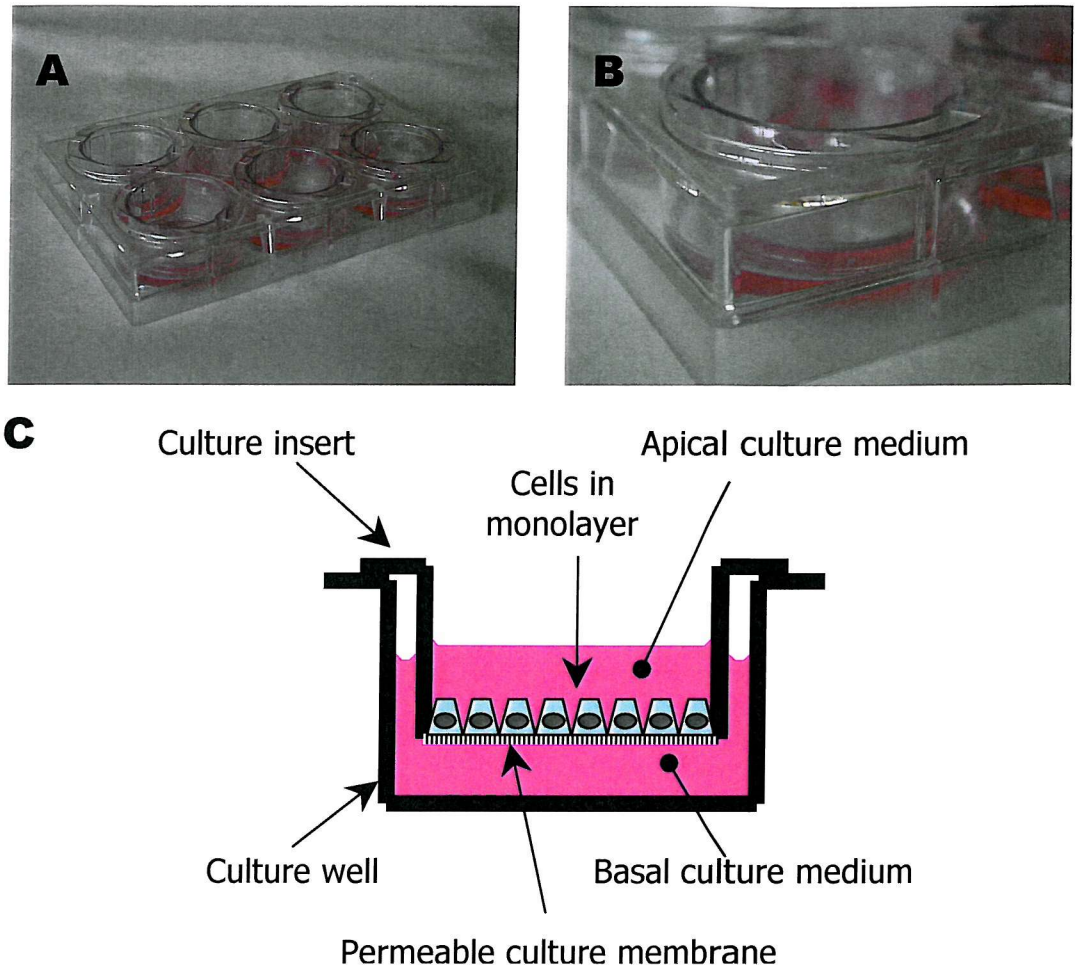

Figure 4. Equipment for culture of polarised cell monolayers: **(A)** whole 6-well plate, **(B)** close-up of one well, **(C)** schematic diagram of one well

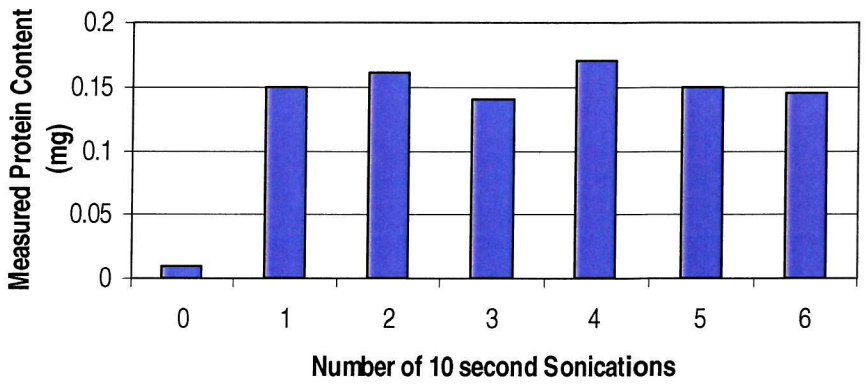

Figure 5. Protein content of identical aliquots of cell suspension subjected to increasing periods of sonication. Maximum protein content is achieved after the first sonication.

Gamma-glutamyl transferase activity estimation

Performed on whole cells using the Sigma 545-A kit. This produces a pink colour in proportion to the GGT-dependent liberation of p-nitroaniline (Protocol 6).

Immunofluorescence techniques

Indirect immunofluorescence was performed on cytocentrifuge preparations of cell suspensions, or monolayers on 8-well chamber slides or cell culture membranes. The samples were fixed, incubated with a mouse monoclonal antibody, then with a fluorochrome-conjugated anti-mouse antibody (Protocol 7). Fluorescence microscopy was performed on a transmission fluorescence microscope (Protocol 8), or a laser confocal microscope (Protocol 9). On the former, composite images of double- or triple-fluorochrome labelled cells can be built up electronically by superimposing images taken of the same field in different wavelengths of laser light (Appendix 3). With the latter, images of multiple fluorochromes can be captured simultaneously. Photomicrographs are produced digitally which are imported to a computer and printed out.

Flow cytometry techniques

Flow cytometry is performed on cell suspensions (Protocol 10). As with indirect immunofluorescence, the samples are fixed, and exposed to a primary monoclonal then fluorochrome-conjugated secondary antibody. Alternatively the cells can be exposed to a soluble fluorochrome, which can accumulate within the cells. Flow cytometry is performed on a flow cytometer, which determines the fluorescence of the cells in laser light and represents this graphically (Appendix 4). More than one "channel" (wavelength of laser light) can be used simultaneously to examine multiple labelling with separate fluorochromes on individual cells (Protocol 11).

Chapter 3 Quiescent Cell culture

Summary

Models of renal tubular epithelium *in vitro* have facilitated the study of tubular function. However, current knowledge has been gained from transformed animal or human cell lines, which are often functionally dissimilar to their normal human equivalents; or from short-term studies of proliferating cells in growth medium, which do not reflect the normal state of cells *in vivo*, and are not appropriate for investigations of longer-term effects.

This study aimed to examine whether novel culture conditions intended to quiesce primary human renal tubular cells of defined phenotype, thus allowing longer-term viability without serial subculture, would provide a more physiological model.

Renal cortical cells were physically then enzymatically disaggregated from the macroscopically normal pole of human nephrectomy tissue. The culture medium was sequentially manipulated from an initial adhesion and proliferation medium containing a synthetic serum substitute to a serum-free hormonally and trace-element defined tubular cell growth medium. At monolayer confluence, the final medium change was made to quiescence medium (DMEM:Ham's F-12, 50iu/ml penicillin, 50μg/ml streptomycin, 2mM glutamine, 25ng/ml epithelial growth factor, 0.5ng/ml parathyroid hormone, 0.1% UltroSerG and 140mM dimethyl sulphoxide). This medium was derived from one previously found to promote maximal differentiation in a human renal tubular cell line [1].

Cellular characterisation was performed by phase-contrast light microscopy, transmission electron microscopy, indirect immunofluorescence, flow cytometry and in-situ enzyme activity. The cells' ability to proliferate on the reintroduction of growth factors was also investigated, as were their cell cycle phases at each stage of culture.

After six weeks in culture, the cellular appearance by light and electron microscopy was consistent with cultured renal tubular epithelium, as was the expression of a panel

of cellular markers and the activity of brush border membrane enzymes. Cell cycle determination showed that the proportion of cells in S-phase in quiescence was 2.5- to 5-fold lower than that in defined growth medium, and the proportion in G2/M-phase was at least halved. The quiescence and not senescence of the cells was confirmed by their ability to be passaged to growth medium at six weeks or greater.

By manipulating the culture medium composition, primary human renal tubular epithelial cells can retain their normal *in vitro* phenotype and may be kept viable in culture without serial subculture for at least six weeks. In this way, reducing the drive to proliferate while maintaining phenotypic markers should provide a more appropriate model for the investigation of chronic renal tubular injury, particularly pharmacological nephrotoxicity.

Introduction

Culture Medium Composition

As discussed previously, in recent years much progress has been made in the development of *in vitro* models of renal tubular epithelium. Manipulation of the composition of the growth medium of tubular epithelial cell cultures [33;35;36;41;48-55] has allowed retention of an approximate *in vivo* phenotype, as confirmed by retention of surface epitope expression, metabolic/biochemical activity and ultra-structure by transmission electron microscopy (TEM) [36;41;48;50;53].

The majority of the commonly used conditions for the culture of human tubular epithelial cells employ FBS as a source of growth factors, either in the culture medium or adsorbed on to the culture surface or matrix. However, data from renal and non-renal human and animal epithelial cell culture suggest that FBS supports fibroblast culture [41;56]; and is also subject to significant inter-batch variation in its composition [57]. UltroSerG (USG, Invitrogen) is a synthetic serum substitute including steroids, whose composition is constant (although not divulged in the product literature) and does not vary between batches (Manufacturer's data sheet), and does not support fibroblast growth [56]. USG is five times more potent than FBS, so a concentration of 2% (v/v) is equivalent to 10% (v/v) of FBS (Manufacturer's data sheet).

As discussed previously, knowledge of CsA nephrotoxicity has been gained from a variety of sources: human renal biopsy studies [30], which will be complicated by a range of confounding factors; animals *in vivo*; *in vitro* transformed human cell lines [58;59], animal cells [35;60;61], or short-term studies on proliferating cells in growth medium [62-68]. However, as already mentioned, (i) transformed cell lines and animal cells differ from primary human tissue in their physiological roles and their responses to insults[1], (ii) renal tubular epithelial cells are mostly in a quiescent state and divide at a very low rate *in vivo* [38], and (iii) the primary human cell studies have been performed with super-pharmacological CsA doses in order to find an effect in the 24 to 120 hours of exposure. Therefore the extrapolation of the chronic effects of toxins from such studies is unlikely to be appropriate.

Quiescence

The aim of this first section was to determine whether primary human renal tubular epithelial cells could be kept in a quiescent state. Quiescence is defined as a state of inactivity, repose or tranquillity [69]. In cell culture it is phenotypic and metabolic normality, with a lack of cellular proliferation [70].

Quiescence in cell culture is normally assumed when both (i) the cells are at confluence, and therefore with maximal contact growth inhibition, and (ii) serum or serum substitutes are removed from the culture medium. However, this state is usually only maintained for up to 48 hours, at which the relevant experiment is usually performed. Clearly longer-term investigations of these cells are not possible.

Early experience with cell culture in defined medium confirmed that the cells overgrow, detach from the culture surface and undergo necrosis (see results below). It became increasingly apparent that longer-term exposure to nephrotoxins would not be possible with these culture techniques. Review of the literature found very little evidence that this problem had been explored before: the only useful previous work was by Racusen [1], while defining her transformed human cell lines.

She studied a number of separate transformed cell lines, and then studied the effect of variation of culture medium composition on the characterisation of these cell lines. Her group determined which of their cell lines was the nearest to normal, and which culture medium maintained this state best. The cell line was HK-5, now commercially available, and the culture medium which promoted the nearest normal (i) brush border enzyme expression, (ii) biochemical properties and (iii) glucose transport, contained low-level FBS, EGF and PTH. They also found that the addition of DMSO (which penetrates living tissues without causing significant damage, resulting in the ability to replace some of the water molecules associated with the cellular constituents) allowed maintenance of morphologically intact monolayers of cells for prolonged periods [1].

It was not within the scope of my study, either in terms of time available or man-power, to replicate this work of varying the composition of culture media for primary human renal tubular cell culture to see which supported the best characterisation and

least proliferation, so I decided to study the effects of what would appear to be the best known culture medium for the purpose, and if successful, continue to the second phase of the study with this medium.

Proliferation

Proliferating cells move through the Cell Cycle (see Figure 6) which has four phases, G_1, S, G_2 and M. Non-proliferating cells such as terminally differentiated cells (muscle cells, nerve cells) and resting lymphocytes are defined as being in the G_0-phase of the cell cycle: when activated, resting lymphocytes can rejoin the cell cycle at G_1. The cells use G_1-phase for RNA synthesis, protein biosynthesis and actual cell growth (increase in cell mass). S-phase is when DNA replication occurs and G_2-involves a re-assortment of cell parts, which must occur before mitosis, in M-phase.

Cellular proliferation *in vivo* and in culture can be detected by a number of methods:

1. Monoclonal antibodies are available against specific antigens expressed during cell cycle cycling, such as Ki-67 and proliferating cell nuclear antigen [38], both expressed at the end of G_1-phase, through S- and G_2-phases into M-phase (Boehringer-Mannheim product literature).

2. Bromodeoxyuridine (BrdU) is taken up by DNA synthesised in S-phase of the cell cycle [71], and can be detected by indirect immunohistochemistry or flow cytometry.

3. Propidium iodide (PI) is a fluorescent marker that binds to nucleotides. It is taken up by the nuclei of cells with permeable cell membranes [72], i.e. non-viable cells, or fixed cells (viable cell membranes are impermeable to PI). It will thus brightly label nuclei, and may also detect cytoplasmic RNA. In S-phase of the cell cycle, cells are duplicating their DNA, and in M- and G_2-phases cells contain twice their normal quantity of DNA. By exposing fixed cells to RNAse, which removes the potential for cytoplasmic fluorescence, an accurate quantification of the cellular content of nuclear DNA can be obtained by detecting nuclear PI by flow cytometry, and thus the position of cells within the cell cycle (see Figure 7).

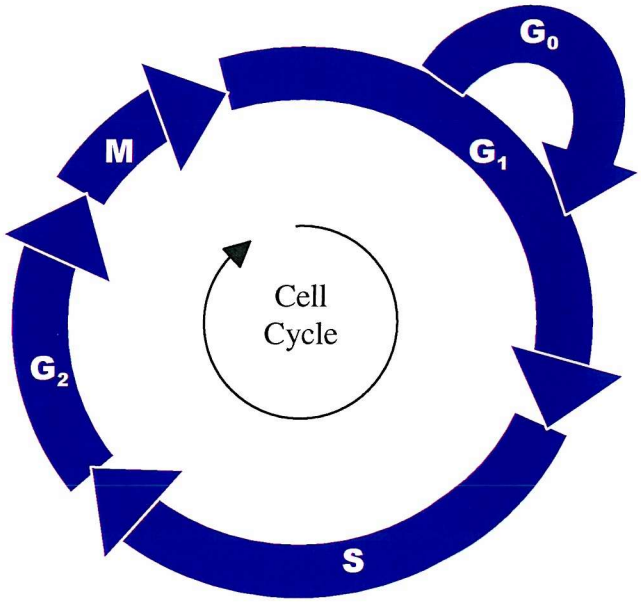

Figure 6 – Cell Cycle: a schematic overview

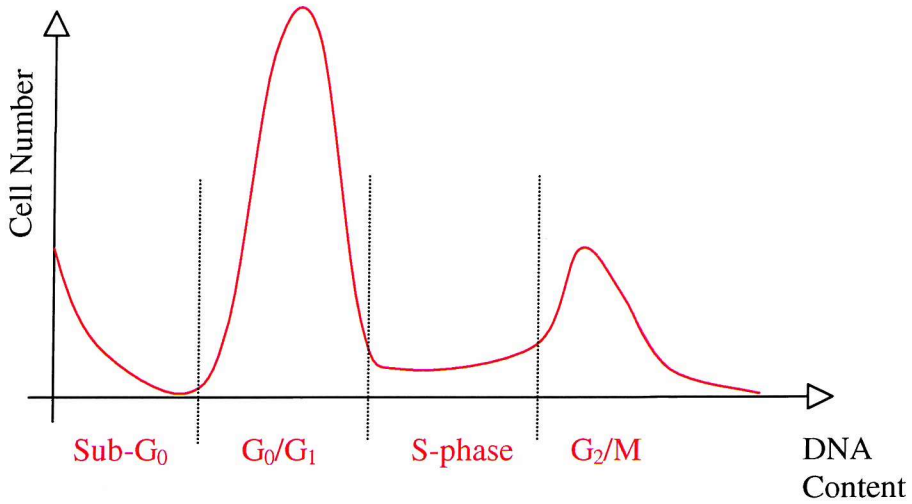

Figure 7 – Cell distribution through the Cell Cycle by DNA content. The sub-G_0-phase represents cells undergoing apoptosis or necrosis, as the DNA content is less than that of normal viable cells

Characterisation

In order to determine the effects of alterations in culture conditions on cells *in vitro*, the cells need to be characterised. The human renal tubular cell character *in vitro* can be built up from a combination of the following.

1. A general human cell character: general cellular markers and DNA content;

2. An epithelial cell character: monolayer formation, cellular polarisation and intercellular tight junction formation.

3. A more specific renal tubular cell character: specific monolayer structure, specific ultrastructural appearance, specific surface epitope expression, and specific metabolic and biochemical activities.

General Human Character

To determine the general human cell character, the cells should express MHC class I, which is variably expressed by all nucleated human cells, and has been reported in tubular epithelial cells [73;74]. The absence of this epitope would represent a wide divergence from the normal *in vivo* phenotype. The relative DNA content of the cells can also be measured, to reveal their positions in the cell cycle.

Epithelial phenotype

The epithelial phenotype can be investigated first by phase contrast light microscopy. Most epithelia should form confluent monolayers of cells, without gaps between the cells [37;41;53]. Epithelial cells should polarise within these monolayers, exhibiting differing apical and basal membranes, and apical / basal distribution of organelles. This can be detected by transmission electron microscopy (TEM) [36;50;55]. Epithelial cells should also form tight junctions between adjacent cells [36;75], which can be identified by TEM or by immunohistochemistry with monoclonal antibodies directed against elements of the junctional complexes.

Specific Renal Tubular Cell Character

A more specific renal tubular cell character would be represented by a whirling appearance of the cell monolayer [41], and the formation of domes, which can be seen on light microscopy. Domes demonstrate that the cells are performing vectorial fluid shift: *in vivo* the cells would line the tubules, and a major function would be the reabsorption of water and solutes from the urine (apical surface) back into the blood (basal surface). *In vitro*, the apical surface of the cells is exposed to the medium, and in culture flasks, the basal membrane is applied to the impermeable flask plastic. If the cells continue their transport functions, then any fluid excreted from their basal surfaces increases hydrostatic pressure between the cells and the flask. The persistence of impermeable tight junctions leads to the formation of a dome of cells separated from the culture flask by excreted fluid [41;76-78].

A further more specifically renal characteristic is the presence of an apical brush border with microvilli, and numerous basal mitochondria [36], visible on scanning electron microscopy (SEM) and TEM, although in culture microvilli tend to suffer blunting and denuding [36;41;79], particularly in the presence of serum [50].

There is a wealth of surface epitopes specific for renal tubular cells. Three of common use in our department were T43 (Proximal Convoluted Tubule Antigen) which is found on both proximal and distal tubular epithelial cells and alkaline phosphatase (ALP), which have both been detected on proximal tubular cells in our department (previous work not shown here) and in published literature [36;41;76;80;81] and Epithelial Membrane Antigen (EMA), which is situated on a variety of human epithelia. In the kidney EMA is found on the distal convoluted tubule (and collecting duct) [82]. These can be detected by immunohistochemistry or flow cytometry.

Specific renal tubular metabolic activities include alkaline phosphatase and γ-glutamyl transferase [1;36;39;41;53;76]. These can be detected on whole cells by immunohistochemistry or by spectrometric methods.

Cell Populations

When initially dissected, homogenised, filtered then plated out on culture flasks, the cell population is widely variable. Filtration removes the majority of the glomeruli, and dissection avoids macroscopic medullary and vascular tissue, but the remainder includes proximal and distal tubular, stromal, vascular and haematogenous cells. Decanting off and replenishing the culture medium at 24 and 48 hours removes the majority of the glomerular, vascular and haematogenous cells, which do not appear to adhere to the culture flask surface (unpublished observations).

The hormonally and trace element defined medium used for cell growth and differentiation promotes the growth of proximal tubular cells over distal cells, and maximal differentiation is achieved after seven days of such culture [49;55]. Furthermore, distal cells that are supported by these culture conditions transdifferentiate to proximal cells, expressing less distal cell markers and more proximal markers (although not ALP) [53].

It is therefore safe to assume that the majority of cells that become established and subsequently proliferate in this defined culture medium, before changing to the study media, exhibit the proximal renal tubular phenotype.

Methods

As in General Methods (Chapter 2), tissue was obtained and plated into 25cm^2 uncoated plastic culture flasks, and serial manipulation of the culture medium was performed until monolayer confluence, as determined by phase-contrast light microscopy.

At confluence, the medium was changed to a novel quiescence medium. The formulation was based on a culture medium previously derived to promote the greatest differentiation of a human transformed renal cell line [1] (see Table 2). The effect of this medium on cell proliferation was initially assessed by BrdU uptake. The effect of the inclusion within this medium of dimethyl sulphoxide, which has been shown to induce differentiation in transformed human renal tubular epithelial cells [1], was also examined in this way.

Table 2. Culture medium composition, Basal medium[a] plus supplements: Comparison of quiescence medium with defined medium

Medium	Antibiotics[a]	USG % v/v	DMSO mM	EGF[b] ng/ml	HC[c] ng/ml	Insulin ng/ml	PGE_1[d] ng/ml	PTH[e] ng/ml	Sel[f] ng/ml	Tf[g] mg/ml	T3[h] pg/ml
DM[i]	50/ml			10	36	5	10		5	5	5
QM[j]	50/ml	0.2	(140)[k]	25				0.5			

[a-i] see Table 1

[j] Quiescence medium

[k] Studies with and without DMSO were performed

Cell Culture – Preparation for Characterisation

In order to obtain appropriate cell samples for the different characterisation procedures, three experimental protocols were followed.

1. For phase contrast light microscopy, immunohistochemistry, flow cytometry, and enzymatic activity, cells were kept in primary passage. At confluence in DM (for all medium compositions – except QM – see Table 1), the medium was changed to QM (see Table 2), which was refreshed every seven days.

2. For BrdU incorporation, primary passage cells at confluence in DM were subcultured 1:2 to 8-well glass chamber slides into DM. At confluence, BrdU incorporation was measured by indirect immunofluorescence (Protocol 12) then the medium was changed as per Table 3. BrdU incorporation was measured again after 24 then 48 hours.

Table 3. BrdU incorporation experiment medium composition, basal medium plus supplements

Medium	USG %v/v	DMSO mM	EGF ng/ml	HC ng/ml	Insulin ng/ml	PGE_1 ng/ml	PTH ng/ml	Sel ng/ml	Tf mg/ml	T3 pg/ml	BSA[a] %w/v
DM[a]	-	-	10	36	5	10	-	5	5	5	-
USG	0.2	-	-	-	-	-	-	-	-	-	-
BSA[b]	-	-	-	-	-	-	-	-	-	-	0.5
QM1	0.2	-	25	-	-	-	0.5	-	-	-	-
QM2	0.2	140	25	-	-	-	0.5	-	-	-	-

[a] serum-free, hormonally defined medium

[b] bovine serum albumin

3. Tight-junction immunostaining and transmission electron microscopy (TEM) required confluent cell monolayers on non-vitreous culture membranes. At confluence (in DM), cells were passaged at a 1:2 subculture ratio to pre-soaked (in BM – basal medium, see Abbreviations) uncoated polyethylene teraphthalate (PET) 0.4µm pore 6-well cell-culture membranes (Falcon, Becton-Dickinson) in HM. After 24 hours, the medium was changed to DM. At confluence, the final change to QM was made (within 2-3 days), which was managed as above.

Light microscopy

Phase contrast micrographs of the cell monolayers were taken regularly, using a Nikon CoolPix 990 digital camera on a Nikon Diaphot-TMD inverted microscope.

Immunostaining

The panel of antibodies for characterisation is shown in Table 4.

Table 4. Characterising Antibodies[a]

	Antigen	Antibody	Source	Fluorescence Concentration
Isotype Control IgG1	Rat IgG[b]	MCA928	Serotec	2µg/ml
Isotype Control IgG2a	Rat IgG	MAB003	R&D Systems	2µg/ml
MHC I	Human MHC[c] Class I common epitope	HB95	Wessex Immunology	0.5µg/ml
T43	Human renal convoluted tubule membrane	Urothelial Antigen T43	ID Labs	25µg/ml
EMA	Human Epithelial Membrane Antigen	EMA	Dako	1.25µg/ml
ALP	Human alkaline phosphatase common epitope	0300-1730	Biogenesis	0.4µg/ml
ZO-1	Human recombinant zonula occludens protein-1 fusion protein	ZO1-1A12	Zymed Labs	5µg/ml

[a] all raised in mouse

[b] immunoglobulin-γ

[c] major histocompatibility complex

Immunohistochemistry

Samples for zonula occludens protein-1 (ZO-1) staining were intact cell monolayers on uncoated PET cell culture membranes. For the remainder of the primary antibodies, cytocentrifuge preparations of cells at confluence in DM and in quiescence in QM were prepared as for passage, then centrifuged on to 3-aminopropyl-triethoxysilane (APES)-coated microscope slides (see Protocol 13). Slides were air-dried then stored at room temperature until staining.

Indirect immunofluorescence was performed per Protocol 7. Slides were fixed in acetone then incubated with the appropriate primary monoclonal antibody (see Table

4) and fluorescein isothiocyanate (FITC)-conjugated rabbit-anti-mouse (RaM) $F(ab')_2$ (Dako) secondary antibody, with propidium iodide (PI) to counterstain the nuclei. Glass coverslips were mounted, and immunofluorescence microscopy was performed on a TCS SP2 laser scanning confocal microscope (Leica) (Protocol 9).

Flow cytometry

Cell suspensions were prepared by brief trypsin / EDTA digestion as above. Protocol 11 was followed: disrupted cell suspension was incubated with 25µg/ml primary monoclonal antibody (or relevant control – see Table 5), then with 20µg/ml FITC-RaM $F(ab')_2$ or 2.8µg/ml Cy5-GaM $F(ab')_2$ secondary antibody. Cytometry was performed on a FACScalibre flow cytometer (Becton-Dickinson – Protocol 10).

Table 5. Flow Cytometry Characterising Antibodies[a]

	Antibody	Fixative	Time / temperature for fixation	Antibody Incubation Time
Isotype Control IgG_1	MCA928	-	-	30mins
Isotype Control IgG_{2a}	MAB003	-	-	30mins
MHC I	HB95	-	-	30mins
T43	Urothelial Antigen T43	-	-	30mins
EMA	EMA	-	-	30mins
ALP	0300-1730	100% Ethanol	-20°C / 10mins	Overnight
Isotype Control IgG_1 (for ALP staining)	MCA928	100% Ethanol	-20°C / 10mins	Overnight

[a] all raised in mouse

Enzyme activity

Cell suspensions prepared as above were assayed:

(i) for ALP activity using the Sigma 104-LS kit. This utilises the phosphatase-dependent liberation from p-nitrophenol phosphatase of p-nitrophenol, the

concentration of which is proportional to phosphatase activity, and can be measured spectrophotometrically by the extinction of light at 400-420nm when converted to yellow complexes by alkalinisation [83] (Protocol 5);

(ii) for Gamma glutamyltransferase (GGT) activity using the Sigma 545-A kit. This produces p-nitroaniline in proportion to the GGT-dependent transfer of the glutamyl group from L-glutamyl-p-nitroaniline to glycylglycine [84]. P-nitroaniline is then diazotised by sodium nitrite in an acid environment [85], and the diazo compound is reacted with N-[1-Naphthyl]-Ethylenediamine to form a pink-coloured azo-dye, the concentration of which can be measured spectrophotometrically by the extinction of light at 530-550nm [86] (Protocol 6).

(iii) Cells in PBS, disrupted by sonication at 14μm for 10 seconds (Soniprep 150, MSE), were assayed for total protein content using Brilliant blue G with the Sigma 610-A kit, utilising a modified Bradford technique of shifting the wavelength of absorbance of the dye from 465 to 595nm on binding with protein [47]. The concentration of protein in the microgram range can then be measured by light absorbance around 600nm (Protocol 4).

The colour intensities were measured on a Microscan Multisoft (Titretek) spectrophotometer, by absorbance at (i) 414, (ii) 540 and (iii) 620nm respectively (once the wavelength with the absorbance of closest correlation to standards was determined). Each sample was measured at least in duplicate. Standards were measured and standard curves calculated for each experiment. Enzyme activity was represented as nmol of substrate·min^{-1}·mg protein^{-1}.

The same protocols were performed on isolated cells (immediately before first culture plating) to determine the enzyme activities on day zero.

Cell viability

At each cell detachment (for passage, characterisation etc.), cell viability was estimated by trypan blue (0.4% solution, mixed 1:1 with 50μl cell suspension) exclusion on a haemocytometer (Protocol 1).

Cell cycle

At each cell detachment, 50µl of cell suspension was added to 450µl 70% ethanol, and stored at –20°C until tested. All assays were performed together (see Protocol 14): washing off the ethanol, incubating with RNAse and staining with propidium iodide, then performing flow cytometry on a Beckton-Dickinson FACScalibre. The resulting peaks were analysed for necrotic (no PI signal [no DNA]), apoptotic (sub-G_0-), G_0/G_1-, S- and G_2/M-phase cells.

Transmission electron microscopy (TEM)

See Protocol 2: membranes holding cell monolayers were rinsed, cut from their mounts and fixed. They were post-fixed, dehydrated, infiltrated and then embedded in resin. Polymerisation was performed, and transverse sections were cut, stained, and examined then photographed on a Hitachi 7000 electron microscope.

Regrowth

Cells in quiescence were removed from the flasks using trypsin / EDTA, and were plated at a 1:4 subculture ratio into 25cm^2 flasks in DM. Once confluent, characterisation was performed on these cells as previously described.

Results

General Culture

The study ran between 1st June 2000 and 28th February 2002. During this period, the urological surgeons in Southampton University Hospitals NHS Trust performed 29 adult nephrectomies.

Once ethical approval had been obtained for identical tissue harvesting from Portsmouth Hospitals NHS Trust, and the necessary procedures put in place, one adult nephrectomy was performed there during the study period.

Twenty-three of these 30 kidneys were suitable for culture. Of the remaining seven, three were unsuitable because of lack of cortical tissue, three had been (mistakenly) placed in formalin prior to leaving theatre, and in one the tumour was too large to allow safe removal of any normal tissue.

Four kidneys arrived after 4pm. Before 1st June 2001, isolated cell preparations were not prepared from these, as the preparation protocol took in excess of four hours. From 1st June 2001, excised renal tissue was kept in medium overnight at 4°C and prepared in the usual way the next day. One kidney was treated in this way.

The 20 patients whose kidneys were prepared for cell culture were equally split male to female, and had a median age of 68.5 years (mean 65.85, standard error of mean 2.84, range 44 to 84 years). All 20 kidneys were removed for presumed malignancy, and this was confirmed macroscopically at dissection, although no histological diagnoses were subsequently sought, as the samples were anonymous as per ethical advice. Likewise no information was recorded of the patients' co-morbidity, previous medical history or current/past medication.

Culture success

Of the 20 samples cultured, two were lost before investigation / subculture due to infection. The first seven of the remainder were subcultured and the other methods

were investigated and perfected on them, including early experiments with the quiescence medium. The results described below are based on the subsequent 11 patient samples.

BrdU incorporation in "quiescing" media

Figure 8 shows the immunofluorescent micrographs of BrdU uptake in passage 1 cultured cells in the quiescent media under investigation. The less the bright green signal seen in the micrographs, the less the BrdU uptake, and therefore the fewer proliferating cells present in each sample. The sample with the least uptake is of the cells in the DMSO-containing medium formulated for the maximal differentiation of a human transformed renal tubular cell line [1], medium consisting of EGF, PTH, USG and DMSO. This is the medium that was used for the subsequent quiescent study.

Figure 9 and Figure 10 shows the cell counts performed on the flasks and the supernatant medium decanted off 25cm^2 flasks of cells initially plated at the same density, grown in serially changing medium as described, and finally in defined medium until confluence at day 11. At day 11 and at each subsequent weekly medium change the supernatant medium was examined for shed cells by Trypan blue exclusion with the haemocytometer (Protocol 1). The cells in one flask were removed by trypsinisation and counted at confluence on day 11. The medium in the remaining flasks was changed in two flasks to quiescent medium with DMSO (QM) and in the other two to quiescent medium without DMSO (QM[–D]). On day 35 after the third medium change, the adherent cells in the four flasks were counted in the same way (Figure 9).

Quiescence success

Quiescence with the final medium formulation was performed on 11 patient samples. All 11 remained quiesced (defined as maintaining their characteristic cobblestone light microscopic appearance without cellular overgrowth) for at least 4 weeks (5 weeks total culture time); three for more than 40 days including one which was still viable at 150 days, at which point the cells were still able to be regrown from culture (see Regrowth below).

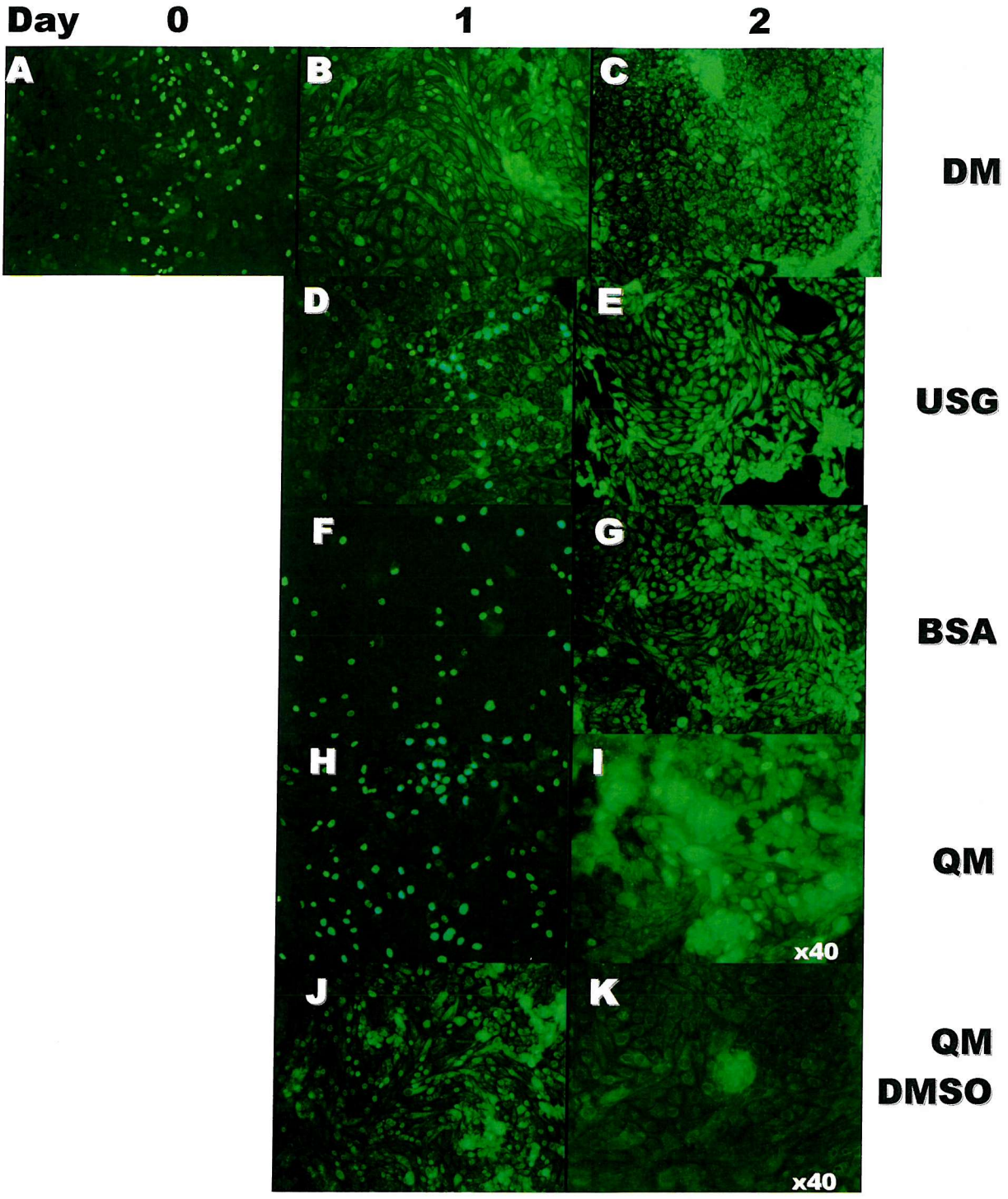

Figure 8. BrdU accumulation immunofluorescent micrographs in different quiescent media: A, B & C – DM; D & E – USG (2%); F & G – BSA (0.5%); H & I – QM[-D] (QM without DMSO); J & K – QM; **at three time points:** day 0 – A; day 1 – B, D, F, H & J; day 2 – C, E, G, I & K. Magnification all × 20, except I & K × 40. **pto…**

The uptake of BrdU is denoted by brightest green nuclear staining. There is non-specific background green staining in the majority of the day 2 photomicrographs. However, the greatest nuclear day 2 staining is in the DM and BSA samples, followed by USG, then QM, then QM-DMSO. This implies that the maximum proliferation occurs in cells in DM and BSA media. The minimum proliferation occurs in cells in QM with DMSO.

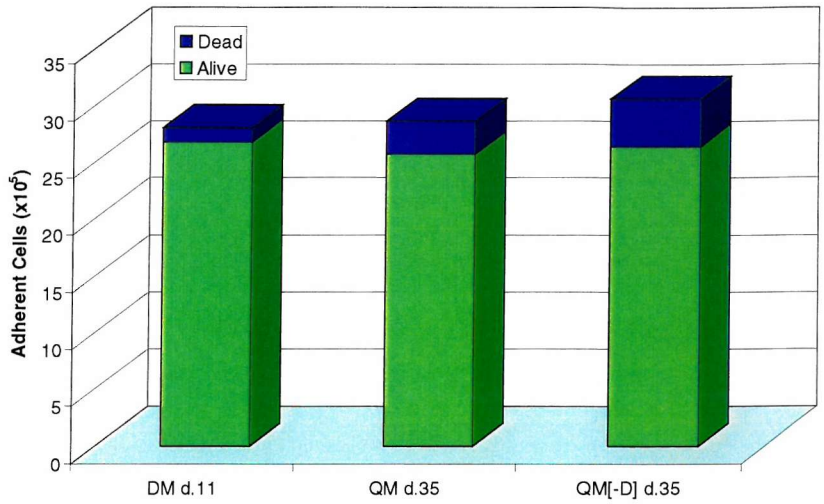

Figure 9. Viability counts of cells remaining adherent to the culture surface: effect of quiescent medium and DMSO (n=2). Results shown for cells in DM at confluence at day 11 (DM) and at day 35 in DMSO-containing (QM) and DMSO-free (QM[–D]) quiescent medium. **Green** = viable cells as determined by trypan blue exclusion, **Blue** = dead cells by same technique; mean of two counts on same cells by haemacytometer. By day 35, the number of cells on the flask surface is lower in QM than QM[–D], and the viable proportion is greater. Thus QM with DMSO appears to be having a greater growth-inhibitory effect on the cells than the DMSO-free QM, while increasing the viability of the cells (proportions viable: DM = 95.7%, QM = 89.9%, QM[-D] = 86.2%).

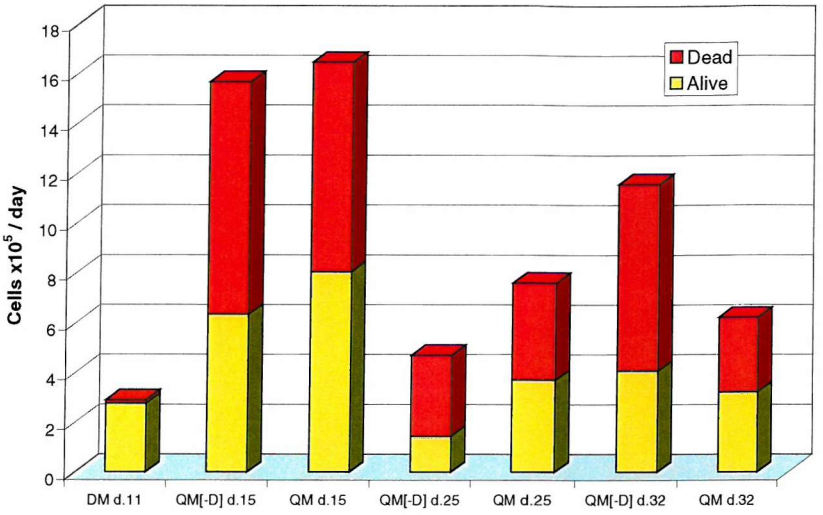

Figure 10. Viability counts of cells removed in supernatant medium (corrected to daily means). Red = non-viable cells, **Yellow** = live cells. Cell count performed on decanted medium, without detaching cells from culture surface (standard medium refreshment = decant off medium and replenish with fresh medium). As medium refreshment is performed thrice weekly, the cell counts may vary according to the interval between medium exchanges. Results therefore corrected to number of days since previous medium change, expressed as mean number per day (daily mean). Results given for cells in DM at confluence at day 11 (DM) and at medium change at days 15, 25 and 32 in DMSO-containing (QM) and DMSO-free (QM[–D]) quiescent medium. By day 32, the total number of cells in the supernatant medium is reduced. Comparing the DMSO-containing medium with the DMSO-free QM, the total number, and the proportion of dead cells in the medium is reduced in the DMSO QM. Therefore, although live cells are still shed into the medium, QM with DMSO appears to be having a greater growth-inhibitory effect on the cells than the DMSO-free QM.

Cells subcultured to permeable cell culture membranes were able to be quiesced successfully (n=6). In two samples, the second passage cells became infected. From one of these infected samples cells were able to be subcultured from quiescence following the reintroduction of growth medium (DM) and re-quiesced for a further 3 weeks before investigation.

Characterisation

Phase-contrast light microscopy

At confluence, in DM, phase contrast microscopy showed the characteristic cobblestone appearance of transport epithelium (Figure 11A) [41]. The cells quiesced in QM (Figure 11B), and those passaged from quiescence (Figure 11C) also showed this normal appearance.

However, some cell margins became less distinct and membrane crenation was noted in places. Despite this, domes (out of focus area in Figure 11B: cells lifted from the impermeable plastic culture surface by vectorial fluid shift [77;78;87]) persisted at least six weeks into quiescence (and have still been found at 150 days – see Figure 12), indicating the continued impermeability of the cell junctions.

When kept in medium (changed weekly) without subculture for 28 days (passage 1 in uncoated plastic 24-wells), cells in QM maintained their monolayer formation, while those in DM overgrew, and attained a fibroblastic phenotype (Figure 13).

Transmission Electronmicrography

The normal ultrastructure of the quiesced cells was revealed by TEM, with cellular organelles and intercellular tight junctions [36;50;55]. The brush border was present, but reduced in height from normal, and the cells were polarised within the monolayers (Figure 14).

Immunostaining

Immunohistochemistry and flow cytometry demonstrated the expression of cell surface epitopes in DM at confluence (Figure 15, Figure 17), and their continued expression in QM (Figure 16, Figure 18). The degree of expression per cell and the number of cells expressing T43, ALP and MHC-I was slightly lower in quiescence for all epitopes but EMA, the expression of which reduced to a greater extent over time. The expression of ZO-1 also persisted on immunohistochemistry (Figure 19).

Cell Viability

The viability of the cells in QM remained remarkably constant. When measured by trypan blue exclusion with a Neubauer haemocytometer (Protocol 1), at confluence in DM, 89.8 ± 3.7% (11 experiments) of the cells were viable. After quiescence for 35 to 70 days, the viable proportion remained very similar at 88.9 ± 3.7% (15 experiments, 8 patient samples).

Cell Cycle

The results from the cell cycle flow cytometry are shown graphically in Figure 20. There were significantly fewer proliferating cells (cells in S- and G_2/M-phase) in QM than in DM.

Enzyme activity

The activities of the brush border enzymes ALP and GGT are shown in Table 6. Both activities vary significantly between subjects, particularly in the quiescent cells, but generally activity in quiescence is the same if not increased when compared to that in DM.

Table 6. Brush-border enzyme activities[a]

	Alkaline Phosphatase	Gamma-Glutamyltransferase
Isolated Cells[b]	194.0 ± 19.8 [2][c]	245.0 ± 4.2 [2]
Confluent Cells in DM[d]	5.5 ± 6.2 [5]	34.4 ± 18.7 [5]
Cells in QM[e]	44.0 ± 47.4 [5]	180.8 ± 280.1 [4]

[a] arithmetic means ± 1 standard deviation in $nmol \cdot min^{-1} \cdot mg\ protein^{-1}$

[b] day zero

[c] number of experiments (from 3 patient samples) in parentheses

[d] days 7-10

[e] greater than day 24

Regrowth

The cells could be regrown to confluence from quiescence of at least six weeks (n=6). Cells in G_0/G_1-phase reduced and the proportions in S-phase and G_2/M-phase increased (see Figure 22). Even cells kept in QM for up to 150 days (n=1) have been treated successfully in this way (Figure 21). Characterisation of the regrown cells by light microscopy is shown in Figure 11C and Figure 21. Characterisation by immunofluorescence and flow cytometry showed continued epitope expression (see Figure 23).

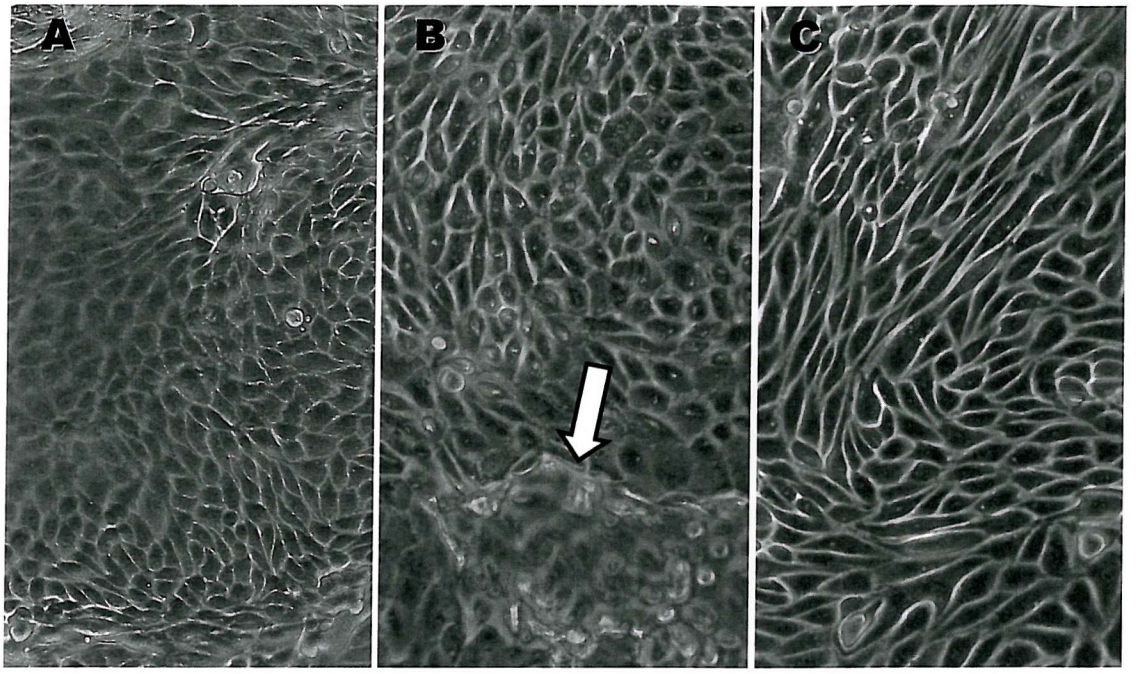

Figure 11. Light microscopic characterisation of cell monolayers. Phase contrast micrographs **(A)** in defined medium, **(B)** in quiescence after six weeks and **(C)** after regrowth from at least six weeks of quiescence. The normal character of the cell monolayer is seen. A dome is seen in (B) (arrow): evidence that the cells are performing vectorial fluid shift and their intercellular junctions are intact (Magn × 10)

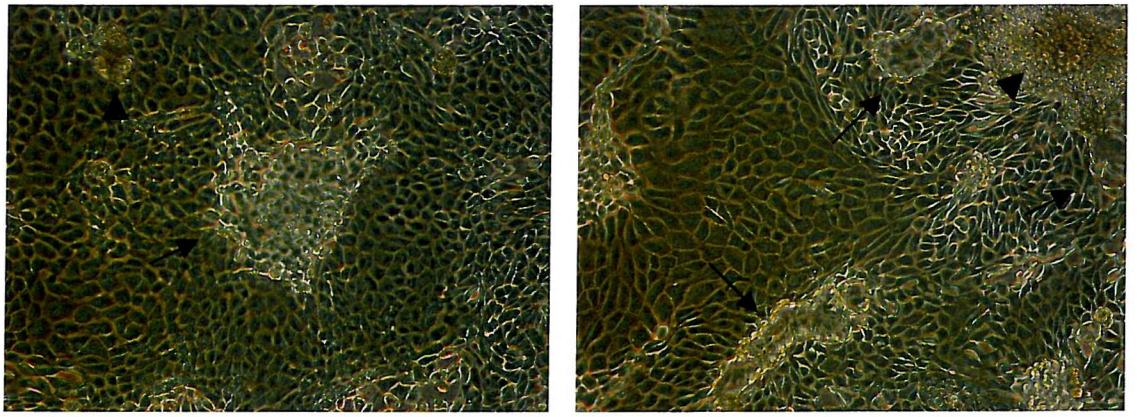

Figure 12. Phase-contrast light micrographs of cell monolayers at confluence, kept in QM (refreshed weekly) for 150 days. The maintenance of domes (arrows) is clearly seen. Some areas of cellular overgrowth are evident, however (arrowheads). Magnification × 10.

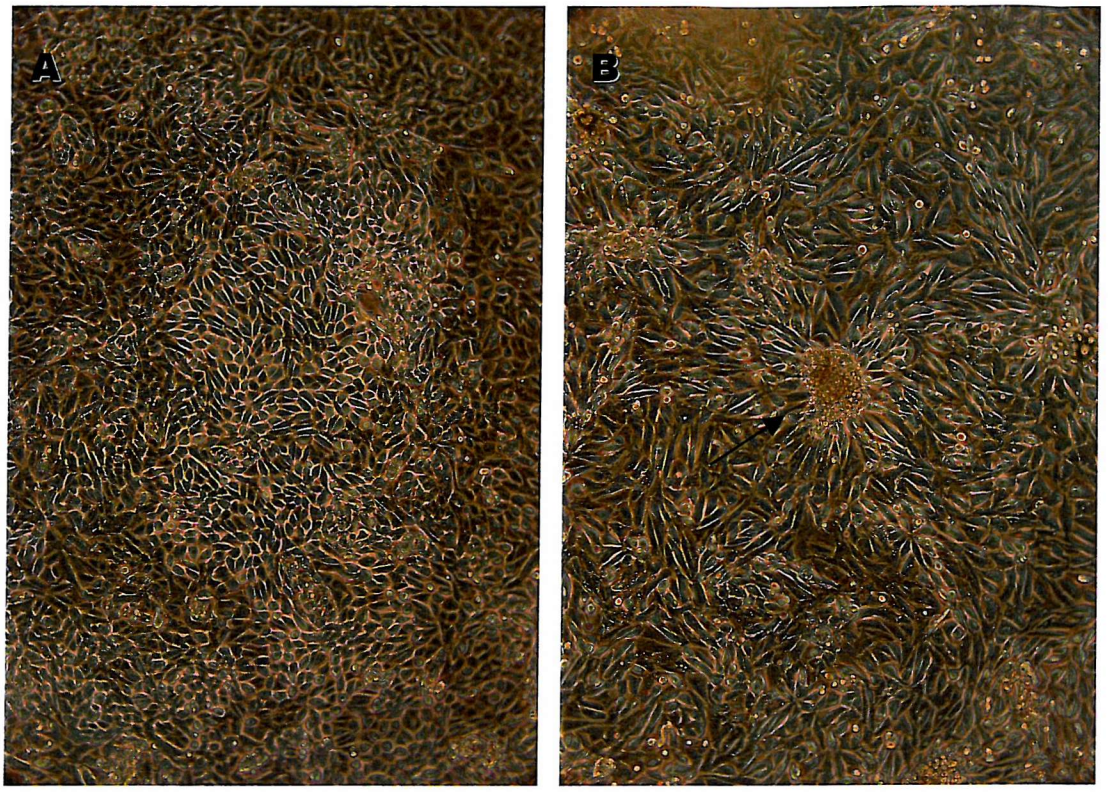

Figure 13. Effect of medium composition on light microscopic character of confluent passage 1 cell monolayers. Phase-contrast light micrographs of passage 1 cell monolayers kept in **(A)** QM and **(B)** DM for 4 weeks. Quiesced cells maintain the epithelial monolayer morphology, while cells in DM elongate and overgrow (arrow). Magnification × 10.

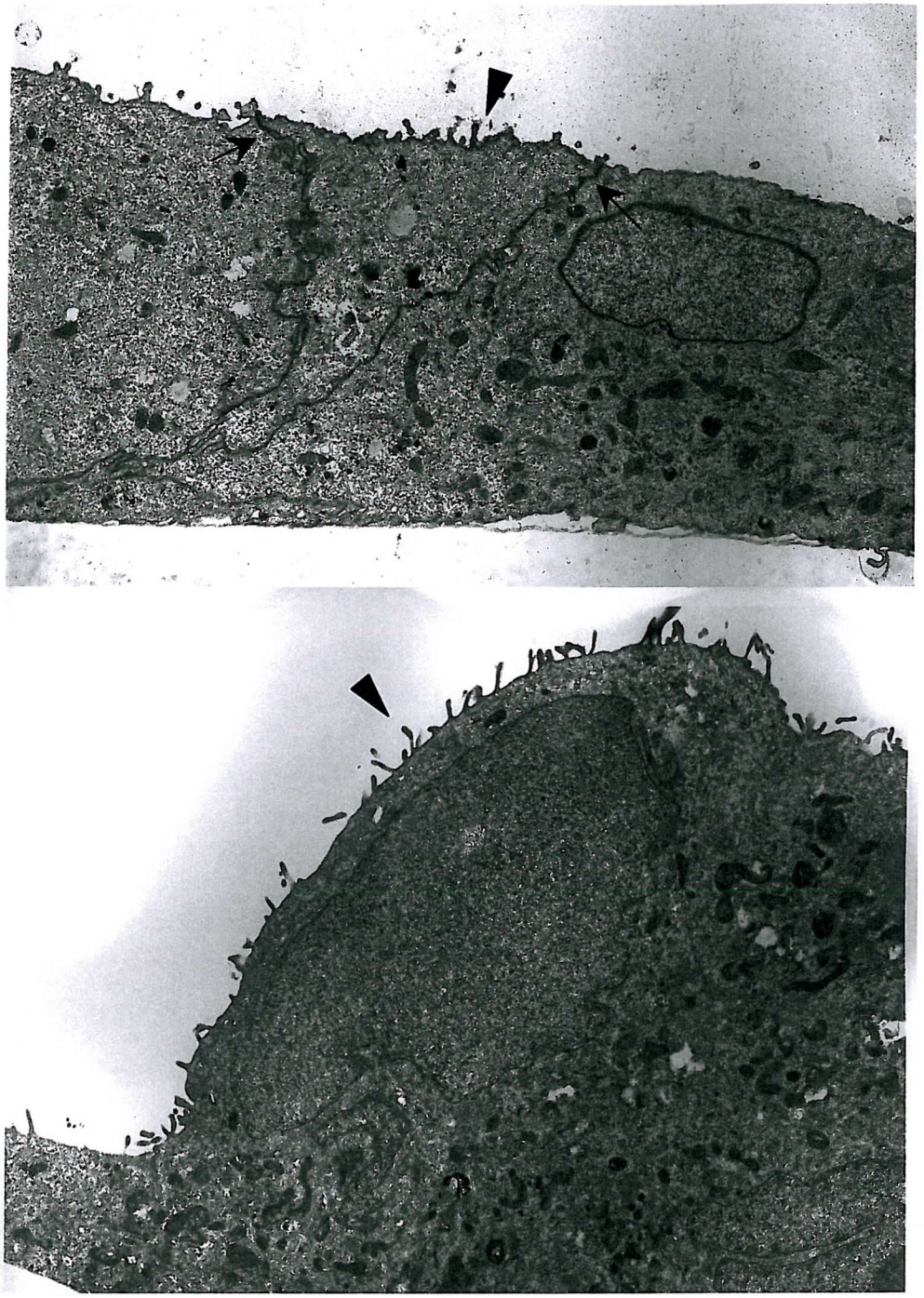

Figure 14. Transmission electron micrographs of confluent cells in quiescence demonstrate monolayer formation (with membrane interdigitations), cellular polarisation (apical brush border, basal mitochondria), intercellular tight junctions (**arrows**), normal cell architecture and cellular organelles (mitochondria, rough endoplasmic reticulum, golgi apparatus and (short) apical microvilli). The brush border is also seen (**arrowheads**), although at reduced height. Magnification × 5000.

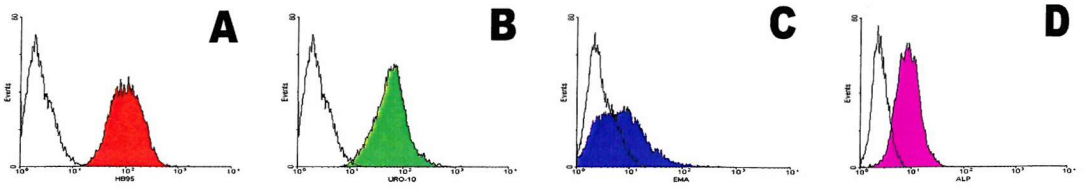

Figure 15. Flow cytometry histograms of characterisation epitopes on cells in confluence in DM. Monoclonal antibodies used: MHC-I **(A)**, T43 **(B)**, EMA **(C)**, and ALP **(D)** (filled peaks; the lines show the respective isotype controls). The strongly positive signals from MHC-I and T43, approximately 50% weakly positive signal from EMA, and 100% slightly stronger signal from ALP are shown.

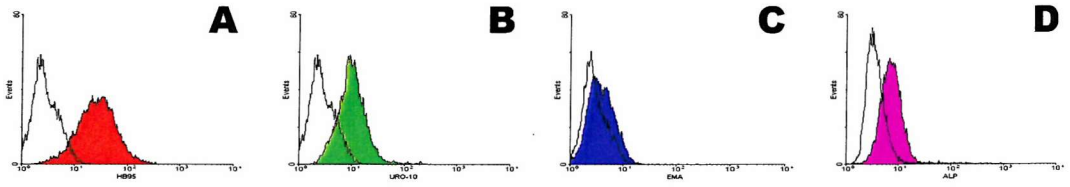

Figure 16. Effect of quiescence for six weeks on characterisation epitopes on confluent cells in 25cm^2 flasks. Flow cytometry histograms of FITC-signal. Monoclonal antibodies used: MHC-I (A), T43 (B), EMA (C), and ALP (D) (filled peaks; the lines show the respective isotype controls). All epitopes show slightly reduced expression, apart from EMA which is significantly lower, consistent with the transdifferentiation of distal cells into a more proximal phenotype.

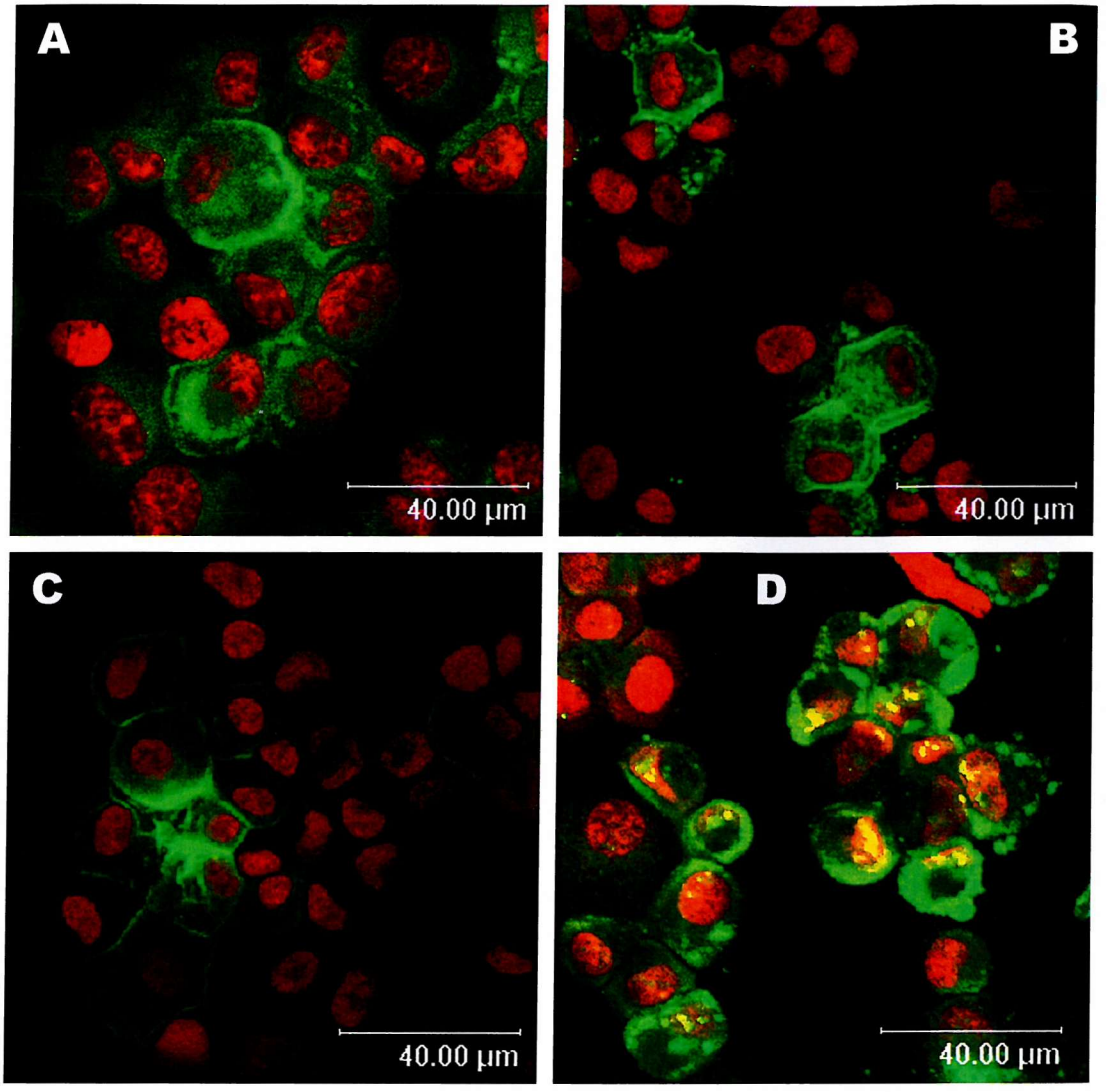

Figure 17. Confocal laser scanning micrographs of indirect immunofluorescence on cytocentrifuge preparations of cells at confluence in 25cm^2 culture flasks in DM. Monoclonal antibodies used: MHC-I **(A)**, T43 **(B)**, EMA **(C)**, and ALP **(D)**. Secondary FITC-conjugated antibody shown by **green** fluorescence. The nuclei are counterstained with PI (**red** fluorescence). (**Yellow** = overlap of red and green signals.) Initial magnification × 40. Bar = 40µm. The membrane localisation of the antigens is clearly seen, although for MHC-I and to some extent ALP there is also some cytoplasmic staining. All cells stain for MHC-I, albeit to varying degrees. The smaller proportion of cells which stain for EMA are likely to be distal tubular cells, and are probably the same cells that do not stain for T43 (double staining could have determined this but was not available).

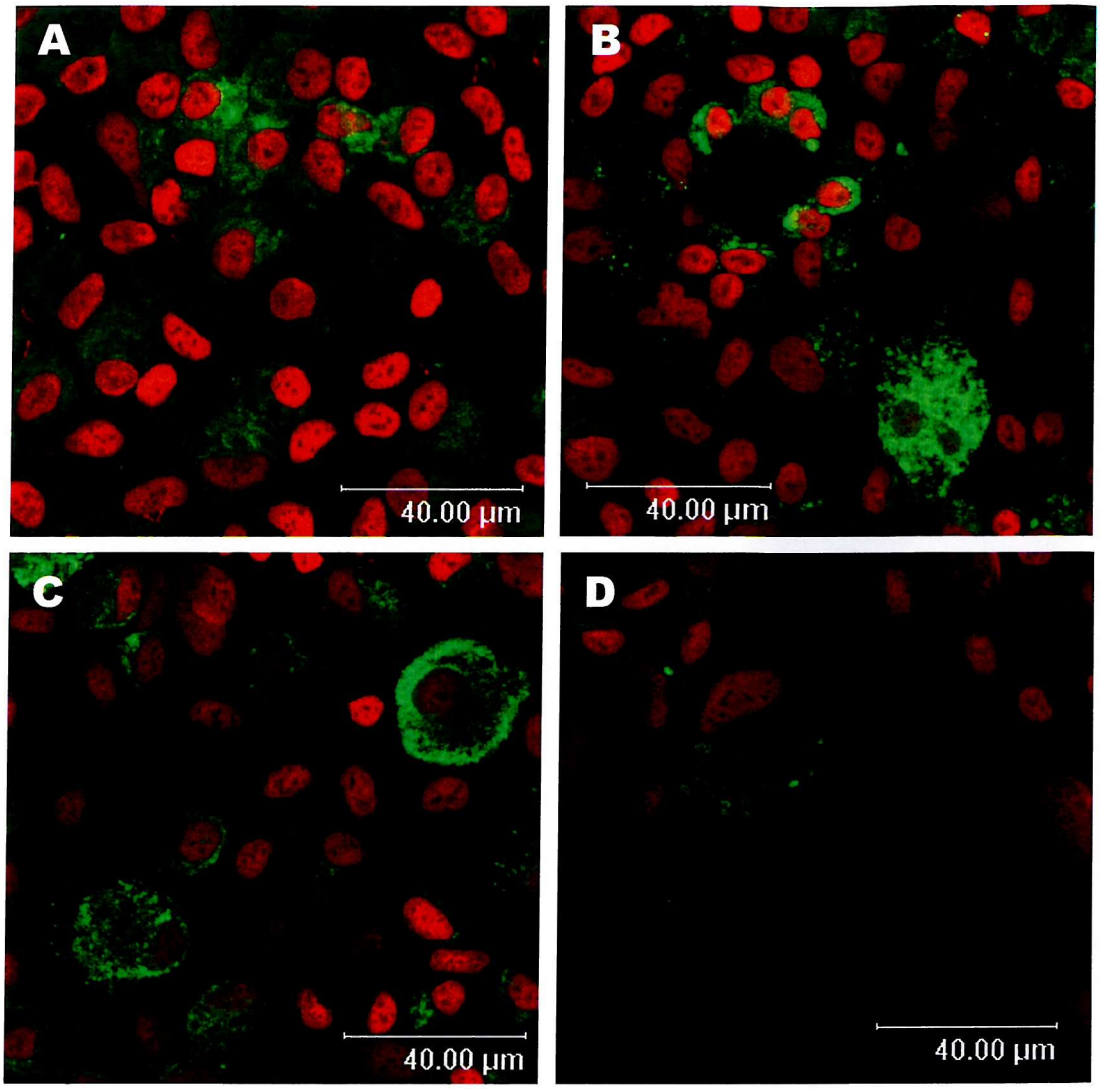

Figure 18. Effect of quiescence for more than 6 weeks on characterisation epitope expression on cytospin preparations of confluent cells in QM from 25cm^2 flasks. Confocal laser scanning photomicrographs of indirect immunofluorescence. Monoclonal antibodies used: MHC-I (**A**), T43 (**B**), EMA (**C**), and ALP (**D**). FITC-conjugated secondary antibody = **green** fluorescence. PI nuclear counterstaining = **red** fluorescence. Initial magnification × 40. Bar = 40µm. The antigen distribution remains on the cell membrane, although slightly reduced and not as distinct as on the cells in defined medium. The proportion of cells staining is reduced also. MHC –I staining remains on all cells, although more cytoplasmic than membranous and less distinct than on the cells in defined medium (Figure 17). The T43 staining is also more cytoplasmic than in defined medium, but more cells are staining. Less cells stain for EMA. Both findings consistent with the selection of and transdifferentiation to the proximal phenotype. The ALP staining is considerably reduced, in keeping with the reduction in the brush border membrane microvilli seen on transmission electron microscopy.

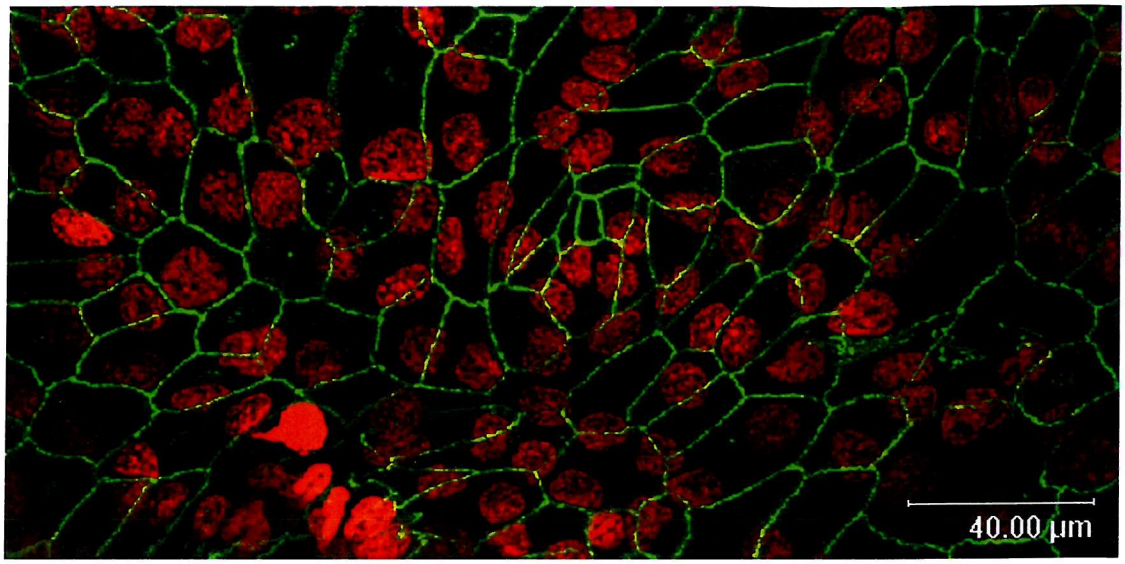

Figure 19. Confocal laser scanning micrograph of indirect immunofluorescence with ZO-1 monoclonal antibody on an intact monolayer of cells in QM for six weeks. **Green** FITC signal: study antibody, **Red** PI counterstain: nuclei. The maintenance of the tight junctional complex is clearly seen (green staining). The overlap of ZO-1 staining with the nuclei is consistent with the intercellular membranes not lying perpendicular to the basal membrane, but the number of nuclei equates to that of cellular outlines, and this micrograph includes the entire depth of the specimen. Initial magnification × 40. Bar = 40µm.

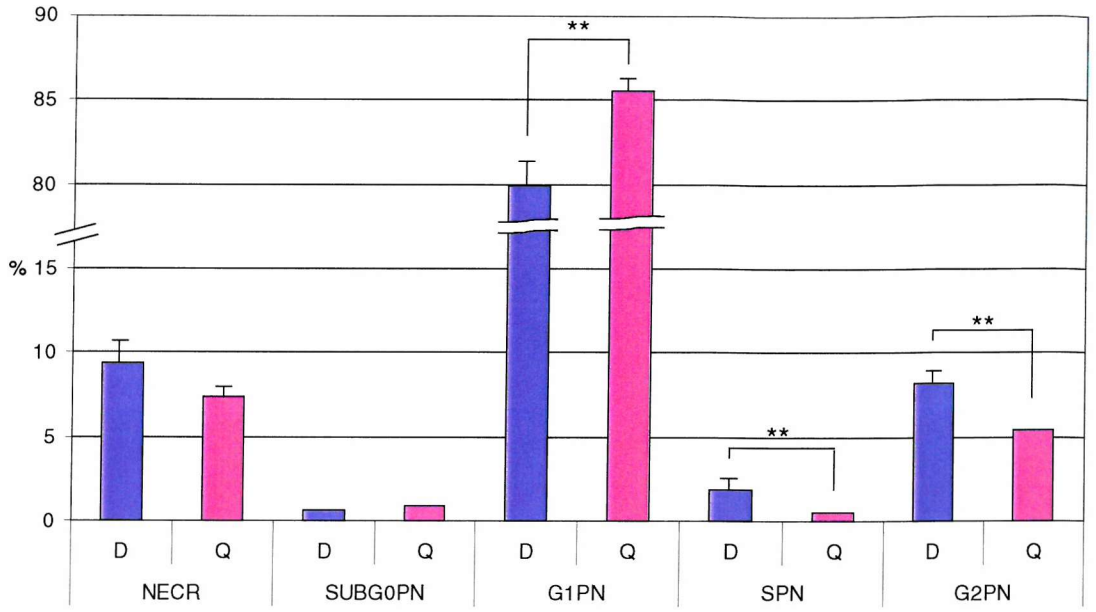

Figure 20. Effect of medium composition on proportions of cells in each cell cycle phase. Bar graph of defined versus quiescent medium. **Pink** bars = quiescent medium, **blue** bars = defined medium. Bars = means (QM, n=28; DM, n=30), error bars = 1 standard error of mean. The decrease of cell proliferation in QM is clearly shown, with significantly greater proportions of cells in G_0/G_1-, and smaller proportions in S- and G_2/M-phases (** = Student's T $p < 0.05$ – G_0/G_1: p=0.003, S: p=0.002, G_2/M: p=0.001).

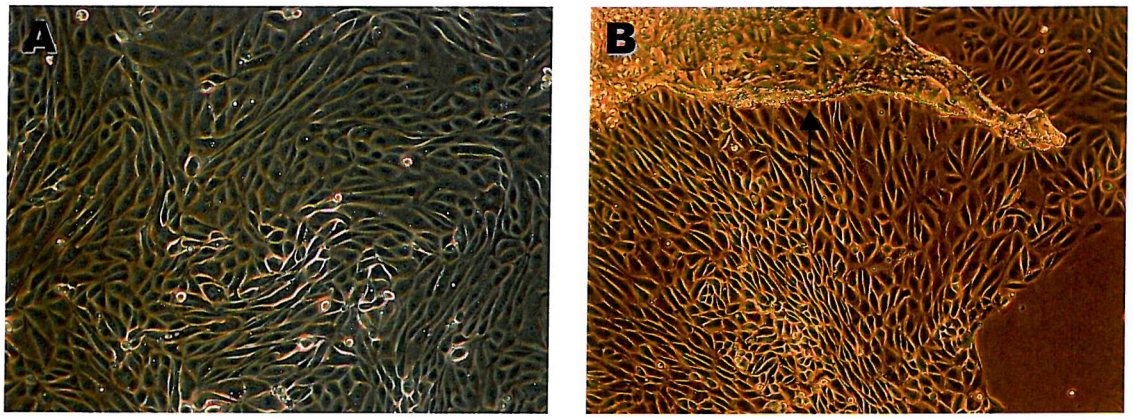

Figure 21. Effect of reintroduction of growth factors and trace elements on cells in quiescence. Phase-contrast light micrograph of cells **(A)** detached from quiescent culture by trypsin after 150 days and allowed to reach confluence in DM, and **(B)** remaining on the same culture surface after quiescence for 29 days then exposed to DM for 1 day. Original (undetached) cells from which remainder have grown are shown by the arrow. Magn. × 10.

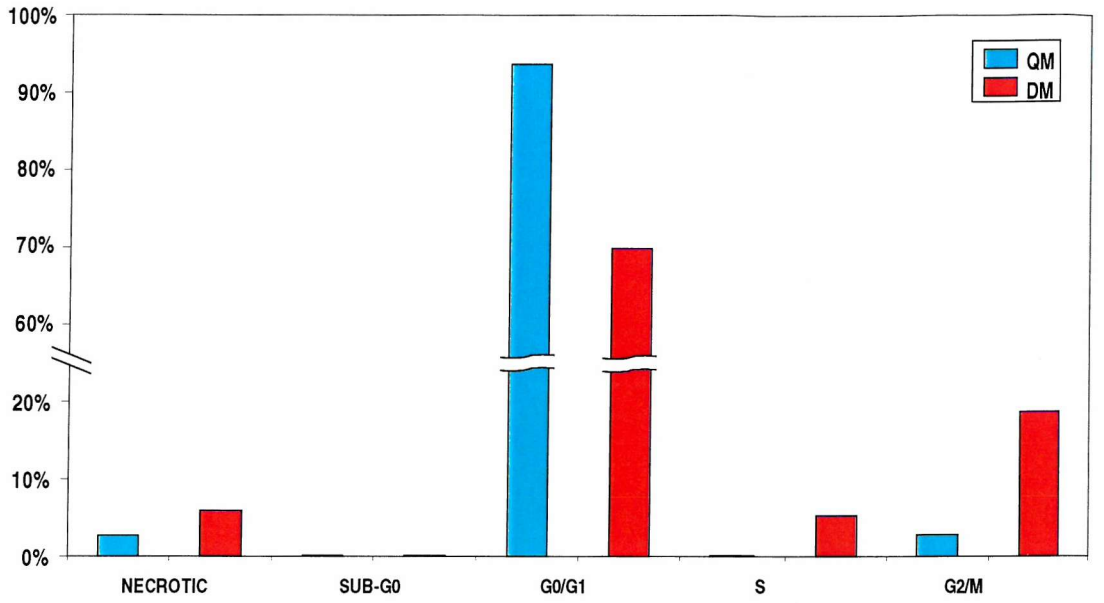

Figure 22. Effect of re-exposure of quiesced cells to growth medium on the proportions of cells in each cell cycle phase. Cells in QM compared to cells trypsinised from quiescence and replated in DM. **Blue** bars = QM, **red** bars = regrown (d.1) in DM (n=1). The ability of cells to proliferate when passaged from QM into DM is clearly shown, with a several-fold increase in the proportions of cells in S and G_2/M phases.

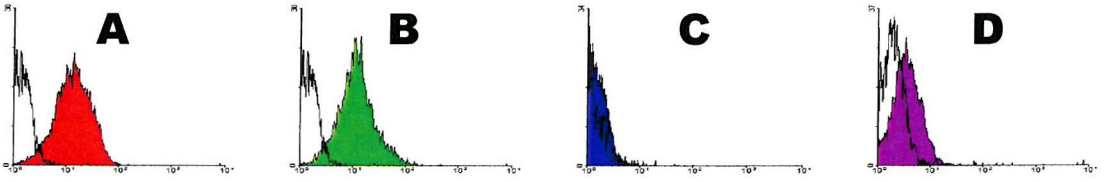

Figure 23. Effect of regrowth from quiescence on characterisation epitopes in confluent cells in 25cm^2 flasks. Flow cytometry histograms of FITC-signal. **(A)** MHC class I, **(B)** URO-10, **(C)** EMA and **(D)** ALP. These cells were kept in quiescent medium for 70 days, then trypsinised from the culture flask and replated into defined medium until confluent (4d). Persistence of MHC-I, URO-10 and ALP is shown. The EMA signal (distal tubular cell marker) is reduced, consistent with the trans-differentiation of distal to proximal cells during the culture period. (The defined medium used for the cell culture selects for and promotes transdifferentiation to proximal tubular cells.)

Discussion

Despite modification of previously described methodologies for the harvest and isolation of primary human renal tubular cells, the morphology and character of cells in DM in this study is very similar to that reported [36;44;49;55]. The significant advance demonstrated here from previous reports is the subsequent quiescence, enabling cells to be maintained in primary passage for at least 5 weeks without the need for subculture.

The characterisation of the cells in QM is consistent with the maintenance of the previously reported *in vitro* phenotype of human renal tubular epithelial cells. There are, however, some differences from those described in the previous studies:

- The crenation of the cell membranes of the quiesced cells, although not described in previous literature, is consistent with the interdigitations described between adjacent tubular cells both *in vivo* and *in vitro* [55]. Certainly, the observation of persisting domes of cells suggests that the intercellular junctions are impermeable to fluid; the ZO-1 expression confirms that the tight junctions between the cells are intact; and the TEM appearance of tight junctions and close cellular invaginations further supports this concept. The failure of previous investigations to maintain cells in hormonally defined medium without subculture for more than 7-10 days may not have allowed this degree of interdigitation to develop.

- The cellular ultrastructure otherwise differs from that seen *in vivo* in the slightly enlarged mitochondria and the rudimentary brush border. Enlargement of mitochondria is described in aminoglycoside exposure [62;88] and these cells have been in streptomycin-containing medium for at least six weeks.

- Although the brush border is less prominent than *in vivo*, similar findings have been previously reported in cells cultured in serum-free hormonally-defined medium [41;55], and to a greater extent in serum-containing medium [50]. The observed decline in ALP activity in culture from that of freshly isolated cells is in accord with that previously reported [49]. However, the persistence into quiescence of the activity found in DM suggests there is no further change in the brush border

conformation from that at confluence, although the sample numbers are small and variations great.

The immunofluorescent and flow cytometric results also support the maintenance of the normal phenotype. The cells express MHC class I and ZO-1 appropriately. Failure to express either would indicate a significant departure from a normal human epithelial phenotype. The proximal tubular phenotype selected for by the DM used in this study [41;49;55] is suggested by the retention of T43 and ALP expression, which are both proximal tubular epitopes, the cells were only in DM for approximately 6 days, and the monolayers examined here are not entirely homogeneous.

As mentioned previously, the defined medium used for initial growth and differentiation of these cultured cells selects for proximal tubular cells. Any distal cells that do grow tend to transdifferentiate to a proximal phenotype during growth, although do not express ALP [53]. Therefore the decrease in EMA expression found was expected.

However, from the flow cytometric data some cells give a positive signal for both T43 and EMA. The most likely explanation for this finding is that the precise localisation of T43 in cultured isolated tubular segments is not known, and some overlap in expression between tubular segments may occur (manufacturer's data sheet suggests so – see Glossary). Another normal activity of these cells is protein uptake and degradation: therefore non-specific uptake of proteins by phagocytosis during culture may also lead to dual staining.

The slight decline in the expressions of all epitopes and in the GGT enzyme activity has been previously described in cultured cells [79] and may be a feature of membrane composition alterations. The growth rates of cells can be altered by a change in the phospholipid composition of their culture medium [89], and their normal membrane phospholipid composition may differ from that of the serum or serum substitute in the growth medium [90].

The ability of the cells to regrow from QM at passage on the reintroduction of growth factors is consistent with their quiescence, rather than senescence, which might otherwise be suspected after six weeks without passage.

The cell cycle data was performed towards the end of the second part of the study, after the majority of the experimental work had been completed. As the cell monolayers were well maintained, the cell counts on the decanted medium were low, and there appeared to be little in the way of overgrowth of cells on the culture surface, it was a surprise to find that there were still 4% of cells in G_2/M-phase in QM. This is an order of magnitude greater than in normal kidneys *in vivo*.

However, proliferation in DM was double this, and resulted in an increased number of necrotic cells as cells were heaped up away from the monolayer. Clearly this is an area for further research, as additional manipulation of the cell culture composition, perhaps to reduce the concentration of the serum substitute or the EGF (hepatocyte growth factor has a more potent effect on differentiation than EGF, so its use may allow lower concentrations and potentially a lower proliferative effect [91]), may further increase the ability of the cells to remain in the G_0 or G_1 phase of the cell cycle.

It could be argued that there was no point in progressing further with this study as the cells were still proliferating so much. Certainly the culture conditions were not perfect, but as can be seen from Figure 13, the overall appearance of the cells in the quiescent medium was much better maintained than in the defined growth medium. This model, although not perfect, would still appear to be better for longer-term investigation of primary human renal tubular cells in culture than any existing *in vitro* model.

Conclusion

These experiments have shown that primary human renal tubular epithelial cells may be kept viable, while retaining normal *in vitro* phenotype for at least six weeks without subculture, and may therefore provide a useful model for the investigation of chronic tubular injury, particularly longer-term pharmacological nephrotoxicity.

Having developed this apparently appropriate model, the next section (but one) describes its use for the assessment of the chronic effects of therapeutic concentrations of CsA on primary human renal tubular epithelial cells in culture.

Chapter 4 Later work on HTECs in quiescence

Summary

Since the completion of my experimental work for this thesis, further investigations have been performed on the cells in the culture described thus far. A number of further characterisation techniques have been employed, involving determination of the cells' cytoskeletal structure, responses to reno-active hormones, transepithelial resistance measurement, transepithelial permeability to known molecular weight molecules and the activity of the Na^+-glucose cotransporter.

The majority of the investigations confirmed the maintenance of a normal phenotype in these cells. Any variations from normal, such as the cytoskeletal appearance reflecting a slight increase in stress fibres and a small reduction in the cAMP response to reno-active hormones, are mild. The majority of the results show little difference between the responses of these cells kept in quiescent medium for more than six weeks and those just at confluence in hormonally and trace-element defined medium.

This work therefore further supports the generally maintained phenotype of cells kept at quiescence as previously described.

Introduction

Since the completion of my experimental work for this thesis, further investigations into the characterisation of the quiesced cells have been ongoing in the same laboratory. I have not personally carried out the experimental work, but have taken an active part in the conception and design of these experiments and the collation of the results. Although this work cannot therefore form a part of my thesis results, it does further support the maintenance of an appropriate phenotype.

Other investigators have characterised primary and transformed HTECs [36;49] by skeletal structure [92;93], by responses to reno-active hormones [94], by measurement of transepithelial resistance [95;96], through their ability to allow or impair the transepithelial passage of known molecular weight substances [97;98] and by the activity of other metabolic processes such as the Na^+-glucose cotransporter [99;100].

The cytoskeleton of HTECs is formed by actin microfilaments. Disruption of this skeleton is common in cytotoxicity [92], and may represent the transdifferentiation of HTECs to myofibroblasts, one of the precursors to renal tubulointerstitial fibrosis. The actin filaments can be visualised microscopically by staining with fluorochrome-conjugated phalloidin [93].

In response to the reno-active hormones parathyroid hormone (PTH), calcitonin (CT) and arginine vasopressin (AVP), adenylate cyclase activity is increased in both proximal and distal HTECs, forming cyclical adenosine monophosphate (cAMP) [36;49;94]. Proximal tubular epithelial cells have a greater response to PTH than to CT or AVP, whereas distal cells have the opposite response.

Epithelial cells are further characterised by their ability to form intercellular tight junctions. The tightness of these junctions can be determined by the TER. TER is measured by electrodes in the medium either side of a confluent cell monolayer: the greater the TER the tighter the junctions between the cells (i.e. the lower the passage of ions across the cell monolayer) [101]. The tightness of the junctions can also be estimated by the ability of the monolayer to prevent or permit the passage of

molecules of known molecular weight from apical to basal medium or *vice versa* [102;103].

The Na^+-glucose cotransporter is a normal and essential component of the basal membrane of epithelial cells, particularly in the proximal renal tubular cell [50;104-106]. Finding normal activity (ability to transport glucose only in the presence of Na^+ and inhibition by the specific inhibitor phlorizin) of this vital transporter protein would further support the normal character of these cells.

General Methods

Cortical cell suspensions were prepared from macroscopically normal, ethically obtained nephrectomy tissue, as previously described.

Freshly prepared cells were grown on 25 cm^2 uncoated plastic culture flasks in 6ml of 1:1 DMEM: Ham's-F12 medium with 2 mM glutamine (basal medium) and UltroSerG (USG - synthetic serum substitute). The medium was removed and refreshed as below (Summary: Table 7):

- Day 1-3: small (~10-cell) colonies. Hormonal and trace element supplements introduced.

- Day 3-5: ~50% flask cover. Medium changed to fully "defined" HTEC growth medium [55].

- Day 7-10: confluence.

At confluence cells were passaged into (i) 6-well PET-membrane culture inserts for immunofluorescence, or (ii) 96-well plate for hormone responses. The same media changes were performed as above.

At confluence in passage 1, half the colonies were processed as below. For the remainder the medium was changed to "quiescent" medium, previously found to promote the greatest differentiation of virally transformed HTECs [1] (see Table 7).

Cells were maintained for six weeks, with media changes every 3 days.

Table 7. Medium composition: basal medium, antibiotics, hormones and trace elements

Day	Basal medium	Antibiotics	USG (%v/v)	EGF (ng/ml)	HC (ng/ml)	Insulin (ng/ml)	PGE1 (ng/ml)	PTH (ng/ml)	S & Tf (/ml)	T3 (pg/ml)	M name
0	✓	100/ml	2	-	-	-	-	-	-	-	
1-3	✓	50/ml	1	5	18	2.5	5	-	2.5	2.5	
3-5	✓	50/ml	-	10	36	5	10	-	5	5	DM
7-10	✓	50/ml	0.2	25	-	-	-	0.5	-	-	QM

Antibiotics=penicillin (IU) and streptomycin (mg), DM=defined medium, EGF=epithelial growth factor, HC=hydrocortisone, M=Medium, PGE1=prostaglandin-E_1, PTH=parathyroid hormone, QM=quiescence medium, S & Tf=selenium (ng) and apo-transferrin (mg), T3=tri-iodothyronine

Method for cytoskeletal appearance

1. Culture cells to confluence on Falcon inserts (six wells).
2. Wash ×2 in RPMI media and remove membrane from the cup using a disposable scalpel (hold the scalpel steady and rotate the cup to obtain the best separation).
3. Cut each membrane into quarters and place on an APES slide. Allow to air-dry overnight.
4. Fix cells in 2% paraformaldehyde (freshly prepared) for 5 mins.
5. Wash in PBS ×2 for 3mins each.
6. Quench excess aldehyde with 0.1M glycine in PBS for 5mins.
7. Permeabilise the cells with 0.1% Triton X-100 for 1min.
8. Incubate with 10^{-6}M rhodamine-conjugated phalloidin for 20 mins.
9. Rinse 3× in PBS 5min/wash.
10. Counterstain with 7AAD at 1:250 for 10mins.
11. Rinse 3× in PBS 5min/wash.
12. Mount in antifade.
13. Confocal microscopy performed using a Leica TCS SP2 laser scanning microscope.

Method for hormonally stimulated adenylate cyclase activity

1. Passage zero (P^0) cells seeded to 96-well plate, cells grown to confluence under our standard culture conditions.
2. Media removed and cells washed twice with RPMI media.
3. Media replaced with 200µl culture media (DM or QM) containing 0.1 mM IBMX and incubated for 20mins at 37°C in a shaking incubator.
4. Thereafter cells incubated in 200µl media containing a, b, c, d for 5 mins as follows:
   a) media alone
   b) 10^{-7}M PTH
   c) 100ng/ml calcitonin
   d) 10^{-6}M AVP
5. Terminate the reaction by adding 125µl ice-cold acid alcohol (absolute ethanol + 1% HCl) to cells.
6. Samples dried overnight at 80°C and stored at –20°C for cAMP estimation.
7. 'Total' (intracellular and cell supernatant) cAMP was determined using the Amersham Pharmacia Biotech Biotrak cAMP enzyme immunoassay (EIA) system. (code RPN 225)

Method for transepithelial resistance

1. Cells for measurement are grown in 6-well culture inserts (permeable membranes)
2. Medium is changed to DM at least 15min prior to measurement
3. 2ml DM at 37°C are placed in the Endohm
4. Blank (no cells) or cell-containing inserts containing 1ml fresh DM are placed into the Endohm cup
5. Inserts are left in the Endohm for 15min to allow equilibration across the monolayer
6. TER is calculated from the raw measurements using the formula: TER = (monolayer measurement – insert measurement) x membrane area (The area of the monolayers was 4.2cm^2)

Method for dextrans

Reagents

4kD dextran

70kD dextran: dissolve 50mg/ml in 10mM HEPES pH 7.4 – 145mM NaCl and dialyse against the same buffer (in the dark, at least twice)

Method

1. Cells cultured to confluence (1 week) in six well culture inserts
2. 1hr before experiment used tissue medium replaced with appropriate new medium, 2ml added to basolateral side (well) and 1ml to apical side (insert) – see Figure 4
3. Start experiment by adding 80µl concentrated Dextran solution to final concentration of 2mg/ml (concentration determined to remain on linear range of standard curve – Figure 28)
4. Incubate for 4hr at 37°C in 5% CO_2
5. Collect 200µl medium from insert and well
6. Construct standard curve for appropriate dextran: 2, 1, 0.5, 0.25, 0.125, 0.0625 and 0.0313mg/ml respectively
7. Transfer 200µl standard solutions and test solutions into blank 96-well plates
8. Determine fluorescence using Bio-Tek FL600 fluorescent plate reader, using FITC filters – excitation 490nm, emission 520nm, and concentration by spline analysis

Method for glucose transport

Reagents

1. Basic Transport Buffer: 187mg KCl, 98mg $MgSO_4$, 99mg $CaCl_2$, 5ml HEPES, made up to 500ml using polished water
2. Sodium Containing Buffer (Na): 250ml basic transport buffer, 2.046g NaCl, pH adjusted to 7.4 using 1M KOH
3. Sodium Deplete Buffer (No Na): 100ml basic transport buffer, 1.9g choline chloride, adjusted to 7.4 using 1M KOH

4. Sodium Phlorizin Buffer (Na Ph): 250ml basic transport buffer, 2.046g NaCl, 0.5mM phlorizin, pH adjusted to 7.4 using 1M KOH
5. αMG Transport Buffers (αMG Na/No Na/Na Ph): 12.5µl αMG tracer (1µCi/5µl current batch – final concentration 0.5µCi/ml), 100µl 50mM 'cold' αMG – final concentration 1mM, made up to 10ml with Na/No Na/Na-Phlorizin buffer
6. 'Blank' Transport Buffers (Blank Na/No Na/Na Ph): 100µl 50mM 'cold' αMG – final concentration 1mM, made up to 10ml with Na/No Na/Na-Phlorizin buffer
7. 'Stop' Buffer (Stop): 0.25M 'cold' αMG (0.485g) made up to 10ml with RO water

Method

1. Seed Biocoat inserts with $1x10^4$ passage 0 primary renal tubular epithelial cells
2. Incubate to confluence under standard tissue culture conditions (defined medium measured at 7 days, quiescence at 7 weeks – 6 weeks in quiescent medium)
3. Remove medium and rinse twice using 1ml of glucose-free medium at 37°C
4. Add 400µl of medium as per Table 8
5. Remove medium and replace with 400µl ice cold Stop buffer
6. Wash x2 with 1ml ice cold Stop buffer
7. Solublise cells by adding 400µl 0.2N NaOH, and incubate for 10min at 37°C
8. Take 200µl aliquots for determination of radioactivity and protein concentrations

Table 8. αMG transport medium composition

<table>
<tr><th>Buffer</th><th>Volume</th><th>Remove?</th><th>Wash?</th><th>Incubate</th></tr>
<tr><td>Blank Na</td><td rowspan="6">400µl</td><td rowspan="3">Immediately</td><td rowspan="3">x2 with Stop at 4°C</td><td rowspan="6">30mins at 37°C in 5% CO_2</td></tr>
<tr><td>Blank No Na</td></tr>
<tr><td>Blank Na Ph</td></tr>
<tr><td>αMG Na</td><td rowspan="3">No</td><td rowspan="3">No</td></tr>
<tr><td>αMG No Na</td></tr>
<tr><td>αMG Na Ph</td></tr>
</table>

9. Count aliquots + 1ml scintillation fluid (Cobra Series Canberra Packard Liquid Scintillation Counting System)
10. Count 200µl of original isotopic solution for total counts
11. Measure protein concentration using Bradford reagent (Protocol 4)
12. Express results as counts per mg protein
13. Dispose of radioactive waste into designated sink and record in radioactive log

Results

Representative photomicrographs are shown in Figure 24 and Figure 25. Figure 24 shows the appearance of a confluent monolayer in defined medium at 7 days, Figure 25 that of a confluent cell monolayer after 6 weeks in quiescent medium. A slight increase in cytoskeletal stress fibres is seen in the quiesced cells, suggesting an early change to a more myofibroblastic phenotype.

Figure 26 shows the cellular cAMP synthesis in response to renal-active hormone exposure. The persistence in quiescence of the response to these hormones and the retention of a generally proximal phenotype (greater response to PTH than AVP or CT) is shown.

In Figure 27 are the TER results for confluent monolayers in defined medium at 7-10 days and in quiescent medium after a further 6 weeks. These show retention in quiescence of transepithelial resistance, a marker of intercellular adhesion.

Figure 28 and Figure 29 show the results of the experiments on the permeability of confluent monolayers to dextrans. The persistence in quiescence of permeability to 4kD dextrans, and retained lack of permeability to 70kD dextrans is shown.

Figure 30 and Figure 31 show the results of the glucose transport experiments. The activity at 30 mins (within the period of transport rate linearity – see Figure 31) of the Na^+-glucose co-transporter is 90% inhibited by Na^+-depletion and 94% inhibited by phlorizin (similar to published evidence). The activity of this vital basal-membrane enzyme is reduced by approximately 40% in quiescence, although only two subjects were examined.

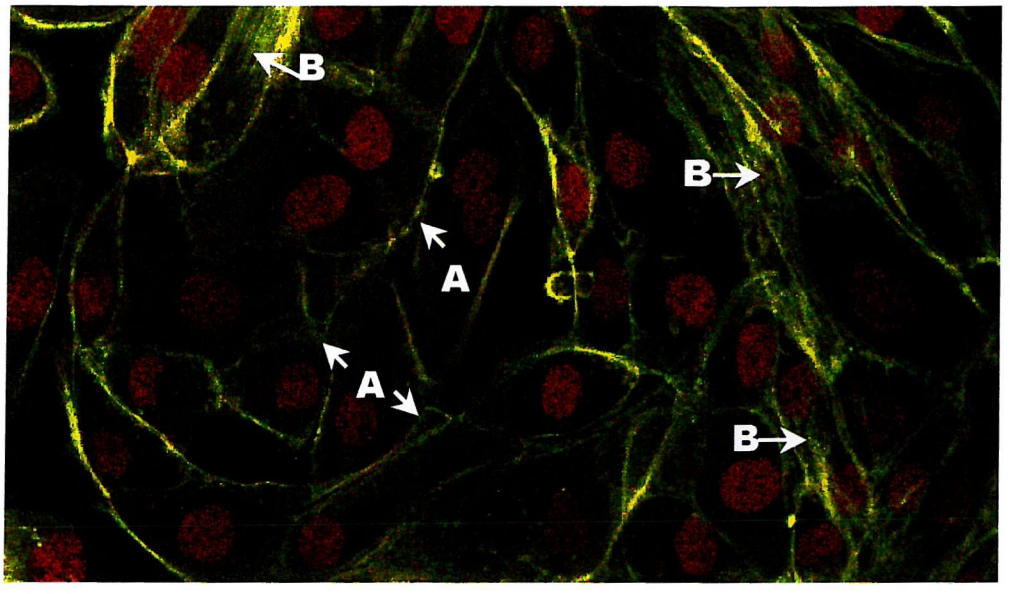

Figure 24: Laser confocal micrographic appearance of cytoskeleton of cells in defined medium at confluence. Rhodamine-phalloidin staining. A mostly normal cytoskeleton is shown, with pericellular peripheral F-actin skeleton (**A**) and minimal cytoplasmic transcellular fibres (**B**). (**Green** = F-actin, **Red** = nuclear counterstain with 7AAD. Original magnification ×40)

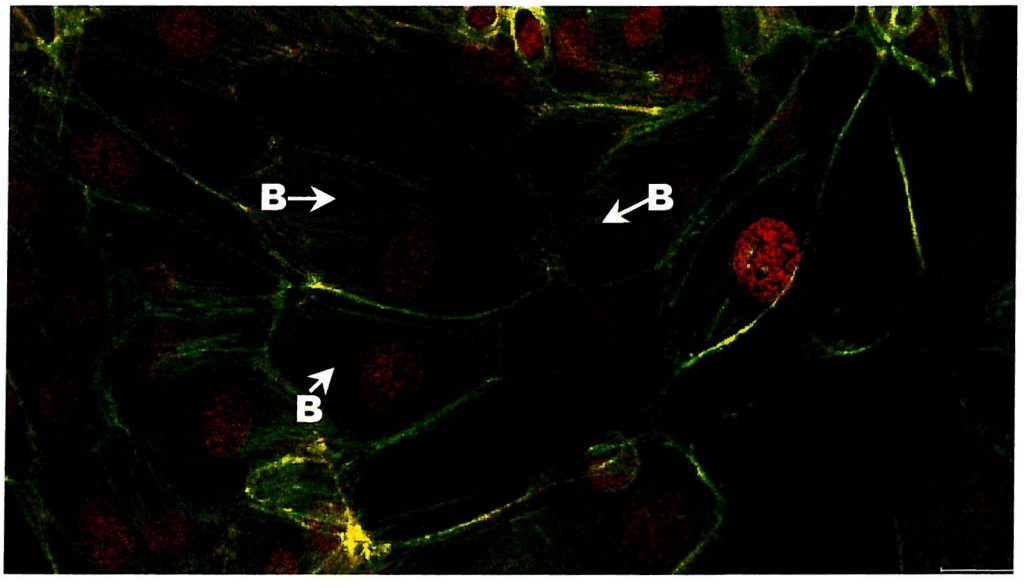

Figure 25: Laser confocal micrographic appearance of cytoskeleton of cells in quiescence medium after 6 weeks. Rhodamine-phalloidin staining. The pericellular F-actin skeleton is maintained, although there are more cytoplasmic stress fibres (**B**). (**Green** = F-actin, **Red** = nuclear counterstain with 7AAD. Original magnification ×40)

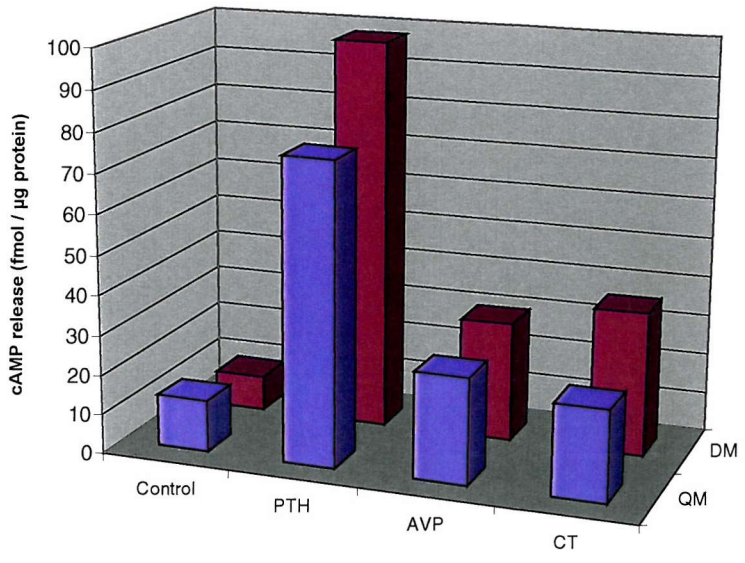

Figure 26. Reno-active hormone-stimulated cAMP release from cells in defined and quiescent medium. DM = cells in defined medium at confluence at 1 week, QM = cells in quiescence medium for 6 weeks (7 weeks in culture). All results n=8 from three subjects. The retained ability to release cAMP in response to PTH, AVP and CT is shown. The greater release of PTH compared to the other two hormones is consistent with the generally proximal phenotype of the cells selected for by the defined medium. Some transdifferentiation of distal to proximal tubular cells also occurs in such culture. The overall cAMP release is slightly but not significantly reduced in quiescence.

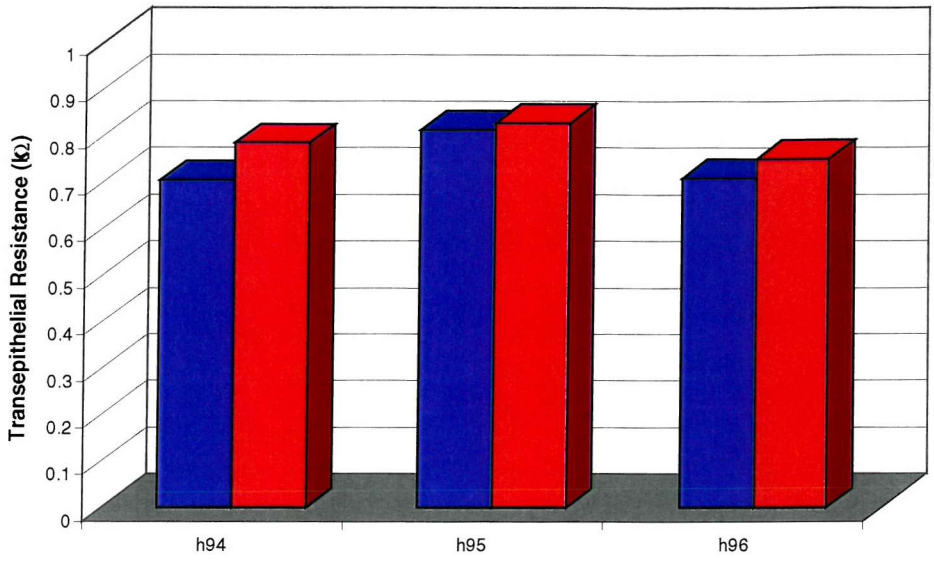

Figure 27. Transepithelial resistance across confluent monolayers of cells in defined and quiescence medium. Blue = cells in defined medium at confluence at 1 week, **Red** = cells in quiescence medium for 6 weeks (7 weeks in culture). All results n=4 from each of three subjects (h94-h96). The retention of TER is clearly seen in all subjects, consistent with the persistence of intercellular tight junctions. The TER is slightly but not significantly increased in quiescence, possible related to a slight increase in the number and decrease in the size of the cells over time.

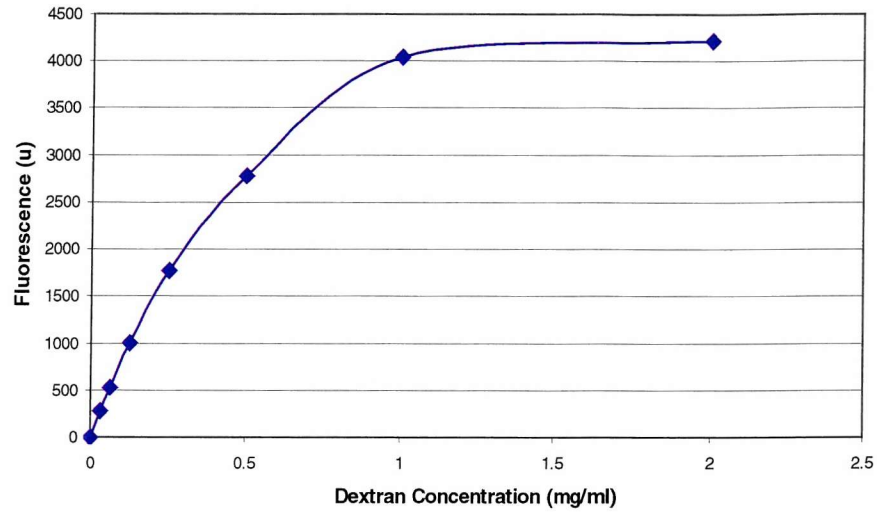

Figure 28. Fluorescence of standard dextran concentrations. Concentrations below 1mg/ml show linear fluorescence vs. concentration.

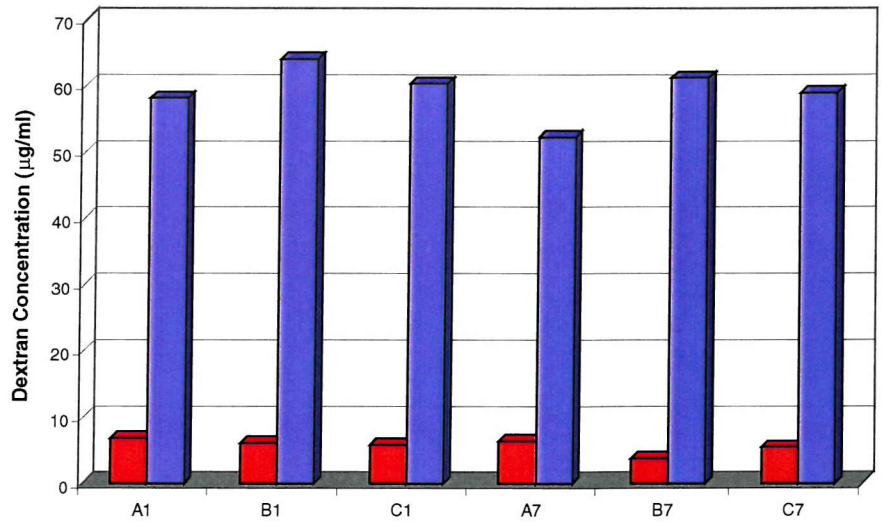

Figure 29. Permeability to dextrans of confluent monolayers of cells after 1 and 7 weeks in culture. Week 1 cells in DM, week 7 cells in QM for 6 weeks. **Bars** = concentration of dextrans (2mg/ml placed in apical chamber of permeable culture wells. Amount shown recovered from the basal chamber after 4 hours – level is inversely proportional to permeability). **Blue** bars = 4kD dextran, **Red** = 70kD. **Titles** = samples A to C, weeks 1 and 7 respectively. The permeability to 4kD, and lack of permeability to 70kD dextrans (normal phenotype), is maintained in quiescence.

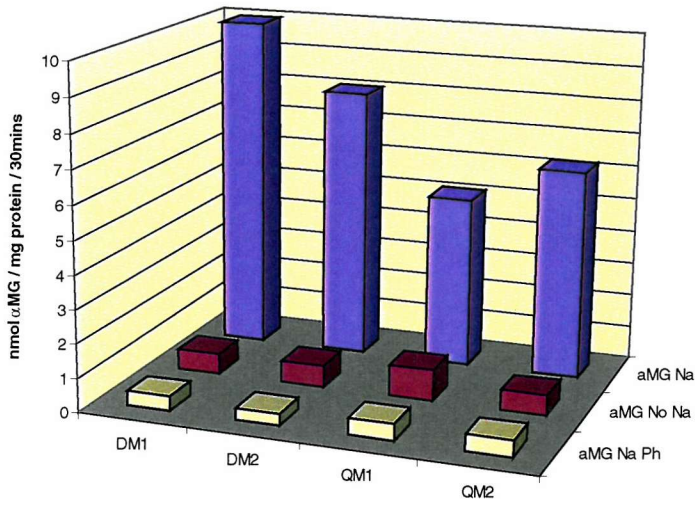

Figure 30. Effect of quiescence on Na^+-dependent αMG uptake. DM = defined medium, cells at confluence at 1 week. QM = quiescence medium, cells at confluence at 7 weeks (6 weeks in quiescence). Results from two subjects shown, n=3. aMG Na = Na^+-containing buffer, aMG No Na = Na^+-deplete buffer, aMG Na Ph = Na^+-containing buffer with phlorizin. The Na^+-dependence of αMG uptake is demonstrated, which is appropriately inhibited by phlorizin. The release in quiescence is slightly reduced.

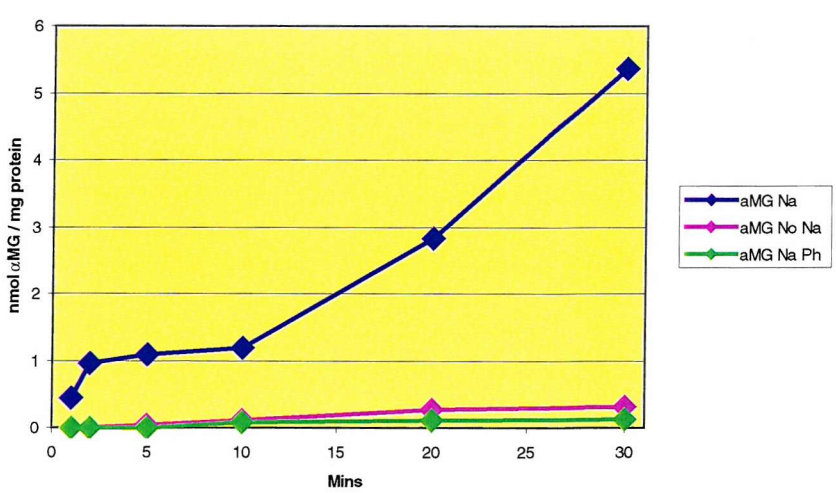

Figure 31. Time courses of αMG release in quiescent culture. Week 7 cells in QM for 6 weeks. The time-dependent release of αMG is shown, which remains Na^+-dependent and appropriately inhibited by phlorizin.

Discussion

Maintenance of cells in quiescent medium allows the maintenance of a near normal cytoskeletal architecture, when compared to cells at confluence in defined medium, with a few more cytoplasmic fibres. HTECs exposed to toxic insults transdifferentiate to a myofibroblastic phenotype, which is shown by a cytoskeletal change to cytoplasmic fibres [92]. These cells have been exposed to aminoglycoside antibiotics for 7 weeks, which may explain the mild change in cytoskeleton.

Cells in quiescence for 6 weeks and those at confluence in defined medium respond to reno-active hormones by releasing cAMP. The greater synthesis of cAMP in response to PTH when compared to that to CT or AVP is consistent with a generally proximal HTEC phenotype [36], as shown previously in this manuscript. The relative reduction in cAMP production in prolonged culture is consistent with the previously reported and observed (in this manuscript) reduction in brush-border membrane structure [36;49].

The maintenance of TER in quiescence is evidence of the retention of intercellular tight junctions, and the confluence of the cellular monolayer. This is further illustrated by the retention of impermeability to 70kD dextrans, while retaining permeability to 4kD dextrans in quiescence.

Activity of the Na^+-glucose co-transporter is demonstrated. This is shown to be Na^+ dependent and appropriately inhibited by phlorizin. The release in quiescence is slightly reduced, which may be related to a reduction in the integrity of the cellular membranes (Na^+-glucose co-transporter is situated across the basal membrane).

Conclusions

Although these results were obtained after I had completed my research, and are therefore not incorporated into general discussion of this thesis, they further confirm that primary HTECs maintained in the quiescent culture described retain an appropriate phenotype.

Such quiescent culture allows the longer-term exposure of cells *in vitro* to known or suspected nephrotoxins without the confounding factors of diet and medication in humans or the different response to toxic insults seen in animals or transformed / tumour cells.

Chapter 5 P-glycoprotein and Cyclosporin A

Summary

Chronic CsA nephrotoxicity is associated with CsA accumulation. CsA is removed from renal tubular epithelial cells by P-glycoprotein (P-gp). P-gp's physiological role is not fully known, but by spanning the apical membrane of a number of epithelia, it is in ideal position to efflux toxic macromolecules by active transport. P-gp efflux activity is increased in multi-drug resistance, where it was first discovered. P-gp acts by transporting bound molecules across cell membranes, through conformational changes involving cysteine-cysteine bonds induced by substrate and inhibitor binding, and ATP hydrolysis. P-gp substrates are diverse in their shapes, sizes and charges. P-gp function can be studied by activity or expression. Activity investigation requires the measurement of the transport of a substrate across a membrane, and the effects on this of other substances. Expression is measured by the detection of the binding of a monoclonal antibody against P-gp to cell membranes. CsA is both a substrate and a modulator of P-gp. CsA increases the expression of P-gp both *in vivo* and *in vitro*. Acutely, CsA inhibits the activity of P-gp. Over time, exposure of P-gp to CsA may increase the activity of drug efflux.

Introduction

Chronic CsA nephrotoxicity *in vivo* is associated with CsA accumulation within tubular epithelial cells. CsA enters renal tubular cells by passive diffusion from the pericapillary lumen, across the endothelium and through the tubular cell basement membrane. It leaves the cell through the apical (brush border) membrane, actively, with saturable kinetics [107]. This efflux pathway has been further characterised as a transmembrane protein called P-glycoprotein (P-gp) [108].

P-glycoprotein

Background

P-gp is encoded in humans by the multi-drug resistance (MDR) type 1 gene, located on chromosome 7 at q21.1 [109]. It belongs to the adenosine-5'-triphosphate (ATP)-binding cassette (ABC) protein superfamily (member B1) and is well conserved through invertebrates, mammals and primates [110-112]. It is situated on the luminal surface of secretory epithelia such as the renal tubules, breast ductules, bile duct canaliculi and small intestine [113-118]. The full physiological role of P-gp is as yet unknown, but its conservation and situation are consistent with the suggestion that it acts as a ubiquitous xenobiotic efflux mechanism, removing from these cells potentially toxic macromolecules, particularly those soluble in lipids [116;119], which would otherwise accumulate within the cellular cytoplasm as there is no other efflux mechanism available for their removal – evidenced by MDR-1 gene knock-out mice [114-120]. P-gp is found in the endothelium at the blood-brain barrier [108;120] and the syncytiotrophoblast on the maternal side of the placenta [121;122], where it is situated to secrete hydrophobic macromolecules back into the blood stream. It is also situated in the adrenal medulla, where it is involved in the secretion of steroid molecules [123;124]. The importance of P-gp in the pharmacokinetics of many drugs is becoming more evident. P-gp is not only involved in the elimination of some drugs to prevent toxicity, but also in absorption, being linked to incomplete and/or slow intestinal absorption of many medications [115;125].

Structure

P-gp is formed as a 140kD molecular weight protein, and acts an N-glycosylated dimer of 264kD. Each monomer is made up of two homologous halves, each comprising six membrane-spanning segments (transmembrane domains: TM1-6, 7-12) and a cytosolic nucleotide-binding domain (ATP Sites – Figure 32) [126;127]. Evidence suggests that the protein performs its efflux function by folding to form a pore through the membrane (Figure 32) [128], whose structure and conformation depends on the binding of substrates and modifiers to the molecule [129-133], the hydrolysis of ATP at either or both of the nucleotide-binding domains [128;133-138], and the integrity and phospholipid composition of the cell membrane [139-142]. In fact latest reports suggest that when the two nucleotide domains each contain ATP, they communicate [143], or dimerise to form a transitional state [144]. The subsequent hydrolysis of ATP at one catalytic site triggers substrate transport by effecting a conformational change, which is then not "reset" until the hydrolysis of ATP at the other nucleotide-binding domain [145;146].

The conformational changes occurring within P-gp on substrate binding [147] involve cysteine-cysteine cross-linking, particularly from TMs 4-6 to TMs 9-12 (Figure 32) [147-150]. Early reports of at least four separate or overlapping substrate binding sites on the molecule were supported by experimental evidence suggesting the majority of these sites transport substrates while the others are regulatory or modulatory. This molecular evidence supports the pharmacological findings that (a) P-gp transports a vast range of substrates with dissimilar structures [151-154], and (b) competitive and non-competitive inhibition occurs between substrates and between substrates and modifiers [129;131;133;151;155;156]. Latest evidence suggests that the promiscuity of P-gp (its ability to bind a larger number of diverse substrates) is mediated by altered packing of the TM segments within the drug binding site depending on the substrate, modulated by the formation of different cross links between TMs [157], while still supporting the binding of different substrates to different parts of the molecule, causing allosteric and conformational inhibition [156]. The proximity of the binding site(s) and the nucleotide-binding domains also explains the reported effects of P-gp substrates/modulators on the activity of P-gp ATPase [134;142;158], which appears to be specific to the structure of TM5 [159].

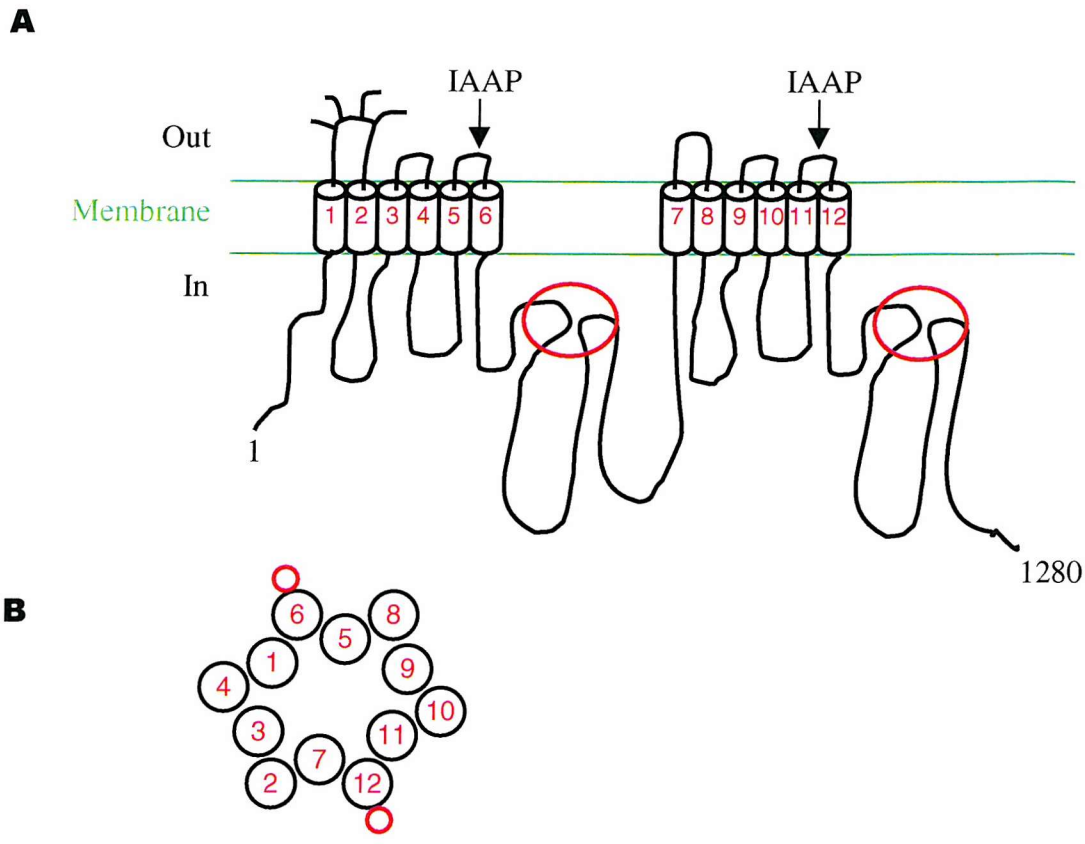

Figure 32 – Diagrams of P-gp structure: A – molecular schematic, based on Ambudkar (1999) [127]; **B** – apical (from extracellular milieu) view of simplified transmembrane domain arrangement, based on Seigneuret (2003) [160] and Rothnie (2004) [161]. Black numbers = amino acid positions, red numbers = transmembrane domains (TMs), red circles = nucleotide binding domains, IAAP = photoaffinity labelled regions [127], also the binding site for Cyclosporin A [162].

Substrates and Inhibitors

After clinical multi-drug resistance in tumours and malignant cells was first encountered [163], "sensitisers" were discovered which could reverse the resistance and restore cytotoxicity [164]. It was deduced that the chemotherapeutic agents were transported out of the tumour cells by P-gp, thereby reducing their cellular toxicity, and that the sensitisers were somehow inhibiting P-gp activity. In a crude sense, inhibitors (sensitisers) and substrates (molecules which are transported by P-gp – i.e. the cytotoxic drugs) can be characterised in this way.

Other *in vivo* approaches have involved studying the competition between P-gp-mediated intestinal absorption [165;166] or renal excretion [167] of compounds, particularly using MDR-gene "knock-out" animals, and comparing their absorbance/excretion with the wild-type (review [168]). In the intestine, P-gp reduces the absorption of P-gp substrates by actively transporting the substrate back into the intestinal lumen, thus preventing it from reaching the blood stream. Competition between P-gp inhibitors and substrates therefore increases intestinal absorption of the substrate in wild-type animals, but has no effect on the (increased) absorption in MDR-gene "knock-out" animals (which do not express P-gp). In the kidney, inhibitors decrease the removal of P-gp substrates from the circulation by blocking active transport into the tubular lumen, and thence into the urine.

In vitro, the accumulation of a substrate within cells or the efflux of one from the cells into medium measures the activity of P-gp. The discovery of a number of fluorescent substrates has led to direct optical determination of the accumulation and efflux of such molecules and the impact of other compounds on handling of these fluorochromes by P-gp. The main fluorescent substrates used are rhodamine 123 and doxorubicin. By pre-incubating cells known to express P-gp with either of these substrates for a standard time (time x), then transferring the cells to medium without the fluorochrome (see Figure 33) for a standard time (time y), the effect of putative competitors on the efflux of the substrate from the cells can be measured, by fluoroscopic or flow cytometric detection of the fluorescent substrate in the medium or the cells, and/or by comparison of the results obtained with and without exposure to the substance under investigation [131;151;155]. Optimum time x can be determined by

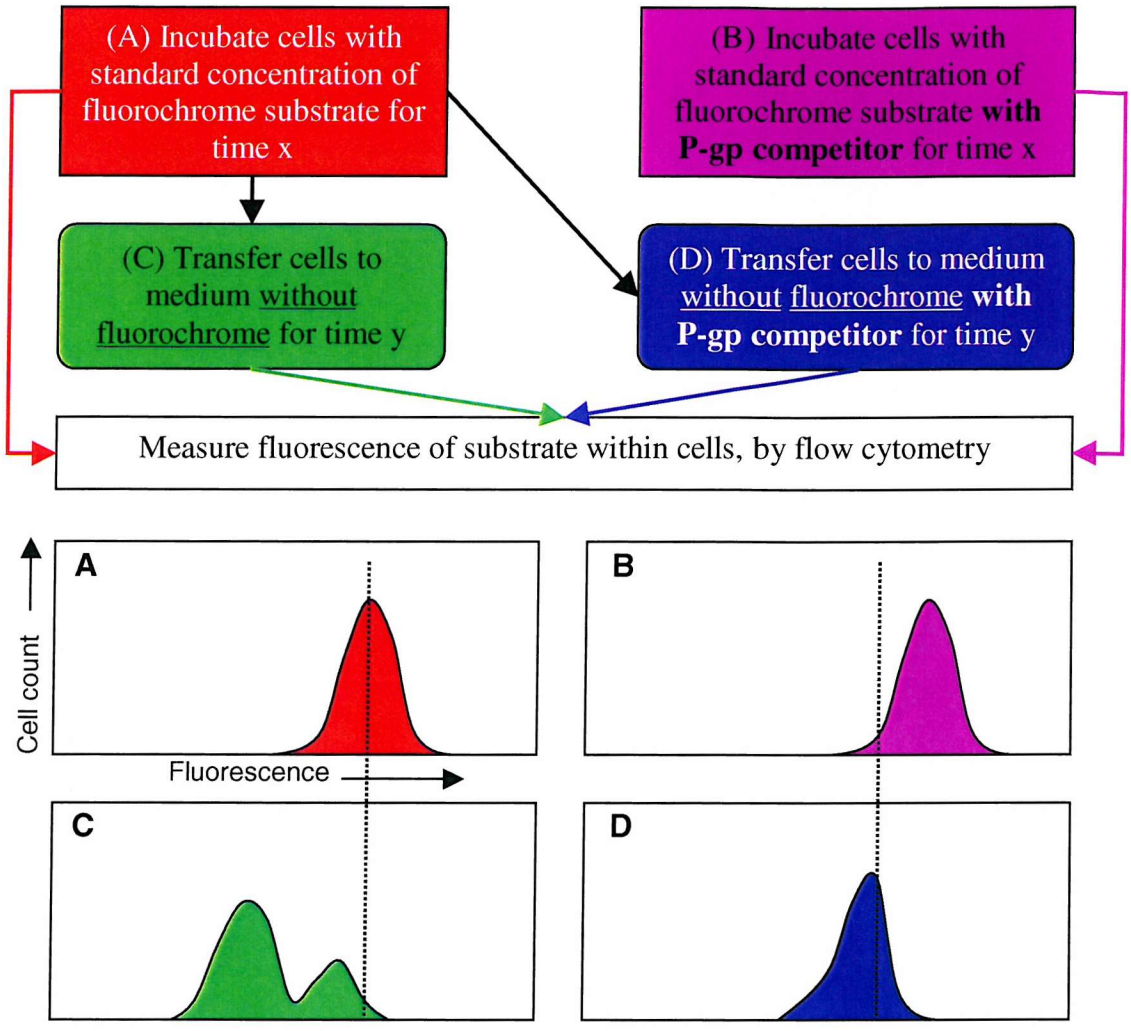

Figure 33 – Diagrammatic representation of fluorescent substrate efflux experiments. In **A**, cells have taken up the fluorochrome and are analysed immediately: the control state (dotted line = mean fluorescence for comparison). In **B**, cells have taken up the fluorochrome in the presence of a P-gp inhibitor, which has blocked P-gp efflux during the accumulation period, and produced maximum uptake. In **C**, in medium without fluorochrome two populations are revealed: the left-hand peak which effluxes the substrate, and the right-hand one, which has lost only a small amount by diffusion. The P-gp-specific transport is confirmed in **D**, when all efflux except diffusion (small shift) is blocked by P-gp inhibition. P-gp efflux activity can be calculated from the ratio of the mean fluorescences in **D** and **B**, which can be used to compare P-gp activities between different cells, or investigate the blocking effects of different inhibitors on the same cells [151;169].

measuring the uptake of the fluorochrome by the cells to find which time allows maximal uptake (or significant uptake in a reasonable time). Optimum time y can be found by determining the time required for the cells to efflux the majority of the fluorochrome. Efflux of the substrate is time-dependent: but reducing the cells' temperature to around 4°C can halt active efflux. By using known substrates and inhibitors in these ways, the efflux activity of P-gp can be determined in and compared across differing cell types.

Vanadate trapping, a technique utilising vanadate ions to competitively block Na^+/K^+-ATPase activity, can be used to compare the efficacy of P-gp blocking of any other inhibitor [170;171]. The activity of ATP hydrolysis of the ABC family of proteins is completely inhibited by vanadate trapping (the half-life of the vanadate-ATPase complex is approximately 72 hours [172]), whereas vanadate blocks the activity of other Na^+/K^+-ATPases in a concentration-dependent manner [173].

Two confounding factors have been reported, however: (i) different species may handle P-gp substrates in different ways. For example, in the isolated perfused rat kidney, Rhodamine 123, a fluorescent P-gp-substrate in the human and other animals, was exclusively excreted by the organic cation pathway, unaffected by known P-gp inhibitors [174] (although its excretion by live rats was unaffected by cimetidine, an organic cation pathway inhibitor [175], despite cimetidine being a P-gp substrate itself [176]). (ii) Other influencing compounds may be present in commercially available solutions – chloroform has been found in a gluconate-Ringer solution, which inhibited P-gp activity, it was presumed, by affecting cell membrane integrity [177].

A plethora of experimental studies too numerous to mention has been published on P-gp activity and the effects of inhibitors. These investigated (a) the movement of substances (putative substrates) across cells known to express P-gp, (b) the handling of known substrates by cells with unknown P-gp expression, and (c) the effects of putative P-gp inhibitors on the movement of known substrates in cells known to express P-gp. The most relevant studies will be discussed in more detail later.

Attempts have been made to classify compounds into P-gp substrates and inhibitors by molecular weight, size, charge and hydrophobicity. All substrates are hydrophobic:

there is little similarity between them otherwise, reflecting the large and diverse range of compounds effluxed by P-gp [151;155;169;178;179]. However, structural analysis of substrates suggests that to interact with P-gp, molecules require two or three electron donor groups with a fixed spatial separation, either of 2.5±0.3 or 4.6±0.6 Å for two, or of 4.6±0.6 Å for the outer two of three [153]. Further analysis suggests that molecules with greater hydrogen-ion acceptance (total ≥8 nitrogen and oxygen atoms), large molecular weight (>400kD) and acid ionisation (pKa > 4) are likely to be P-gp substrates, whereas those with lower numbers of N and O atoms, smaller molecular weight and alkali ionisation are not [178].

Inhibitors also appear to require lipophilicity and large molecular weight, but in addition a large molecular volume or length (>18 atoms in length, which can bridge more than one binding site / P-gp molecule), a high energy occupied orbital (increasing the ability to donate electrons), and a basic tertiary nitrogen atom (forms a hydrogen bond with P-gp residues) in the molecular structure [179]. From these differences between substrates and inhibitors one may infer that it may be the strength of the molecular bond to P-gp which separates substrates and inhibitors – substrates bind loosely and can therefore be transported then dissociate again, while antagonists bind strongly and block the transportation pathway [155].

Expression

P-glycoprotein expression – the concentration of functional protein molecules on the cell surface – can be examined using monoclonal antibodies (MAbs), either on the cell surface by tissue or live- / fixed-cell immunohistology / -cytology, or in cell homogenates (disrupted cells) by protein detection by Western blotting. There are many commercially produced antibodies against human P-gp, and those commonly used are listed in Table 9.

Expression of P-gp has also been examined using photo- or autoradiographic labelling with azide dyes, which bind to the sites shown in Figure 32. However, the binding site for the most commonly used azide, [^{125}I]-iodoaryl azidoprazosin (IAAP), overlaps the same binding site as CsA [127;162]. If this molecule were used to study the effect of CsA on P-gp, a reduction in binding of IAAP, which would be perceived as a down-

regulation of P-gp expression, could in fact be the stoicometric blockade of IAAP binding to P-gp by CsA, and therefore produce erroneous results.

The expression of functional P-gp protein can also be deduced from the measurement of its mRNA signal (MDR-1 mRNA) using Northern blotting or PCR [114]. For this deduction to be correct, all MDR-1 mRNA must be translated by the ribosomes to correctly formed protein, which is then trafficked to the cell surface. This assumption is not always true: in cellular hypotonic shock there is translational block to P-gp production [180] and P-gp protein trafficking [180-182] can be reduced by chemotherapeutics [183].

Table 9. Anti-P-gp monoclonal antibodies

Antibody	Epitope	Internal/External	Cross Reaction
4E3		External	None known [184]
C219	Sites just distal (C-terminal side) to each ATP-binding site [162]	Internal	Other species (mammals & catfish) [185] and other tumour proteins [186]
C494	C-terminal between TM 12 and ATP binding site [162]	Internal	Pyruvate carboxylase [187]
JSB-1	N-terminal amino acid sequence [188]	Internal	Pyruvate carboxylase [189]
MRK16	First & fourth extracellular loops [190]	External	None known (manufacturer's data sheet)
UIC-2	Third extracellular loop [191]	External	No data available

There are also problems with using these MAbs, however. Several of the anti-P-gp antibodies cross-react with other molecules (e.g. JSB-1 with pyruvate carboxylase [189]). To use those directed against internal epitopes, the cells in question need first to be permeabilised, which requires fixation and kills the cells, preventing simultaneous measurement of expression and activity, and may lead to loss of substances held within the cytoplasm. The internal MAbs are also less detectable by flow cytometry,

leading to false negative results [192]. Antibodies may share binding sites with substrates under investigation (e.g. C219, C494 and C32 with azidopine and ATP binding to P-gp [193]), and there are also reports of the modulation of multi-drug resistance by the use of monoclonal antibodies [194;195]. There is therefore great scope for provoking erroneous experimental results: the antibody probe may interfere with substrates' interactions with P-gp, or the substrate may compete with the binding of the antibody probe with the P-gp molecule.

Substrates not only modulate P-gp activity by competition between substrates, but can also affect the cellular expression of the P-gp protein. Up-regulation of P-gp expression (induction) by substrates and other molecules has been observed – see Table 10.

The mechanism of this induction is not currently known, but is a true increase in functional P-gp protein on the cell surface, not just an increase in MDR-1 mRNA. The nuclear transcription factor NF-κB may be involved, which has been shown to be required for the transcription of the MDR-1 gene [196] and a consensus NF-κB binding site has been found on the intron of the MDR-1 gene in human colonic carcinoma cells [197], which have a high expression of P-gp.

It may be that MDR mRNA levels are 'superinduced' by inhibition of transcription and/or a reduction in mRNA destruction, leading to an increase in the nuclear / cytoplasmic mRNA half-life [198].

The structures of P-gp inducers have also been examined. It is suggested that to up-regulate P-gp, the molecular structure should contain two (or two of more) electron donor groups separated by 4.6±0.6 Å. The observation that P-gp expression is also increased by physical stress such as X-ray irradiation, ultraviolet light irradiation and heat shock further supports this hypothesis. Such insults generate nucleic acid fragments. Free nucleotide bases contain electron donor groups separated by 4.6±0.6 Å, and although free nucleotides are lipid insoluble and therefore not effluxed by P-gp, it is assumed that as such fragments can assume nearly any structure, some could be hydrophobic, and therefore presented to P-gp in the membrane. These observations and assumptions lead to the hypothesis that P-gp may also be responsible for the

removal of cellular genetic waste, which would otherwise interfere with the mechanism of correct genetic translation [153]. The recent finding that P-gp communicates with the proteasome [199], the cellular mechanism for presentation of peptides to the cell surface, may also support this hypothesis.

Table 10. P-gp expression up-regulators, tissues affected and references

Inducer	Tissue	Reference
CsA	MDCK cells *in vitro*	del Moral (1995)[30]
CsA	rat kidney, intestine, liver	Jette (1996)[200]
CsA and Hydroxyethyl-cyclosporin	rat liver	Vickers (1996)[201]
CsA	rat kidney	del Moral (1997)[202]
Ecto-5'-nucleotidase protein expression	MDCK cells *in vitro*	Ledoux (1997)[203]
CsA	rat tubule cells *in vitro*	Hauser (1998)[204]
Cyclosporin analogue SDZ-PSC 833	rat kidney	Jette (1998)[205]
CsA	human kidney	Koziolek (2001)[206]
CsA	rat liver	Bai (2001)[207]
2-acetylaminofluorene	human hepatoma cells *in vitro*	Kuo (2002)[208]
Digoxin	Caco-2 cells	Takara (2002)[209]
Cyclo-oxygenase 2	rat hepatocytes *in vitro*	Ziemann (2002)[210]
CsA	rat liver *in vivo*	Daoudaki (2003) [211]
Lopinavir	human intestinal carcinoma cell line	Vishnuvardhan (2003) [212]

The previous reports presented above describe a number of ways in which both the efflux activity and the protein expression of P-gp can be modulated / altered. The net rate of efflux of substrate by P-gp should approximate to the product of P-gp efflux activity and the protein expression [213]. Moreover, each can be altered separately from

the other – indeed, it has recently been reported that the function of P-gp *in vivo* is not necessarily related to its expression [182;214;215]. Thus, for any *in vitro* investigation into P-gp and the effects of putative substrates / modulators, both the activity and expression of the protein must be examined.

P-glycoprotein and Cyclosporin A

The literature on interactions between P-gp and CsA is extensive and not conclusive.

In vivo

The majority of the *in vivo* studies have been performed on animals. The absorption of CsA from the intestine is increased by co-administration of the P-gp inhibitors grapefruit juice [216] or verapamil [217], and reduced by the P-gp inducers St. John's Wart [218] and rifampicin [219], confirming that CsA is a P-gp substrate (gut effects of P-gp are reversed: increased efflux from the cell is back into the intestinal lumen, decreasing the amount of drug within the cell available for absorption into the blood stream). In general, CsA exposure increases the tissue expression of P-gp in the kidney [206] and liver [207].

To examine the effect of CsA on human kidneys *in vivo*, a percutaneous renal biopsy would be required, which is a relatively traumatic and complicated procedure (4.5% complication rate [Abstract: Leach and Stevens, Native Renal Biopsy Performance: One Unit's Experience, Nephrol Dial Transplant 2002; 17(suppl 1): 115]). Therefore, in a patient being given CsA for a medical treatment, biopsies would only be taken when renal disease is expected. The coexistence of disease and another renal injury or insult would potentially confound any correlation of P-gp expression with CsA exposure.

As above, a patient receiving CsA for an indication other than renal transplantation would only undergo a renal biopsy for renal dysfunction. The most likely renal diagnosis would be CsA toxicity. If CsA toxicity is related to P-gp hypo-function (greater renal cellular CsA-accumulation), then a negative correlation between CsA and P-gp expression would be expected, at odds with the published findings in animal

studies (see below). However, P-gp hyper-function may lead to an increase in the dosage of CsA (by monitoring levels of CsA or the pharmacological effects of CsA) through increased biliary excretion or efflux from white blood cells where the immunosuppressive activity occurs. Such an increase in exposure could overwhelm the renal tubular P-gp and lead to CsA toxicity.

The exception to this situation would be biopsies taken from renal transplant recipients on CsA. Although biopsies would still be taken for renal dysfunction, some of that dysfunction would be likely to be unrelated to CsA (as 'protocol biopsies' – biopsies taken routinely at set time points in the post-transplant period, so the most likely to yield meaningful results – are not standard practice in many renal units). However, in this setting, acute graft dysfunction is most likely to be due to acute rejection (the immunological attack of the graft kidney by the recipient). The majority of acute rejection is cellularly-mediated, and as the response of the T-cells to CsA may be blunted by P-gp overactivity (as has been found in heart and lung transplant recipients [220;221]), there may still be more of an interaction between P-gp expression and CsA exposure than just a straightforward or cause-effect one.

In vivo investigations of P-gp responses to the effects of drugs such as CsA will be further confounded in human studies by other factors. The co-administration of other pharmaceutical agents is one such confounder. There are reports of corticosteroid effects on P-gp expression: in asthma sufferers treated with prednisolone, P-gp expression decreased in B-lymphocytes [222]; in rheumatoid arthritis patients on corticosteroid therapy, P-gp expression was greater on peripheral blood lymphocytes than in patients not on steroids, or in controls [223].

Uraemia (the progressive deterioration of physiologic functions as a result of the retention in the body of compounds that normally are ex-/secreted into the urine by the healthy kidneys [224]) is another confounder. There are (conflicting) reports of the effects of uraemia on P-gp function, which could further confound studies of P-gp expression in renal transplant recipients: acute renal failure in rats inhibits renal and hepatic P-gp function [214;225] but increases expression [214;226], while increasing intestinal P-gp function [217]. Chronic renal failure decreases intestinal P-gp activity, while increasing expression [182].

Further confounding factors include the increase of P-gp activity by the products of cyclo-oxygenase 2 (COX-2), an enzyme closely related to regulation of intra-renal blood flow, particularly in states of glomerular hypo-perfusion [227]; the down-regulation of P-gp expression by IL-2 , a major pro-inflammatory cytokine [228;229] and an increase in P-gp expression by other pro-inflammatory cytokines [230].

Despite these potential problems, up-regulation of P-gp has been reported in biopsy samples from (a) transplant kidneys of patients receiving CsA for immunosuppression [30;206] (although not in biopsies showing CsA toxicity [206]) and (b) small intestine of normal volunteers given rifampicin [213].

In renal transplant recipients' peripheral blood lymphocytes, CsA has variable and unexpected effects: P-gp expression is either down-regulated [231], or unaffected [117;232;233], although in one cross-sectional study of 32 renal transplant recipients, none of the 9 patients with graft survival of greater than 40 months expressed P-gp on their T-lymphocytes [234], suggesting either that CsA exposure of greater than 40 months has down-regulated P-gp expression, or (more likely) that only those patients with maximal T-lymphocyte exposure to CsA, i.e. those which have effluxed CsA less (as a result of low expression of P-gp), were protected from graft immunological attack.

Animal studies have shown that renal P-gp expression is up-regulated by exposure to CsA in rats [200-202;235]. However, the extrapolation of this animal work to humans is limited by the different sensitivities of human and animal cells to the effects of CsA. To induce an effect in renal P-gp in rats, doses of CsA of 20-100mg·kg^{-1}·day^{-1} are required [201]. The same dose in humans would be profoundly toxic – doses of a maximum of 18mg·kg^{-1}·day^{-1} were originally used in cardiac transplantation [4], but this was quickly found to be damaging to the renal cortical cells [236], and subsequent reductions in CsA dose improved renal longevity [237]. The dose of CsA used in human renal transplantation remains initially approximately 10mg·kg^{-1}·day^{-1}, reducing over several weeks to 6mg·kg^{-1}·day^{-1}, with a longer-term maintenance dose of around 3-5mg·kg^{-1}·day^{-1} [238;239]. The adjustment of CsA dosage has historically been made on trough levels [238], although more recently the area under the curve (AUC) of blood concentration versus time has been found to correlate better with anti-rejection effect and toxicity [240]. The accumulation of CsA within cells, however, bears little

relationship to peak or trough levels [241-243], suggesting that other factors such as P-gp function are playing a part, although reducing the dose to adjust the AUC does have an impact on nephrotoxicity [244].

Conclusion: *in vivo* results are conflicting and confounded by disease and administration of medications. Is better evidence available from *in vitro* studies?

In vitro

The majority of the *in vitro* published studies have been performed on cell lines (tumour, or virally transformed normal human and animal cells), with the remainder on cultured primary (not virally-transformed) animal cells and haematological cells.

Specifically with respect to CsA, it is generally found that in the kidney, CsA inhibits P-gp efflux activity [225;245-249]. The same is true on peripheral blood mononuclear cells, where CsA exposure either increases the intracellular accumulation of a substrate studied in normal or malignant lymphocytes [250;251], or improves the malignant cell death rate of cytotoxic medications (secondary effect of increased accumulation of cytotoxic drugs) when co-administered [252-254]. These reports illustrate a clear difference between the effects on P-gp of acute and chronic exposure to CsA: acute exposure inhibits the efflux activity of P-gp while chronic exposure up-regulates the expression of the protein.

Only one study has investigated the effects on P-gp activity of incubating cells *in vitro* with CsA or other putative inhibitors / modulators for a period of time. Hauser [204] incubated human arterial endothelial cells and rat proximal tubular cells for 7 days in CsA at pharmacological doses (concentrations from 100nM to 1.6μM [120–1920ng/ml] – subculturing 1:10 twice per week). They measured intracellular accumulation of calcein-AM as a marker of P-gp efflux activity. Calcein-AM is a substrate of P-gp that enters the renal tubular cell passively and is then actively effluxed by P-gp. Any calcein-AM that remains within the cell is cleaved by endogenous esterases into a fluorescent metabolite whose concentration – which they measured by spectrophotometry – is inversely related to the P-gp efflux activity. They measured P-gp expression in the same cells by immunoblotting with C219 and immunocytochemistry with MRK16 (both monoclonal anti-P-gp antibodies). They found that both the efflux activity and protein expression were increased by CsA co-incubation. They compared this effect with that of FK506 (Tacrolimus (TAC) – another calcineurin-inhibiting immunosuppressant P-gp substrate / modulator). In the therapeutic range, no effect was found on either P-gp activity or expression. However, increases in both activity and expression were seen when the dose of TAC was increased to a toxic range. In cultured mouse brain capillary endothelial cells a

difference was observed in the acute toxic effects of CsA and TAC (less toxic) although both suppressed P-gp function in the short term [124], suggesting that although similar drugs, the mechanisms of toxicity and P-gp up-regulation are different. Certainly the target proteins for the two compounds are different [255].

The binding site for CsA has been determined between the ends of TMs 11 and 12 [162] (see Figure 32). It is assumed that the interaction between CsA and other P-gp substrates is related to either (i) their sharing of the same binding site, (ii) the stereotactic blockade of a separate but close binding site (including that of ATP, which is in close proximity to TM12) by the CsA molecule, or (iii) a conformational change in P-gp induced by the binding of CsA which prevents the binding of further substrates. The finding that CsA inhibits the labelling of P-gp with IAAP unless the cells are washed (repeated incubation in medium without CsA, to allow dissociation of CsA from the P-gp molecule) between CsA incubation and IAAP labelling [205] would tend to support these hypotheses, but not necessarily differentiate the most likely.

Therefore in order to study the effects of longer-term CsA exposure on P-gp expression and activity in cultured human renal tubular epithelial cells, immunohistochemistry and flow cytometry could be performed using monoclonal antibodies to P-gp, as long as a wash-out period, as above, was incorporated to minimise any direct binding interactions between CsA and the MAb (any CsA still bound to the P-gp would stereotactically block the binding of a MAb to the same or an adjacent binding site). The activity of P-gp could be measured using Rhodamine 123 efflux and studying the effect of blocking P-gp activity with vanadate and/or CsA. The effect of CsA on P-gp over time should be determined by the use of control cells, from the same patient and treated in the same way throughout, but without CsA exposure.

CsA is nephrotoxic. Prolonged exposure of cells in culture to CsA may therefore cause cellular damage, or perturbation of function. In order to investigate such effects in cells in such culture, the following can be determined (for details, see Chapter 3):

- the cells' viability,

- their position in the cell cycle,
- the cellular character by scanning and transmission electron microscopy, surface markers and biochemistry, and
- other markers of damage / impairment such as the release of LDH (a cytosolic enzyme, which is responsible for trans-mitochondrial membrane hydrogen-ion transfer [256], released by cells in culture during cell death and other toxic effects such as membrane perturbations [62;257]).

In vivo, oral CsA is administered twice daily. CsA concentrations in the blood of treated patients therefore follow a diurnal rhythm: varying from the pre-dose trough of 50-150ng/ml to a peak between 1-2 hours post dose of approximately 700-1300ng/ml, giving a daily AUC of approximately 4,000-10,000ng·24hr·ml^{-1}. Pharmacological data have shown that both the immunosuppressive actions, and also the toxicity, of CsA are directly related to the AUC [240]. *In vitro*, this variation could be reproduced by the perfusion of the cells with culture medium containing a changing concentration of CsA. If this is not possible, the CsA dose in the culture medium should be maintained to keep the AUC appropriate.

Therefore, in order to detect any effect of prolonged CsA exposure on human renal tubular cells, avoiding as many confounding factors as possible, the following would be appropriate:

- use human cells – to avoid any differing response in another species
- use cells in culture – to avoid multiple confounding factors in giving CsA to human subjects / patients
- use cells in stable culture – cells in the healthy human kidney turn over at a rate of 0.2% per day [38]
- keep the cells exposed to CsA for a number of weeks – acute toxicity develops within days, while chronic toxicity takes longer (although the mechanism is not fully understood)
- use therapeutic doses of CsA – to avoid doses acutely toxic to the cells, and achieve an appropriate AUC (exposure to CsA)
- measure the effect of CsA through:
  1. cellular characterisation, viability and metabolism

2. P-gp activity by efflux/accumulation of known measurable substrate(s)
3. P-gp expression by monoclonal antibodies
4. Activity and expression in the same cells by non-competing substrates / antibodies, and

- compare the results in CsA-exposed cells with control non-exposed cells

Methods

Cell Culture

Cells were obtained and plated as per General Methods (Chapter 2) and Quiescent Cell Culture (Chapter 3). Cells used for CsA exposure were confluent monolayers in 6-well (~4cm^2 per well) culture inserts (see Figure 4). 1ml of QM ± CsA was added to the apical chamber, and 2ml to the basal chamber.

For all experiments the effect of CsA was compared to a control, treated in the same way but without CsA exposure. *In vivo*, renal tubular epithelial cells would be exposed to CsA by diffusion from the peritubular capillaries on their basal surface, with their apical surface being exposed to urine, through which effluxed CsA is removed. Although urinary CsA concentrations exceed those in the blood [258], movement of CsA into the cells through the apical membrane is negligible compared to that across the basal membrane [107]. In the cell culture inserts, differential culture medium composition is possible, as the cells form a selectively-permeable barrier to solute movement.

As the cells were to be exposed to CsA over a number of weeks, culture medium would need to be changed regularly. This was achieved by careful pipetting of the medium from the apical then the basal chambers, and gentle replacement of fresh medium. Used medium was kept frozen at –80°C for the measurement of CsA and LDH, both performed in batches.

CsA was measured by radioimmunoassay using the CYCLO-Trac SP kit (Protocol 15) from Diasorin (Germany).

LDH was assayed using the Roche 1 644 793 kit (Protocol 16), measuring LDH activity by (i) the formation of NADH+H$^+$ by LDH from lactate; (ii) the subsequent addition of the catalyst diaphorase transfers H/H$^+$ to the yellow tetrazolium salt 2-[4-iodophenyl]-3-[4-nitrophenyl]-5-phenyltetrazolium chloride, forming a red formazan salt. The concentration of formazan, determined by spectrophotometry, is in direct proportion to the activity of LDH (Manufacturer's Data Sheet).

In static culture it is not possible to reproduce the diurnal variation of CsA blood concentrations. An average dose of 200-500ng/ml corresponds to a daily AUC of 5,000-12,000ng·hr·ml^{-1}.

The exposure to CsA was studied twice: preliminarily at 100ng/ml (low trough dose) and 500ng/ml ("high-average" therapeutic dose) concentrations for more than 5 weeks with the medium being changed at weekly intervals; subsequently at 300ng/ml ("low-average" therapeutic dose) for more than 3 weeks with the medium changed thrice weekly. The rationale for this is explained in the results.

Any short-term effects of CsA, or effects of CsA masked by or affected by the quiescence process, were also investigated by (i) growing cells in DM + CsA, (ii) adding CsA to cells at confluence in DM for up to 7 days, and (iii) serially subculturing cells in DM + CsA.

The transport of CsA across the cells was quantified separately towards the end of the study using ^{125}I-CsA (Protocol 17).

P-gp activity and expression

A panel of MAbs was examined for the determination of P-gp expression (see Table 11). For flow cytometry Protocols 10 and 11 were followed. For indirect immunofluorescence Protocols 7 and 9 were followed, initially on 8-well chamber slides or cytocentrifuge preparations of cells, subsequently on confluent cell monolayers on culture-well membranes.

Table 11. Flow cytometry / immunofluorescence fixatives and permeabilisation

Monoclonal Antibody	Flow cytometry Fixative / Time	Flow cytometry permeabil-isation?	Immunocytology Fixative / Time	Immunocytology Concentration
JSB-1	2% PFA / 60mins	0.05% Saponin	Acetone / 10mins	5µg/ml
Neomarkers anti-P-gp	2% PFA / 60mins	No	-	-
MRK16	2% PFA / 60mins	No	4% PFA / 4mins	5µg/ml

To determine P-gp activity, the accumulation and efflux of Rhodamine (R)123, with and without the effect of vanadate (and the effect of the addition of and variation in concentration of Mg-ATP, which may be important for the blockade of P-gp Na^+-K^+-ATPase[172]) and CsA as inhibitors or cimetidine, ethanol (CsA vehicle) and sodium hydroxide (vanadate vehicle) as controls was measured. The relative P-gp activity was calculated from the efflux of R123 with and without CsA or vanadate in the efflux medium [151].

Protocol 18 was followed to measure P-gp activity and expression: first at the confluent monolayer in DM stage (around days 7 to 10) immediately before passage into the 6-well culture plates, then at the end of each study at between 3 and 6 weeks of culture.

The protocol was adjusted subsequently (Protocol 19 – see results for explanation) to measure activity and expression separately (but in parallel) for the final studies

Results

Cell culture success

Weekly CsA culture

Three specimens (two from males aged 55 & 70 years, one female age 56) were plated out in 6-well culture inserts at passage 1 and exposed to none, 100ng/ml and 500ng/ml CsA respectively, refreshed weekly.

All survived quiescence for greater than 6 weeks (43, 48 & 48 days) without loss of monolayer integrity by phase-contrast microscopy.

Thrice-weekly CsA culture

Three specimens (two male, 58 & 72, and one female aged 84 years) at passage 1 were kept in 6-well culture inserts and exposed to none or 300ng/ml CsA, refreshed three times weekly (at 1-4 day intervals).

All survived quiescence for greater than 3 weeks (23, 25 & 26 days) without phase-contrast microscopical abnormality.

Characterisation

Phase contrast microscopy

The monolayer appearance at 23 days of quiescent culture on 6-well culture inserts with medium refreshment thrice weekly is shown in Figure 34. Although the photomicrography of cells on these membranes is not as clear as those on uncoated plastic, the normal appearance of the majority of cells can still be seen. The inhomogeneity of the cell populations remains, with "islands" of cells of similar morphology visible. The cells retain their low ratio of length to width, however (an increase in the length:width ratio would suggest trans- / de-differentiation to a myofibroblastic phenotype).

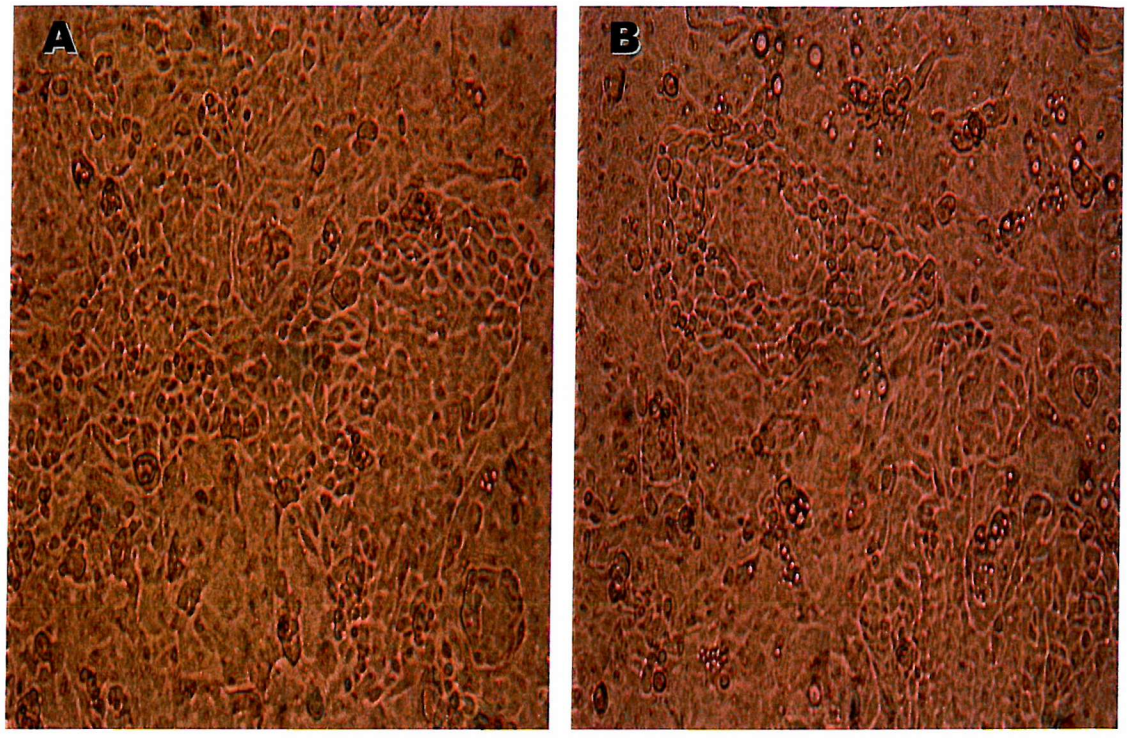

Figure 34. Effect of 23 day CsA-exposure on confluent monolayers of passage 1 cells on 6-well culture membranes. Phase-contrast photomicrographs of cells in **(A)** QM and **(B)** QM + CsA 300ng/ml, refreshed thrice weekly. Although the photomicrography of cells on these membranes is not as clear as those on uncoated plastic, the normal appearance of the majority of cells can still be seen. The inhomogeneity of the cell populations remains, with "islands" of cells of similar morphology visible. The cells retain their low ratio of length to width, however (an increase in the length:width ratio would suggest trans- / de-differentiation to a myofibroblastic phenotype). (Original magnification × 10)

Although representative photomicrographs are not available, the cells on 6-well culture membranes behaved similarly to those on uncoated plastic. For comparison, the photomicrographs in Figure 35 are of cells in passage 1 on uncoated plastic culture 24-wells, quiesced for 24 days with or without CsA 300ng/ml, with refreshment of the medium only performed weekly. Both photomicrographs show features suggestive of transdifferentiation towards a fibroblastic phenotype.

The apparent change in morphology, and the phenotypic alteration suggested by this change when the medium was refreshed only every 7 days, was the first of the results that led to the change in experimental protocol to thrice-weekly medium refreshment with a reduced CsA dose. Both increasing the frequency of medium refreshment and reducing the CsA exposure promoted the maintenance of a more normal appearance, suggesting a reduction in transdifferentiation to a myofibroblastic phenotype.

Transmission electron microscopy

TEM was performed on once- and thrice-weekly refreshed cells in quiescence for 6 and 3 weeks respectively, with and without CsA exposure.

Figure 36 to Figure 38 show the TEM results. They generally show the maintenance of the cellular ultrastructure previously shown in quiescence (Chapter 4), with appropriate cellular polarisation (apical brush border microvilli in 2 of the 3 subjects, and basal mitochondria and cellular invaginations), cellular organelles (rough endoplasmic reticulum, mitochondria, golgi apparatus, lysosomes, nuclear membrane and nucleolar chromatin), intracellular tight junctions and membrane interdigitations. The cell monolayer appeared to be maintained, although without multiple consecutive sections, and with the significant intracellular membrane interdigitation associated with the proximal tubular cell phenotype, it was not possible to determine this accurately.

The cellular ultrastructure in the CsA-exposed cells was less normal. In 5 of the 6 subjects the brush border microvilli were reduced or absent altogether. The cellular junctions were less prominent, the cellular heights were generally less, and the nuclei and cytoplasm were more electron-dense. In one subject the mitochondria were

bizarrely-shaped and enlarged (one feature of CsA toxicity [23] - Figure 37H), and all had an increased number of lysosomes, some being particularly dense.

A comparison of the cells in quiescence whose medium was change weekly with those cells whose medium was changed thrice-weekly (Figure 36 versus Figure 37 & Figure 38) shows that the ultrastructure of the cells with the more frequent medium change is much better preserved (particularly in the control cells: Figure 36 A,B, Figure 37 A,B,D,F and Figure 38).

Scanning electron microscopy

SEM was performed only once. However the results show a difference between cells quiesced in the presence of 300ng/ml CsA and without (see Figure 39). The reduction of cellular height in the CsA-exposed cells is clearly seen, as is the reduction in length of the microvilli (although there are not many seen in the control cells). In the control cells the junctions between the cells are intact, and the cells form a monolayer. There are holes clearly visible within the monolayer of the cells exposed to CsA.

Immunostaining

Immunofluorescence characterisation was performed first on the cells quiesced with no CsA, CsA 100 or 500ng/ml on 6-well culture membranes, with the medium refreshed weekly. It proved impossible to remove the background non-specific staining even on the IgG_1 isotype control (the control antibodies should not stain the samples: some slight non-specific (negative-control) staining is often seen, which is removed / minimised by adjusting the software settings for the microscope, ensuring that the same settings are used for all samples in each experiment). Non-specific staining is seen on cells whose membranes are disrupted, as more (and bizarre) antigens are exposed to the antibodies, and washing of the cells between antibody incubations does not remove the internalised antibodies. However, the HB95 (MHC class I) and ZO-1 (tight junction constituent protein) staining was still clearly discernable, except on the CsA 500ng/ml cells, which appeared to be bizarre and to have lost much of their integrity (Figure 40).

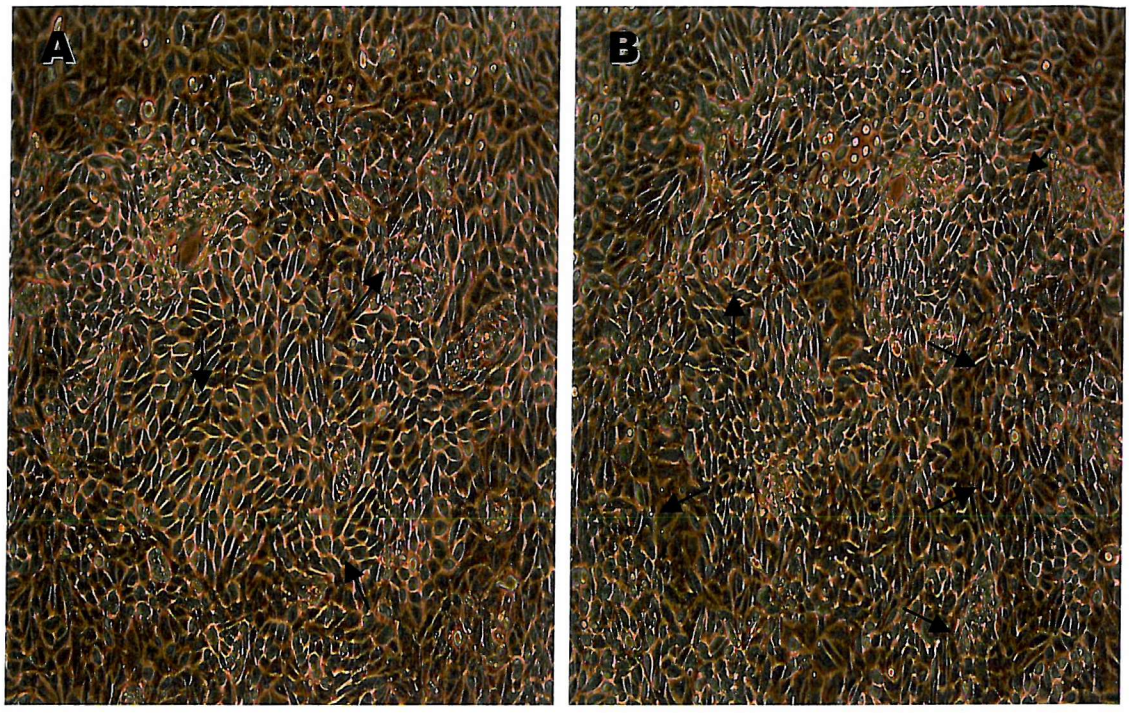

Figure 35. Effect of 24 day CsA-exposure on confluent monolayers of passage 1 cells on uncoated plastic culture 24-well plates. Phase-contrast micrographs in **(A)** QM and **(B)** QM with CsA 300ng/ml, refreshed weekly. A proportion of cells in both fields show shrinkage/rounding (arrows), consistent with apoptosis/necrosis. This is more marked in the cells exposed to CsA (B). Both groups of cells also exhibit an elongation of their shape (an increase in the length:width ratio), which can be associated with a change to a fibroblastic phenotype.

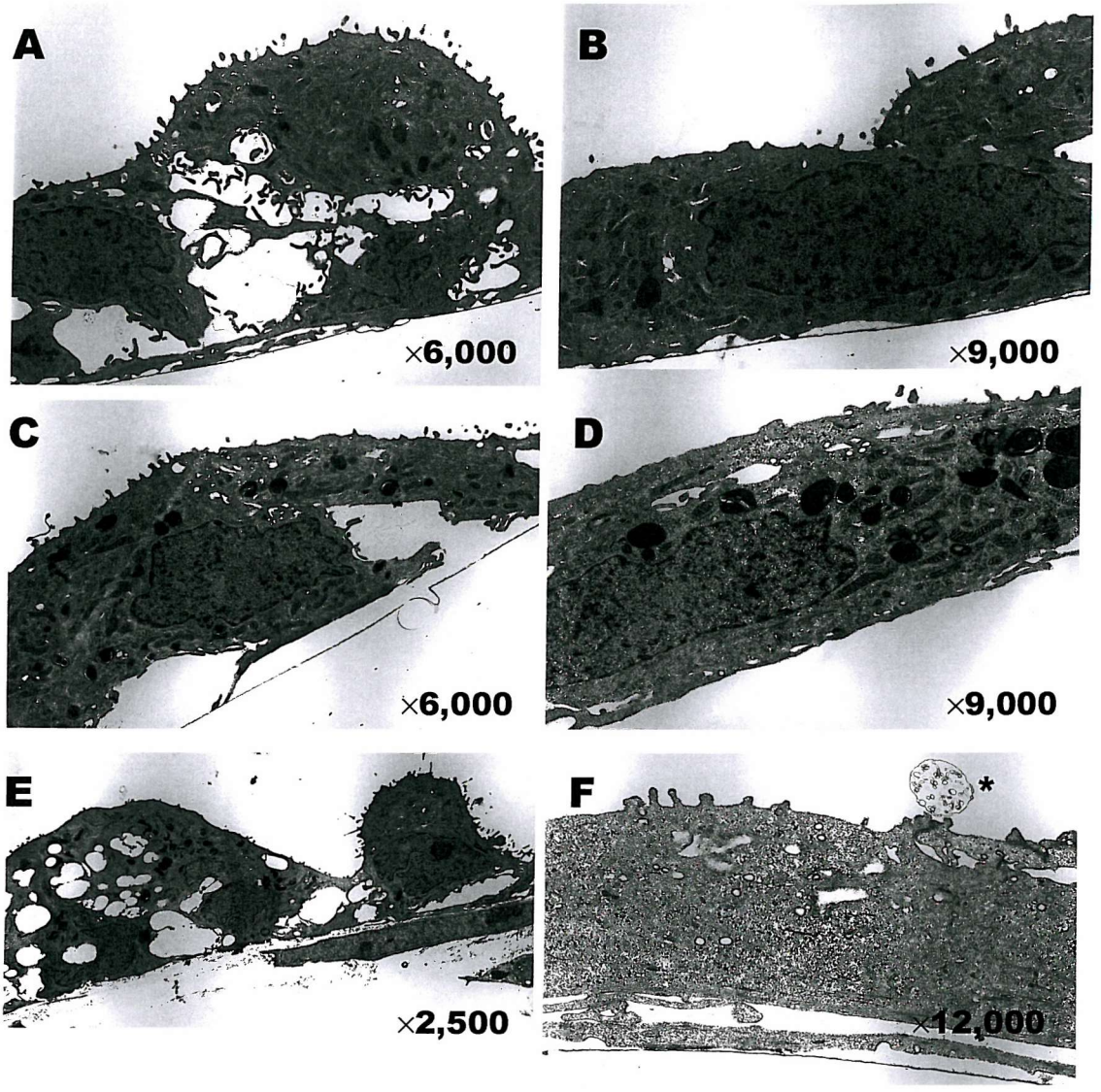

Figure 36: Effect of different concentrations of CsA on cells quiesced on 6-well culture membranes for 45-48 days, medium exchanged weekly. Transmission electron micrographs, original magnifications (varied) as shown. **(A,B)** control cells with no CsA, **(C,D)** CsA 100ng/ml, **(E,F)** CsA 500ng/ml. Cell ultrastructure abnormalities in the CsA-exposed cells is shown, with reduction of the brush border membrane, an increase in lysosome number and size, and enlargement of mitochondria (particularly in **D**). Cells exposed to the highest CsA concentrations exhibited multiple cytoplasmic vacuoles (**E,F**), and presumed exocytosis of cellular contents (* in **F**).

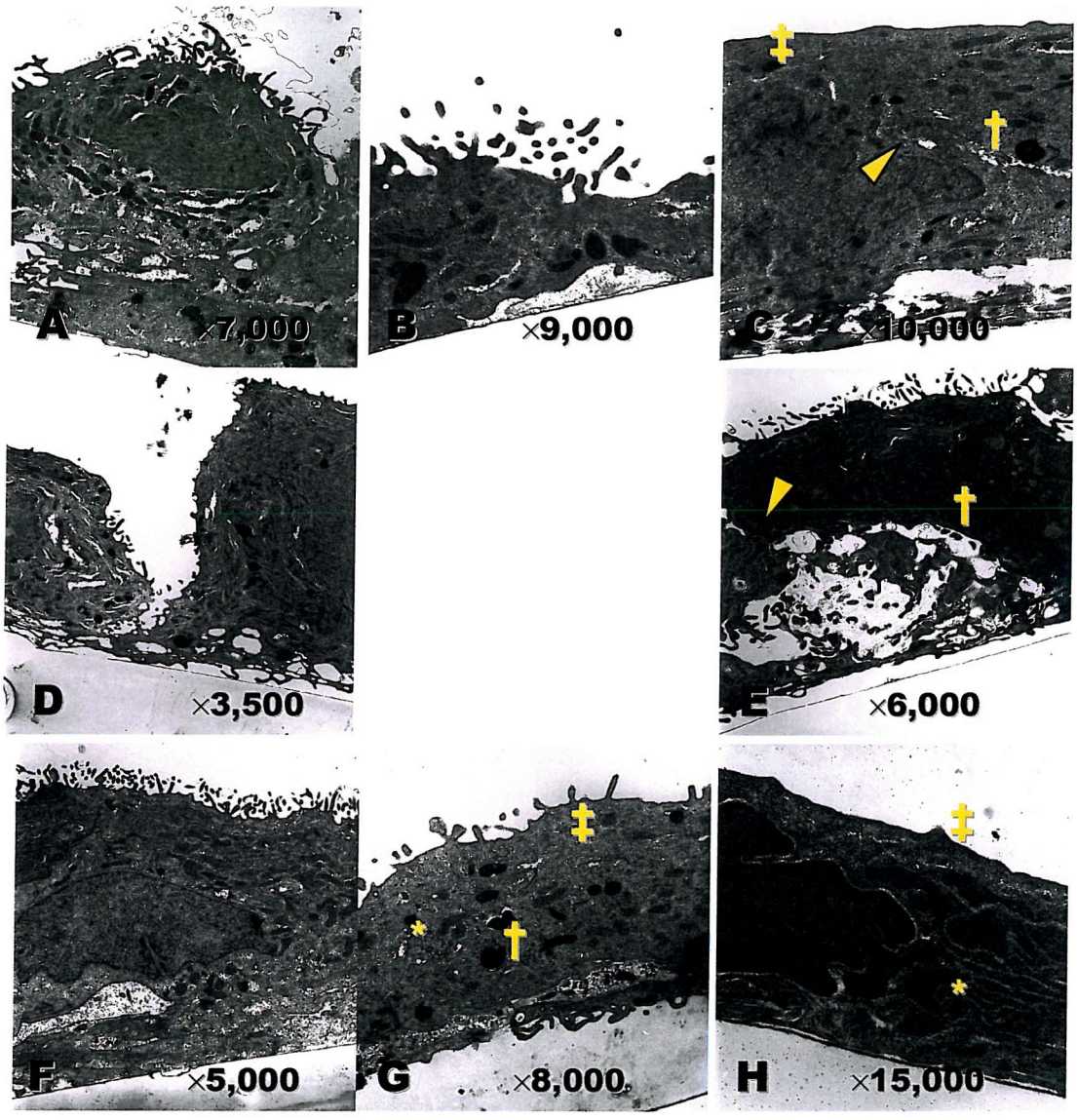

Figure 37: Effect of exposure to CsA with thrice-weekly medium change on confluent monolayers of cells on 6-well culture membranes over 23 to 25 days. Representative transmission electron micrographs – magnifications as given. **(A,B,D,F)** without and **(C,E,G,H)** with 300ng/ml CsA. The overall appearance of the CsA-exposed cells is not normal, with loss of cell height, condensed nuclear chromatin, increased cytoplasmic density, abnormal organelles (swollen and distorted mitochondria *) and prominent lysosomes (†). The brush border (‡) is variable, but generally reduced in height (particularly in the CsA-exposed cells – **C** and **G,H**) and cellular junctions are not prominent (arrowheads).

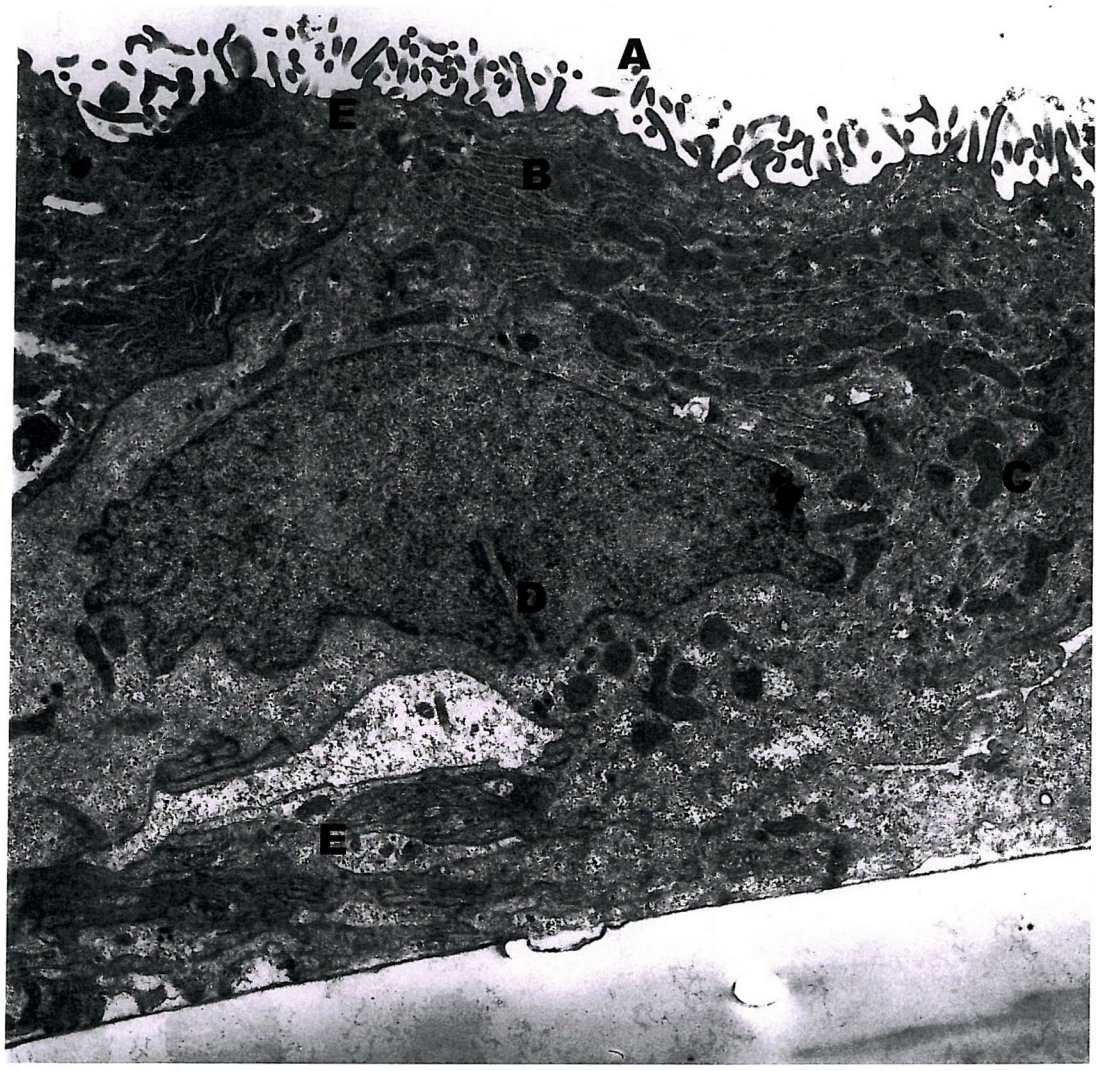

Figure 38. Transmission electron micrograph of control cells (without CsA exposure) quiesced for 26 days with medium change thrice weekly. The well-preserved brush border (A), rough endoplasmic reticulum (B), mitochondria (C), nucleus and nuclear membrane (D) and intercellular junctions / interdigitations (E) are well shown (original magnification ×5,000).

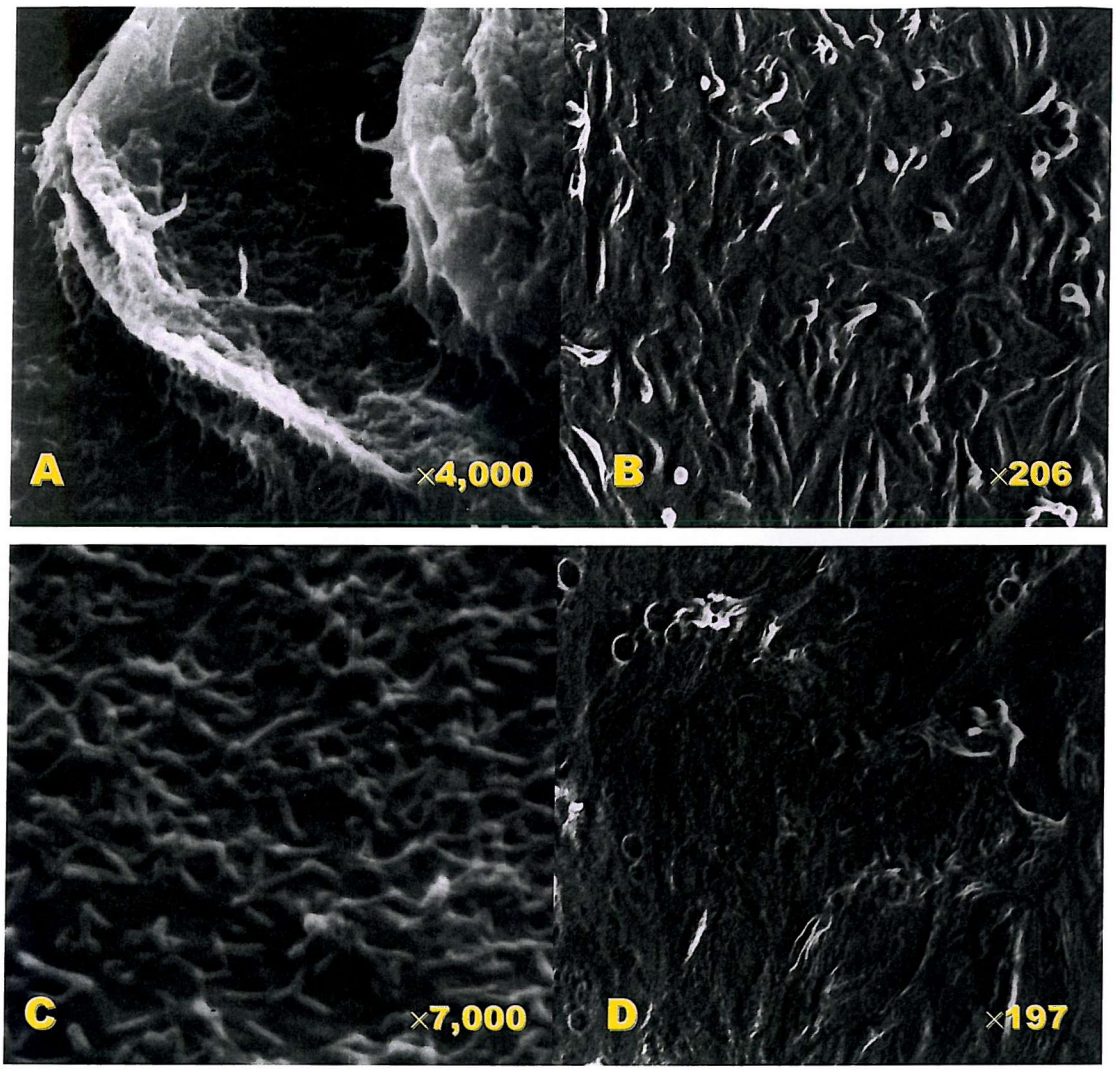

Figure 39: Effect of CsA exposure on surface ultrastructure of confluent cells on 6-well culture membranes. Scanning electron micrographs – magnifications as given. **(A,B)** without and **(C,D)** with 300ng/ml CsA. Medium was refreshed thrice-weekly. The brush border microvilli are seen, although their orientation and length are not normal. When exposed to CsA the cellular height is less and the maintenance of the monolayer is impaired compared to the controls.

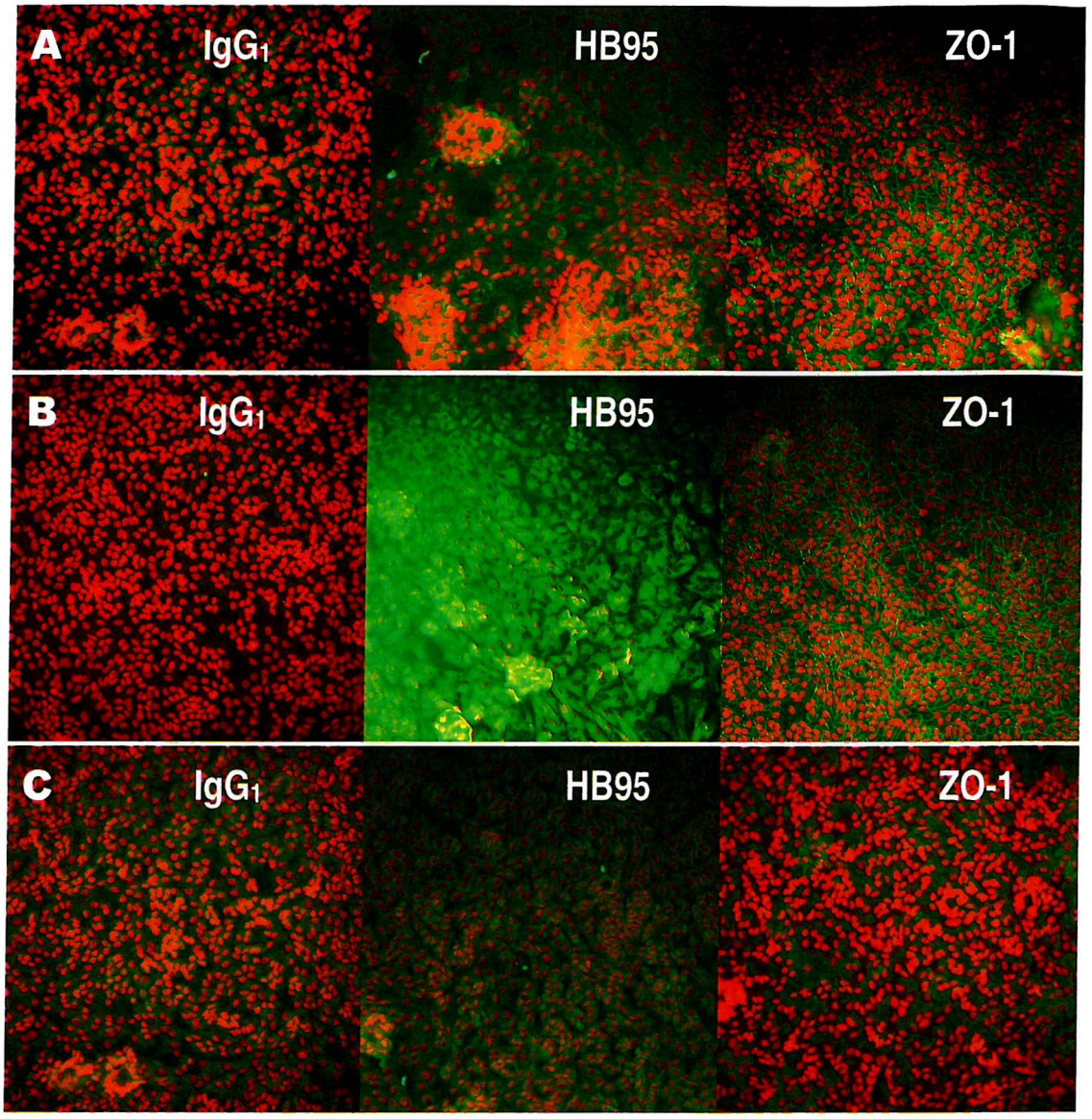

Figure 40. Effect of CsA exposure on immunofluorescence characterisation of cell monolayers in passage 1 on 6-well culture membranes kept in QM for 43 days. **(A)** without, or with **(B)** CsA 100ng/ml or **(C)** CsA 500mg/ml, refreshed weekly. The antibody signal is the **green** fluorescence, the **red** is PI counterstaining, which is taken up by nuclei. **IgG_1** = isotype control, **HB95** = MHC class I, **ZO-1** = zonula occludens protein-1. Background non-specific staining is present even on the IgG_1 isotype control (particularly in **B** HB95). However, the HB95 (MHC class I) and ZO-1 (tight junction constituent protein) staining was still clearly discernable, except on the CsA 500ng/ml cells, which appeared to be bizarre and to have lost much of their integrity. Magnification × 25.

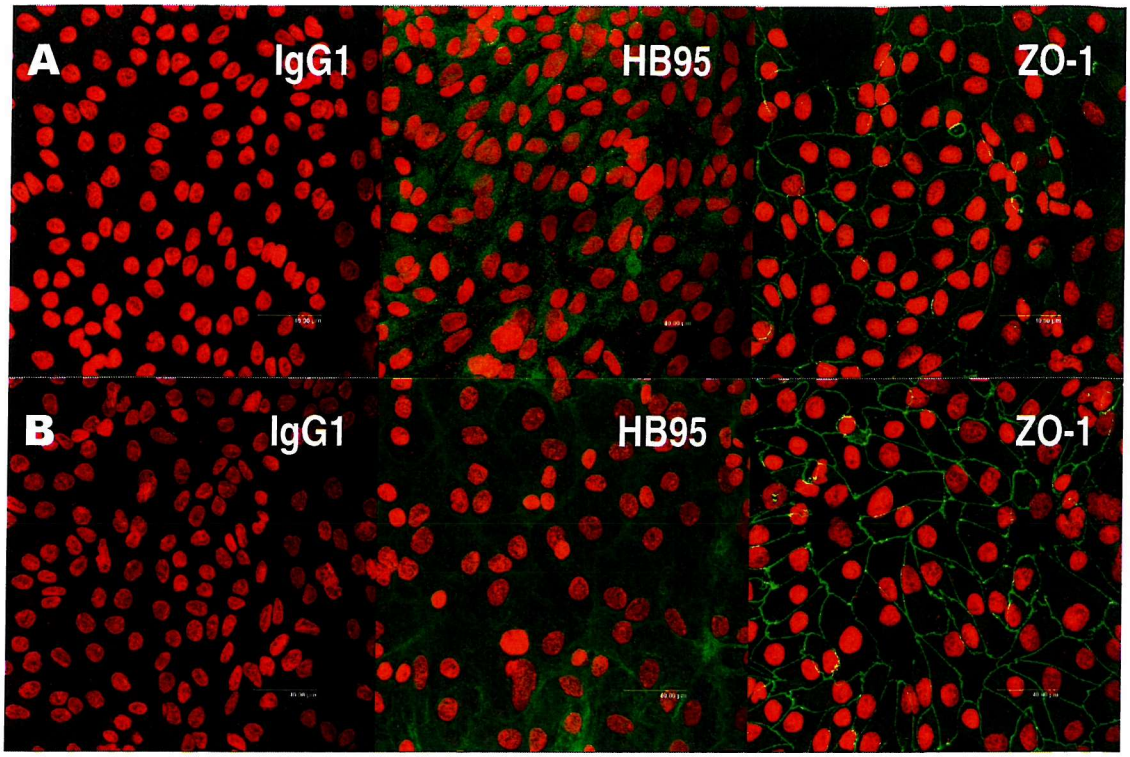

Figure 41. Effect of CsA exposure on confocal laser fluorescence characterisation of confluent monolayers of passage 1 cells kept quiesced on 6-well culture membranes for 21-23 days (A) without and **(B)** with CsA 300ng/ml, refreshed thrice weekly. Antibody signal = **green**, PI nuclear counterstain = **red**. The generally better cellular morphology is seen. It was possible to exclude background staining from the photomicrographs. ZO-1 staining is well preserved in these cells. Magnification × 63.

This was another result leading to the change of experimental protocol from the once- to thrice-weekly change of medium, and the reduction of CsA from 500 to 300ng/ml.

Figure 41 shows representative laser confocal fluorescent micrographs from the three subjects, whose passage 1 cells were quiesced with and without CsA 300ng/ml for 21-23 days, the medium being refreshed thrice weekly.

It was possible to exclude control fluorescence in these samples. The cellular tight junction morphology remains normal (although there is some cellular shedding in the CsA-exposed monolayers). MHC class I is still expressed – possibly slightly less widespread in the CsA-exposed cells than the controls.

Flow cytometry

Flow cytometric characterisation was performed on the cells with and without CsA exposure using the same protocols and monoclonal antibodies as for quiescent cell characterisation (Chapter 3).

Again, infection and technical error prevented full results, a full antibody panel only being performed on one sample (with all but ALP being performed on one other) – see Figure 42.

The only apparent difference in the characterisation between cells exposed to CsA for around 3 weeks and the control cells was the shift in ALP signal from an obvious positive-negative biphasic result without CsA to a skewed, possibly small negative and larger positive, peak with CsA exposure, suggesting either a greater proportion of proximal tubular cells in culture (ALP is a proximal marker) or an up-regulation of ALP on these cells. Unfortunately this was a single result, and although of interest, there were no repeated results to confirm this finding.

Cell cycle

Cell cycle determination was performed on cells kept in quiescence without and with CsA 300ng/ml (see Figure 43). The difference between the groups appeared to be the reduction of proliferation of cells in CsA-containing medium (greater $G_0/_1$ cell proportion, lower S- and G_2/M-phase proportions), with significantly fewer cells in S-

phase in CsA. The expected increase in the proportion of apoptotic cells was not found.

Brush border enzyme activity

Technique failures (infections ×1 and protocol error ×1) prevented results on all quiesced cells or CsA-exposed cells. The available results are shown in Table 16 and Figure 44. Given the small numbers and wide variation, no trends / patterns emerge from these results.

Table 16. Brush border enzyme activities in passage 1 cells in QM on 6-well culture membranes for 23-26 days, medium refreshed thrice weekly. Results in nmol·min^{-1}·mg protein^{-1} ± 1 standard deviation. [number of experiments].

	Alkaline Phosphatase	Gamma-Glutamyltransferase
Cells in QM	68.5 ± 47.1 [3]	343.0 ± 360.7 [2]
Cells in QM + CsA 300ng/ml	53.8 ± 32.4 [3]	405.3 ± 450.8 [2]

Cyclosporin A transcellular transport

After finding an apparent lack of effect of CsA on the cells after weekly medium change (no effect on P-gp activity or function: see CsA exposure in quiescence medium and P-gp expression and activity – preliminary experiments, Figure 88 to Figure 90), the concentration of CsA in the medium retrieved from the wells at the weekly medium changes was measured. In four wells over two weekly periods, it proved impossible to detect CsA. This was initially thought to be due to a failure of the technique, but after spiking the samples with CsA, CsA could be retrieved, suggesting that, in fact, there were undetectable levels of CsA within the samples.

The degree of cellular exposure to CsA was therefore investigated in cells whose medium was changed thrice-weekly. The results of this are shown in Figure 45.

These cells had been exposed to CsA for 8 days before the medium was taken (medium being changed on day 0 of exposure, then days 3 and 5). CsA was added to

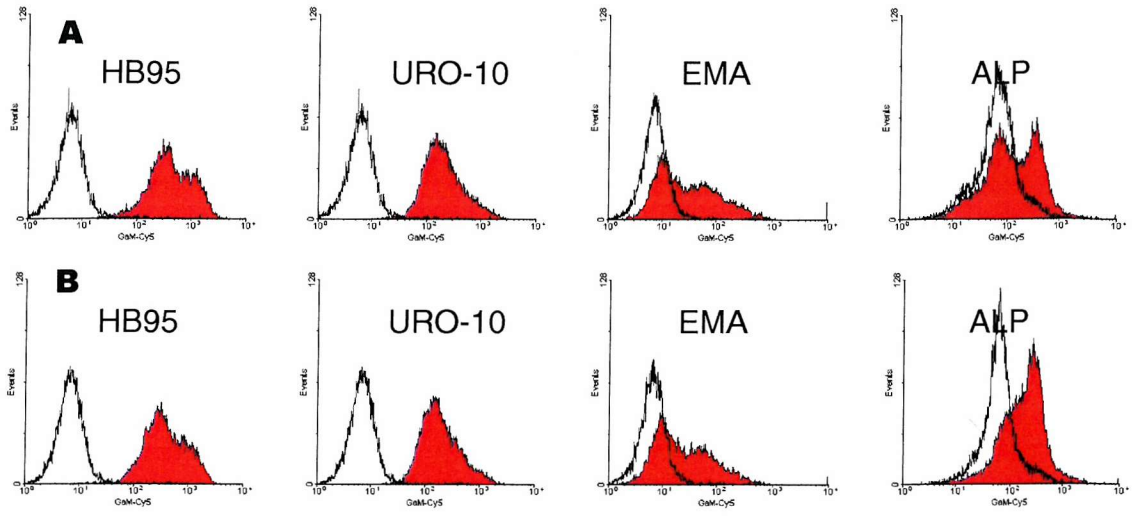

Figure 42. Effect of incubation with CsA on flow cytometric characterisation of passage 1 cells on 6-well culture membranes in QM for > 21 days. **(A)** without CsA and **(B)** with CsA 300ng/ml. Coloured trace = sample, black line = relevant control antibody. **HB95** = anti-human MHC class I antibody, **URO-10** = anti-human straight segment proximal tubule, **EMA** = anti-human epithelial membrane antigen antibody, **ALP** = anti-human alkaline phosphatase common epitope antibody. Apart from an apparent increase in the proportion of ALP-positive cells (right-hand peak higher in **B**) the flow cytometry character of the cells was maintained.

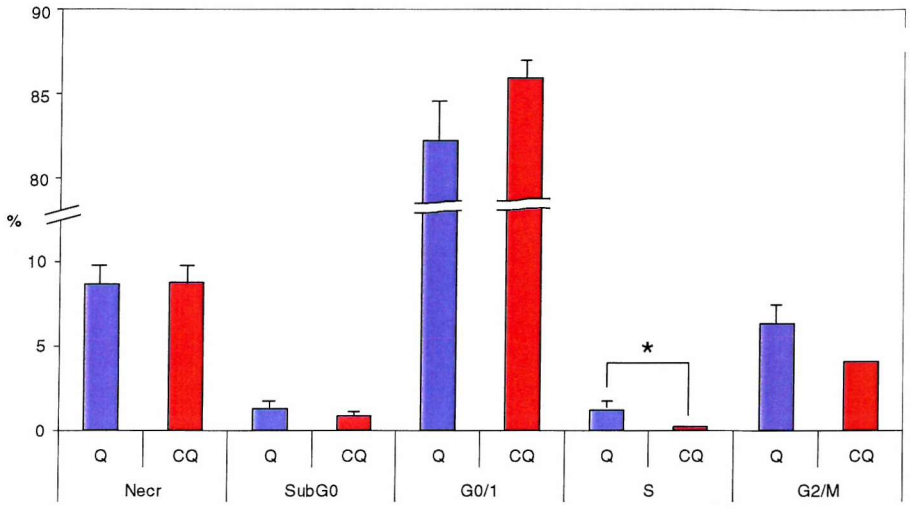

Figure 43. Effect of CsA exposure on cell cycle. Data for cells in quiescent medium without **(Q, blue)** or with **(CQ, red)** CsA. Bars = means (Q, n=10; CQ, n=13), error bars = standard error of mean. **Necr** = necrotic, **others** = phases of cell cycle. * = significant difference at 5% limit (p=0.041 Mann-Whitney U). The reduction when exposed to CsA of the proportion of cells in S-phase was significant.

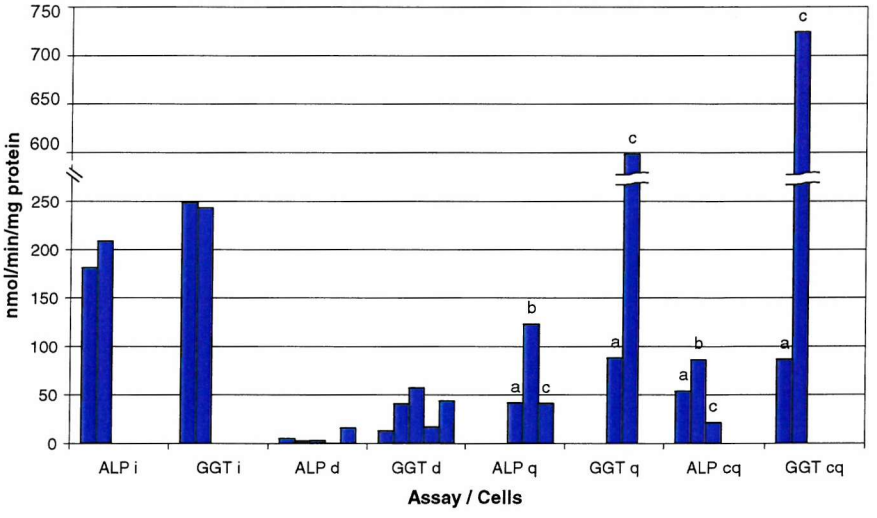

Figure 44. Brush border enzyme activities. ALP = alkaline phosphatase activity; **GGT** = γ-glutamyltransferase activity; **i** = day 0 original cell isolate; **d** = passage 0 cells at confluence in DM; **q** = confluent cells on 6-well culture membranes in QM; **cq** = confluent cells in QM; **a**, **b** and **c** = individual subjects. The wide variation in enzyme activity is shown. There is no consistent effect of quiescence or CsA exposure on these activities.

the QM from aliquots of 0.1mg/ml before pipetting 2ml into the basal medium chamber – hence 6µl of stock solution was added to each basal chamber (600ng per well).

It was therefore expected that 600ng would be recovered from each well, but as can be seen from Figure 45 the amount recovered varied substantially, and never approximated 600ng. As can be seen from Figure 46 (explanation below) the amount of CsA within the cells on the culture membrane was very small in comparison with the amount in the culture medium, so the accumulation of CsA within the cells in culture was not the reason for the reduced amount recovered.

The exposure of the cells to CsA is therefore less than intended, and was initially thought to be due to inaccurate pipetting of small volumes, but subsequent repeated testing of the original stock solution suggested that the initial vial of 100mg of CsA actually contained about 55mg. This was a salutary lesion to an inexperienced investigator (after the fact) that laboratory supplies do not necessary contain what they say on the tin (as was assumed by extrapolation from clinical pharmaceutical supplies (generally) and confirmed by communication to and from the manufacturers). A second sample of CsA was purchased, measured to be correct and used subsequently.

However, as can also be seen from the results, the amount of CsA in the basal chamber (well) reduces with increased time between medium exchanges, and it was shown that over 7 days the amount of CsA remaining un-transported in the basal chamber was minimal.

The transcellular transport of CsA was further examined in passage 1 cells in QM in culture membrane inserts over a 25-hour period, with cell-free controls. The results are shown in Figure 46. Unfortunately this could not be repeated, owing to time and equipment constraints.

The results support a hypothesis of transport of CsA across the membrane from the basal to the apical chamber at a rate less than diffusion (cell-free control insert results c2 and c25 are greater than their experimental equivalents), fortunately confirms that the culture membranes are permeable to CsA (although slowly – not reached

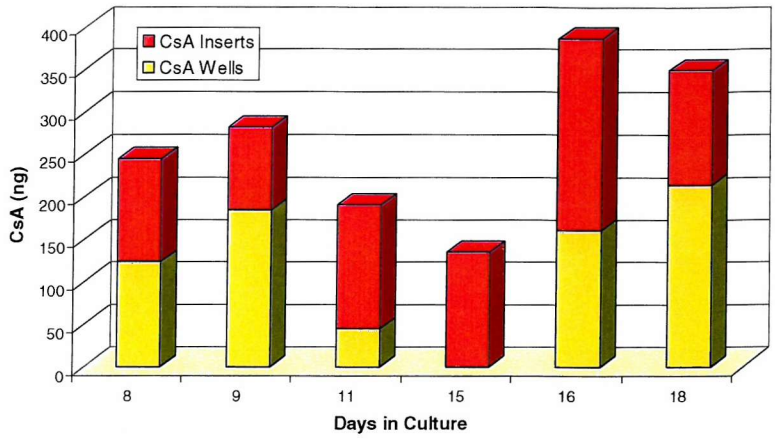

Figure 45. CsA concentrations in medium from passage 1 cells in confluent monolayers grown on 6-well culture membranes in medium with 300ng/ml CsA initially placed in the well (basal) medium. CsA wells (yellow) = concentration of CsA left within medium from the well (basal medium compartment), **CsA inserts (red)** = concentration of CsA transported to the medium in the insert (apical medium compartment). X-axis = days in culture when medium was refreshed – previous refreshment performed on day 5. In the wells, the reduction of CsA, and in the inserts, the accumulation of CsA with time is seen.

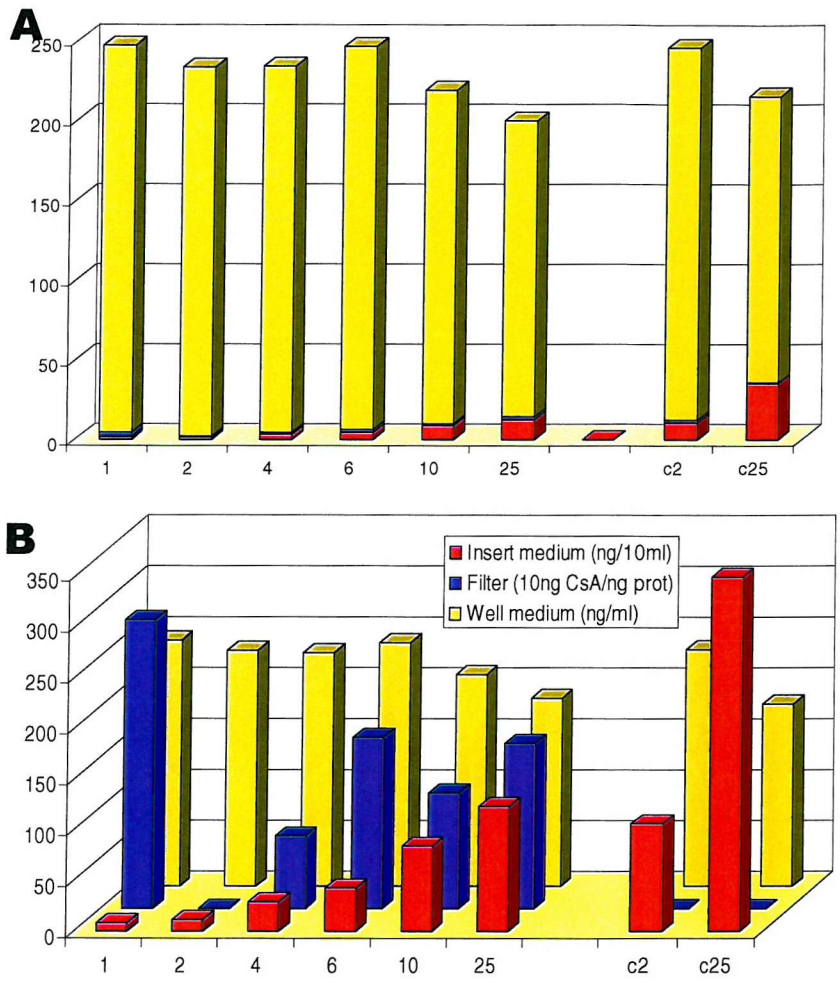

Figure 46. Bar charts showing CsA transport results: Insert medium (red) = concentration of CsA within culture insert medium; **Filter (blue)** = concentration of CsA per ng protein (cells on the culture membrane); **Well medium (yellow)** = concentration of CsA within culture well medium. X-axis = hours of incubation, c-values = control wells without cells, Y-axis = concentration of CsA, **(A)** unadjusted values in ng/ml, **(B)** insert ng/10ml, filter ng/0.1ng protein, well ng/ml. The transport of CsA from the wells to the apical chamber, once the cells are loaded with CsA is shown (the cells were not pre-loaded, so the 1 hour filter uptake of CsA appears to be artefactual – experiment needs to be repeated). The transport of CsA across the membranes was faster than that across the cell monolayer (2 & 25 results less than c2 & c25).

equilibration by 25 hours) and shows that the cells accumulate CsA.

The results also suggest that the transport of CsA depends on prior loading of the cells with CsA, as it would appear that CsA transferral to the insert (apical) medium only occurs once the cells contain CsA (the 1 hour cellular content result appears to be a significant outlier from the rest of the results, may be artefactual, and would have been repeated if time had allowed).

Lactate dehydrogenase release

Figure 47 and Figure 48 show the cellular release of LDH into the medium during culture. There are two cell populations represented:

1. cells whose medium is refreshed thrice-weekly; and
2. those undergoing medium change only every 7 days.

The assumption that fresh cell culture medium does not contain LDH was made, as this was not listed in the contents. The results show that (i) cells incubated with CsA release more LDH and (ii) cells release more LDH with increasing time in culture, although (iii) the release of LDH in culture is not linear over time.

P-gp expression experiments

Immunohistology

In order to determine the baseline expression of P-gp in the human renal tissue from which each population of cells was taken, immunohistology was performed on frozen sections of tissue. Light microscopy was used first, as a simple technique. Indirect immunohistology involves incubating tissue with primary antibodies against the epitope under investigation (which may require fixation to be unmasked – tissue preparation techniques often mask proteins and fixation (exposure of the cells, membranes and contents to compounds which may cross-link or otherwise modulate protein structures to expose or stabilise epitopes) is required to allow the antibodies to bind to the protein epitopes), then with secondary antibodies that bind to the primaries. These secondary antibodies can be bound to molecules that can be seen under the microscope, or more often bound to molecules that can cause a colour

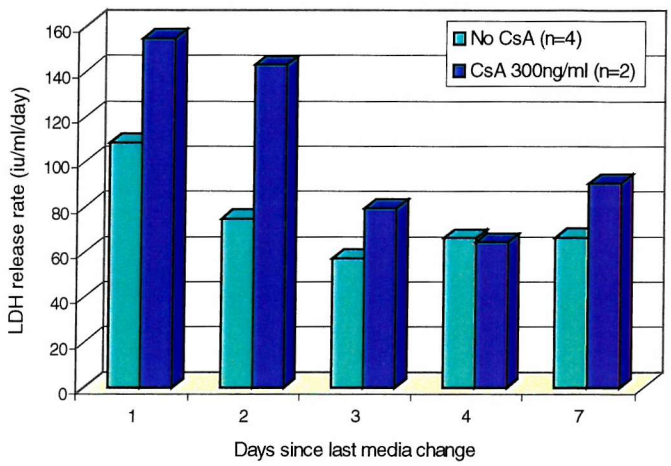

Figure 47. LDH concentration in refreshed medium from passage 1 cells in confluent monolayers on culture membranes in 6-well plates. No CsA (light blue) = medium from cells cultured without CsA, **CsA (darker blue)** = medium from cells exposed to 300ng/ml CsA in the basal chamber, **X-axis** = number of days since medium was refreshed. This shows that cells incubated with CsA release more LDH and that LDH release is not linear over time.

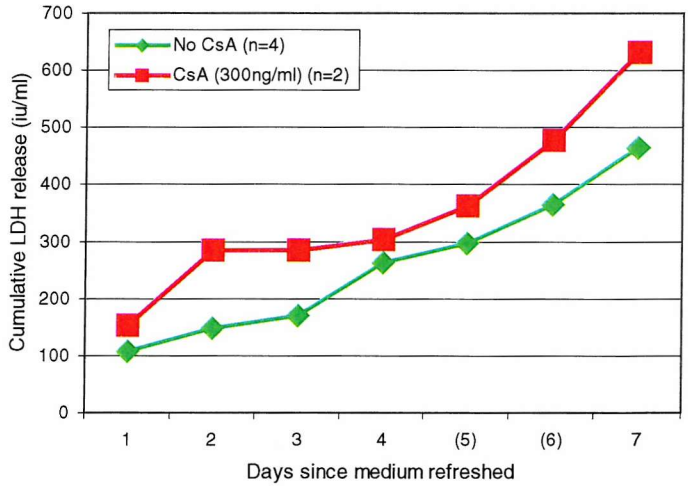

Figure 48. Extrapolated total LDH content of medium from passage 1 cells in confluent monolayers on culture membranes in 6-well plates. No CsA (green) = medium from cells incubated without CsA, **CsA (red)** = medium from cells exposed to 300ng/ml CsA in the basal chamber. **X-axis** = days since medium was refreshed (days 5 and 6 extrapolated from results for days 4 & 7). These graphs were calculated from the differences in mean LDH quantities in 1, 2, 3, 4 and 7 day samples. They imply that the release of LDH increases with increasing time in culture.

change in a third chemical added to the specimen, or attract coloured chemicals to the antibody to be seen under the microscope.

P-gp can be detected in paraffin sections, which produce much better preservation of tissue structure. However, only the MAb JSB-1 can be used on paraffin sections. This MAb has two major problems in its routine use: (i) it has been shown to cross-react significantly with pyruvate carboxylase, which is abundant in the many mitochondria of renal tubular cells, hence positive staining could be not from P-gp, and (ii) JSB-1 requires complicated unmasking / signal enhancing techniques to reliably stain P-gp, which are beyond the expertise of this laboratory. Dual staining on paraffin sections, a technique employed to identify two (or more) epitopes on the same tissue, is equally difficult.

Immunohistochemistry was therefore performed with MRK16, a human P-gp-specific antibody that is widely commercially available and can be reliably used on frozen sections. Initial attempts at streptavidin-biotin (SAB) peroxidase staining proved ineffective on sections (Figure 49 – the difference between the non-specific background staining of the negative control and the specific staining of the proximal tubules for P-gp is minimal), which was largely attributed to the widespread location of biotin and endogenous peroxidases within the kidney, causing a high degree of background 'noise' (staining in negative control sections) and reducing the 'signal-to-noise' ratio (the difference between positive staining and negative controls) of such staining techniques.

The SAB technique is shown graphically in Figure 50. While the technique is designed to reveal epitopes where there are endogenous biotin and peroxidases present, the extreme concentration of these molecules within renal tissue prevented the use of streptavidin/biotin for imaging.

Subsequent attempts with immunofluorescent techniques did not fare much better:

- FITC-conjugated secondary antibodies were limited by dramatic autofluorescence of the renal tissue (Figure 51). This shows tissue only treated with the PI red nuclear counterstain. The extensive green signal, which occupies the same wavelength as FITC emission, is attributed to autofluorescence of collagen, as it is

emitted from basement membranes and areas of tissue that appear to contain fibrosis.

- TRITC-conjugated secondary antibodies emit light further from the autofluorescence wavelength. This is shown in Figure 52, where the red light signal is obtained from a TRITC-conjugated secondary Ab binding MRK16, which shows P-gp expression. Nuclear counterstaining (very useful to further define the tissue content) is however prevented as TRITC-emitted light shares the same emission wavelength as PI and 7AAD.
- The use of Cy5-conjugated secondary antibodies was more promising, as its emission wavelength is separated from those of PI and of the (FITC-similar) collagen autofluorescence (see Figure 78). The resultant photomicrographs were still disappointing, however (Figure 53), as more Cy5-staining is visible in the interstitium than in the tubules. This may have been a problem with the blocking of non-specific epitopes, or some cross-reaction between the primary antibodies, but was not explored further.

Immunocytology

The detection of P-gp on cultured cells proved more straightforward. Cytocentrifuge preparations of cells, then monolayers of cells on 8-well chamber slides were initially investigated with the monoclonal antibody MRK16 using the SAB peroxidase technique (Figure 54). Again, however, the lack of definition of the positive staining, and the high background in the negative controls from (presumably) the endogenous biotin and peroxidases (despite the use of several different peroxidase blocking techniques) made the routine use of this light microscopic technique inappropriate to determine P-gp expression in these cells.

Immunofluorescent techniques, however, proved very useful. Titration of the antibody concentrations and variations in times of incubation led to very good definition photomicrographs being obtained (see later in this chapter).

Both transmission fluorescence and laser confocal fluorescence microscopy were possible. The optical definition of the images was slightly greater with transmission, but autofluorescence from the synthetic cell membranes with transmission, and the

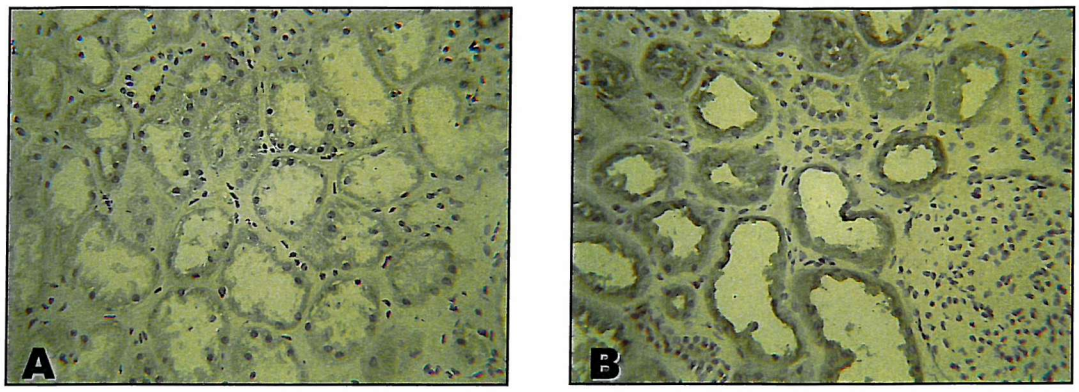

Figure 49. Streptavidin-Biotin immunoperoxidase staining of frozen sections of human renal cortical tissue. **(A)** Isotype control antibody, **(B)** MRK16 monoclonal antibody. Brown staining = positive antibody signal, blue / purple = haematoxylin counterstain. These are the best photomicrographs available and still the difference between the non-specific background staining of the negative control and the specific staining of the proximal tubules for P-gp is minimal, which was largely attributed to the widespread location of biotin and endogenous peroxidases within the kidney, causing a high degree of background 'noise' (staining in negative control sections) and reducing the 'signal-to-noise' ratio (the difference between positive staining and negative controls) of such staining techniques. Magnification × 25.

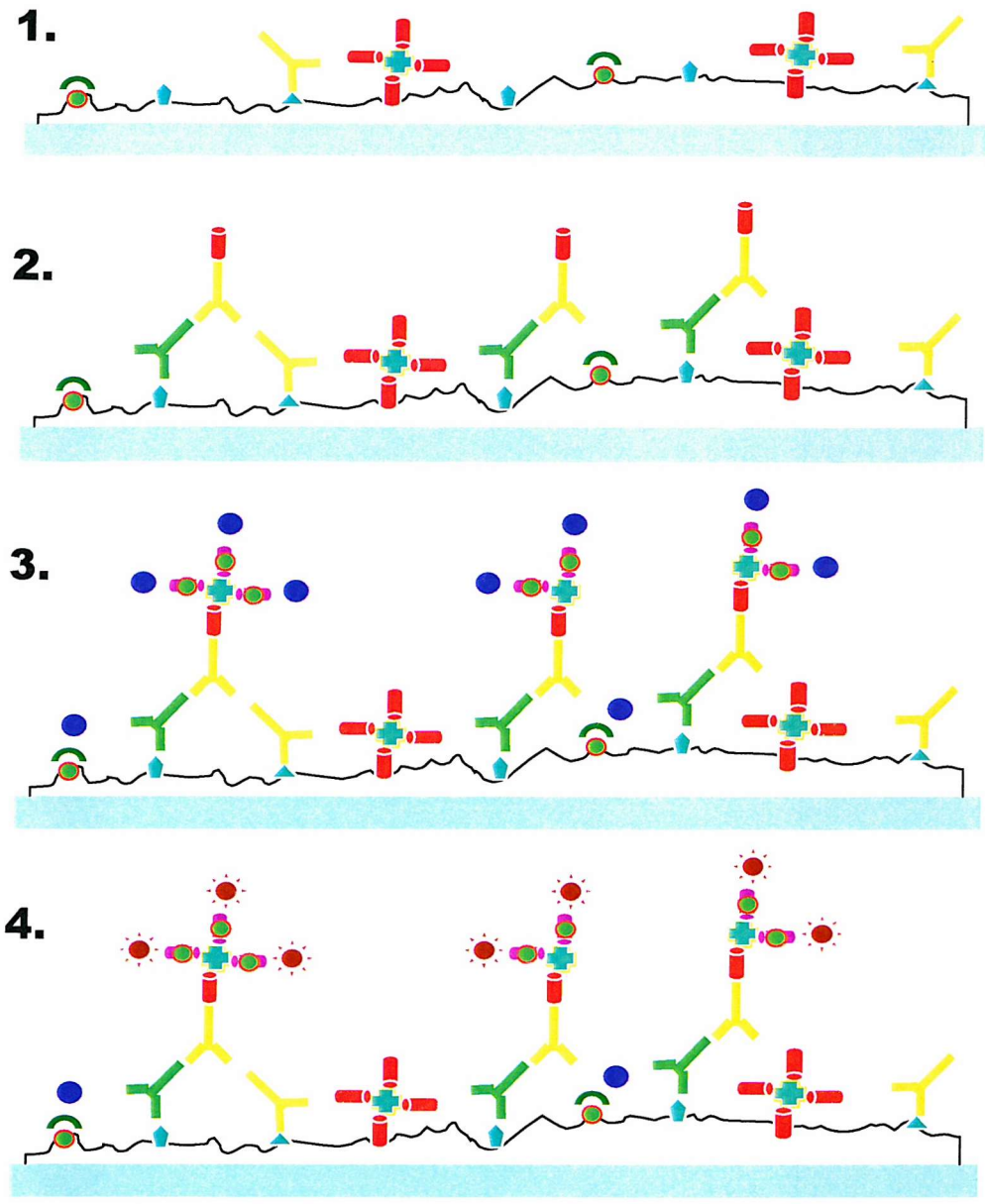

Figure 50 – Diagrammatic representation of the Streptavidin-Biotin indirect immunohistochemistry technique. = avidin, = biotin, = DAB (diamino-benzidine) substrate, = peroxidase, = peroxidase block,, = peroxidased (coloured) DAB, = mouse-like epitopes, = biotin-conjugated sheep anti-mouse secondary antibody, = streptavidin/peroxidase-conjugated biotin complexes, = target epitope, = non-specific sheep antibodies. **1.** Endogenous peroxidases, mouse-like epitopes and biotins are blocked, and the added avidin blocked with biotin (each biotin binds only one avidin). **2.** Mouse MAb binds the target epitope, then the biotin-conjugated secondary sheep anti-mouse Ab binds the primary. **3.** Streptavidin/ peroxidase-conjugated biotin complexes are added, the avidin of which binds to any available biotin. DAB substrate is added, which **4.** is converted to a coloured product by unblocked peroxidase, revealing and amplifying the presence of the target epitope.

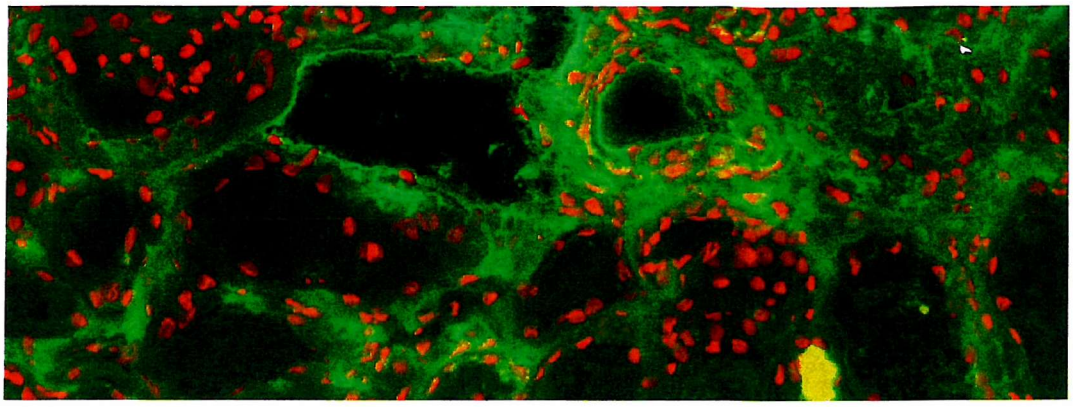

Figure 51. Immunofluorescence micrograph of frozen section with no primary or secondary antibodies, counterstained with PI (red nuclear stain**).** Magnification × 63. The **green** autofluorescence of endogenous collagen is clearly seen, which prevents staining with FITC-conjugated antibodies as these would fluoresce in the same wavelength and be indistinguishable from the autofluorescence.

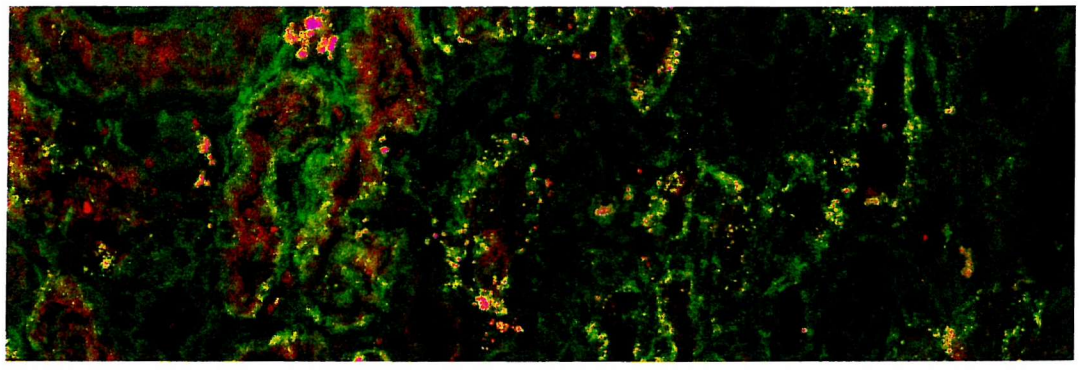

Figure 52. Laser confocal micrograph of frozen section, stained with MRK16 and TRITC-conjugated secondary antibody, without counterstaining. Magn. × 40. Again the **green** autofluorescence is clearly seen. The MRK16 (**red**) staining is present and reasonably discernable. This would not able to be differentiated from nuclear counterstaining using PI or 7AAD, which is useful to define the tissues and cells being stained.

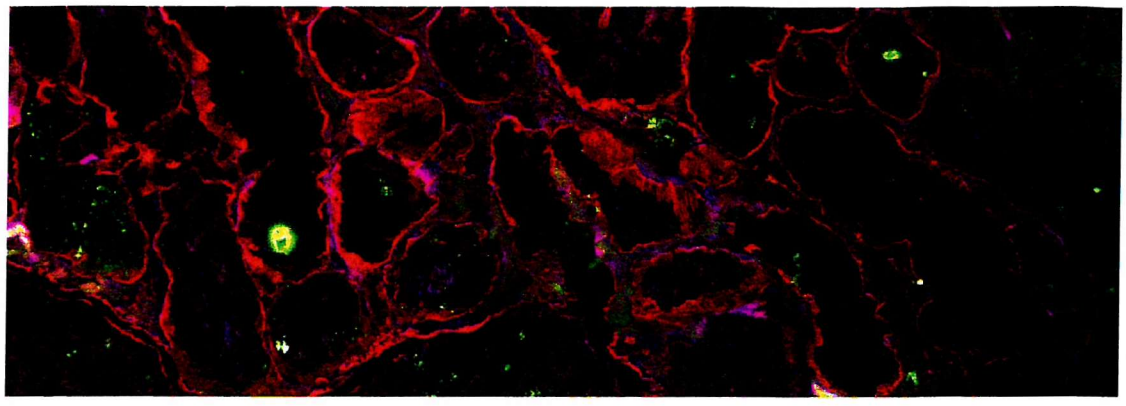

Figure 53. Laser confocal micrograph of frozen section with MRK16 and α_1-antitrypsin. Blue staining = Cy5-conjugated secondary and MRK16 primary: which should highlight brush border within the proximal tubules. **Red** staining = TRITC-conjugated secondary to α_1-antitrypsin (tubular basement membrane protein [259]). FITC channel signal reduced significantly. Magnification × 25. The blue MRK16 staining is seen in the (proximal) tubules, but is also seen strongly in the interstitium. This may have been a problem with the blocking of non-specific epitopes, or some cross-reaction between the primary antibodies, but was not explored further.

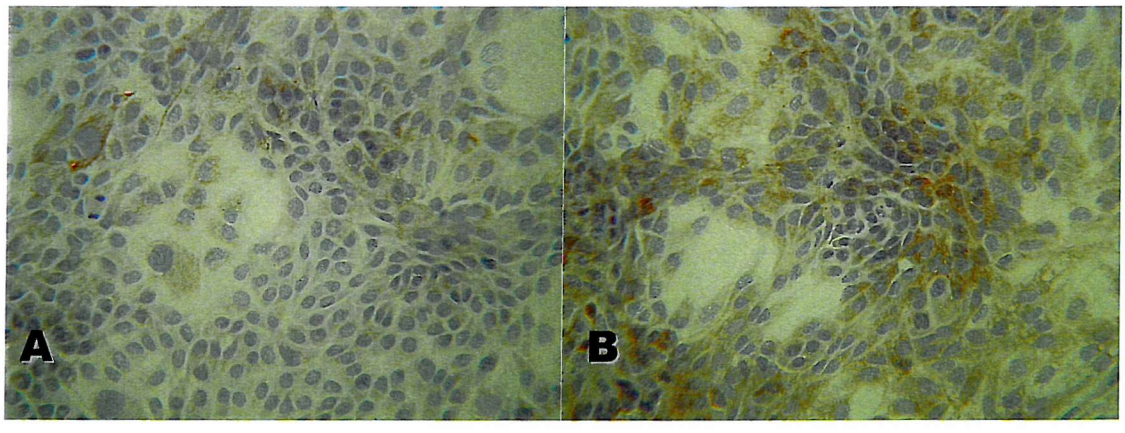

Figure 54. Streptavidin-Biotin immunoperoxidase light micrographs of confluent cells in DM on 8-well glass chamber slides. (A) Isotype control, **(B)** MRK16 primary antibody (**brown** staining). Haematolxylin nuclear counterstain = **purple**. Magnification × 25. The lack of definition of the positive staining, and the high background in the negative controls from (presumably) the endogenous biotin and peroxidases (despite the use of several different peroxidase blocking techniques) makes the routine use of this light microscopic technique inappropriate to determine P-gp expression in these cells.

greater ability to determine positive from negative signals with laser confocal microscopy (results not shown), led to the latter being adopted as the method of choice for the remainder of the project. Laser confocal microscopy also has the advantage over transmission of being able to investigate the relation of immunostaining to cell ultrastructure, as microscopic sectioning through the specimen is possible (see Appendix 3).

With the subsequent culture of cells on permeable and flexible cell culture membranes, cytocentrifuge preparations of cells became unnecessary as it became possible to image the monolayers *in situ* by cutting the membranes from their holders and mounting them directly on microscope slides. This obviously had advantages in the imaging of confluent cell monolayers and in the retained polarisation of the cells (Figure 55), which was not possible on the disrupted cells of the cytocentrifuge preparations.

Flow cytometry

In order to determine more accurately populations of cells with different cellular marker expression (which can be internal or external, endogenous or exogenous), flow cytometry can be used.

The cells under investigation need to be disrupted from the culture surface, therefore no polarisation or localisation is possible, but the degree of expression of the marker in question can be accurately defined, as can the proportions of expressing / not expressing cells.

Three anti-P-gp primary monoclonal antibodies were investigated for their appropriateness for determining P-gp expression in this cell population.

- **JSB-1**: this is one of the original monoclonal antibodies directed against P-gp. As described above the main drawbacks of its use are the cross-reactivity against (a) pyruvate carboxylase, which is present in mitochondria (which are abundant in renal tubular epithelial cells), and (b) the fact that it is directed against an internal

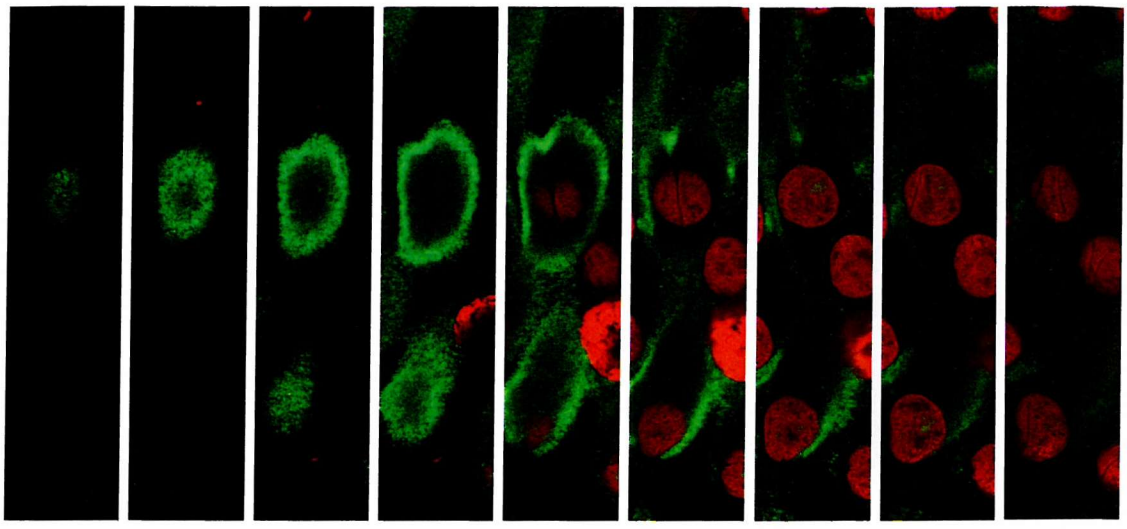

Figure 55. Laser confocal micrograph "sections through" a confluent monolayer of cells on 6-well culture membrane, stained with FITC-secondary and MRK16. **Green** signal = FITC-labelled MRK16, i.e. P-gp protein. **Red** signal = nuclei (counterstained with PI). Sections left → right are 1μm thick from the apical surface of the cells to the basal surface. The polarisation of the P-gp-staining to the apical membrane, with none intracellularly, is clearly seen. Original magnification × 63.

epitope of P-gp and the cells therefore require being permeabilised to achieve staining.

In order to specifically determine P-gp expression in these cells using JSB-1, the cells would need to be permeabilised sufficiently to expose the internal epitope of P-gp, but not enough to expose the intra-mitochondrial pyruvate carboxylase.

A variation on Protocol 11 was used, which added a permeabilisation step prior to each addition of antibody (primary and secondary), and involved washing the cells with permeabilising agent instead of wash buffer.

The results of a standard permeabilisation with varying fixation techniques are shown in Figure 56. The lack of a right-shift of the trace from the control trace (i.e. positive result) after no fixation, which is present after fixation with paraformaldehyde, shows that fixation is required for binding of JSB-1 to P-gp.

The results of a variety of permeabilising agents are shown in Figure 57. Anti-vimentin (an intracellular cytoskeletal component [260]) antibody was used as a positive control to determine that the cellular membrane had been permeabilised, and an anti-mitochondrial inner-membrane antibody [261] was used to determine whether the mitochondrial membranes had been permeabilised. In the unfixed, un-permeabilised results on the top line of Figure 57, although a proportion of cells have a strong JSB-1 signal (right-most peak greater signal than right-most control peak), and the anti-mitochondrial antibody signal is negative (trace same as control), only a proportion of cells are vimentin-positive, when all should stain for this ubiquitous structural element. Both the second and third lines of Figure 57 show positive vimentin and JSB-1 signals, but slightly positive anti-mitochondrial antibody results. Repeating this on subsequent subjects (n=12) produced no standard results. Although it appeared that JSB-1 staining was possible, the permeabilisation was not reliable, so this MAb was not used further.

- **MRK16**: this anti-P-gp monoclonal antibody is directed against a human-specific external epitope, and therefore cellular permeabilisation is not necessary for P-gp binding.

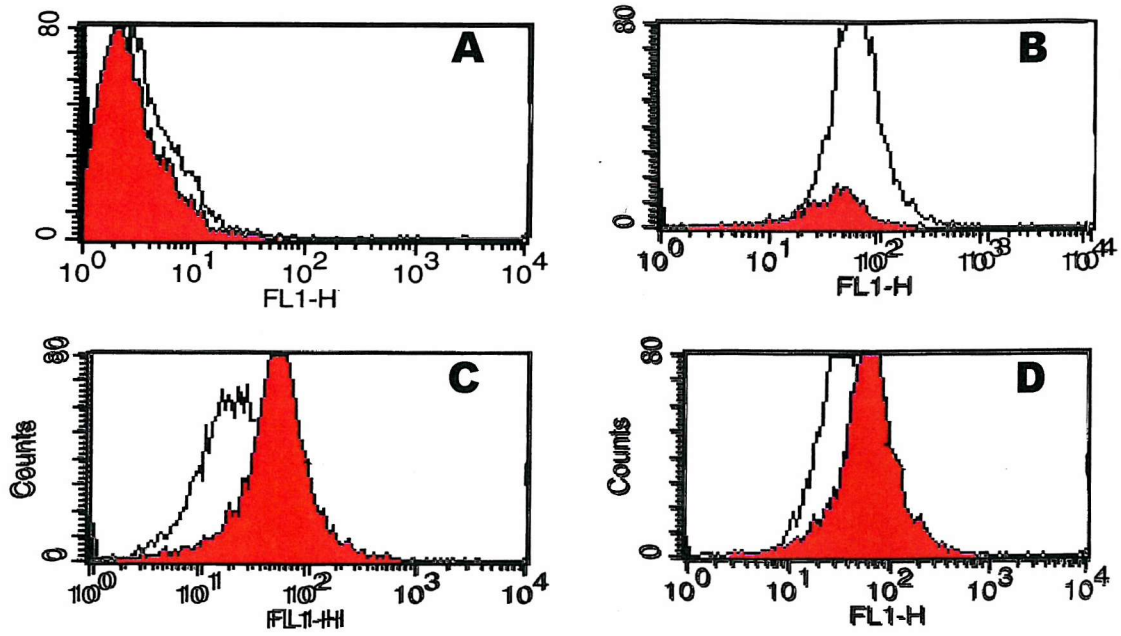

Figure 56. Representative flow cytometry histograms of confluent cells disrupted from DM and stained with JSB-1 using differing fixation techniques. All panels: **filled trace** = JSB-1, **line** = appropriate isotype control; **(A)** = no fixation or permeabilisation: subsequent traces all permeabilised with 0.05% Saponin; **(B)** = 2% PFA fixation for 10mins **(C)** = 2% PFA for 30mins **(D)** = 2% PFA for 60mins. The requirement for fixation and permeabilisation is shown (only with saponin and sufficient time in PFA does the antibody signal become distinct (right shift) from the control.

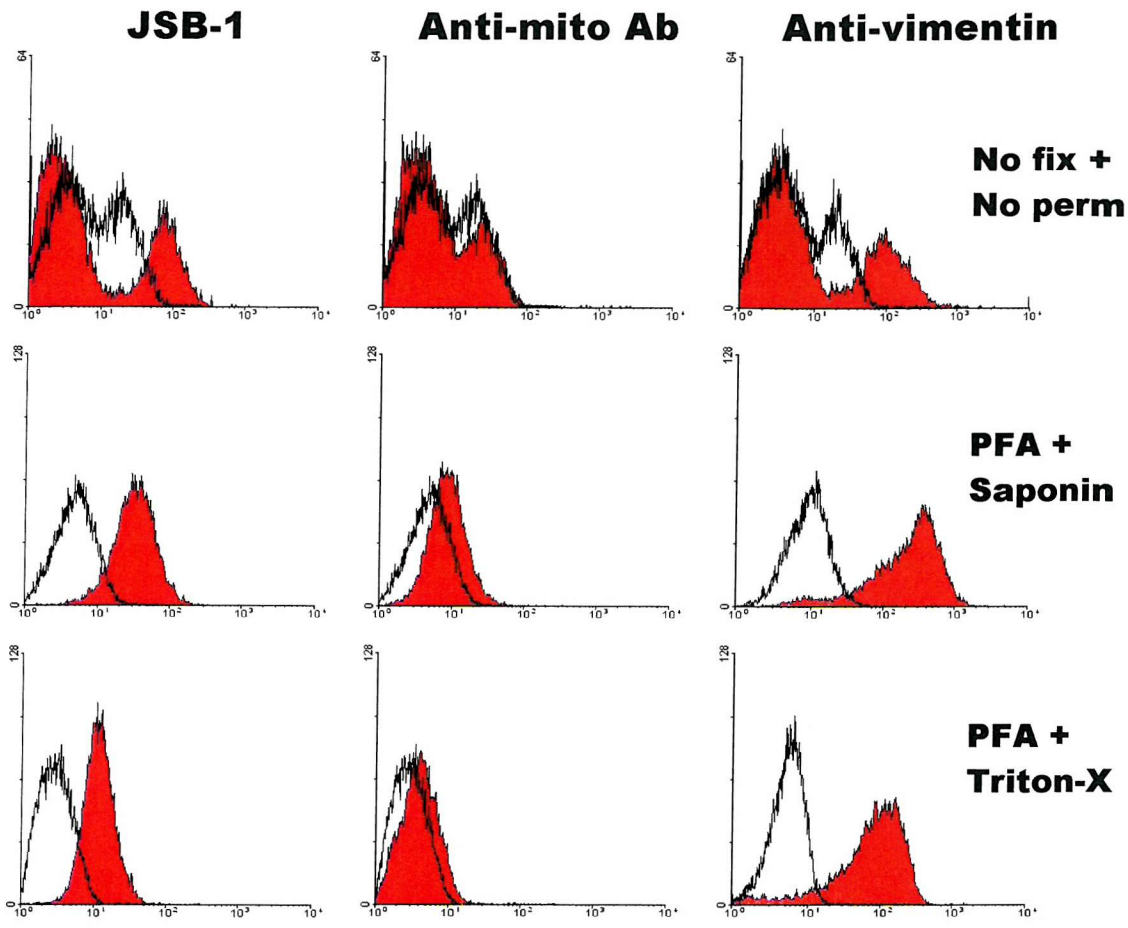

Figure 57. Representative flow cytometry histograms of confluent cells disrupted from DM and stained with JSB-1 using differing permeabilisation techniques. All panels: **filled trace** = relevant antibody, **line** = appropriate isotype control; **Anti-Mito Ab** = Anti-Mitochondrial inner membrane antibody, **PFA** = 2% PFA fixation for 60mins, **Saponin** = permeabilisation with 0.05% Saponin, **Triton-X** = permeabilisation with 0.1% Triton X-100. The requirement for fixation and permeabilisation is shown (all cells should be Vimentin positive). However, the non-permeabilised JSB-1 trace is more appropriate than the permeabilised, as not all cells should be positively staining (right (positive) and left (negative) peaks). The anti-mitochondrial inner membrane antibody signal should be negative, if the interior of the mitochondria is not being exposed to the antibodies. This is likely to explain the single positive JSB-1 peak, as JSB-1 would be allowed to bind to pyruvate carboxylase within the mitochondria. Moreover, the effects of fixation and permeabilisation vary greatly between subjects.

However, as can be seen from Figure 58, fixation is still required for P-gp detection (there was no positive [vs. control] peak for the MRK16 signal without fixation or with fixation with 2% PFA for less than 30 minutes).

In the next section it will be shown that fixation of the cells interferes with the simultaneous investigation of P-gp activity, therefore a third anti-P-gp monoclonal antibody, whose product literature suggested that it might be used without fixation, was investigated in the same way:

- **Neomarkers' Anti-P-gp monoclonal antibody** is also directed against an external epitope, and was suggested to not require fixation to unmask its binding site on the P-gp molecule.

The results of the determination of the appropriate concentration for P-gp detection, and of the fixation required are shown in Figure 59. Without fixation there is no difference between the traces for the antibody under investigation and the negative isotype control, suggesting no binding to P-gp. When fixed, 2.5µg of the Neomarker's antibody was sufficient to produce a positive peak, so the lack of a positive signal without fixation was felt to be due only to the lack of fixation.

These results showed that this antibody also required fixation for P-gp binding, so had no advantage over the more commonly reported MRK16 and was therefore not used in further experimentation.

P-gp activity experiments

In order to determine the activity of P-gp, a substrate of P-gp that would be reliably taken up by these cultured primary human renal tubular epithelial cells and mainly actively effluxed from the cells by P-gp, was required. The available literature suggested Rhodamine (R)123 as an appropriate substrate, the intracellular concentration of which could easily be determined by flow cytometry.

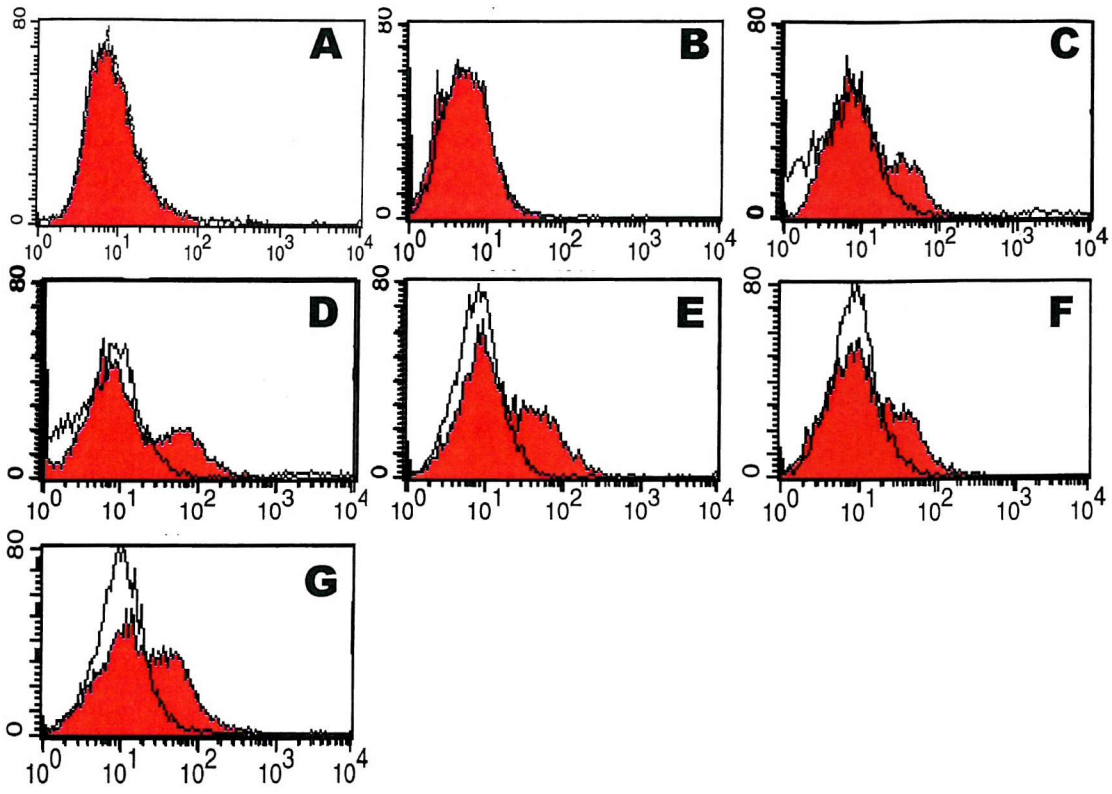

Figure 58. Representative flow cytometry histograms of confluent cells disrupted from DM and stained with MRK16 using differing fixation techniques. All panels: filled trace = relevant antibody, line = appropriate isotype control; **(A)** = no fixation, **(B)** = fixation with 2% PFA 20mins, **(C)** = fix. with 2% PFA 30mins, **(D)** = fix. 2% PFA 60mins, **(E)** = fix. 4% PFA 10mins, **(F)** = fix. 4% PFA 30mins and **(G)** fix. 4% PFA 60mins. The requirement for fixation is shown. The greatest signal and differentiation from the negative cells (highest peak and shifted furthest to the right) is seen with 2% PFA for 60mins **(D)**: this was therefore used for subsequent studies.

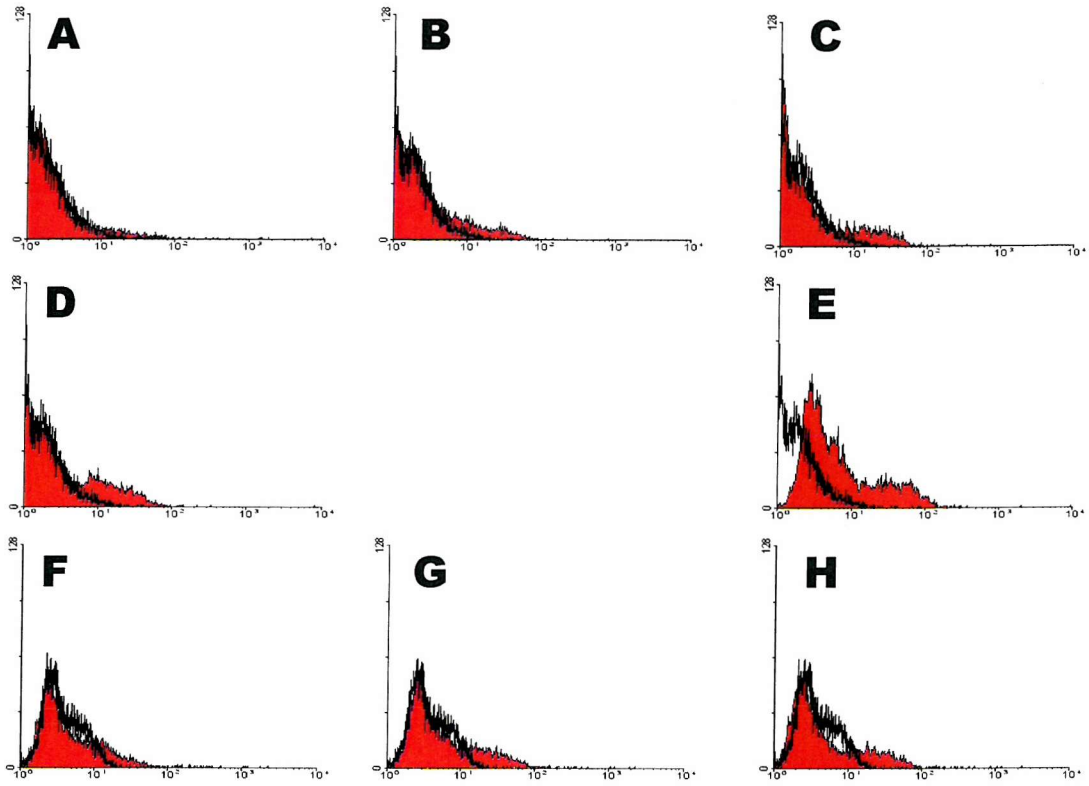

Figure 59. Representative flow cytometry histograms of confluent cells disrupted from DM and stained with Neomarkers' Anti-P-gp monoclonal antibody 2.5µg/ml using differing fixation techniques, and effect of Ab concentration. All panels: filled trace = relevant antibody, line = appropriate isotype control; **(A)** = no fixation, **(B)** = fixation with 2% PFA 10mins, **(C)** = fix. with 2% PFA 30mins, **(D)** and all subsequent = fix. with 2% PFA 60mins, **(E)** = MRK16 on same cells for comparison, **(F) =** Neomarkers' anti-P-gp Ab 1µg/ml, **(G)** = 2.5µg/ml and **(H)** = 5µg/ml. The requirement for fixation of the Neomarkers' antibody is shown (lack of positive signal peak without PFA fixation).

Determination of R123 uptake

The reliability of the uptake of R123 into the cells, and the determination of its concentration by flow cytometry was examined first.

Figure 60 shows representative flow cytometry results from cells disrupted from their culture surface and incubated for 30 mins at 37°C with R123 0.5μg/ml in DMEM:Ham's-F12 medium / 10% FBS.

From the literature, it is assumed that the uptake of R123 is passive, therefore probably follows first-order kinetics and the total amount of R123 which each cell can accumulate is finite (presumably determined by the cells' volume and dependent on the concentration of R123 in the external medium). The effect of time of the uptake of R123 into the cells is shown in Figure 61, which confirms these assumptions (cells saturated by 40mins, final cell R123 fluorescence proportional to forward scatter, i.e. cell size).

Efflux pathway(s) will be removing R123 from these cells while they accumulate it by diffusion. It can be assumed from these results that as the cells accumulate R123 and reach steady state / saturation the rate of passive uptake exceeds the efflux rate. The impact of efflux on accumulation is detectable but not large, and is shown later.

As can already be seen, it was not always possible to use the same number of cells for each experiment. Indeed, the numbers of cells often varied between different tubes within the same experiments (the same volume of cell suspension was used for each separate tube, but with volumes such as 10-20μl significant variations in cell numbers were inevitable).

The effect of the variation of cell numbers between samples on the uptake of R123 was therefore investigated, as any significant difference in the accumulation and therefore the R123 fluorescence signal would interfere with and probably confound any experimental results. Figure 62 shows the negligible effect of cell number on the accumulation of R123.

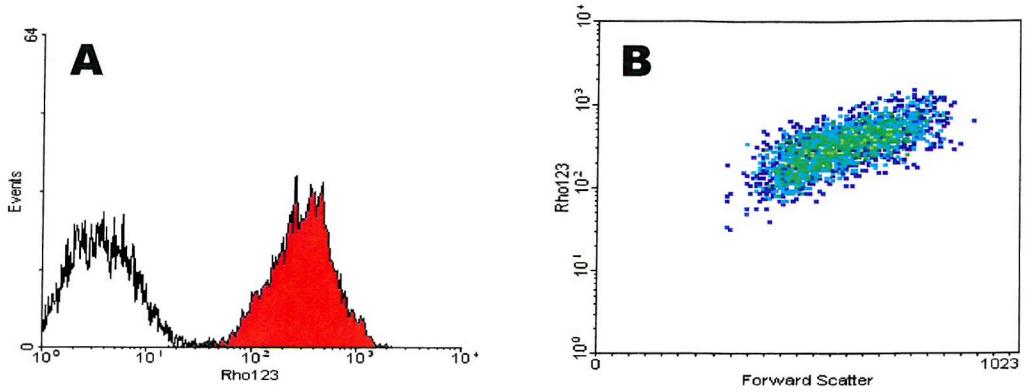

Figure 60. Flow cytometric investigation of cells incubated with R123. (A) histogram of the first fluorescence channel (FL-1) signal and **(B)** density plot of FL-1 against Forward Scatter (FSC – measure of cell size, blue = low to red = high density). Cells incubated for 30mins with R123 0.5µg/ml. The filled trace is of the cells exposed to R123, the line is the control – cells incubated in the same medium for the same time without R123. Each result is of 5000 cells. The normal distribution and narrow spread of the signal is evident: the majority of the spread is due to a positive correlation of R123 signal with cell size.

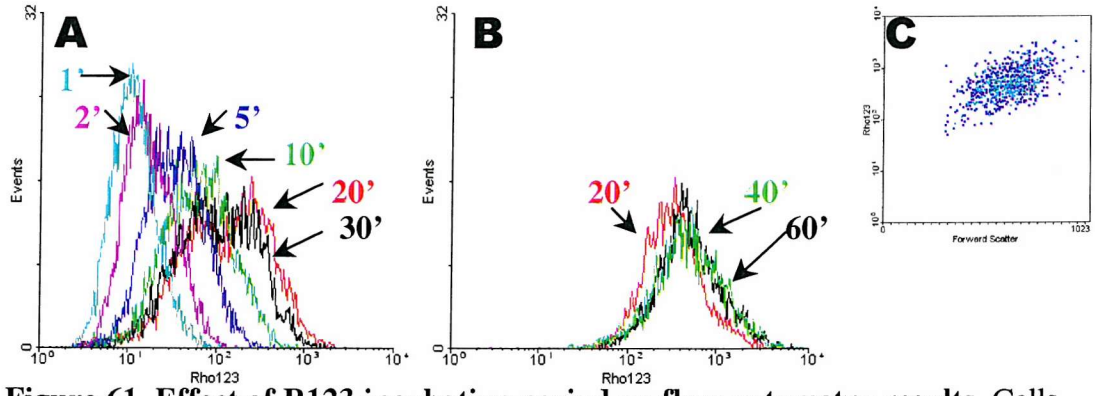

Figure 61. Effect of R123 incubation period on flow cytometry results. Cells incubated with R123 0.5µg/ml. **(A)** plots of 1, 2, 5, 10, 20 and 30min incubations (5000 cells each); **(B)** plots of 20, 40 and 60min incubations (2500 cells each: **A** and **B** = separate experiments); **(C)** density plot of cells incubated with R123 for 60mins (from experiment **B**) – again shows signal is proportional to and spread is mainly due to variation in cell size (forward scatter signal). For clarity, control cell histograms are not shown, but all had minimal FL-1 signal as shown previously. Incubation times indicated (' = mins).

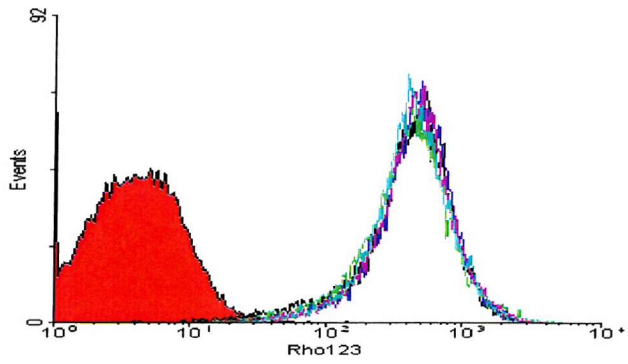

Figure 62. The effect of variation of sample cell number on the accumulation of R123. The numbers vary by 16-fold between the lowest and the highest samples (approximate numbers ($\times 10^4$): 2, 4, 8, 16 and 32). The **filled trace** is the control cells, the **coloured lines** the individual sample histograms. (Geometric means 403, 406, 466, 473 and 446 respectively – control cells 4.35, Pearson's correlation GM versus cell number R^2= 0.2443.) There is clearly no effect on the accumulation of R123 of the number of cells in the sample.

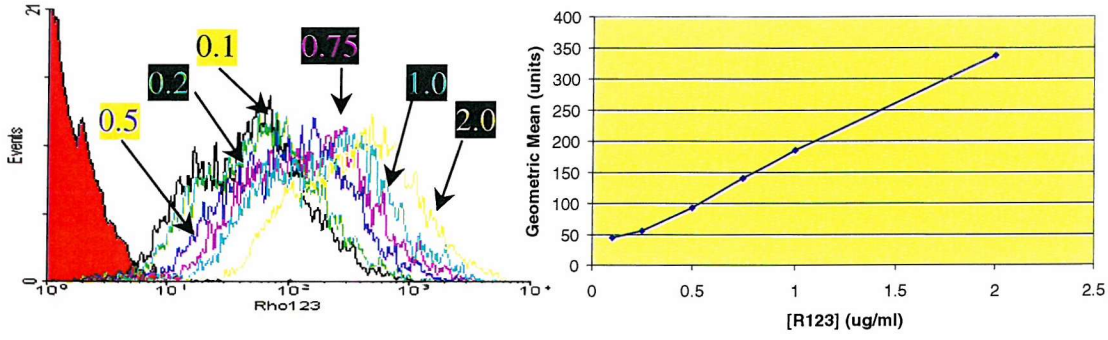

Figure 63. The effect of R123 concentration on FL-1 flow cytometric fluorescence signal. Coloured unfilled lines = traces for each R123 concentration (0.1, 0.25, 0.5, 0.75, 1.0 and 2.0µg/ml), **filled line** = control cells. **Line graph** = correlation of FL-1 geometric mean versus R123 concentration. The expected linear relationship between the concentration of R123 and the GM of the FL-1 signal is clearly shown.

The effect of a variation in the concentration of R123 was also investigated, to confirm the initial assumptions that passive accumulation would lead to a maximal intracellular concentration of R123 equivalent to that of the surrounding medium. The accumulation over 30mins was found to be proportional to the concentration of R123 (see Figure 63). In order to detect the entire population of cells with the higher concentrations of R123, the amplification of FL-1 signal was reduced, leaving the control cells as mainly undetectable (zero fluorescence, reducing the accuracy of any mathematical calculation of differences between control and sample cells).

These findings, and the easy discrimination of cells accumulating R123 at 0.5μg/ml from those that had not, led to the adoption of 30 minutes accumulation and this concentration of R123 as the standards for subsequent experimentation (n.b. higher control cell signals in previous figures = higher FL-1 amplification).

Determination of R123 efflux

According to the literature, R123 is a substrate of P-gp. As such it should be actively pumped (if available to P-gp) from the cultured human renal tubular cells (which should express P-gp) in a time-dependent manner.

The efflux of R123 should be competitively inhibited by inhibitors of P-gp activity, and should not be apparent in cells that do not express P-gp, which should moreover not be affected by P-gp-activity inhibitors.

The time-dependent efflux of R123 was therefore determined, the results of which are shown in Figure 64. From this it can be inferred that the complete efflux of available R123 is achieved by 60mins, although subsequent efflux experiments used 90mins as standard.

The influence of P-gp activity on R123 efflux was examined in a number of ways:

1. by comparing the efflux from primary human renal tubular epithelial cells (which should express P-gp) with that in LLC-PK1 cells (a porcine renal tubular epithelial cell line which expresses negligible P-gp [262;263]) – see Figure 65.

2. by determining the effect of competitive inhibitors of P-gp function on R123 efflux – see Figure 66 to Figure 69.

3. by determining the effect of inhibitors of other pathways, such as the organic cation efflux pathway, in case R123 efflux is partly / fully mediated through this pathway rather than P-gp [174;263]– see Figure 70.

To summarise these results:

1. When pre-incubated with R123 then placed in R123-free medium, there was a much greater loss of R123 from cells that should express P-gp (human tubular epithelial cells) than from those which do not (LLC-PK1 cells). This finding supports the literature that R123 is a P-gp substrate, and the assumption that these cultured human cells express P-gp.

2. The reduction of the efflux of R123 from the human cultured cells by known P-gp inhibitors in a concentration dependent manner further supports the assumption that the efflux is P-gp mediated.

3. The lack of effect of these P-gp inhibitors on the efflux of R123 from cells that do not express significant levels of P-gp supports the R123-efflux-P-gp link still further.

4. The true effect of the P-gp inhibitors on R123 efflux was further strengthened by the lack of effect of Mg-ATP, ethanol and sodium hydroxide on efflux (and/or accumulation). These experiments also showed that Mg-ATP was not required for vanadate-mediated P-gp inhibition.

5. The lack of the inhibition of R123 efflux by cimetidine refuted the literature (in rats[174]) that R123-efflux was mediated by the organic cation pathway, although there was a dose-related *increase* in R123 loss from the cells exposed to cimetidine which is not explained (i.e. potentiation of P-gp activity (cimetidine is a substrate of P-gp [264] – perhaps the activity of P-gp is enhanced acutely by cimetidine [c.f. chronically by CsA[235]]) or other route of R123 efflux: possibly a

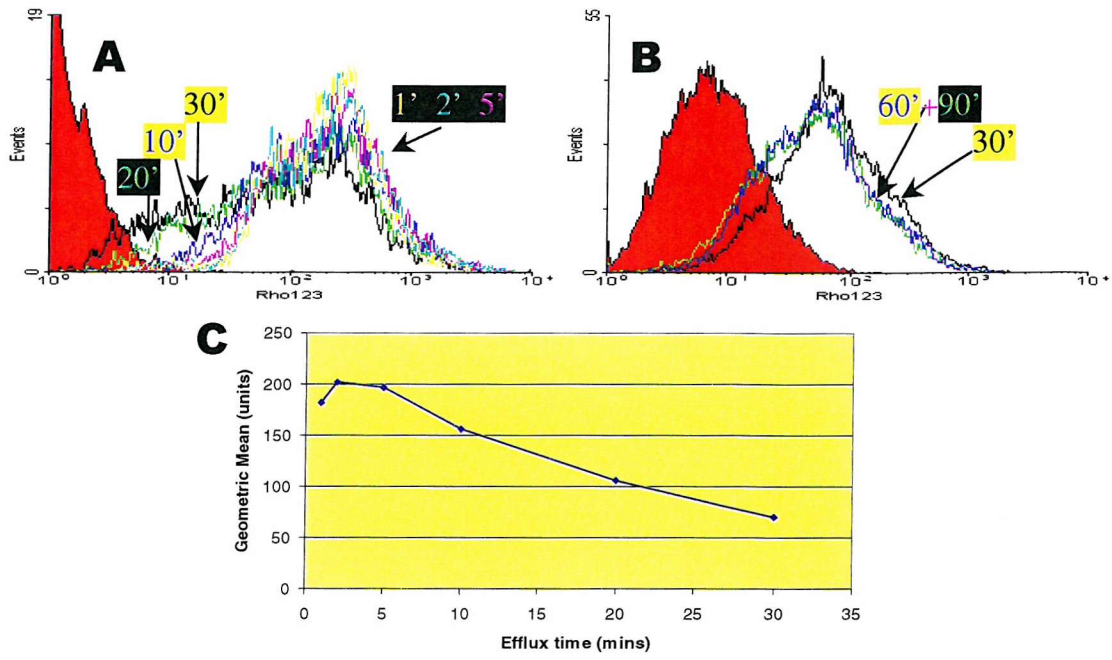

Figure 64. Effect of efflux time on flow cytometry histograms of cells pre-incubated with R123. 30min pre-incubation with R123 0.5µg/ml. **(A)** Efflux times 1, 2, 5, 10, 20 and 30mins; **(B)** Efflux for 30, 60 and 90mins (different experiment); **(C)** line graph of geometric means of traces from experiment **A**. The efflux appears to be exponential after 5 mins as expected, and completed by 60 minutes (some residual signal remains – R123 is taken up by mitochondria).

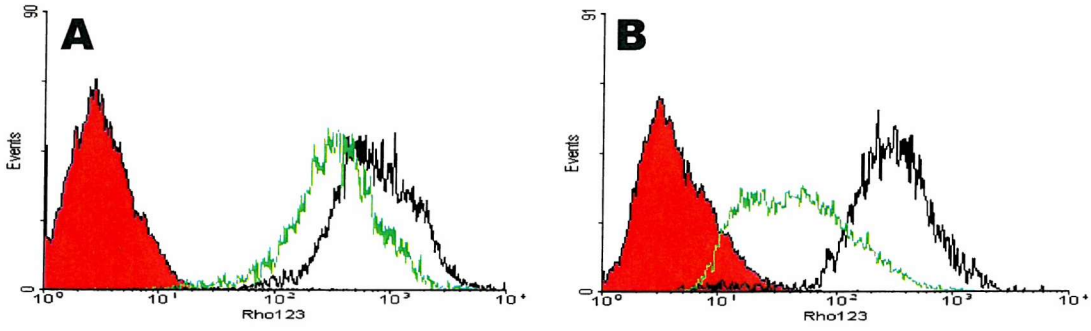

Figure 65. Comparison of R123 efflux between a commercial porcine cell line and primary cultured human renal tubular epithelial cells. **(A)** LLC-PK1 cells, **(B)** primary human cells. In both histograms filled line = control cells, black line = cells accumulated R123 0.5µg/ml for 30mins, green line = cells pre-accumulated R123 0.5µg/ml for 30mins then transfered to R123-free medium at 37°C for 90mins. Minimal efflux from the porcine cells (consistent with diffusion) is seen, while much greater efflux from the P-gp expressing HTECs is seen.

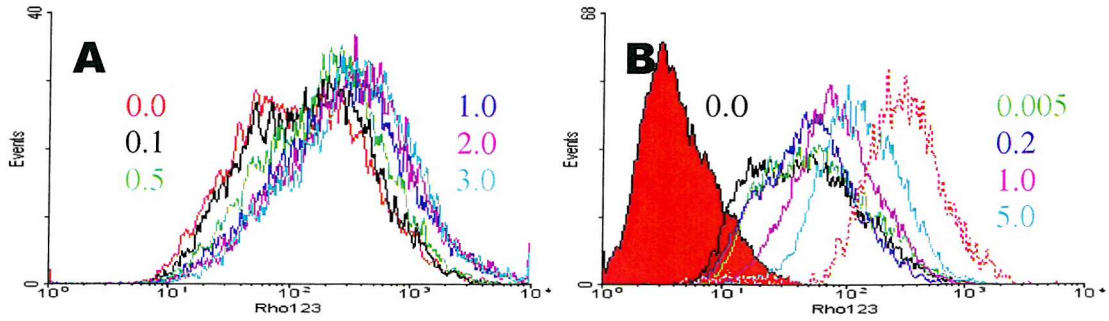

Figure 66. Effect of different concentrations of known inhibitors of P-gp activity on R123 efflux. (A) Cyclosporin A (concentrations in µg/ml), **(B)** Sodium orthovanadate (V_i – concentrations in mM) + 0.8mM Mg-ATP. **Red lines** in **(B)** = controls: **filled** = no R123, **dotted** = accumulation with no efflux. **All others** pre-incubated with R123 as above, then effluxed in R123-free medium for 90mins. Increasing concentrations of V_i increasingly reduce the efflux of R123 from these cells, suggesting an increasing inhibition of P-gp efflux activity.

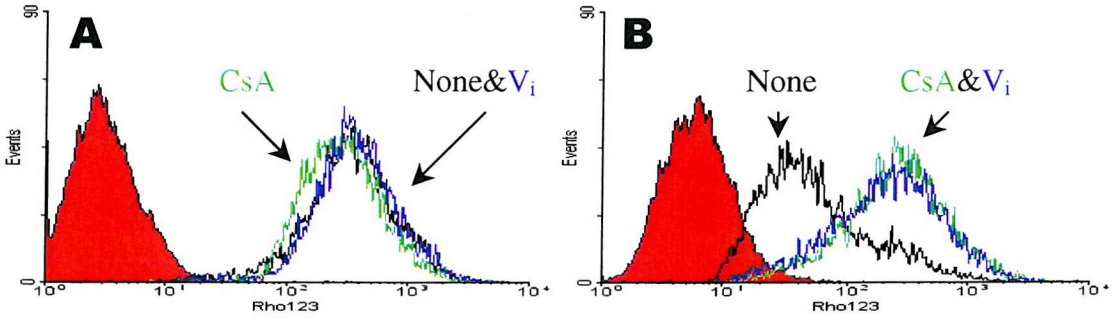

Figure 67. Comparison of effects of known inhibitors of P-gp activity between transformed porcine cell line and primary human cells. (A) LLC-PK1 cells, **(B)** primary human cells. Filled red lines = controls, all others pre-incubated with 0.5µg/ml R123 for 30mins, then effluxed in R123-free medium for 90mins. Black line = efflux in medium only, green line = efflux in medium with 2.5µM CsA, blue line = efflux in medium with 5mM sodium orthovanadate (V_i) + 0.8mM Mg-ATP. The lack of difference between CsA, V_i and none signals in the porcine cells, and the reduction of efflux in the HTECs with both CsA and V_i, support the hypothesis that P-gp effluxes R123 from HTECs but not LLC-PK1 cells.

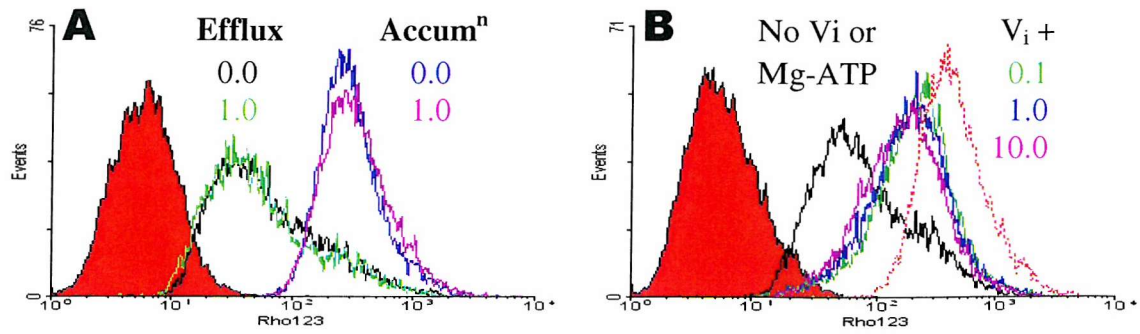

Figure 68. Effect of different Mg-ATP concentrations with sodium orthovanadate on R123 efflux. **(A)** effect of Mg-ATP on R123 accumulation (0.5µg/ml R123 for 30mins) and efflux (pre-incubated in 0.5µg/ml R123 for 30mins then placed in R123-free medium for 90mins), **(B)** effect of different Mg-ATP concentrations on V_i-inhibition (5mM) of R123 efflux (pre-incubated and effluxed as previous). Concentrations of Mg-ATP = mM. **Filled lines** = R123-free controls. **Dotted line** = control: R123 accumulation (0.5µg/ml R123 for 30mins) without efflux. There is no effect of Mg-ATP alone on efflux or accumulation. There appears to be no effect on the efflux of R123 of the concentration of Mg-ATP with V_i.

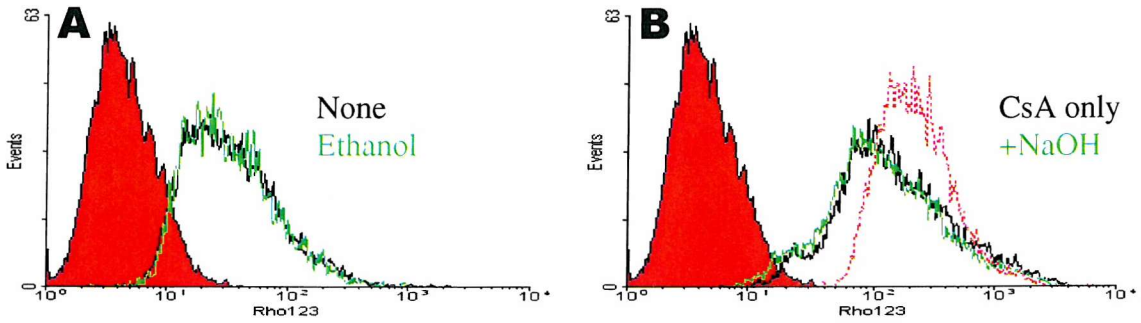

Figure 69. Effects of the vehicles of cyclosporin A and sodium orthovanadate on the efflux of R123. **(A)** 0.2% ethanol, **(B)** Cyclosporin A ± 0.05N sodium hydroxide (NaOH). **Filled lines** = R123-free control cells. All others pre-incubated with 0.5µg/ml R123 for 30mins. All but dotted red line: then effluxed ± vehicles in R123-free medium for 90mins. There is no effect of the vehicles on efflux.

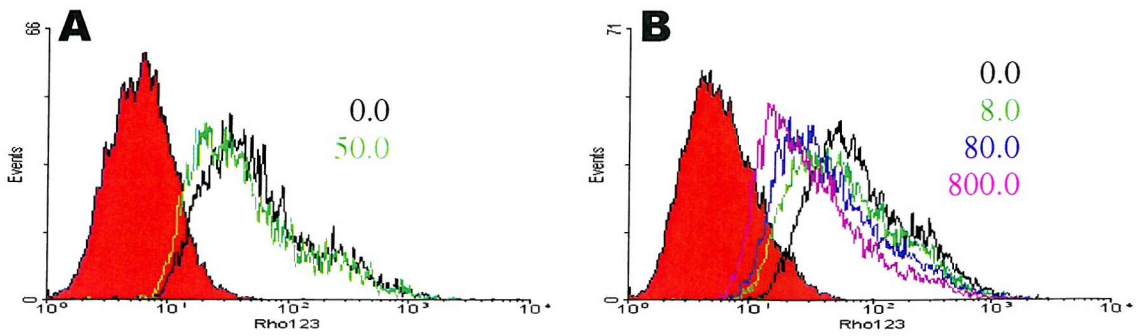

Figure 70. Effect of cimetidine on R123 efflux. (A) cimetidine 50μM versus none, **(B)** different concentrations of cimetidine (μM). **Filled lines** = R123-free control cells. **All other lines** = cells pre-incubated with R123 0.5μg/ml for 30mins then effluxed ± cimetidine in R123-free medium for 90mins. There appears to be an increase in efflux of R123 from these cells with increasing concentrations of cimetidine, an organic cation pathway inhibitor. In rats, cimetidine blocks the efflux of R123 as this is mediated through the cation pathway, which does not appear to be the case with these human cells. The increase in efflux may be related to displacement of the R123 from the cellular mitochondria, or a cellular membrane permeabilisation effect.

direct cell / mitochondrial membrane-permeabilisation effect, or maybe by increasing the availability of R123 to P-gp by displacing it from mitochondria).

The aim of the determination of the efflux of R123 was to gain a measure of the efflux activity of P-gp in a cell population. The reproducibility of this measurement can be seen in most of the figures (the overlapping of histogram lines in efflux implies the same degree (of spread) of efflux across the population).

Further evidence for P-gp activity

While the cells are accumulating R123, P-gp efflux, an active process and therefore possible against a diffusion gradient, should still be occurring, reducing the maximum uptake of R123. Theoretically, greater R123 accumulation could be achieved by the addition of P-gp inhibitors to the R123 solution (see Figure 71).

The effects of the P-gp inhibitors CsA and sodium orthovanadate on the accumulation of R123 in human primary cultured tubular cells and porcine transformed tubular cell line are shown in Figure 72. In the human cells, a small but reproducible increase in uptake is associated with incubation with the P-gp inhibitors. This was a representative result from at least 35 similar experiments, each with more than 5,000 cells per sample. No similar finding is seen with the porcine cells, where CsA decreased and V_i increased the R123 fluorescence. The lack of effect of cimetidine on R123 accumulation is also shown and is contrary to the two reports that R123-efflux is mediated through the organic cation pathway alone [174] or through that pathway in combination with P-gp [263].

Calculation of P-gp activity

According to Van der Kolk *et al* [265], an "efflux blocking factor" (EBF) can be calculated for any P-gp inhibitor by determining the ratio of the R123 fluorescence of cells pre-incubated with R123 then allowed to efflux for a set time with and without the P-gp inhibitor (see Figure 73). The geometric mean of the cells' R123 fluorescence signal is used as it gives a more accurate estimate of the average population signal (the fluorescence signal is measured on a logarithmic scale and the

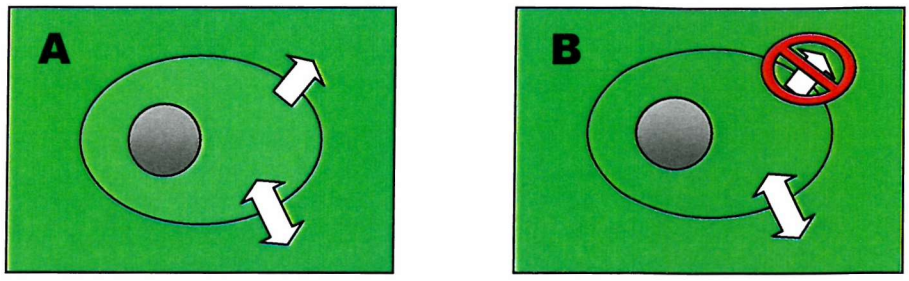

Figure 71. Schematic diagrams of the effect of the blockade of P-gp by P-gp inhibitors on the accumulation of R123. **(A)** without P-gp inhibitor, **(B)** with P-gp inhibitor. **Double arrow** = diffusion of R123 between medium and cell cytoplasm. **Single arrow** = P-gp-mediated efflux of R123. The blockade of the unidirectional efflux pathway allows greater accumulation of R123 (P-gp-mediated transport appears faster than movement by diffusion).

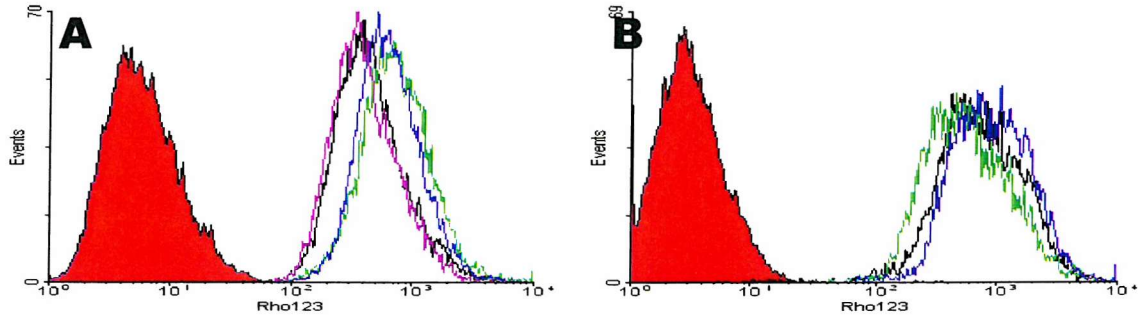

Figure 72. The effect of P-gp inhibition (and cimetidine) on R123 accumulation in primary human cells and transformed porcine cells. **(A)** Human cells (n=13,000), **(B)** LLC-PK1 cells (n=10,000). **Filled lines** = control R123-free cells. **Black lines** = R123-only, **Green lines** = R123 and CsA 3μg/ml, **Blue lines** = R123 + V_i 5mM, **Purple line** = R123 + cimetidine 80μM. The lack of effect of cimetidine on the uptake of R123 in the human cells is seen (equivalent uptake = overlapping traces). The increase in uptake (i.e. decrease in efflux) in human cells with CsA and V_i is seen by the right-shift of the traces. The lack of a similar effect on LLC-PK1 cells, which do not express P-gp, is seen (although CsA appears to reduce the uptake / increase efflux, possibly by a toxicity / membrane perturbing effect).

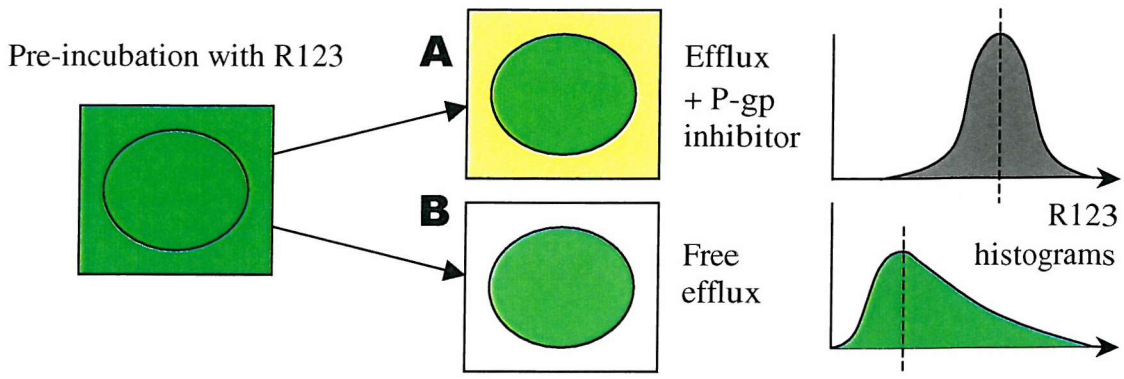

Figure 73. Schematic diagram of van der Kolk et al's [265] experiments. The flow cytometric fluorescence signals (peaks) are directly related to the cellular retention of R123. The geometric means (dashed lines) give a numeric representation of the R123 signal. The ratio of blocked efflux signal **(A)** to free efflux **(B)** gives the "efflux blocking factor" of the P-gp inhibitor.

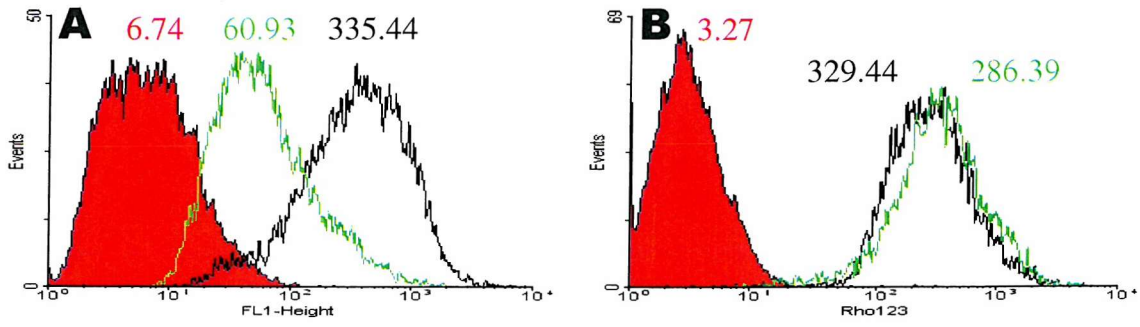

Figure 74. Flow cytometric determination of the "Efflux Blocking Factors" of CsA on renal cells. (A) primary human cells, **(B)** transformed porcine cell line LLC-PK1. **Filled lines** = R123-free controls, **Black lines** = CsA-inhibited efflux, **Green lines** = free efflux. Respective geometric means (GM) are shown above each trace. EBFs ([black GM – red GM] / [green GM – red GM]) = (A) 6.07 and (B) 0.86. The higher the EBF the greater the P-gp activity (if the same blocking substance / concentration is used), showing that LLC-PK1 cells exhibit no P-gp activity.

geometric mean calculates the average on a log scale) and therefore smoothes the effect of outliers [266].

The geometric mean of the R123 signal from the inhibited cells is proportional to the degree of blockade, and the ratio between the inhibited and un-inhibited cells gives the "strength" of the activity-reduction by the inhibitor under investigation. They used this technique with the synthetic CsA analogue PSC833 to determine the degree of P-gp activity in paediatric patients' leukaemic cells, in an attempt to correlate this with the clinical failure of chemotherapeutic agents in this disease.

Figure 74 shows this calculation performed on primary human tubular epithelial cells and the porcine transformed cell line, using the P-gp inhibitor CsA. The inhibition of R123 efflux in the human cells, and the lack of effect on the porcine cell line are clearly shown. The geometric means are provided by the flow cytometry software (Beckton Dickinson CellQuest®).

The determination of the EBF for each cell population depends on the R123 fluorescence signal on flow cytometry. As well as being influenced by the accumulation and subsequent efflux of R123, the strength of the signal is related to the background autofluorescence of the cells (hence the subtraction of the GM of the control R123-free cells in Figure 74) and the amplification of the flow cytometer photomultipliers, which is set manually at the start of each investigation (see Protocol 10).

Figure 75 shows the effect of adjustment of the photomultiplier amplification on the EBF. This adjustment is usually performed to keep the background autofluorescence to a minimum, while capturing the entire cell population, thus achieving maximum accuracy of the geometric mean.

As the R123 signal varies so much with the photomultiplier amplification, and the relationship does not appear to be mathematical, an FL-1 amplification figure of 400 was chosen for subsequent P-gp activity experiments (much less than this prevented all the control cells being sampled, much more led to the highest cell fluorescence

(e.g. when pre-incubated with R123 and CsA and not effluxed) overlapping the top of the scale – see Figure 75, black line of histogram [F]).

Simultaneous measurement of P-gp activity and expression in the same cells

Having determined the optimum conditions for the determination of P-gp expression and activity by flow cytometry, the next aim was to perform both techniques on the same cells, in order to assess both P-gp expression (MRK16 + fluorochrome-conjugated secondary antibody) and activity (inversely related to R123 fluorescence signal) on the same cell simultaneously.

The first attempt at this is shown in Figure 76. Cells were allowed to accumulate and then efflux R123, then were fixed and stained for P-gp expression with MRK16 and a TRITC-conjugated secondary antibody (R123 is detected by FL-1 on the flow cytometry, where FITC-emission is detected too).

Despite numerous repeat attempts at the same protocol it proved impossible to reproduce these findings (Figure 77). Careful dissection of the flow cytometric procedure showed that it was impossible to separate the R123 signal from the FL-2 detector (despite the quoted lack of overlap between TRITC and R123 emission spectra [Figure 78]) leading to the proportional signal of FL-1 and FL-2 (the 45°diagonal spread of the dots shows that there is overlap between the R123 fluorescence and the FL-2 detector).

A different fluorochrome, which would not be detected by the FL-1 detector, was therefore required. Such a marker is Cy5 (for spectrum see Figure 78). Figure 79 shows the results of the first experiment investigating R123 accumulation and simultaneously staining for P-gp with MRK16 and Cy5 (goat-anti-mouse Cy5-conjugate).

Initially these results of the simultaneous activity and expression experiments looked promising, in that the MRK16 and R123 signals appeared to be inversely

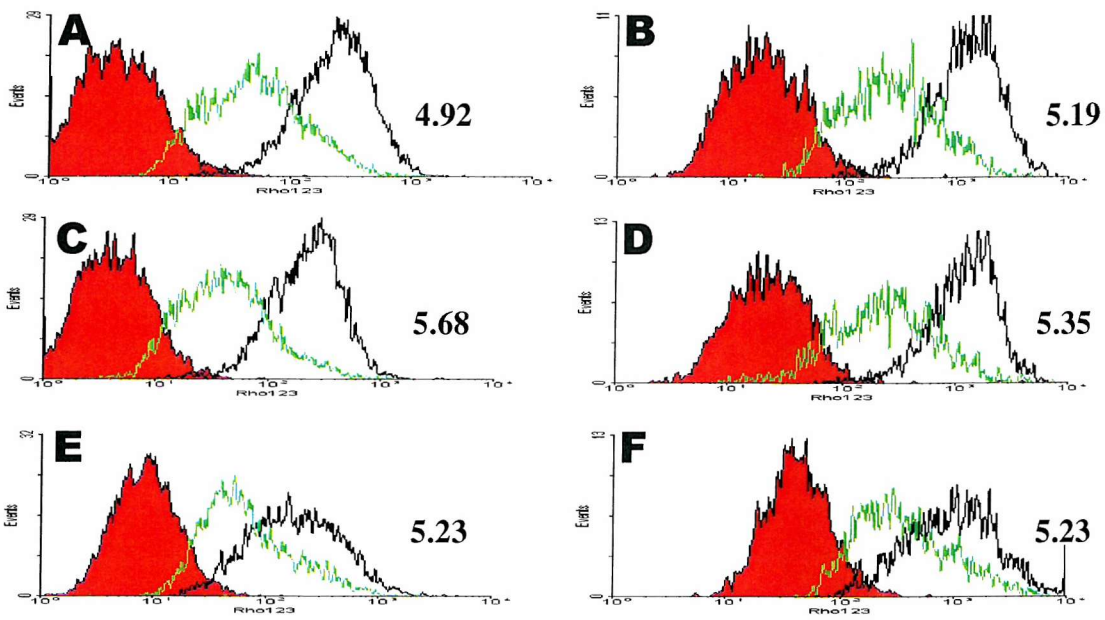

Figure 75. The effect of changing FL-1 photomultiplier amplification on R123 signal and Efflux Blocking Factors. (A+B, C+D, E+F) = three separate cell populations, **(A,C,E)** = FL-1 PMT 400, **(B,D,F)** = FL-1 PMT 500. **Filled**, **Green** and **Black** lines = control, CsA-free efflux and efflux with CsA respectively. EBFs are shown with each group of histograms. There is no relationship between the EBFs for PMTs of 400 and 500. There is therefore no mathematical calculation that can be made to adjust for PMT variation, so a standard PMT setting must be used.

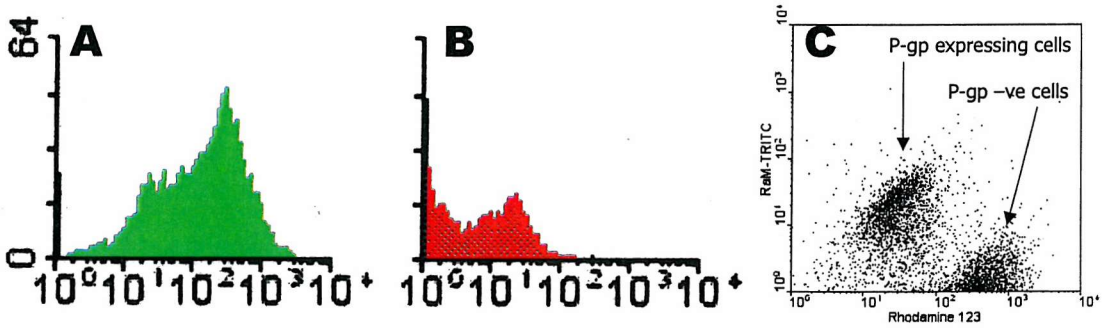

Figure 76. Flow cytometry histograms of R123 and TRITC-MRK16 signals, and dot plot of simultaneous detection. (A) R123 (FL-1), **(B)** TRITC (FL-2), **(C)** TRITC-MRK16 against R123 (FL-2 versus FL-1). The inverse relationship between R123 signal and MRK16 staining is clearly seen. This suggests that cells which express P-gp (higher FL-2) efflux R123 (lower FL-1), while cells without P-gp (lower FL-2) retain more R123 (↑ FL-1).

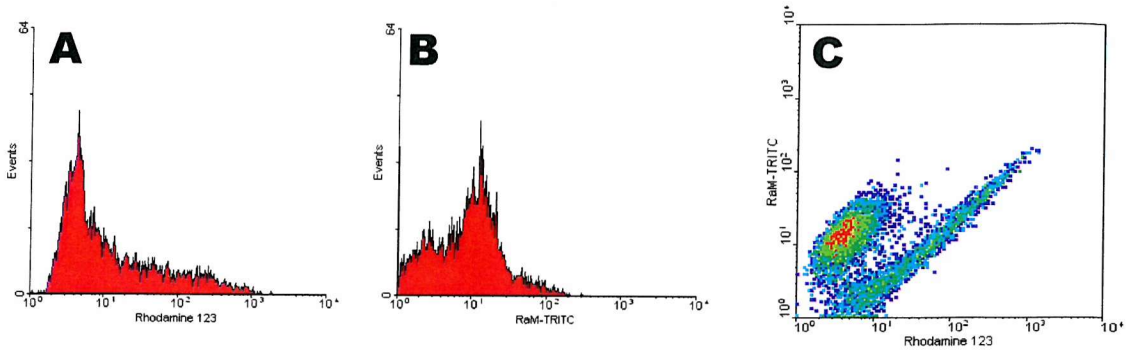

Figure 77. Flow cytometry histograms and density plot of R123 and TRITC-MRK16 on double-stained cells. All cells pre-incubated with R123 (30mins), effluxed (90mins), fixed then stained. **(A)** R123 signal, **(B)** TRITC-MRK16 signal, **(C)** density plot of simultaneous R123 and TRITC-MRK16 detection (density blue= low to red=high). Careful dissection of the flow cytometric procedure showed that it was impossible to separate the R123 signal from the FL-2 detector (despite the quoted lack of overlap between TRITC and R123 emission spectra [Figure 78]) leading to the proportional signal of FL-1 and FL-2 (the 45°diagonal spread of the dots shows that there is overlap between the R123 fluorescence and the FL-2 detector).

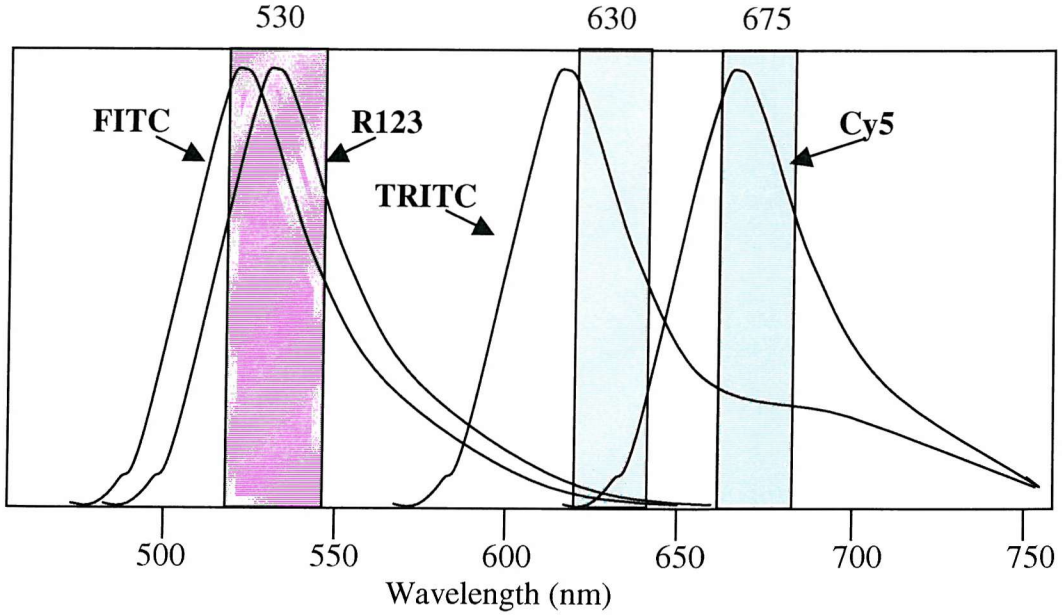

Figure 78. Emission spectra of fluorochromes. The overlap of the FITC and R123 fluorescence spectra is clearly seen. Although TRITC and R123 do not significantly overlap in this diagram, they were not possible to separate flow cytometrically.

proportional, as expected. However, on closer inspection, several problems soon became apparent, which are listed below:

1. The vast majority of the cells did not express P-gp (low on the density plot Y axis).

2. The cells that were positive for MRK16 did not accumulate R123 at all (cells higher on the Y-axis are low on the x-axis), even when exposed to CsA (data not shown).

3. The R123 histograms were generally reduced in value from those previously obtained without MRK16 staining (c.f. Figure 72). There was also a double peak of R123 signal, with a peak of significantly lower R123 signal (i.e. content) seen even in the cells not allowed to efflux at 37°C, which should have retained R123 as in Figure 72.

The obvious protocol difference between the single and dual staining was the MRK16 staining. This required fixing the cells with 2% Paraformaldehyde for 60mins, then washing, incubating with MRK16, then re-washing and incubating with the Cy5-conjugated secondary antibody, all at 4°C. The literature suggests that lowering the temperature to 4°C will prevent P-gp-mediated efflux [267].

Figure 80 shows the investigation of these aspects:

1. sitting on ice – the green traces are reduced in signal with respect to the black traces, but generally exhibit the same spread of signal, suggesting that efflux has occurred from all cells, rather than just those expressing P-gp;

2. sitting on ice with paraformaldehyde – this produces a greater loss of signal (blue lines) than just sitting on ice, again suggesting an efflux from all cells, at a greater rate than just on ice. This implies that the cell membranes have been slightly permeabilised by fixation, allowing greater diffusion.

3. accumulation with CsA – the traces in B are generally right-shifted compared to those in A, confirming that P-gp-mediated efflux is blocked during accumulation, but the loss of R123 signal with ice and fixation still occurs, suggesting that it is not a failure of the lowered temperature at preventing P-gp-mediated efflux, but diffusion from the cells which causes the lower R123 signal.

Therefore, in order to determine the expression and activity of P-gp on cells in further experiments, the same protocols would therefore be followed, but the R123 and MRK16 staining would be performed in parallel on separate cell samples of the same population, rather than in series as above. The results of cells treated in these ways are shown in Figure 81.

Unfortunately, without being able to double stain the same cells, it now has to be assumed that the cells which are effluxing R123 – which can be prevented by co-incubation with the P-gp inhibitors CsA and V_i (and not affected by the organic cation pathway inhibitor cimetidine) – express P-gp.

P-gp expression and activity experiments

The parallel determinations of P-gp expression and activity, and the effects of cell passage, medium composition and CsA exposure, were performed on cell samples from some or all of 4 subjects.

CsA exposure in defined medium and P-gp expression and activity

The first attempt at investigating the effect of increasing exposure to CsA on culture cells is shown in Figure 82. These cells had been kept in passage 0 quiescence for 49 days before subculture to 25cm^2 uncoated plastic culture flasks, and then regrown to confluence in defined medium. At confluence, the passage 1 cells were exposed to CsA for increasing periods. The control cells were kept in defined medium only: to the others CsA 500ng/ml was added at day 0 (4d), day 2 (2d) and day 3 (1d). The experiments were performed on day 4.

There is a trend towards increasing EBF with increasing time exposed to CsA, although the time of exposure is small.

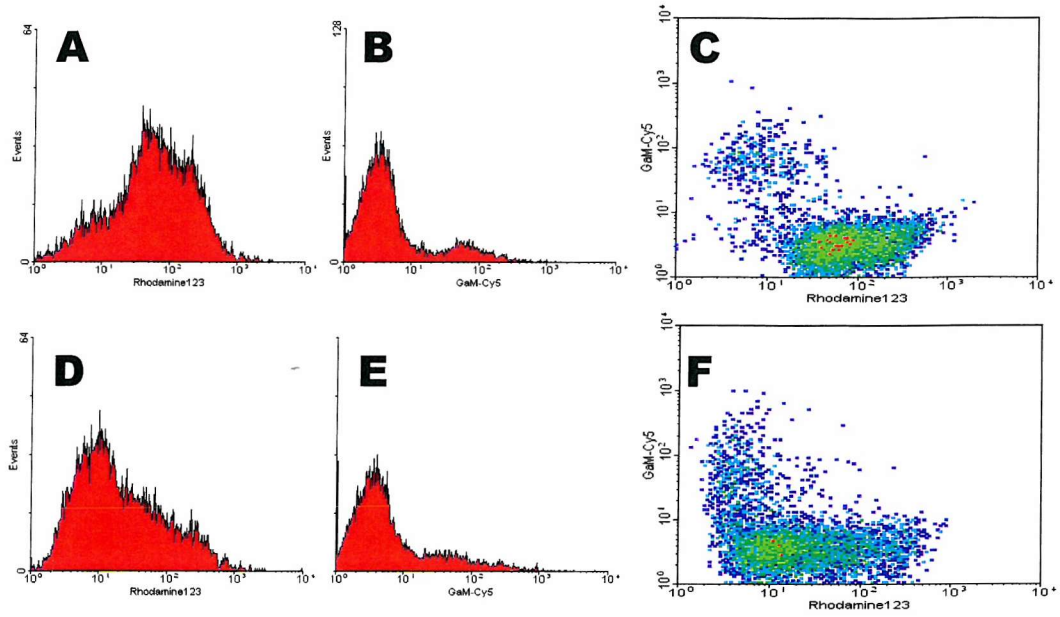

Figure 79. Flow cytometry histograms and density plots of simultaneous R123 fluorescence and MRK16 staining with Cy5-conjugated secondary antibody. **(A-C)** R123 accumulation only, **(D-F)** R123 accumulation and efflux. **(A,D)** R123 histograms, **(B,E)** MRK16 histograms, **(C,F)** R123 versus MRK16 density plots. The vast majority of cells do not stain for P-gp. Those cells that do stain for P-gp do not accumulate R123. The R123 histograms are generally reduced in signal: even those cells without an efflux period have a significant left (negative) peak.

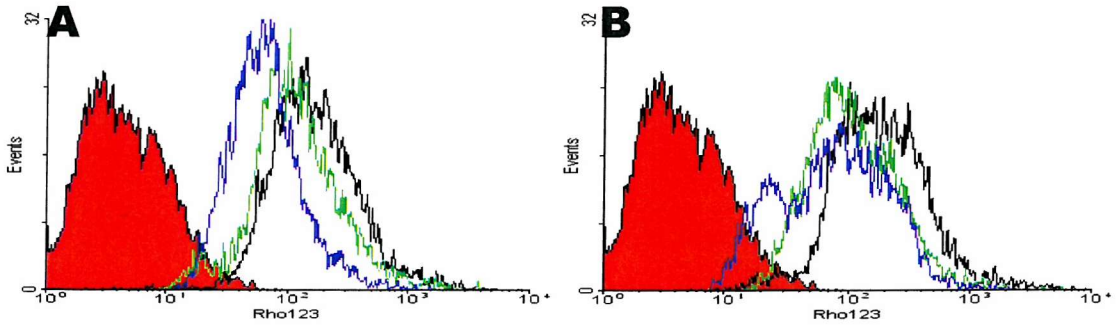

Figure 80. Effects of incubation on ice, and fixation on ice with 2% Paraformaldehyde, on R123 retention. **(A)** R123 only, **(B)** R123 + CsA 3.0μg/ml. **Filled line** = control R123-free cells, **Black lines** = accumulate R123 then facs, **Green lines** = accumulate R123, stay on ice for 60mins then facs, **Blue lines** = accumulate R123, fix with 2% PFA on ice for 60mins then facs. The reduction in the cellular R123 content with time on ice, and especially with fixation, is shown.

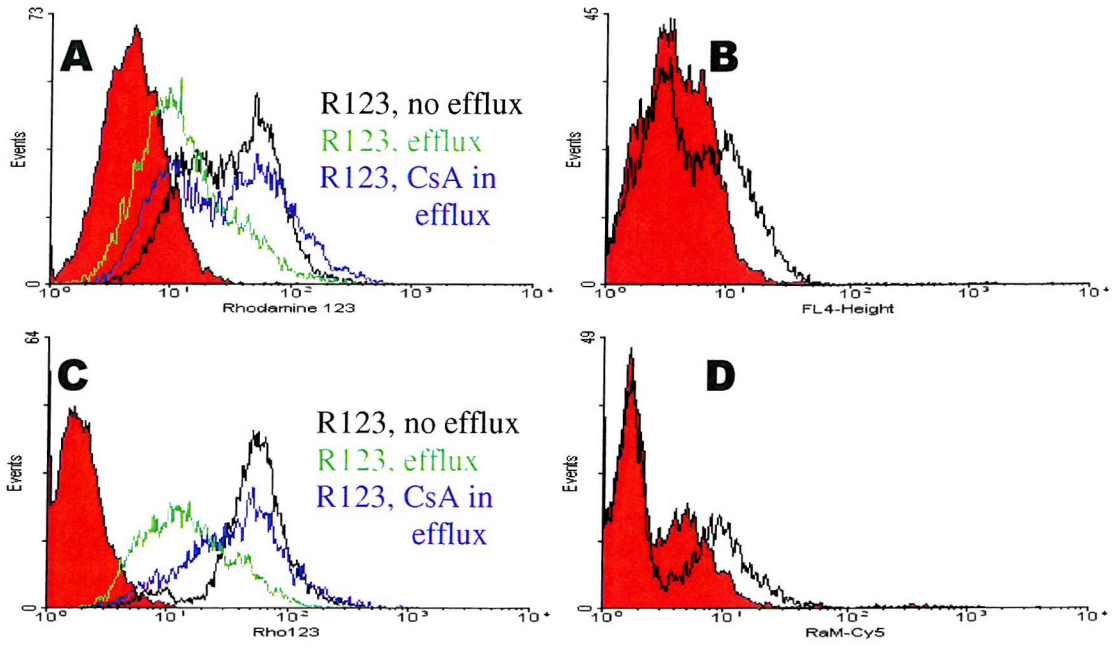

Figure 81. Flow cytometry histograms of R123 accumulation and efflux and the effect of fixation and staining with MRK16. **(A,B)** R123 and MRK16 in series, **(C,D)** R123 and MRK16 in parallel on the same cells. **(A,C)** R123 signal (FL-1), **(B,D)** MRK16 staining (Cy5 signal measured on FL-4). **Filled lines** = negative control (R123-free or isotype control Ab). The return of the R123 traces (**C**) to the 'cleaner' results previously achieved, with no lower-signal peak / left-shift of the traces (**A**), is clearly seen. The same is true of the MRK16 signals, with reduced control signal and an increased differentiation between the positive and negative peaks (**D** cf. **B**).

Passage and P-gp expression and activity

In order to expose cells in defined medium to CsA for longer periods, the cells would have to be subcultured serially. The effect of cell passage was investigated in two subjects: cells at confluence in defined medium were serially subcultured to 25cm^2 uncoated plastic culture flasks, in defined medium (Figure 83) and defined medium + CsA 500ng/ml (Figure 84).

In order to investigate the longer-term effect of CsA exposure on cultured cells in defined medium, it would be necessary to subculture every 3 to 4 days for 3 to 6 weeks. The cells in Figure 84 failed to achieve confluence, i.e. lost their growth potential, by passage 4 (16 days) in subject 1 and passage 3 (11 days) in subject 2. This implies that to expose cells for long enough to reliably affect P-gp expression or activity, serial subculture in defined medium with CsA is not sufficient.

To allow the cells to remain exposed to CsA for longer periods, quiescence was therefore required. First, the effect of quiescence medium on P-gp expression and activity was examined.

Quiescence and P-gp expression and activity

Quiescence was investigated in three ways: (i) in passage 0 cells (in 25cm^2 culture flasks) and in passage 1 cells (ii) on uncoated plastic 24-well plates and (iii) on permeable 6-well culture membranes. The effect in passage 0 cells was examined in 3 subjects (Figure 85), in passage 1 cells in 24-well plates in 1 subject (Figure 86) and on 6-well culture membranes in 3 subjects (Figure 87). In order just to examine the effects of quiescence, these cells were not exposed to CsA.

The 3 subjects' cells in 25cm^2 culture flasks showed a dramatic reduction in MRK16 signal (P-gp expression) and a slight reduction in EBF (P-gp efflux activity) over 3 to 5 weeks in quiescence. The 1 subject's cells in 24-well plastic culture plates showed a significant reduction in P-gp expression and an increase in P-gp activity. The 3 subjects' cells on the permeable 6-well culture membranes maintained their MRK16

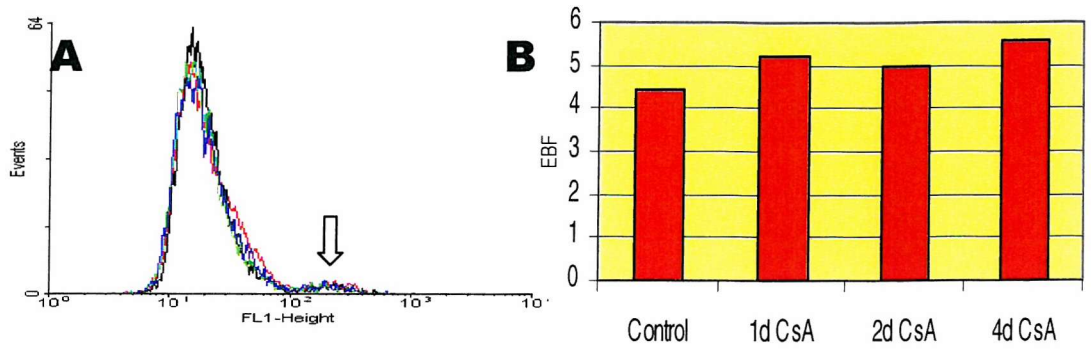

Figure 82: Effect of duration of CsA incubation of confluent passage 1 cells in defined medium. **(A)** Histograms of MRK16 staining (P-gp expression – small rightward peaks arrowed), **(B)** histogram of CsA Efflux Blocking Factors (flow cytometry histograms of R123 fluorescence not shown – calculations performed as above). There is no apparent effect on the (very small) expression of P-gp. There is a trend towards increasing EBF with increasing CsA exposure time (n=1).

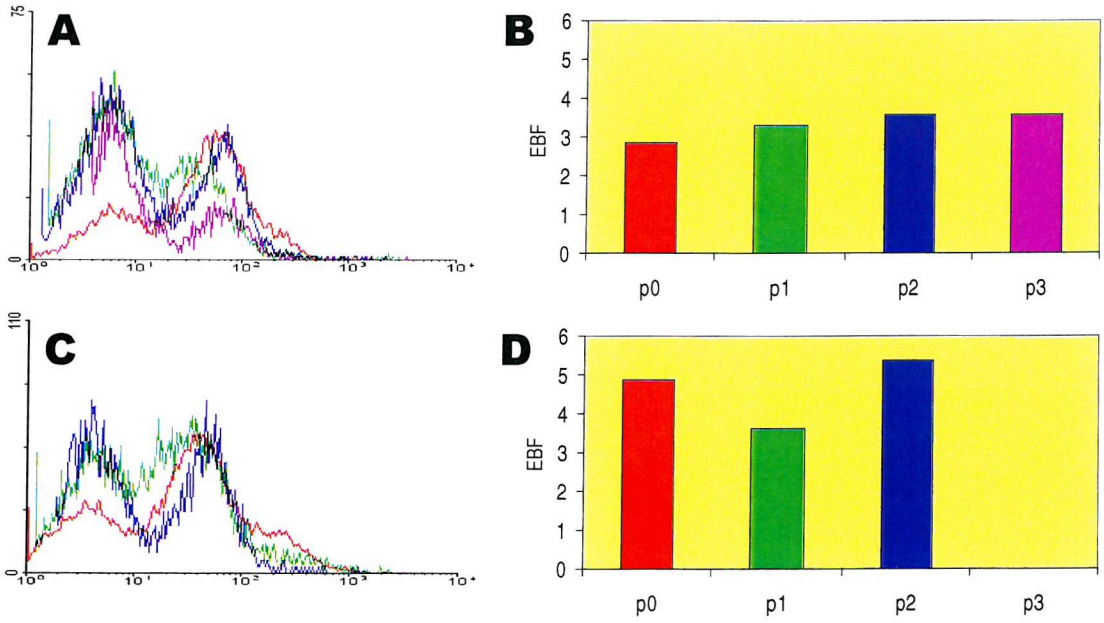

Figure 83: Effect of cell passage in defined medium without CsA on P-gp expression and activity. **(A,C)** flow cytometry histograms of MRK16 staining (P-gp expression), **(B,D)** histograms of Efflux Blocking Factors of each passage. **(A,B)** subject 1, **(C,D)** subject 2. Colours in each represent separate passages. Subject 1 shows a trend towards a reduction in the proportion of cells expressing P-gp (height of rightward peak of flow cytometry histogram) and an increase in P-gp activity (EBF) with increasing passage number. Subject 2 has no such association. (MRK16 histograms adjusted to align negative peaks.)

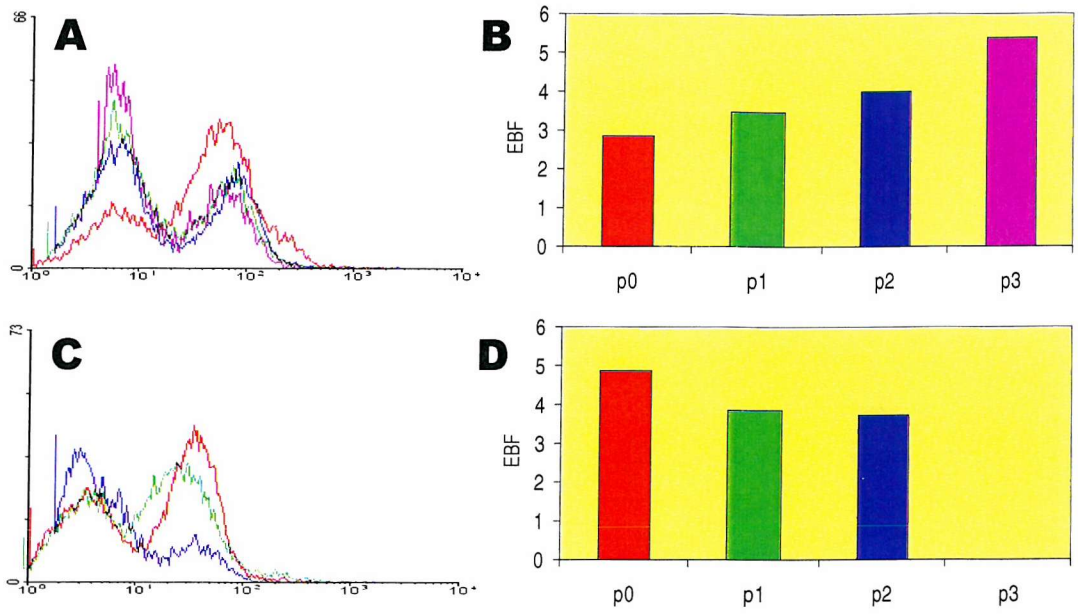

Figure 84: Effect of cell passage in defined medium + CsA 500ng/ml on P-gp expression and activity. **(A,C)** flow cytometry histograms of MRK16 staining (P-gp expression), **(B,D)** histograms of Efflux Blocking Factors of each passage. **(A,B)** subject 1, **(C,D)** subject 2. Colours in each represent separate passages. Both subjects show a trend towards a reduction in the proportion of cells expressing P-gp with increasing passage number. Subject 1 shows an increase in P-gp activity with passage, subject 2 exhibits the reverse association. (MRK16 histograms adjusted to align negative peaks.)

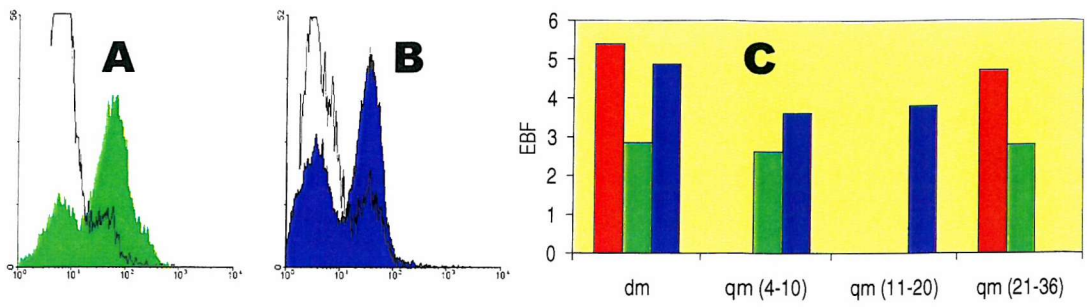

Figure 85: Effect of time in quiescent medium without CsA on P-gp expression and activity in passage 0 cells in 25cm^2 culture flasks. (A,B) flow cytometry histograms of MRK16 signals (2 subjects, filled line = cells in dm, line = cells longest in qm), **(C)** histogram of EBFs against medium composition (3 subjects, dm = defined, qm = quiescent) and time in quiescence (days in quiescence in parentheses). The colours represent individual subjects. There is a large decrease in the proportion of cells expressing P-gp with time in quiescence, and a trend towards a slight decrease in P-gp activity with time in quiescent culture in all subjects.

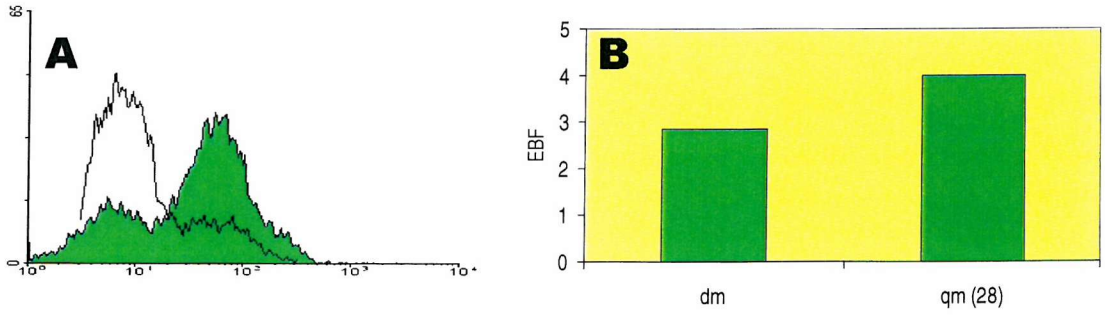

Figure 86: Effect of time in quiescent medium without CsA on P-gp expression and activity in passage 1 cells in 24-well culture wells. (A) flow cytometry histograms of MRK16 signals (filled line = dm, line = qm), **(B)** histogram of EBFs against medium composition (dm = defined, qm = quiescent, days in quiescence in parentheses). There is a large decrease in the proportion of cells expressing P-gp with time in quiescence, but an increase in P-gp activity with time in quiescent culture.

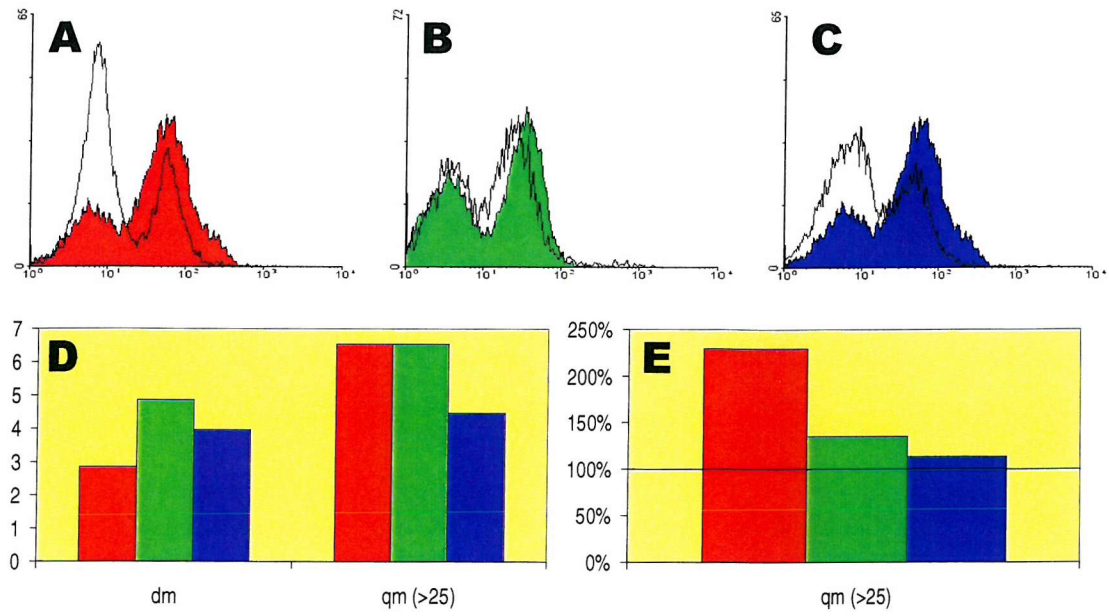

Figure 87: Effect of time in quiescent medium without CsA on P-gp expression and activity in passage 1 cells on 6-well culture membranes. **(A-C)** flow cytometry histograms of MRK16 signals (3 subjects, filled line = dm, line = qm), **(D)** histogram of EBFs against medium composition (3 subjects, dm = defined, qm = quiescent) and time in quiescence (days in quiescence in parentheses), **(E)** percentage increase of EBF in qm over dm. The colours represent individual subjects. There is a decrease in the proportion of cells expressing P-gp with time in quiescence, but to a much smaller degree than on the plastic culture surface. There is an increase in P-gp activity with time in quiescent culture in all subjects, although to quite different degrees.

signals the best and at least maintained their EBFs (if not increased over at least 3 weeks in culture).

These results suggest that P-gp expression, as measured by flow cytometric detection of MRK16 staining, is best maintained in quiescence by culture of these human primary cultured renal tubular epithelial cells on permeable culture membranes.

The activity of P-gp, as measured by the efflux of R123 and its blockade by the P-gp inhibitor CsA, in contrast to that on the impermeable plastic culture surfaces, is at least maintained by this culture method. However, in 2 of the 3 subjects the EBF increased dramatically in quiescence. This may mask any CsA-effect in the next section: the longer-term exposure of these cells to CsA.

CsA exposure in quiescence medium and P-gp expression and activity – preliminary experiments

This penultimate results section examines the expression and activity of P-gp in primary human renal tubular epithelial cells cultured for 6 weeks with CsA in quiescent medium, and compares them to cells kept in identical conditions without CsA.

When these experiments were first performed:

(i) the detrimental effects of CsA 500ng/ml on the immunofluorescence characterisation had not been shown,

(ii) the LDH and cell cycle experiments showing that thrice weekly medium exchange was less damaging to the cells had not been performed,

(iii) the reduction of R123 signal caused by fixation during the serial measurement of MRK16 staining and R123 accumulation was not known, and

(iv) the requirement for the standardisation of the FL-1 photomultiplier settings for comparison of Efflux Blocking Factors between subjects had not been discovered.

Therefore cells from the first 3 subjects were cultured in quiescent medium with 0ng/ml (control), 100ng/ml and 500ng/ml CsA, which was exchanged weekly. The P-gp expression and activity flow cytometry experiments were performed simultaneously (in 2 subjects) without FL-1 photomultiplier standardisation. P-gp expression was also examined by MRK16 immunofluorescence.

The flow cytometry results of the P-gp expression from these first 3 subjects are shown in Figure 88, P-gp expression by immunofluorescence results in Figure 89, and P-gp activity by flow cytometry results in Figure 90.

It was previously shown that the cellular retention of R123 was reduced following the subsequent fixation and staining of cells with MRK16. Here a further interference between R123 and MRK16 flow cytometry signal is shown, with a reduction in the discrimination of positive MRK16 from background (a decrease in the strength of the MRK16 staining compared to background) with double staining.

Again, as shown previously, the results of the immunofluorescence characterisation of cells grown in CsA 500ng/ml are complicated by the inability to fully remove background fluorescence, the loss of membrane specific staining and an appearance consistent with the loss of or a reduction in cellular integrity.

As previously discussed, the lack of results from the P-gp activity experiments shown in Figure 90 is likely to be due to problems with the methodology:

(i) cellular R123 retention is reduced by the fixation required to double-stain the cells with MRK16, which significantly reduces the R123 geometric mean figures and potentially masks any CsA effect,

(ii) the lack of standardisation of the FL-1 photomultiplier settings prevents the comparison of EBFs between subjects,

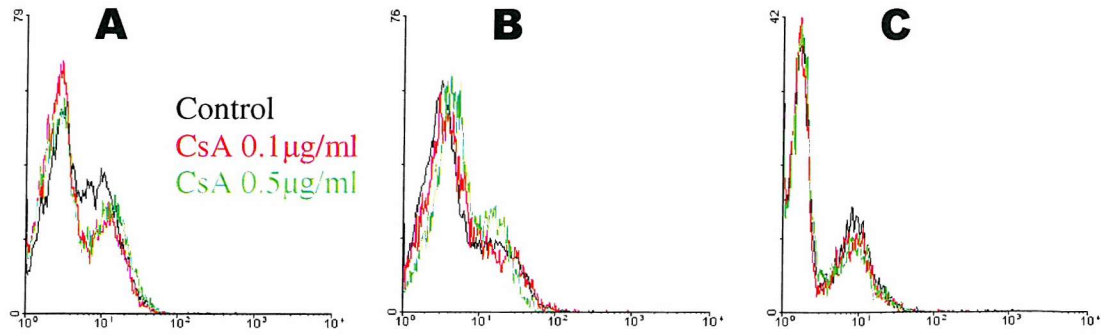

Figure 88: Effect on P-gp expression of incubation of confluent passage 1 cells on 6-well permeable culture membranes in quiescence medium for 43-48 days with different CsA concentrations. (A-C) MRK16 signal histograms – 3 subjects. **Coloured traces: black / red / green** = CsA 0 / 100 / 500ng/ml. There is no consistent effect of CsA incubation (a reduction in **A**, a small increase in **B,** and no effect in **C**). **A** and **B** were simultaneously exposed to R123, **C** was not. A greater separation of positive from negative signal is shown when not simultaneously exposed.

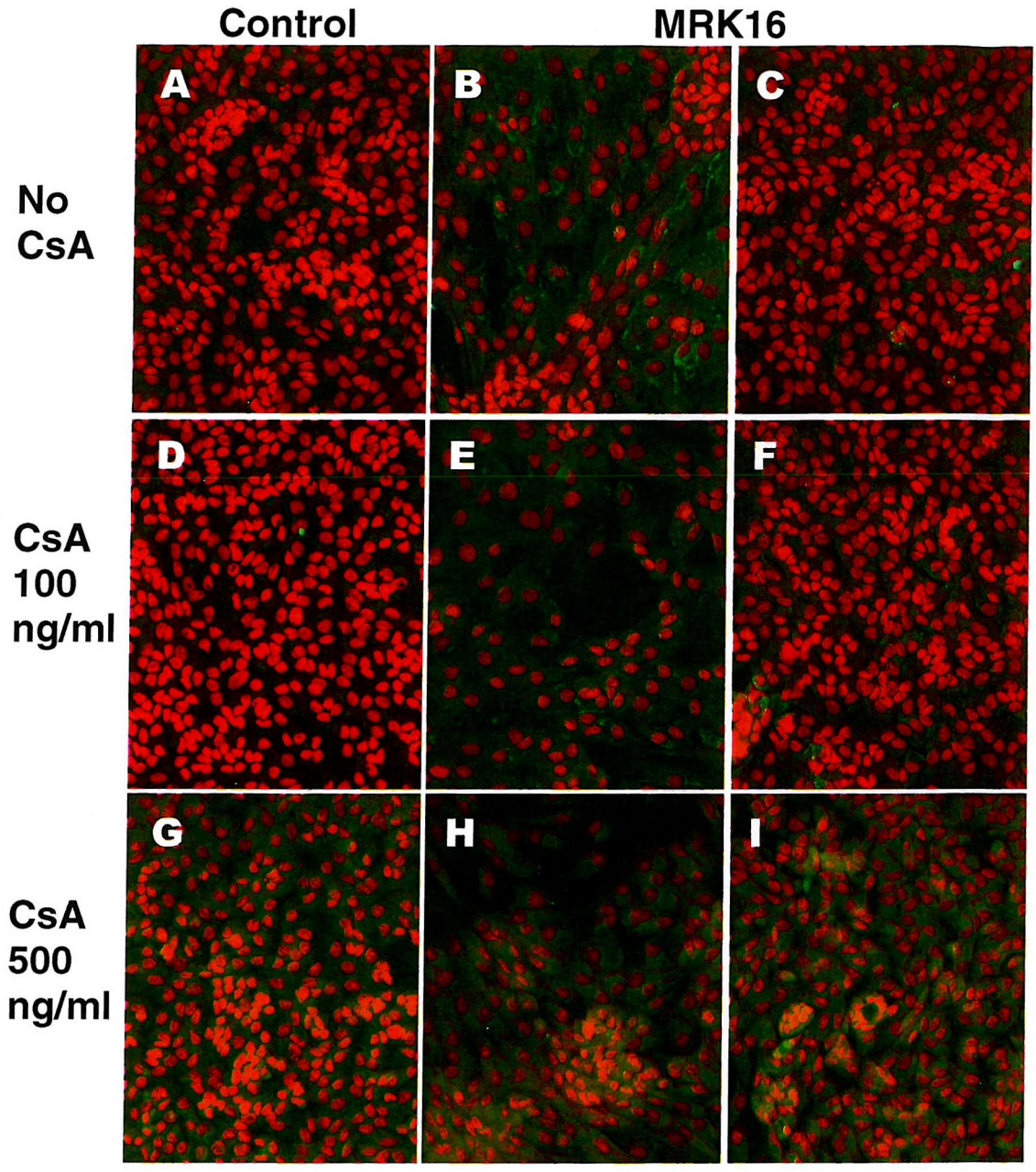

Figure 89: Effect of incubation with different CsA concentrations in quiescence medium for 43-48 days on P-gp expression in confluent passage 1 cells on 6-well permeable culture membranes. Control = IgG_{2a} isotype control antibody fluorescence micrographs, (FITC-conjugated secondary antibody = **green**, PI nuclear counterstain = **red**). This was performed on only 1 subject because of interference with the staining at the highest CsA dose (there should be no green signal on the control cells – also the membrane-situated MRK16 staining seen in the CsA 0 and 100ng/ml is heavily cytoplasmic in the 500ng/ml sample (Magn×25)

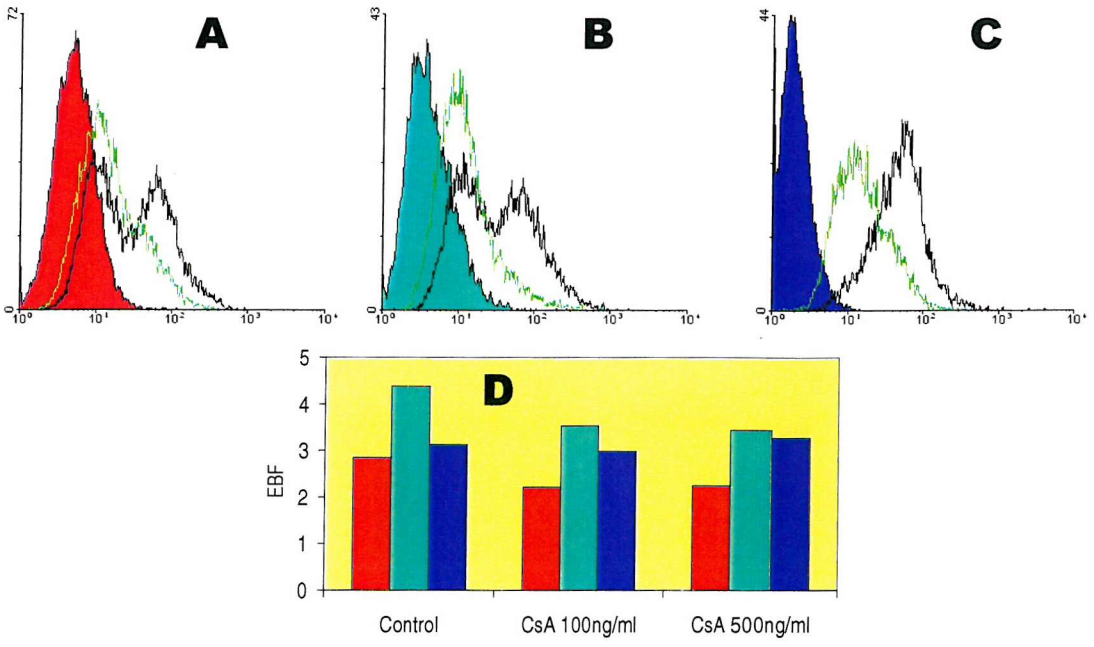

Figure 90: Effect on P-gp activity of incubation of confluent passage 1 cells on 6-well permeable culture membranes in quiescence medium for 43-48 days with different CsA concentrations in cell samples from 3 subjects. **(A-C)** R123 signal flow cytometry histograms – CsA 500ng/ml for each subject, **(D)** histogram of the EBFs for the 3 subjects. Separate colours are used for each subject. Flow cytometry histograms consist of three traces: **appropriate-colour filled line** = R123-free control, **green line** = CsA-free efflux, **black line** = CsA-blocked efflux. The decreased cellular retention of R123 with fixation and double-staining with MRK16 **(A,B)** is shown, which confounds the EBF. This is unaffected when not simultaneously exposed **(C)**, although the FL-1 photomultiplier settings were not standardised, and such EBF comparison between subjects is therefore not valid.

(iii) the incubation of cells in quiescence medium for more than 6 weeks with 500ng/ml of CsA appears to impair their membrane integrity – this may add to the reduction in cellular R123 retention by allowing diffusion through the membrane, and

(iv) the exchange of medium only weekly limits the exposure of P-gp to CsA. This is because a large proportion of CsA is transported to the apical side of the cells early in the period, preventing further basal and therefore cytoplasmic exposure to P-gp. The weekly medium refreshment also reduces the cell viability.

CsA exposure in quiescence medium and P-gp expression and activity – final experiments

The final results section examines the expression and activity of P-gp in primary human renal tubular epithelial cells cultured for more than 3 weeks with CsA in quiescent medium, and compares them to cells kept in identical conditions without CsA.

Drawing on all the prior results, the final methodology involved:

(i) the subculturing of passage 0 cells at confluence in defined medium on to pre-soaked 6-well permeable culture membranes, in half-defined medium for 24 hours, then in defined medium until they reached confluence. The medium was then changed to quiescent medium with / without CsA 300ng/ml, which was exchanged thrice weekly;

(ii) after the required incubation period (greater than 3 weeks) the performance of the P-gp expression and activity protocols in parallel;

(iii) the measurement of P-gp expression by laser confocal microscopic examination of cells *in situ* on the membranes, fixed and stained with

MRK16 and Cy5-antibody, and counterstained with PI, compared to an isotype control;

(iv) the measurement of P-gp expression by flow cytometric examination of cells trypsinised from the membranes, fixed, incubated with MRK16 monoclonal primary antibody, and an anti-mouse Cy5-conjugated secondary antibody, compared to an isotype control;

(v) the measurement of P-gp activity by flow cytometric examination of cells trypsinised from the membranes then incubated with R123. The activity was measured by calculating the ratio of retained R123 in cells allowed to efflux R123 in the presence of CsA to cells allowed CsA-free efflux (Efflux Blocking Factor).

(vi) All these were compared to cells kept in identical culture conditions without CsA, investigated in the same ways at the same times.

Time constraints prevented taking the cells out to 6 weeks, so all investigations were performed after 3 weeks of quiescence (greater than 4 weeks in culture – 7-10 days in defined medium, 1-3 days reaching confluence on the 6-well membranes, then at least 21 days in quiescence).

The results of these experiments are below: indirect immunofluorescence P-gp expression in Figure 91 to Figure 93, flow cytometry P-gp expression in Figure 94, and flow cytometry P-gp activity in Figure 96.

The results of the P-gp expression by immunofluorescence experiments were fraught with technical problems: Paraformaldehyde fixation appeared to cause a disruption of the nuclear membranes, and the spillage of nuclear contents into the cytoplasm. This increased the uptake of PI and caused the cells to appear completely red. Laser confocal microscopy builds up the composite picture by adding the colours from separate channels, so the green FITC signal could be examined and acquired separately, but this was also impaired. This happened twice on the same day, and

affected the results for subjects 4 and 5. No other tissue was available for these subjects so only the results from subject 6 were available for investigation.

The MRK16 samples for subject 6 were therefore cut, fixed, stained and examined in duplicate! This left only this sample to determine whether CsA made any difference to the expression of P-gp, as investigated by indirect immunofluorescence.

Image analysis was performed on the subject 6 photomicrographs (see Protocol 20). The proportion of positive cells was determined by counting the number of cells with staining density above an arbitrary cut-off (deciding on a sample of 10 obviously negative cells, and 10 obviously positively-stained cells, measuring the staining density of each cell and determining a cut-off density value which excludes all the negative cells while including the positive cells). The cut-off values were very similar for the control and CsA-exposed cells (20.8 and 18.6 arbitrary density units respectively), and using these gave positive cell counts of 84 out of 169 (49.7%) for the control cells, and 83 / 161 (51.6%) for the CsA-exposed cells.

Figure 94 shows the flow cytometric measurement of the expression of P-gp in each subject. The proportion of cells can be estimated from the flow cytometry histograms as shown in Figure 95. These estimates are relatively inaccurate depending on the peaks as described: however, the flow cytometric measurement of P-gp expression also (compared to immunofluorescence measurement) shows minimal effect of CsA-exposure in quiescence in these 3 subjects.

Figure 96 shows the P-gp activity results for these 3 subjects. As shown before, the activity of P-gp increases in cells in quiescent medium. The further increase in activity in the CsA-exposed cells shown here must be an additional effect of CsA over and above the quiescence effect. The increase is found across all subjects, and appears to be due mainly to a decrease in the R123 retention in the CsA-free efflux period in the cells maintained in CsA-containing quiescence medium when compared to the control cell histograms.

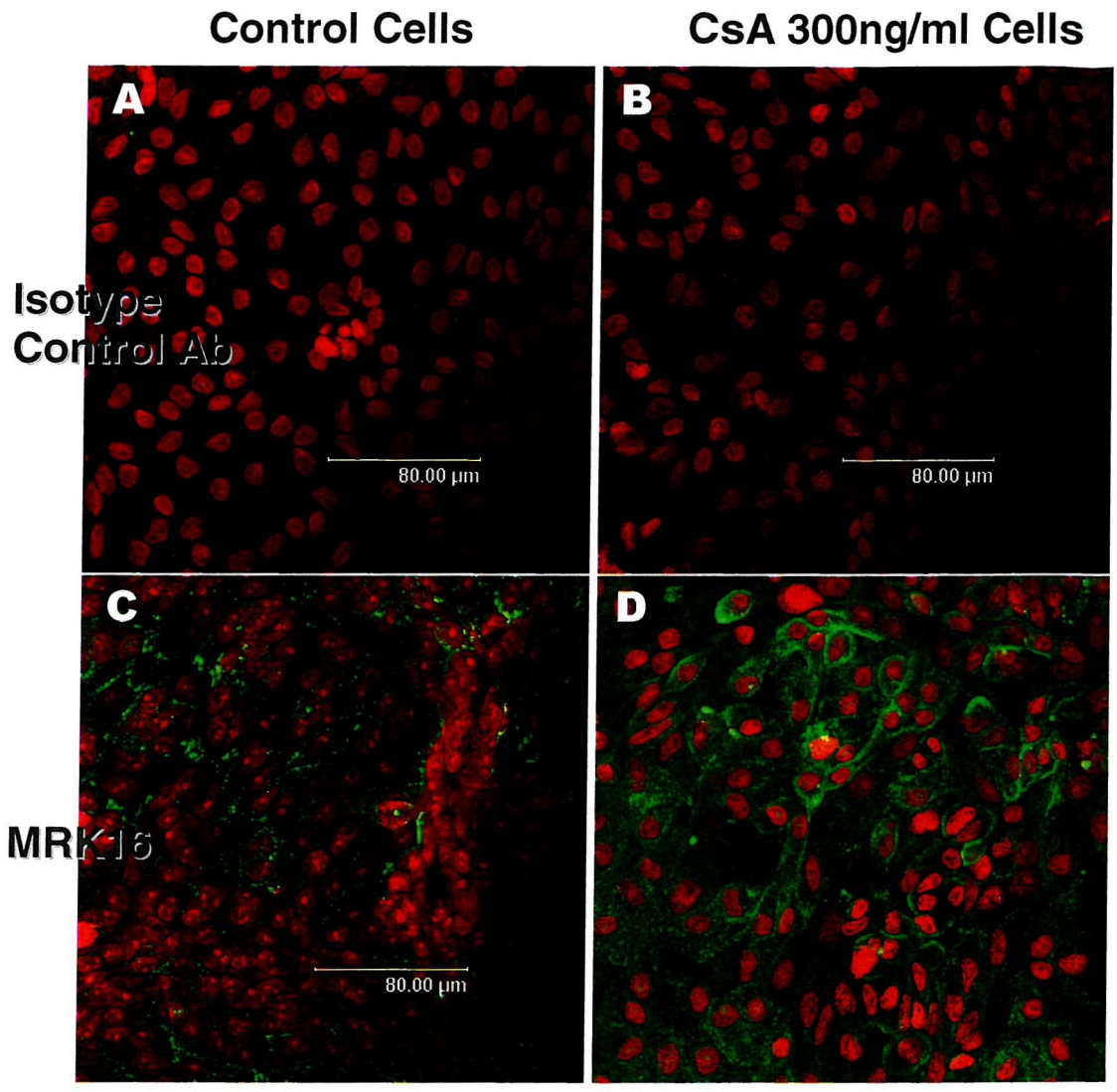

Figure 91: Effect of CsA exposure on confluent cell monolayers in quiescence medium for 21 days – Subject 4. Control = IgG_{2a} isotype control antibody fluorescence micrographs, (FITC-conjugated secondary antibody = **green**, PI nuclear counterstain = **red**). The fixation of the control MRK16 cells affected the nuclei, so it is not possible to determine any change in the expression of P-gp, although P-gp should be membrane bound and therefore unaffected by cytoplasmic masking. (Original magnification ×25)

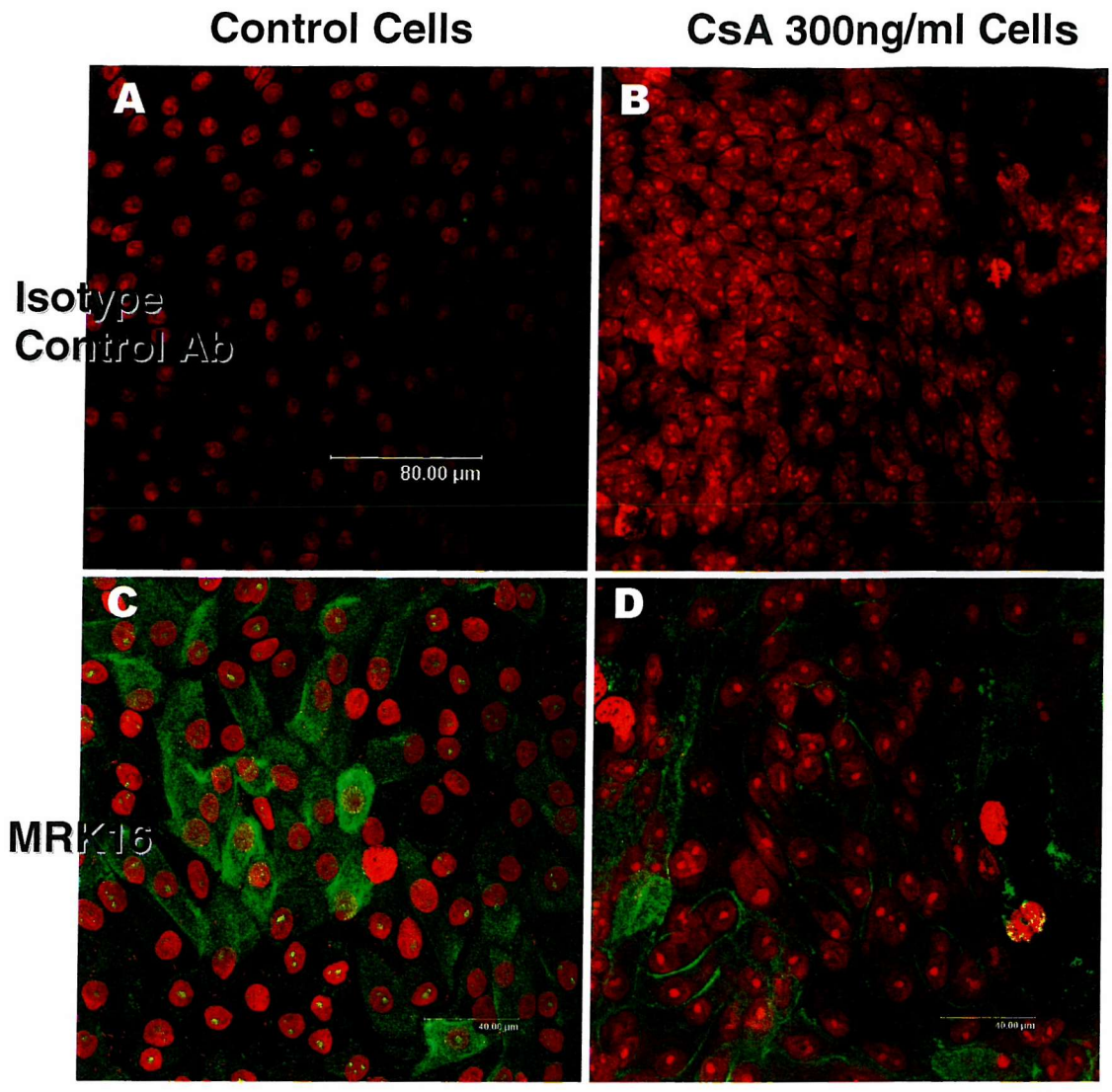

Figure 92: Effect of CsA exposure on confluent cell monolayers in quiescence medium for 22 days – Subject 5. Control = IgG_{2a} isotype control antibody fluorescence micrographs, (FITC-conjugated secondary antibody = **green**, PI nuclear counterstain = **red**). The fixation of the CsA-exposed MRK16 cells affected the nuclei (only the second time ever!), so it is not possible to determine any change in the expression of P-gp. Comparing this result with Subject 4 suggests that the fixation problem has affected the MRK16 staining, as the control cells stain greater in this subject, when the CsA-exposed cells stained greater in Subject 4. (Original magnification **A,B** ×25, **C,D** ×63)

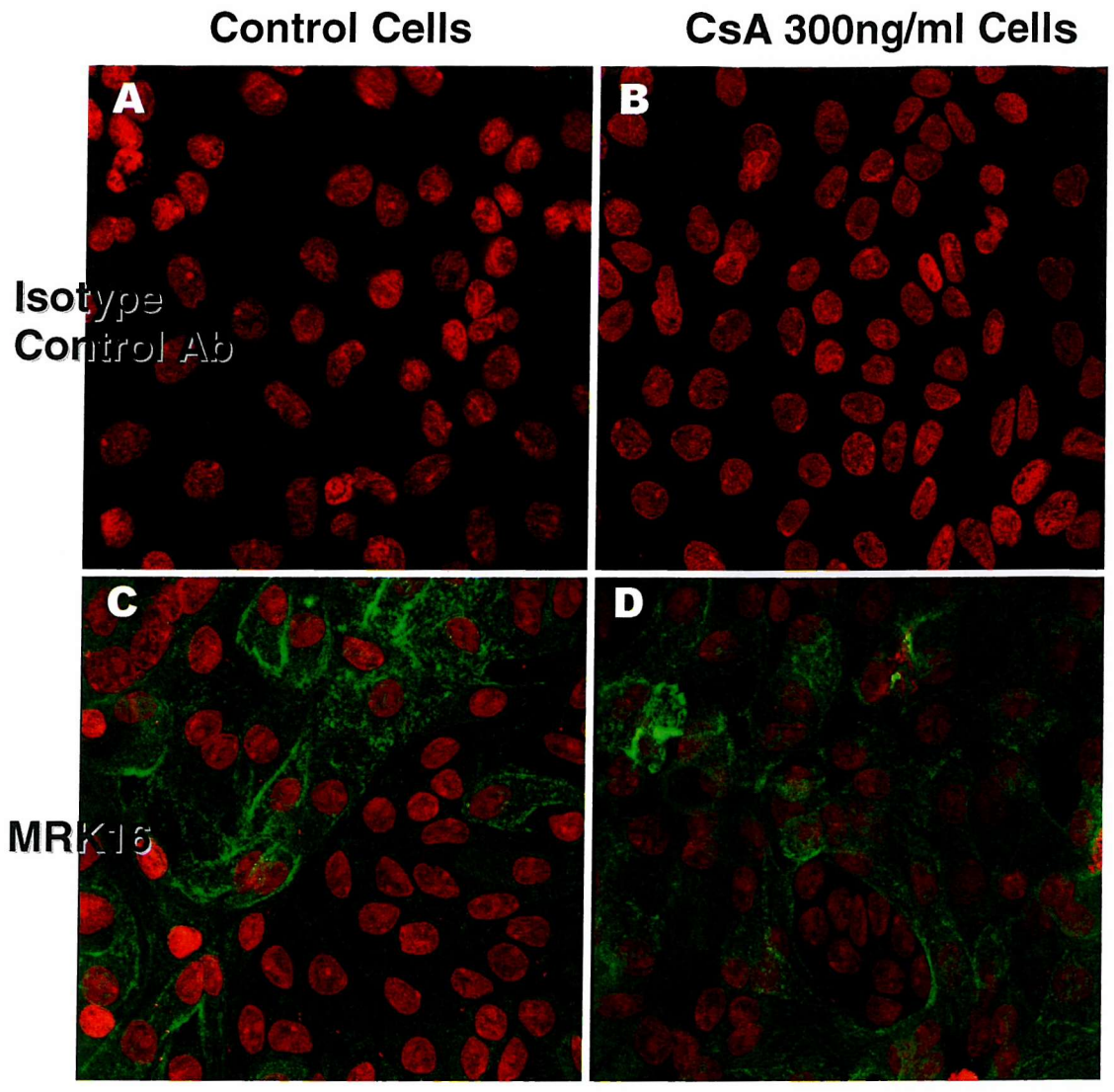

Figure 93: Effect of CsA exposure on confluent cell monolayers in quiescence medium for 23 days – Subject 6. Control = IgG_{2a} isotype control antibody fluorescence micrographs, (FITC-conjugated secondary antibody = **green**, PI nuclear counterstain = **red**). (The fixation worked this time!) The appearance of the MRK16 staining is very similar between the control and CsA-exposed cells. The proportion of cells positive in each is approximately 50% (49.7 & 51.6%). The degree of staining is also very similar (see text). (Original magnification ×63)

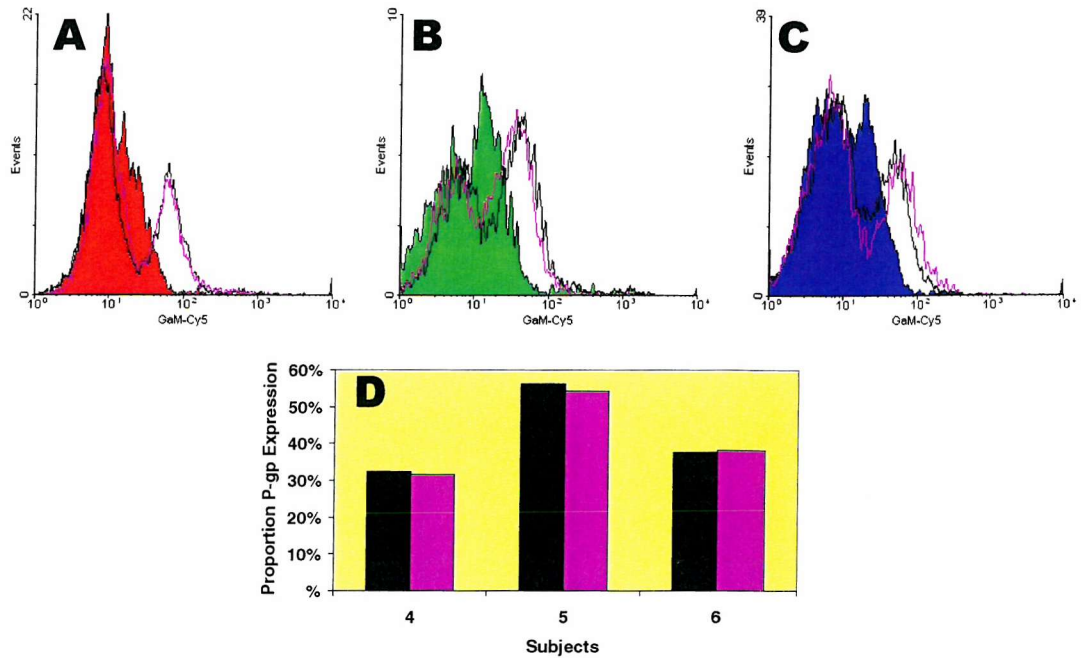

Figure 94: Effect of CsA-exposure on P-gp expression in confluent cells on 6-well culture membranes in quiescent medium for 21 to 23 days. **(A-C)** MRK16 flow cytometry histograms for Subjects 4 to 6 respectively, **(D)** P-gp expression histogram. For each histogram: **colour-filled peak** = isotype control, **black** = control cells, **purple** = CsA-exposed cells. The expression of P-gp measured by flow cytometry in these quiescent cells is unaffected by exposure to CsA (**D** – proportions positive [control : CsA] = 32.4 : 31.6, 56.2 : 54.3 & 37.6 : 38.2% respectively).

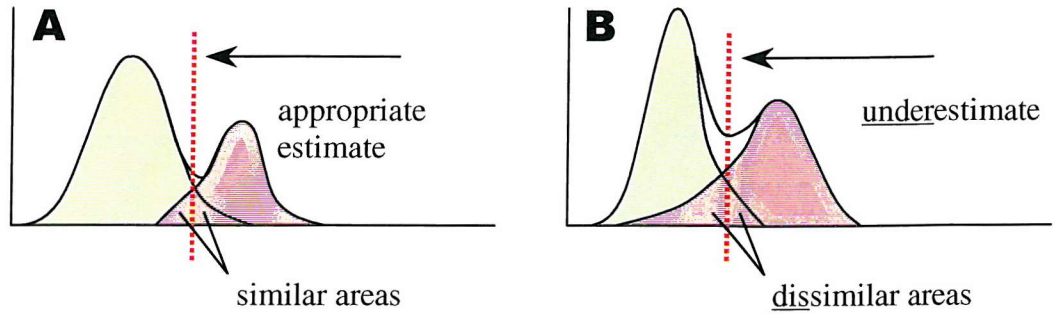

Figure 95: Measurement of antigen expression by flow cytometry. The flow cytometry histograms obtained are generally composites of two peaks of cells: the 'green' negative population, and the 'red' stained population, as represented in **A** and **B**. Taking the cut-off of positivity as the lowest point on the histogram between the two peaks is reasonable, and represents a point from which to estimate the proportion of cells stained (which the flow cytometry software will measure), if the overlapping areas are similar, as in **A**. This will however produce an under- (or over-) estimate of the proportion when the overlapping areas of the two populations are dissimilar, as in **B**.

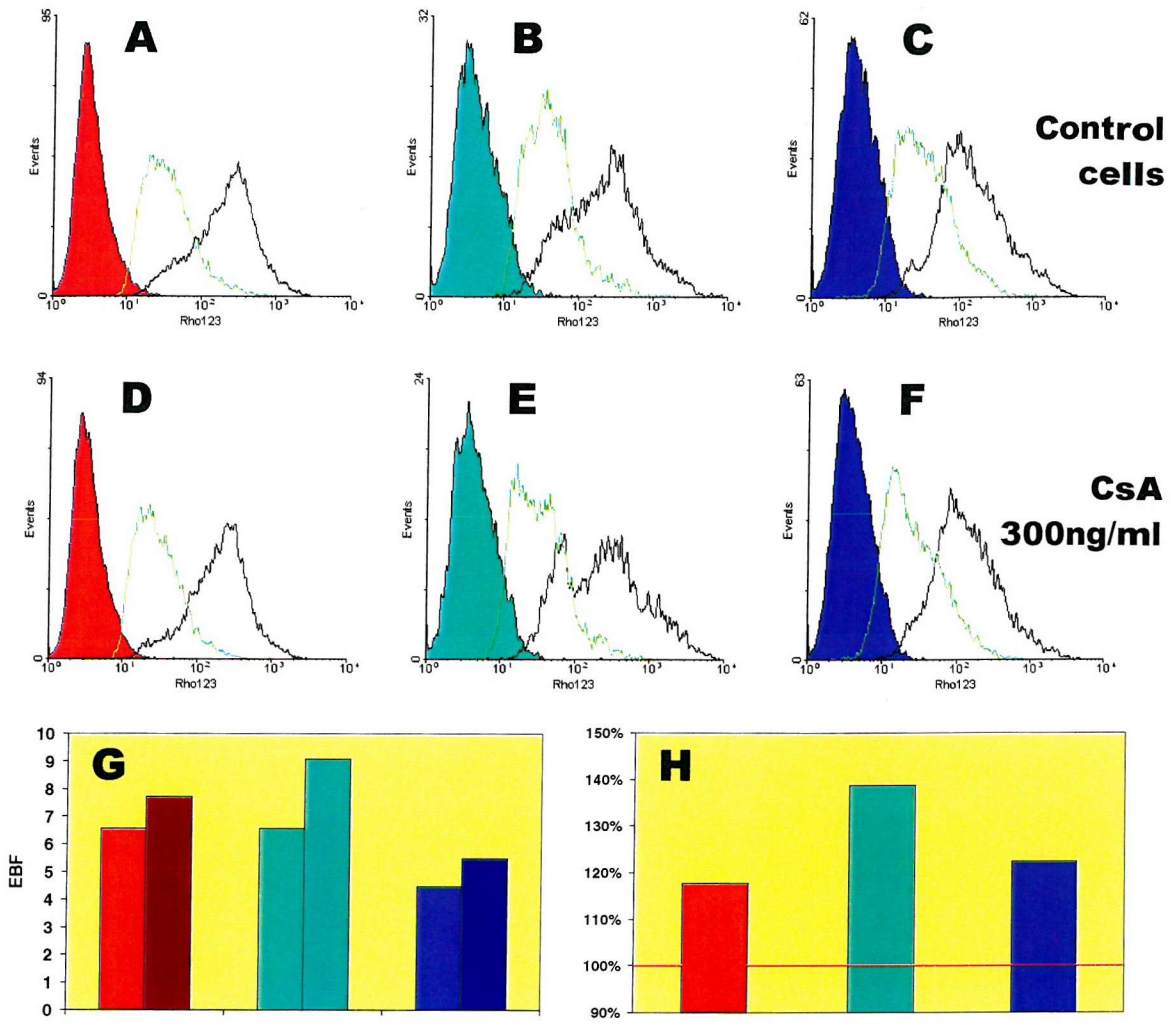

Figure 96: Effect on P-gp activity of incubation of confluent passage 1 cells on 6-well permeable culture membranes in quiescence medium for 21-23 days with different CsA concentrations. **(G)** histogram of the EBFs for the 3 subjects, **lighter bars** = control cells **(H)** histogram of increase of CsA-exposed EBF over control. Separate colours are used for each subject. Flow cytometry histograms: **appropriate-colour filled line** = R123-free control, **green line** = CsA-free efflux, **black line** = CsA-blocked efflux. The cellular retention of R123 when not fixed and double-stained is seen. The FL-1 photomultiplier settings were standardised, allowing comparison between subjects. The increase in EBF in the CsA-exposed cells is clearly shown, of 17.7, 38.6 and 22.4% over the control value.

Discussion

The near normal phenotype of primary human renal tubular cells kept in quiescent culture for up to 6 weeks has already been demonstrated. The second novel aspect of this work is the co-incubation of such cells with a potentially nephrotoxic agent, in this case CsA. The impact of therapeutic levels of CsA is investigated here, in a number of ways.

Appropriateness of Model

In static quiescent culture, the phenotype of tubular cells was maintained by changing the medium only every 7 days. In the CsA culture, early results suggested that changing medium at this frequency damaged the cells. Both the phase-contract microscopy in Figure 34 & Figure 35 and the TEM in Figure 36 to Figure 38 show an altered cell monolayer appearance and cellular ultrastructure when changing the medium only once weekly when compared to changing thrice weekly. This may have been a result of the CsA being transported to and then staying in contact with the apical membrane. *In vivo* CsA would be removed from the cellular milieu in the urine. Although the concentration of CsA in urine is greater than that in the peritubular capillaries, this is the final concentration in the bladder which is likely to be greater than that in the proximal tubule (much urine concentration occurs in the loop of Henle, distal convoluted tubule and collecting ducts, distal to the cells investigated here) and will be flowing from the cells through the tubules. By remaining in contact with the apical membrane the CsA may have caused direct toxicity. Certainly the cells exposed to a greater concentration of CsA exhibited greater abnormalities (Figure 36), and it was subsequently shown that there was minimal CsA remaining in the wells after 7 days. However, this effect may have been confounded by the more regular medium changes, as the control cells appearance was also worse with a reduced frequency of medium exchange.

By increasing the frequency of the medium exchanges, the phenotype of the cells was maintained. This was shown by monolayer formation, cell ultrastructure, normal cellular surface marker expression and brush border enzyme activity.

The same distribution of proximal and distal phenotypes appeared to be present, with approximately 50% expressing ALP by flow cytometry (a proximal tubular cell marker), and a similar proportion with a positive signal for EMA (a distal tubular cell marker).

In order for this to be a suitable model for the investigation of the effects of CsA exposure on P-gp, both P-gp expression and activity need still to be detectable in quiescence. By immunocytology, the appropriate apical distribution of the P-gp protein by indirect immunofluorescence is shown. The expression of P-gp is also shown by flow cytometry, although even the most discriminating anti-P-gp monoclonal antibody requires fixation.

For the measurement of P-gp activity in quiescence, R123 is an appropriate substrate. It is easily detectable by flow cytometry. It enters the cells by diffusion: therefore its accumulation is proportional to the exposure duration and concentration. The loss of R123 from the cells is also time dependent, is much greater than from cells which do not express P-gp, and is able to be blocked by known P-gp inhibitors, while unaffected by their vehicles or inhibitors of other efflux pathways. In the quiescent cells, R123 exhibited all these features, although the degree of activity tended to increase with time in quiescence. It would be tempting to infer that cellular membranes in quiescence are more permeable than those in defined medium; therefore more R123 is lost from the cells during the experiments. However, this would mean that both the P-gp expressing and non-expressing cells should experience "background" loss of R123 to the same extent, and should therefore have the same EBF, which is not the case. Certainly the cellular membranes could be different in quiescence, as mentioned in the first discussion section of this thesis (p.73), and any potential difference in the membrane composition of, for example, cholesterol or other lipids / phospholipids, could have a direct effect on P-gp activity [268;269].

Further investigations could use an alternative substrate to R123, as similar findings would provide additional evidence that P-gp activity is being measured.

Exposure to CsA

Initial results of experiments examining the effects of CsA on quiescent cells showed no effect. These were both on the activity and expression of P-gp. However an increase in the frequency of medium exchanges (with supplemented CsA) did produce an effect on the cells.

Subsequent measurements of CsA concentrations within the cell culture media showed that CsA moved more slowly through cell monolayers than by diffusion through the bare culture membranes.

As expected, the movement across the cells was unidirectional, from basal to apical membrane, and with increasing time between culture medium exchanges the amount of CsA present in the basal medium decreased, and increased in the apical medium. While exchanging the culture medium only weekly, it was likely that the cells were exposed to CsA for a lesser time (certainly CsA was not detectable in the basal medium), and therefore its effect on the cells was reduced.

The unidirectional nature of CsA movement is further evidence that P-gp function is appropriate in these cells.

Attempts to determine R123 movement across the monolayer were thwarted by an inability to reliably determine the R123 concentration in the supernatant medium by spectrophotometry (results not shown). Measurement the movement of other P-gp substrates across the cell monolayer would further confirm the activity of P-gp.

Measurement of P-gp activity

As above, R123 efflux was due to P-gp. The activity of P-gp could be deduced from a reduction of R123 within the cells, but there were technical problems with this. In an attempt to measure P-gp expression at the same time, the cells needed to be fixed (thus their cellular membranes disrupted). It was shown that the intracellular accumulation of R123 reduced with fixation, and was not able to be counteracted. This effect was even greater with the cell membrane permeabilisation required for the

detection of an internal epitope. Thus double staining for efflux and expression on the same cells was not possible.

Further studies could use antibodies directed against different external epitopes of P-gp in an attempt to find one that did not require fixation to label the P-gp molecule, allowing simultaneous measurement of activity and expression.

The quantification of P-gp activity was possible by comparing the efflux of R123 with and without a known P-gp-inhibitor between treatment and control cell groups. This was reproducibly measurable in quiescent and CsA-exposed quiescent cells. CsA exposure consistently increased the activity of P-gp over several weeks. The degree to which the activity increased varied between subjects, but all increased. This is in keeping with human and animal *in vivo* literature [200;202;206], and with reported animal cell culture studies [204]. However, unlike this study, these reports do not differentiate between an increase in substrate efflux due to increased P-gp ATPase activity (true activity increase – surmised by the increased efflux without increased protein expression) and that which would be found as a result of an increase in protein expression alone.

An apparent increase in P-gp activity, as measured by R123 efflux, could be confounded by any other loss of R123 from the cells. As CsA-exposure affects the character of these quiesced cells, the increased loss of R123 from the cells could just be reflecting a disruption of the cellular membranes. However, when co-incubated with CsA, R123 accumulation in the CsA exposed cells remains increased, suggesting that P-gp-mediated efflux is still having a significant effect above any diffusion, even the potentially increased diffusion of cell membrane disruption.

In Figure 96, the CsA-free (green) and CsA-blocked (black) efflux histograms for each subject's cells both co-incubated with and without CsA are very similar, suggesting no increased R123 loss from the CsA co-incubated cells of any subject. Moreover, in all the subjects, the efflux of R123 was greatly reduced by inhibiting P-gp activity, either by co-incubation in the efflux period with CsA or by pre-treatment with vanadate, implying that diffusion from the cells is minimal when compared to the efflux by P-gp.

The reports that R123 is taken up by cells and their mitochondria according to the cellular and mitochondrial membrane potentials [270] suggests that any change in the cellular content of R123 could be mediated by membrane changes. Further investigations with alternative P-gp substrates would address this point, and the above observations from this study still support the hypothesis that an increase in R123 efflux as a result of an increase in P-gp activity is most likely to be present.

While the inhibition of P-gp efflux has been studied in this model, further evidence for the appropriate function of P-gp could be obtained by co-incubation with known P-gp activity inducers such as Rifampicin [271].

Measurement of P-gp expression

Under the culture conditions described, no change in P-gp expression was detected. This is at odds with literature on (i) animal cells in short-term culture [204], although these were still growing (subcultured 1:10 twice) and exposed to a (human) toxic dose of 0.8μM CsA (960ng/ml) so not a direct comparison; and (ii) continually dividing transformed human cells whose P-gp expression increased when co-incubated with 1μM CsA for 4 days [272].

Other problems with *in vitro* studies are that only serum-free culture conditions allow the true effects of P-gp modulators to be determined, as effective concentrations of such compounds are often not attainable in culture conditions with serum [273].

In vivo reports of an increase of P-gp expression by exposure to pharmacological doses of CsA for a longer period, both in animals [30;200;202;235] and in humans [30] may be confounded by the known side-effect of CsA of renal micro-vascular ischaemia [274]. There are complex interactions between CsA, protein kinase-C (PKC), endothelin (ET) and P-gp activity (see Figure 97): PKC phosphorylates P-gp, increasing its activity [275-277], although one subsequent report suggests that it is competition by PKC-inhibitors, rather than a direct PKC effect, that modulates P-gp function [278]. *In vitro*, ET-1 inhibits P-gp activity in killifish tubules through tubular cell ET(B) receptors, the effect being reversed by protein kinase-C (PKC) inhibitors [279;280]. Cyclosporin

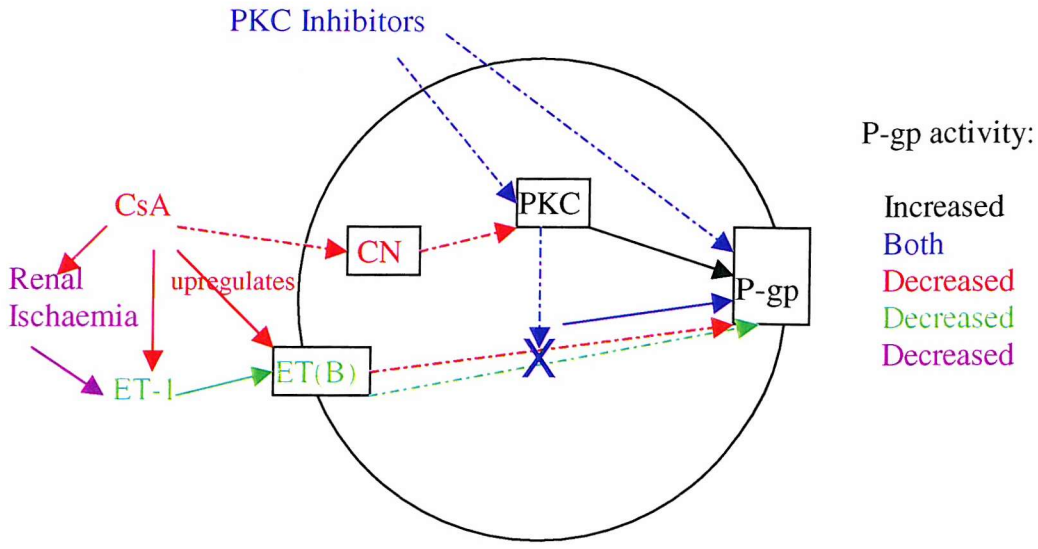

Figure 97: Effects of CsA and PKC on P-gp activity. PKC effect, PKC inhibitors effect, CsA effect, ET effect, Renal Ischaemia effect. Solid arrow = upregulatory effect, dashed arrow = inhibitory effect

increases the production of ET-1 *in vitro* by rabbit proximal tubular cells (partially inhibited, interestingly, by EGF) [281], and *in vivo* also upregulates ET receptors on renal epithelial cells [282]. CsA inhibits PKC activity through calcineurin (CN) inhibition [283]. Renal ischaemia further induces ET production [284].

These same interactions may play a part in alterations of P-gp expression, particularly as TAC at therapeutic dosage has a lesser effect than CsA on ET release [281], and does not induce P-gp expression *in vitro* [204]. However, the pro-fibrotic cytokine $TGF\beta_1$ is known to increase P-gp protein expression [285] and activity (via reactive oxygen species formation and subsequent PKC activation) [286]. CsA at therapeutic concentrations increases $TGF\beta_1$ production from fibroblasts, macrophages and renal tubular cells [21], whereas this effect is much less marked with TAC [287]. Reactive oxygen species are also formed in renal tubular epithelial cells by angiotensin II (AT2) activity (leading to further PKC activation) and CsA (and TAC) activates the renin-angiotensin system both directly and through renal ischaemia, increasing the production of AT2 [202], which also induces $TGF\beta_1$ production [288]. Hence the reported CsA-induced increase in P-gp expression *in vivo* may be modulated or influenced by renin production, renal ischaemia and increased $TGF\beta_1$ production by other non-tubular cells leading to up-regulation of MDR-1 gene transcription. SMADs could also be implicated in this pathway, as they are mediators of gene transcriptional activation by members of the $TGF\beta_1$ superfamily and could have an impact on MDR-1 transcription. The rate of P-gp activation has also been shown to depend on the metabolic state of the cell [289], so starvation of the cells of glucose, or acidification of the milieu, both of which occur in ischaemia, may increase the activity of P-gp without an increase in expression.

These aspects could be investigated in this model by adjustment of the culture conditions to induce ischaemia, to include $TGF\beta_1$ and/or renin/angiotensin administration and analysis of the effects of SMAD inhibition. The effects in this model of co-incubation with other immunosuppressant medications such as TAC, or newer drugs such as Sirolimus or Mycophenolate mofetil, may also further define their interactions with and influences on P-gp.

NF-κB activity has been shown to be increased by chronic CsA administration to rats [290] (despite one of the immunosuppressive actions of CsA being the downregulation of NF-κB activity in lymphocytes [and other tissues] [291]) which may have a role in the increase of P-gp expression in response to continued CsA exposure, particularly as this transcription factor has been shown to be required for the transcription of the MDR-1 gene [196]. Moreover, a consensus NF-κB binding site has been found on the intron of the MDR-1 gene in human colonic carcinoma cells [197], suggesting that NF-κB upregulates MDR-1 gene transcription. NF-κB activity can be inhibited in this model to further investigate this aspect.

Cellular differentiation reduces P-gp expression [292]. The reduced differentiation of the CsA-exposed cells may lead to an increased expression, although it would seem to be unlikely that the expression of P-gp would increase with a reduction in differentiation. It should be safe to infer that any loss of P-gp expression with differentiation would not be reversible with de-differentiation. The slight increase in expression over time may reflect the slight reduction in cell size – which occurs during quiescent culture – i.e. there is a greater membrane to cytoplasm ratio.

Potential Limitations of Expression Studies

Unfortunately a number of technical problems invalidated several of the results, and true conclusions proved difficult to draw from the immunocytology. Flow cytometric results were available on more subjects, however. Certainly further research into this aspect should contain greater numbers of subjects.

None of the available techniques for the detection of P-gp in cells was without problems. The main problem encountered with immunocytology was with the fixation of the cells, which was required for all the monoclonal antibodies in common usage. This was also a problem for the dual staining of cells for simultaneous flow cytometric measurement of P-gp activity and expression, as the fixation increased the efflux of the fluorescent substrate.

Other techniques for direct protein detection involve immunoblotting (Western), which may not require fixation but still disrupts cells preventing the simultaneous

measurement of protein activity and expression. Western blotting would however confirm or refute the finding in this study of no increased expression of P-gp in these cells when exposed to therapeutic concentrations of CsA for several weeks and should be performed in further studies.

Indirect techniques involve the measurement of the appropriate mRNA for gene expression. This assumes that all mRNA will be transcribed (which is not true when exposed to some inhibitors [293]), and still requires the cells to be disrupted. Admittedly the antibody techniques assume that the fluorescent signal is marking functional protein, but the antibody used did not detect an internal isotope of P-gp, so was not likely to detect any cytoplasmic or golgi-body- / endoplasmic reticulum-situated P-gp. Polymerase chain reaction to measure MDR-1 mRNA could be employed in further experiments, again as a confirmation that expression is not increased in these cells. This would also show whether MDR-1 gene transcription and P-gp protein expression are directly related in this model.

Another potentially confounding factor is the unknown drug history of the study patients. If their P-gp expression was already upregulated pharmacologically (they were patients with malignancy who may have received chemo-therapeutic agents) then it may not have been possible to increase the expression further. No aspects of the patients' histories were recorded, to maintain anonymity, so this potential effect could not be addressed further. The patient's age or genotype for P-gp may also have an effect on their cells' response to P-gp modulators. An increase in P-gp expression and activity is seen in lymphocytes from older people [294], which may also be true for the P-gp in their kidneys. Any further research with this model should ensure that demographic details including racial origin and drug histories of the patients are recorded, in order to define and investigate any such potentially confounding factors.

As this study was being performed, the impact of genotype on P-gp function was discovered. There are genetic polymorphisms of the MDR-1 gene in humans, which affect the efflux activity of the molecule ± its expression. The principle effective polymorphism is a single nucleotide polymorphism (SNP) in exon 21 of the MDR-1 gene, at nucleotide number 3435 (SNP C3435T)[213]. The C allele is the wild-type (normal) and occurs in 83% of Ghanaian, 83% of Kenyan, 84% of African American

and 73% of Sudanese populations studied. The British Caucasian, Portuguese, South-west Asian, Chinese, Filipino and Saudi populations had lower frequencies of the C allele compared to the African group (48%, 43%, 34%, 53%, 59%, and 55%, respectively) [295-298], but this was 84% in Polish Caucasians [299], 78% in a Spanish cohort [300] and 64.5% in Portuguese [301]. Heterozygotes have functionally normal P-gp, but the TT mutation confers between 40% and 75% lower P-gp activity than the CC or CT alleles. Twenty-two studies to date have found an effect of MDR-1 genotype on substrate absorption, substrate-inhibitor interactions or tertiary effects (e.g. Parkinson's disease or inflammatory bowel disease susceptibility, HIV-treatment response etc.) [302-323]. Nineteen studies have found little effect however (similar spread of investigations) [324-342]. This variation in findings has been explained by the size of the molecule (>1260 peptides), the large number of SNPs found and a lack of linkage disequilibrium (polymorphisms are spread along the MDR-1 gene and the presence of one particular polymorphism does not indicate the presence of any others). Haplotype analysis, the definition of finite phenotype groups of SNPs, is the current vogue hoped to determine the effect of genotype on P-gp expression and activity [343-348].

Conclusions

This is the first study of P-gp activity and expression in primary human cultured renal tubular cells, and also the first to expose stable cells to immunosuppressants / nephrotoxic compounds *in vitro* for a number of weeks. Direct comparison to other studies is therefore not easy.

The study shows that stable quiescent cultures of human primary cultured renal tubular cells express functional P-gp and the activity of this protein can be modulated by known inducers and inhibitors, as has been shown before both *in vivo* and *in vitro*. This should therefore be a suitable model for the further study of reactions to other immunosuppressive or nephrotoxic medications.

P-gp expression is not shown to be increased in quiesced cultured renal tubular cells exposed to CsA for at least 3 weeks, despite an increase in efflux activity. Notwithstanding the small sample size, this suggests that the mechanism of the increase of P-gp expression in renal tubular cells exposed to CsA may not be a direct one, but may be confounded *in vivo* by other factors such as renal ischaemia or interactions with other cells / cytokines.

Chapter 6 Presentations

Preservation of phenotype in longer-term culture of primary renal tubular epithelial cells

Leach TD, Campbell SK, Bass PS, Albano JDM, Mason JC

(Poster Presentation) Renal Association meeting, Nottingham, Spring 2001

(Abstract) *Renal Association* 2001: The study of diseases, processes and toxins affecting human renal tubular epithelial cells (HTECs) has been enabled by the ability to culture primary HTECs. However, current experimental evidence has been obtained from confluent monolayers of cells maintained in culture for just a few days.

Our study aimed to determine the culture conditions whereby viable characterised HTECs may be maintained in "quiescent" culture for several weeks, thus providing a suitable model for the longer-term study of nephrotoxic drugs in vitro.

Cell suspensions were prepared and seeded as previously described (1). The initial medium was Ham's F12:DMEM, 2mM glutamine (FDGM) with 100IU/ml Penicillin and Streptomycin, 2% UltroSerG®. The cells were weaned to FDGM, 50IU/ml antibiotics, no UltroSerG®, 10ng/ml epithelial growth factor (EGF), 36ng/ml hydrocortisone, 5ng/ml insulin, 10ng/ml prostaglandin E1, 5ng/ml selenium and transferrin, and 5fg/ml tri-iodothyronine, by confluence at days 7-10, when the final medium change to "quiescent" (FDGM, 50IU/ml antibiotics, 25ng/ml EGF, 0.5ng/ml parathyroid hormone and 0.2% UltroSerG®) was performed.

Phase-contrast microscopy revealed that overgrowth of cells with cell rounding and detachment continued after quiescence. Total cell counts fell during 53 days of culture by 23.9±7.6% while viability of adherent cells remained constant (91.2±3.1%).

Fluorescence microscopy of cytocentrifuge preparations from day zero, and in quiescent medium at days 11 and 42 showed maintained expression of cell surface molecules (epithelial membrane antigen, T43, MHC class I, P-glycoprotein, Phaseolus vulgaris-binding carbohydrate). Expression of the brush-border enzyme alkaline phosphatase fell by day 11 with subsequent restoration on quiescence. Flow cytometry confirmed these results.

We have shown that HTEC monolayers retain expression of surface markers and cellular viability for at least 8 weeks in quiescent culture.

Measurement of metabolic activity and examination of ultrastructure by electron microscopy should confirm the suitability of these HTEC cultures for further studies.

1. Carr *et al* Immunopharmacology 44 (1999) 161-167

Primary human renal tubular epithelial cells in quiescent culture: evaluation of phenotype

Leach TD, Campbell SK, Bass PS, Albano JDM, Mason JC

(Poster Presentation) World Congress of Nephrology, San Francisco, Oct 2001

(Abstract) *J Am Soc Nephrol* 2001 Sep; 12: 615A: The study of a wide range of pathophysiological processes affecting human renal tubular epithelial cells (HTECs) has been facilitated by the ability to culture HTECs. However, current experimental evidence has often been obtained from confluent monolayers of cells maintained in culture for just a few days.

Our study aimed to determine the culture conditions by which viable HTECs may be maintained in "quiescent" culture for several weeks, thus providing a suitable model for the longer-term study of nephrotoxic drugs in vitro.

Cell suspensions were prepared and seeded as previously described (1). The initial medium was Ham's F12:DMEM and 2mM glutamine (basal medium), with 100IU/ml Penicillin and Streptomycin and 2% UltroSerG® (USG - synthetic serum substitute) (growth medium 1). The cells were weaned to basal medium, 50IU/ml antibiotics, no USG, 10ng/ml epithelial growth factor (EGF), 36ng/ml hydrocortisone, 5ng/ml insulin, 10ng/ml prostaglandin-E1, 5ng/ml selenium and transferrin, and 5pg/ml tri-iodothyronine. At confluence (days 7-10) the medium was replaced by "quiescent" medium (basal medium, 50IU/ml antibiotics, 25ng/ml EGF, 0.5ng/ml parathyroid hormone, 0.2% USG), refreshed weekly.

Although cellular overgrowth with rounding and detachment continued after quiescence, and total adherent cell numbers fell during 53 days of culture by 23.9±7.6%, adherent cell viability remained constant (91.2±3.1%).

Fluorescence microscopy of cytocentrifuge preparations from day zero, and in quiescent medium at days 10 and 42 showed maintained expression of cell surface molecules (alkaline phosphatase, epithelial membrane antigen, T43, MHC class I). Flow cytometry confirmed these results.

We have shown that HTEC monolayers in quiescent culture are suitable for longer-term studies. They retain cellular viability and expression of surface markers for at least 7 weeks. The confirmation of phenotype by metabolic activity and ultrastructural examination by electron microscopy is ongoing.

Functional P-glycoprotein is expressed on cultured primary renal tubular epithelial cells in longer-term culture

Leach TD, Campbell SK, Mason JC, Bass PS, Albano JDM

(Poster Presentation) Federation of American Societies of Experimental Biology Meeting, New Orleans, Apr 2002

(Abstract) *FASEB J* 2002 Mar; 15(6): A955: P-glycoprotein (P-gp) is a cellular transmembrane protein involved in the active elimination of exogenous molecules including cytotoxic drugs. In the renal tubular epithelium P-gp underactivity may contribute to Cyclosporin A (CsA) toxicity, although to date, human P-gp studies in vitro have been limited to tumour, haematological or transformed cell lines. This study aimed to detect functional P-gp on primary human tubular epithelial cells (PHTECs) in longer-term culture. PHTECs in passage 1 were quiesced for 6 weeks (1). P-gp expression was assessed by indirect immunofluorescence and flow cytometry with the monoclonal antibody MRK16. P-gp activity was measured by flow cytometry using the fluorescent P-gp substrate Rhodamine (R)123. The transcellular transport of R123 and the effects of the putative P-gp modulator CsA were determined. P-gp was expressed in 11.5% (2-25%, n=6) of the cells, in a membrane distribution. The activity of P-gp was confirmed by the increased accumulation and decreased efflux of R123 when exposed to CsA. Therefore this in vitro model may be useful for studies of the role of P-gp in chronic pharmacological tubular toxicity.

Ref: 1. Leach *et al.* J Am Soc Nephrol 2001; 12: 615A (Abstract)

Cyclosporin A exposure upregulates P-glycoprotein activity, but not expression, in longer-term cultured primary renal tubular epithelial cells

Leach TD, Campbell SK, Farrer A, Bass PS, Albano JDM, Mason JC

(Poster Presentation) American Society of Nephrology 35th Annual Meeting & Scientific Exposition, Philadelphia, November 2002

(Abstract) *J Am Soc Nephrol* 2002;

P-glycoprotein (P-gp) is a cellular transmembrane protein involved in the active elimination of exogenous molecules including cytotoxic drugs. In the kidney, P-gp is present on the apical membrane of the proximal tubular epithelium. Chronic Cyclosporin A (CsA) nephrotoxicity is related to tubular epithelial intracellular CsA accumulation, so underactivity of P-gp may contribute to toxic damage. Human P-gp studies *in vitro* have been limited to tumour, haematological or transformed cell lines, and most have been short term (3-5 days). These results should be extrapolated to the normal *in vivo* situation with caution, particularly for longer-term effects.

Our group has previously demonstrated functional P-gp on primary human renal tubular epithelial cells (PHTECs) in longer-term quiescent culture[1]. The present study aimed to investigate the effects of incubation with therapeutic concentrations of CsA for up to 4 weeks on the expression and efflux activity of P-gp in this model.

PHTECs were prepared from nephrectomies from 3 individuals. Cells from each were maintained for 3-4 weeks in passage 1 without subculture in quiescent medium with (CQ) or without (NQ) 300ng/ml CsA. By flow cytometry, P-gp expression was assessed using the monoclonal antibody MRK16 and activity was measured using the fluorescent P-gp substrate Rhodamine (R)123. The accumulation and subsequent efflux of R123 were determined, and relative P-gp efflux activity (ratio CQ:NQ) was calculated.

The proportion of cells expressing P-gp (~45%) and the degree of P-gp expression per cell (~1.9 x Control fluorescence) was similar in CQ and NQ. However, relative P-gp activity was 1.26±0.11 (mean±1s.d - range: 1.18 to 1.39).

Although preliminary, these experiments show that longer-term exposure of quiescent PHTECs to therapeutic concentrations of CsA produced a strong trend toward an increase in P-gp activity, whereas P-gp expression was unaffected, at variance with published data.

[1]Leach *et al. FASEB J* 2002; 16(5): A955 (abstract)

Primary human renal tubular epithelial cells after six weeks of quiescent culture retain F-actin cytoskeleton and maintain cAMP response to renal hormones

Leach TD, Campbell SK, Bass PS, Mason JC, Albano JDM

(Poster Presentation) International Society of Nephrology Annual Meeting, Berlin, Apr 2003

(Abstract) *Nephrol Dial Transplant* 2003; 18(suppl 4): 609: The study of a wide range of pathophysiological processes affecting human renal tubular epithelial cells (HTECs) has been facilitated by the ability to culture these cells. Current experimental evidence has often been obtained from confluent monolayers of cells maintained in culture for a few days.

Our group has determined culture conditions by which viable HTECs may be maintained in "quiescent" culture for several weeks, thus providing a suitable in vitro model for the longer-term study of nephrotoxic drugs.

We have previously demonstrated that such cells exhibit electron microscopic appearances consistent with a tubular epithelial ultrastructure, retain tubular epithelial markers (alkaline phosphatase, T43 and MHC class I), maintain appropriate metabolic functions (alkaline phosphatase, gamma-glutamyl transferase and P-glycoprotein function) and preserve the ability to proliferate again on the reintroduction of growth factors.

The aim of this study was to further characterize primary HTECs maintained in quiescent culture by assessing renal hormone receptor status and cytoskeleton integrity.

Cell suspensions were prepared and seeded to uncoated plastic 96-well plates for the receptor studies and 6-well permeable culture membranes for F-actin localization. The culture conditions were manipulated as previously described [1], from a fully hormonally defined growth medium to a final culture medium of Ham's F-12:DMEM and 2mM glutamine, with 50IU/ml Penicillin, 50mg/ml Streptomycin, 25ng/ml epithelial growth factor, 0.5ng/ml parathyroid hormone (PTH) and 0.2% USG (UltroSerG® - synthetic serum substitute), which was refreshed twice-weekly for 6 weeks.

Cyclic adenosine monophosphate (cAMP) responses to 10^{-7}M PTH, 10^{-6}M arginine vasopressin (AVP) and $3x10^{-8}$M calcitonin (CT) were measured by ELISA.

Responses of cells in quiescent medium for 6 weeks were compared to those of cells in defined medium at 7 days. Intracellular actin microfilaments were localized by laser confocal imaging using rhodamine-linked phalloidin, under both medium conditions.

Hormone responses:

Hormone	Defined medium Median (range)	Quiescent medium Median (range)
None (control)	8.82 (8.80-16.58)	13.09 (6.54-23.62)
PTH	97.78 (72.16-120.77)	75.73 (58.11-106.18)
AVP	29.96 (26.73-34.15)	26.70 (15.61-39.93)
CT	36.09 (32.15-40.85)	22.94 (22.05-44.62)

All results fmol/μg protein (3 cell preparations, n=8)

F-actin was localized at the cell membrane in both media.

In this study we have shown that HTEC monolayers after 6 weeks in quiescent culture retain their response to renal hormones although the magnitude was reduced. F-actin localization indicates a stable polarized epithelium. The absence of cytoplasmic filaments provides additional confirmation of their epithelial phenotype.

This is further evidence that primary HTECs in quiescence are suitable for longer-term studies.

[1] Leach TD *et al.* J Am Soc Nephrol 2001 Sep; 12: 615A (abstract)

Appendix 1 Southampton Ethical Application

Hampshire and Isle of Wight NHS
Strategic Health Authority

Ref: CPW/HPH

SOUTHAMPTON & SOUTH WEST HAMPSHIRE
LOCAL RESEARCH ETHICS COMMITTEES
1ST Floor, Regents Park Surgery
Park Street, Shirley
Southampton
SO16 4RJ

Tel: 023 8036 2466
023 8036 3462
Fax: 023 8036 4110

General Enquiries: sharon.atwill@gp-j82203.nhs.uk
clair.wright@gp-j82203.nhs.uk

27 March 2003

Dr PA Bass
Department of Histopathology
MP 002, Level E, SAB
SGH

Dear Dr Bass,

Submission No. 192/00/w – Culture of human renal tubule cells from nephrectomy tissue

In response to your letter dated 19th March 2003, I am pleased to confirm ethical approval for the protocol amendment, time extension of 3 years and the change in personnel for the above study.

The following documents were reviewed:

- **Letters dated 23rd of January and 19th of March 2003**
- **Amended LREC Application Form**
- **SUHT Consent Form**
- **Amended Protocol**
- **SUHT Patient agreement to investigation or treatment Consent Form I**

This approval has been granted under Chairman's action by the Chairman Dr Audrey Kermode, and will be recorded at the committee meeting in April.

Yours sincerely,

Mrs Clair Wright
Research Ethics Manager

Chairmen: Dr Audrey Kermode/ Dr David Briggs
Manager: Mrs Clair Wright

Appendix 2 Portsmouth Ethical Application

Isle of Wight, Portsmouth and South East Hampshire
Health Authority

Finchdean House
Milton Road
Portsmouth PO3 6DP

Tel: 023 9283 8340
Fax: 023 9273 3292

Direct Line: 023 9283 5139
Fax: 023 9283 5073

Dr Timothy Leach
MP813
Southampton General Hospital
Southampton SO16 6YD

31 August 2001

Dear Dr Leach

REC Prop No: **07/01/1203**
Title: **Culture of human renal tubule cells from nephrectomy tissue**

This is to inform you that the Chair of the Local Research Ethics Committee has approved the above study. Approval for the study is only granted until the end of **August 2002**. If your study continues after this date further Ethics Committee approval will be required.

Thank you for completing the data protection questionnaire. We hope that this was not an onerous task. All applications to the LREC are now required to complete one of these forms so that we can document compliance with the Data Protection Act and increase the awareness of researchers of the implications of the Act. Our current LREC application form has the data protection question removed from it.

The following documents were reviewed:

Protocol	not dated
Patient consent form	not dated
Patient information sheet	not dated
Consultant information letter	not dated
Researcher's CV	Timothy Leach

The Ethics Committee will require a copy of the completed study for its records, you are therefore requested to submit a copy of the completed study to the address above.

The Committee must be informed of any untoward or adverse events which occur during the course of the study.

Please inform the Committee if the study is withdrawn, or does not take place.

The Ethics Committee must also be informed of, and approve, any proposed amendments to your initial application.

Appendix 3 Laser Confocal Microscopy

Laser Scanning Confocal Microscopy is now established as a valuable tool for obtaining high-resolution images and 3-D reconstructions of a variety of biological specimens. It makes use of fluorescence microscopy with computer controlled optics and image storage / interpretation.

Fluorescence

Some molecules emit colour of a different wavelength when exposed to light. This is fluorescence. The molecules absorb high-energy light (blue, for example), which increases the energy state of the molecules. Some of the energy from each blue photon is lost internally and then the molecules emit a photon with less energy, e.g. green. Fluorescein is a common dye that acts in exactly this way, emitting green light when hit with blue excitation light. The colour of light emitted is material dependent, and likewise the excitation light wavelength depends on the material.

Fluorescence microscopy

The advantage of fluorescence for microscopy is that fluorescent dye molecules can be attached to specific parts of the sample, so that only those parts are seen at microscopy. More than one type of dye can be used. By changing the excitation light, one type of dye can be caused to fluoresce, and then another, to distinguish different parts of the sample.

The microscope uses a *dichroic mirror* (or more properly, a "dichromatic mirror"), which reflects light shorter than a certain wavelength, and passes light longer than that wavelength. Thus the photomultiplier sees only the emitted red light from the fluorescent dye, rather than seeing scattered purple light (Figure 98).

This particular style of fluorescence microscopy is known as epi-fluorescence, and uses the microscope objective to illuminate the sample (rather than illuminating the sample from the other side, which would be trans-fluorescence).

Confocality

Two microscope lenses focus light from the focal point of one lens to another point (see Figure 99), represented by the blue rays of light. The red rays of light represent light from another point in the sample, which is not at the focal point of the lens, but which nonetheless gets imaged by the lenses of the microscope. (The red and blue rays in the picture are meant to distinguish the two sets of rays, not different wavelengths of light.)

The image of the red point is not at the same location as the image of the blue point. To image just the blue point, that is, the point directly at the focus of the lens: a screen with a pinhole at the image of the blue point (where the blue rays converge) will block rays from the out of focus areas.

This solves one of the problems of regular fluorescence microscopy. Normally, the sample is completely illuminated by the excitation light, so the entire sample is fluorescing at the same time. Of course, the highest intensity of the excitation light is at the focal point of the lens, but nonetheless, the other parts of the sample do get some of this light and they do fluoresce. This contributes to a background haze in the resulting image. Adding a pinhole/screen combination solves this problem. Because the focal point of the objective lens of the microscope forms an image where the pinhole is, these two points are known as "conjugate points" (or alternatively, the sample plane and the pinhole/screen are conjugate planes). The pinhole is **con**jugate to the **focal** point of the lens, thus it is a **confocal** pinhole.

Laser confocal microscopy

See Figure 100: a laser is used to provide the excitation light (in order to get very high intensities). The laser light (blue) reflects off a dichroic mirror. From there, the laser hits two mirrors that are mounted on motors; these mirrors scan the laser across the sample. Dye in the sample fluoresces, and the same mirrors that are used to scan the excitation light (blue) from the laser descanned the emitted light (green). The emitted light passes through the dichroic and is focused onto the pinhole. A detector, i.e. a photomultiplier tube, measures the light that passes through the pinhole.

So, there never is a complete image of the sample – at any given instant, only one point of the sample is observed. The detector is attached to a computer that builds up the image, one pixel at a time. In practice, this can be done perhaps 4 times a second, for a 512x512 pixel image. The limitation is in the scanning mirrors.

Advantage of using a confocal microscope

By having a confocal pinhole, the microscope is efficient at rejecting out of focus fluorescent light. The practical effect of this is that the image comes from a thin section of your sample (a small depth of field). By scanning many thin sections through the sample, a very clean three-dimensional image of the sample can be built up.

Also, a similar effect happens with points of light in the focal plane, but not at the focal point – the pinhole screen blocks emitted light from these areas. So a confocal microscope has slightly better resolution horizontally, as well as vertically. In practice, the best horizontal resolution of a confocal microscope is about 0.2 microns, and the best vertical resolution is about 0.5 microns.

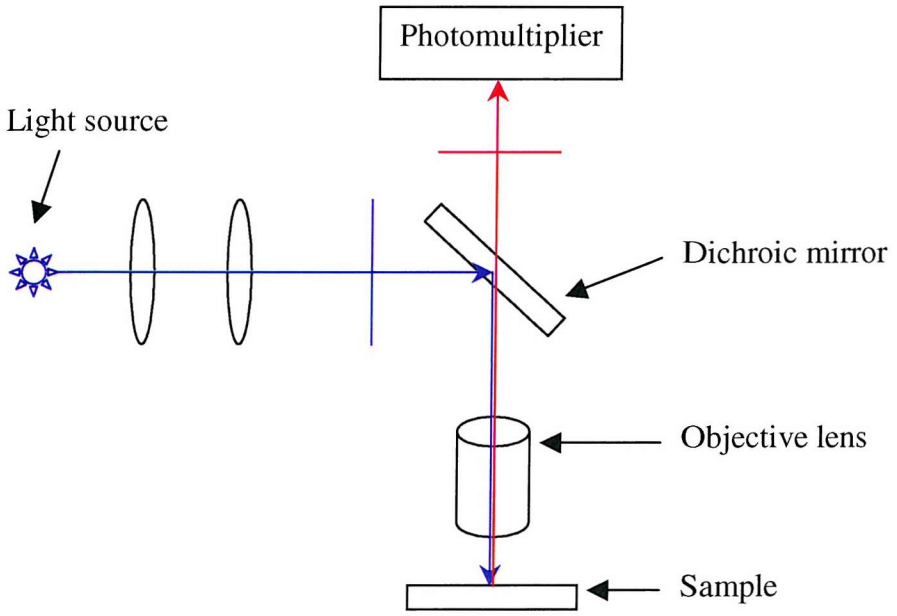

Figure 98. Schematic of epi-fluorescence microscope. Excitation light is blue, emitted light is red. Focusing lenses after the light source. Perpendicular lines = filters.

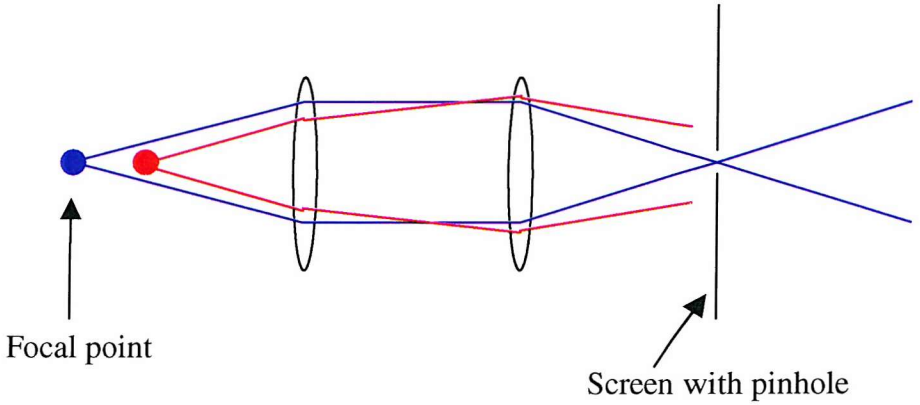

Figure 99. Focusing objective with pinhole screen. Paths of light from different focal points represented by red and blue lines. Pinhole placed at blue focusing point. Two objective lenses shown.

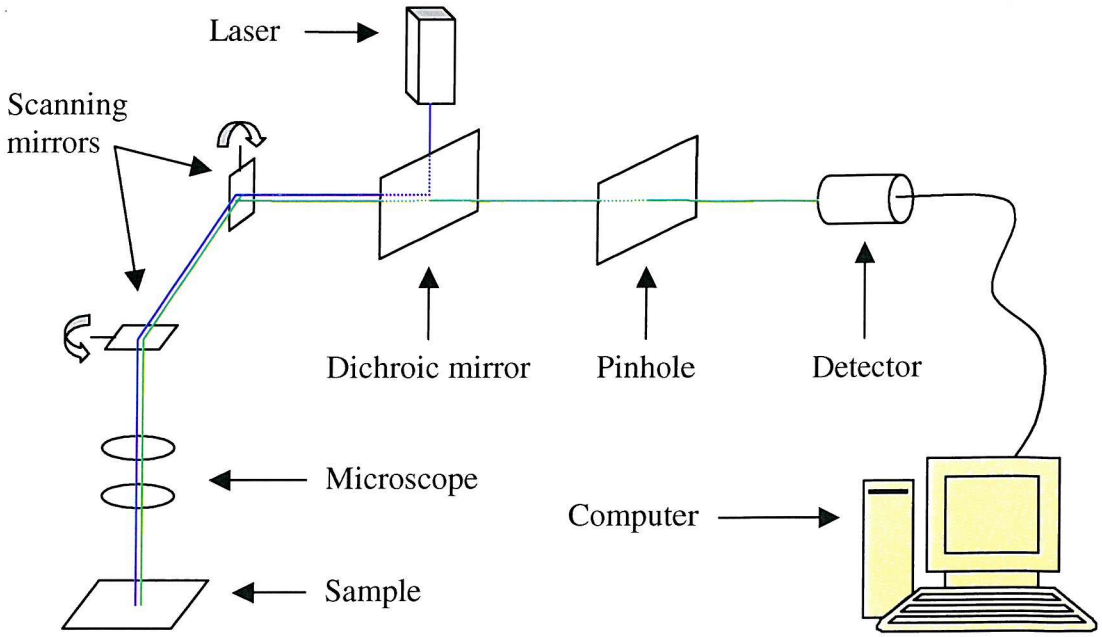

Figure 100. Schematic of scanning laser confocal microscope. The computer also controls the scanning mirrors and laser.

Appendix 4 Flow cytometry

Introduction

In order to appreciate the value of flow cytometry it is first of all necessary to consider what alternative techniques are available. Flow cytometry essentially allows the same sorts of measurements to be made that could be made by conventional light or fluorescence microscopy.

However, conventional microscopy has the following disadvantages:

- Conventional microscopy is labour intensive and slow. Realistically one may expect to count a hundred cells or so in a minute but if more demanding measurements are required such as sizing, identification or characterisation in terms of stain uptake then analysis times will be greatly increased.
- Microscopic analysis of samples leads to operator fatigue, which will affect the reliability of the results.
- As a result of the above problems, typically only a few cells (10s or 100s) will be analysed. This will adversely affect the statistical significance of the results obtained and thus the conclusions that can be safely drawn from the data.
- Microscopic analyses are qualitative or at best semi-quantitative. Generally for example, it will be possible to distinguish between an unstained cell and a cell stained with a blue dye, but it will not be possible to differentiate between cells on the extent of their staining except in extreme cases.
- The accuracy of conventional microscopic measurements is very dependent upon the operator performing the measurements.

Background

Flow cytometers are used to rapidly count and identify bacteria, cells, and other biological particles. Although flow cytometers measure only one cell at a time, they are capable of processing thousands of cells in just a few seconds. The cells may be living or fixed at the time of study, but in either case they must be in a single cell suspension. Flow cytometers function by passing cells through a laser beam in a continuous single-file stream. Each cell scatters some of the laser light, and also emits fluorescent light excited by the laser.

The cytometer measures a number of factors based on scattering and emission and uses this data to differentiate between and count the types of cells in the mixture. Some of the main aspects measured include low angle forward scatter intensity (approximately proportional to cell diameter); orthogonal (90 degree) scatter intensity (approximately proportional to the granularity of the cell); and fluorescence intensities at several wavelengths. This data creates a "histogram" of each cell.

The machinery

There are several components that make up a flow cytometer which include:

- The fluidics system which is required for sample delivery
- The optical system which makes the measurements
- The electronics used for signal detection, data processing and automation
- The computer interface - i.e. the software and hardware used to control the flow cytometer and to collect, display and store the data

Fluidics

The important characteristic of *flow* cytometry is that measurements are made as the cell sample flows through the instrument. If a simple tube were used to deliver the sample, the cells (represented by black dots in the Figure 101A) would not be delivered reproducibly to the measuring point (yellow dot). If a narrower tube were used to ensure reproducible sample delivery it would be likely that blockages would result. To overcome these problems, a method known as *hydrodynamic focusing* is used (Figure 101B). This involves introducing a slowly moving stream of cells into a quickly moving carrier fluid. The carrier (or sheath) fluid constrains the cells to the centre of the tube and thus the cells are reproducibly delivered to the measuring point.

Optics

The optical system of a flow cytometer is composed of one or more light sources, together with a series of lenses, filters and detectors. The lenses and filters act to deliver the light source to the measuring point and also to transfer scattered light and fluorescence from the measuring point to the detectors.

Laser light is used as this has the advantage of monochromasia – i.e. light is of a single wavelength. This helps when separating light scatter from fluorescence. The

most commonly used laser is the Argon Ion laser with a wavelength of 488 nm. HeNe lasers e.g. 544 nm or 633 nm are also often used.

Filters

Optical filters allow light of selected wavelengths to pass through while limiting transmission of other wavelengths. The two most commonly used in flow cytometry are:

- Dichroic filters are selective mirrors that allow transmission of long wavelengths while reflecting short wavelengths. In the example shown in Figure 102, cells were illuminated with 488 nm light from an Argon ion laser. This has resulted in scattering at the incident wavelength and fluorescence at longer wavelengths. By using a 500 nm dichroic the majority of the scattered light is reflected downwards to one detector, whilst the majority of the fluorescent light is transmitted to another detector;
- Band pass filters allow light of a specific wavelength, or narrow band of wavelengths, to pass through. In the example in Figure 103, a mixed light source resulting from scattering and fluorescence reaches a 630 nm band pass filter. This filter is designed to allow transmission of a narrow band of wavelengths between 620 and 640 nm. In this way fluorescence from a single cellular component or added stain can be isolated and quantified.

The optics and fluidics combine to provide a method of delivering the sample in a reproducible manner to the focused light source. A series of filters are then used to split the resulting light into bands representing scattering by the cells and fluorescence from different compounds within them (Figure 104).

Computer

The flow cytometer is connected to a computer (in our case an Apple Mackintosh) running specific software (CellQuest from Becton Dickinson). The software acquires the data from the cytometer, stores it and creates histograms etc. of the data recorded.

Figure 101. Schematic of cell flow within a flow cytometer. (A) flow through a simple tube, (B) flow within a fluid-focused column of cells. **Black dots** = cells, **yellow dot** = sampling point. In **A** the cells cannot reliably be delivered at the sampling point. In **B**, a fast-flowing fluid sheath around the column of cells keeps them focused to a narrow beam.

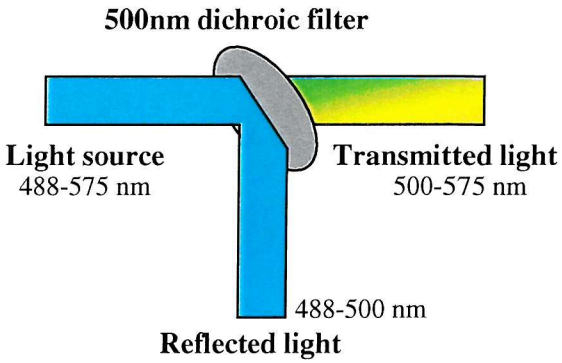

Figure 102. Schematic of dichroic filter. The filter transmits light above a defined wavelength, while reflecting light below that wavelength. Scattered light tends to be around the wavelength of the incident light, whereas emitted fluorescence has a higher wavelength (lower frequency). Thus scattered and emitted light can be separated.

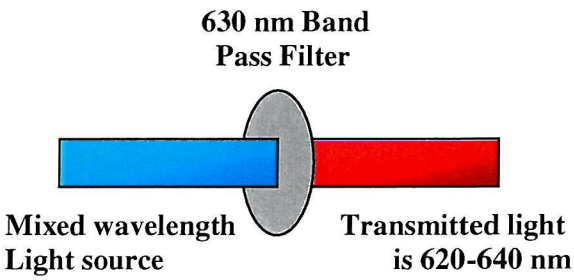

Figure 103. Schematic of a band pass filter. Such filters limit transmitted light to a narrow band width, reducing interference and increasing the specificity of a light detector.

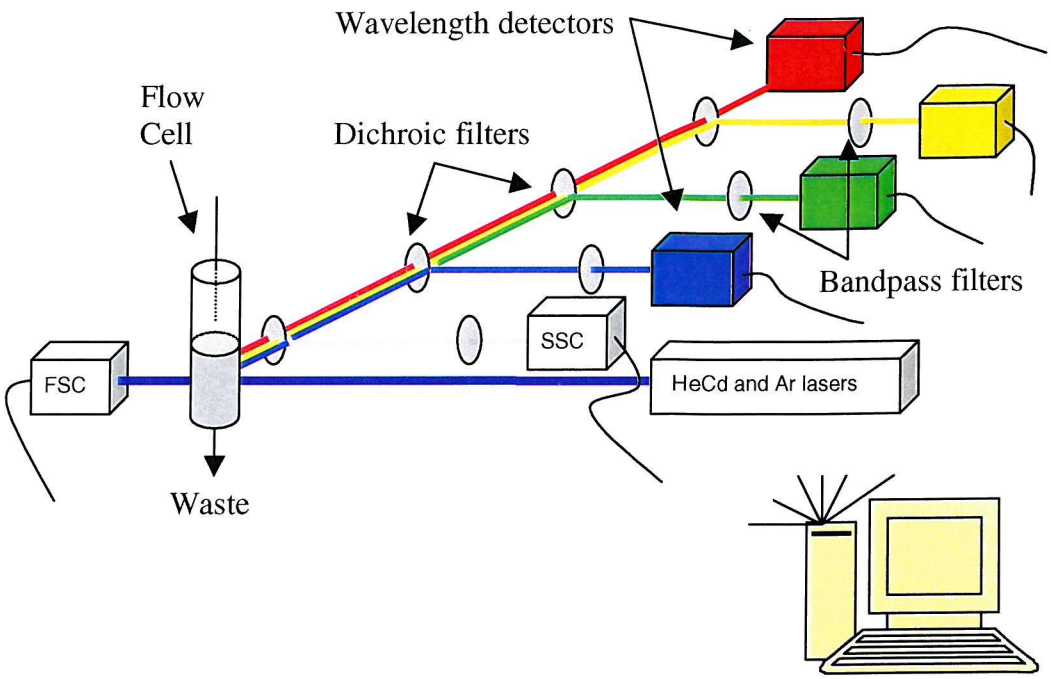

Figure 104. Schematic of flow cytometer. Laser light is shone onto the narrow column of cells within the flow cell. Scattered light transmitted is measured by the Forward Scatter (FSC) detector, and passed to the computer. Scattered and emitted fluorescence light is reflected off and transmitted through dichroic filters of specific wavelengths, defined further through band pass filters, and measured by wavelength detectors, before being passed to the computer for acquisition, recording, analysis and graphical/data output.

Appendix 5 Experimental Protocols

General procedures

Preparation of Phosphate Buffered Saline

Materials required

Disodium hydrogen phosphate

1.0N Hydrochloric acid

Potassium chloride

Potassium dihydrogen phosphate

Reverse osmosed water

Sodium chloride

Equipment Required

>40g balance

5.0L beaker

Magnetic stirrer, and "flea"

pH buffers: pH 4.0, 7.0 and 10.0

pH meter

500ml screw top bottles

(Autoclave)

Method

PBS:

1. Weigh out 40g sodium chloride
   1g potassium dihydrogen phosphate
   5.75g disodium hydrogen phosphate
   1g potassium chloride
2. Measure out 5L reverse osmosed water and add chemicals, stirring continuously
3. Calibrate pH probe using standard buffer solutions @ pH 4.0, 7.0 and 10.0
4. Insert pH probe and correct pH slowly to 7.3 using 1.0N hydrochloric acid
5. Dispense into 500ml bottles

6. Autoclave if needed sterile
7. Keep at 4°C until required

10x PBS:

1. Weight out 80g sodium chloride
   2g potassium dihydrogen phosphate
   11.5g disodium hydrogen phosphate
   2g potassium chloride
2. Measure out 1L reverse osmosed water and add chemicals, stirring continuously
3. Calibrate pH probe using standard buffer solutions @ pH 4.0, 7.0 and 10.0
4. Insert pH probe and correct pH slowly to 7.3 using 1.0N hydrochloric acid
5. Dispense into 500ml bottles
6. Keep at 4°C until required

Hazards

- Wear gloves and laboratory coat at all times
- See end of chapter for further details

Preparation of Tris Buffered Saline

Materials Required

1.0N Hydrochloric acid

Reverse osmosed water

Sodium chloride

TRIS hydroxymethyl methylamine

Equipment Required

>80g balance

10.0L beaker

Magnetic stirrer, and "flea"

2-5L Measuring flask

pH buffers: pH 4.0, 7.0 and 10.0

pH meter

500ml screw top bottles

Method

1. Weigh out 80g sodium chloride
   6.05g TRIS hydroxymethyl methylamine
2. Measure out 10L reverse osmosed water and add chemicals, stirring continuously
3. Calibrate pH probe using standard buffer solutions @ pH 4.0, 7.0 and 10.0
4. Insert pH probe and correct pH slowly to 7.6 using 1.0N hydrochloric acid
5. Keep at 4°C until required

Preparation of Bovine Serum Albumin

Materials required

Bovine Serum Albumin (BSA)

Phosphate buffered saline (PBS)

TRIS buffered saline (TBS)

Equipment Required

>10g balance

200ml Beaker

Magnetic stirrer and "flea"

10ml Measuring flask

100ml Measuring flask

1ml Pipette

Method

10% BSA:

1. Weigh out 10g bovine serum albumin
2. Measure out 100ml PBS and add BSA slowly, stirring gently continuously
3. Keep at 4°C until required

1% BSA:

1. Pipette or measure out 1 or 10ml 10% BSA
2. Make up to 10 or 100ml with TBS or PBS
3. Use immediately or keep at 4°C until required

Preparation of Paraformaldehyde

Materials required

Paraformaldehyde

Phosphate buffered saline (PBS)

100°C spirit thermometer

Equipment Required

>4g balance in fume hood

200ml Beaker

Fume hood

Heated magnetic stirrer and "flea"

100ml Measuring flask

1ml Pipette

Method

4% Paraformaldehyde:

1. In fume hood:
2. Weigh out 4g Paraformaldehyde
3. Measure out 100ml PBS and add paraformaldehyde, stirring continuously
4. Gently heat, while stirring, to 60°C
5. Continue stirring until solution clears
6. Allow to cool, cover, remove from fume hood, and keep at 4°C until required
7. Keep for up to 7 days in the dark at 4°C

2% Paraformaldehyde:

1. Pipette out 4% Paraformaldehyde
2. Make up to double volume with PBS
3. Use immediately or keep at 4°C until required (≤7 days)

Preparation of Antifade

Materials required

1,4-diazobicyclo-(2,2,2)-octane (DABCO)

Glycerol

Trizma buffer pH5

Equipment Required

2g Balance

10ml measuring flask

20ml Universal container

Method

10× Antifade solution:

1. Weigh out 2g DABCO
2. Dilute in 10ml Trizma buffer pH5
3. Store at –20°C

Antifade solution:

1. Add 2ml 10× Antifade to 18ml Glycerol

Preparation of Media

Materials required

DMEM : F-12 Ham (1:1 mixture) medium (sterile)

RPMI 1640 medium (sterile)

200mM L-Glutamine (sterile)

Penicillin (10,000 u/ml) – Streptomycin (10mg/ml) (sterile)

Equipment Required

0.2μm syringe filter (sterile)

5ml syringe (sterile)

Tissue culture hood

Method

Basal medium:

1. In tissue culture hood, filter sterilise (draw up into sterile syringe, pass through syringe filter) 5ml L-glutamine into 500ml DMEM : F-12 Ham medium
2. Store at 4°C

RPMI with 2× antibiotics:

1. In tissue culture hood, filter sterile 10ml Penicillin – Streptomycin mixture into 500ml RPMI 1640 medium
2. Store at 4°C

Basal medium with ½ antibiotics:

1. In tissue culture hood, filter sterilise 5ml L-glutamine into 500ml DMEM : F-12 Ham medium
2. Filter sterilise 2.5ml Penicillin – Streptomycin mixture into medium
3. Store at 4°C

Hazards

- DABCO is corrosive, and is harmful by skin contact, inhalation and ingestion: avoid exposure to dust
- Disodium hydrogen phosphate is hygroscopic: care must be taken when handling stock to avoid excessive exposure to air
- DMEM : F-12 Ham medium should be used with caution
- L-Glutamine should be used with caution
- Glycerol is hygroscopic and should be used with caution: avoid excessive exposure of stock to air
- 1.0N hydrochloric acid is toxic by skin contact and inhalation, and causes burns: pour within a fume hood and keep bottle stopped
- Paraformaldehyde is harmful by contact, and toxic by inhalation: use fume cupboard at all times when handling powder
- Penicillin and streptomycin are toxic by skin contact and inhalation, may cause sensitisation and harm the unborn child: avoid exposure, particularly if pregnant
- Potassium chloride is harmful by skin contact or inhalation, and is hygroscopic: avoid excessive exposure of stock to air, avoid breathing dust
- Potassium dihydrogen phosphate may be harmful, and is hygroscopic: avoid excessive exposure of stock to air
- RPMI 1640 medium should be used with caution
- Sodium chloride is irritating to eyes: avoid contact with eyes
- TRIS hydroxymethyl methylamine is irritant by skin, eye and respiratory contact: avoid exposure to dust
- Trizma buffer is irritant by skin, eye and respiratory contact: avoid contact

Specific procedures

Protocol 1 Cell counting and viability estimation

Materials required

Cell suspension(s)

Trypan blue (0.1% in PBS)

Equipment Required

Improved Neubauer Haemocytometer slide with coverslip

50µl pipette

Method

1. Suspend cells in 1ml of medium (if very few cells, can use less).
2. Ensuring suspension is well mixed, remove 50 or 100µl to a test tube.
3. Dilute cell suspension 1:1 with Trypan blue
4. Ensuring the cytometer is clean and dry, condensate the centre by breathing on it
5. Centre a coverslip on the cytometer
6. Using the pipette, place just enough of the mixed cell/trypan blue suspension on each end of the cytometer to be drawn under the coverslip and fill area beneath. Do not use too little to leave bubbles/unfilled edges, or too much to spill out into the grooves either side or in the centre
7. Count the number of cells within each of the two grids (see Figure 105, one each side of the central divide). Dead cells will have taken up the dye and appear blue, viable cells are clear. Do not count cells which lie on the left or top triple lines of each large square
8. Repeat 2-4 times (= total number of counts, ½ total number of grids counted)
9. The area of each grid is $1mm^2$. The depth of the film beneath the coverslip is 0.1mm. The volume of each grid is therefore $0.1mm^3$
10. $1ml = 1cm^3 = 1000mm^3$. Therefore the volume of each grid is $10^{-4}ml$

11. The concentration of cells in the film on the grid is therefore the number of cells on the grid x10^4/ml
12. The original cell suspension is twice the counted concentration as this has been diluted 1:1 with trypan blue, i.e. the number of cells per grid x 2x10^4/ml, or the total number of cells in two grids x10^4/ml

13. If the original suspension was in less than 1ml, multiply the final cell number by the original volume (in ml), as the cells would be less concentrated by that factor had they been suspended in 1ml
14. Thus:

$$\text{Cell number in original suspension} = \text{Total cell count} \times 10^4 \times \text{Original suspension volume (ml)} / \text{Number of counts}$$

Hazards

- Risk of infection from human tissue: always wear gloves and laboratory coat, ensure all used cells are disposed of into 10% Virkon disinfectant, clean haemocytometer well with water then with 70% ethanol
- Trypan blue is toxic by skin contact: always wear gloves and laboratory coat

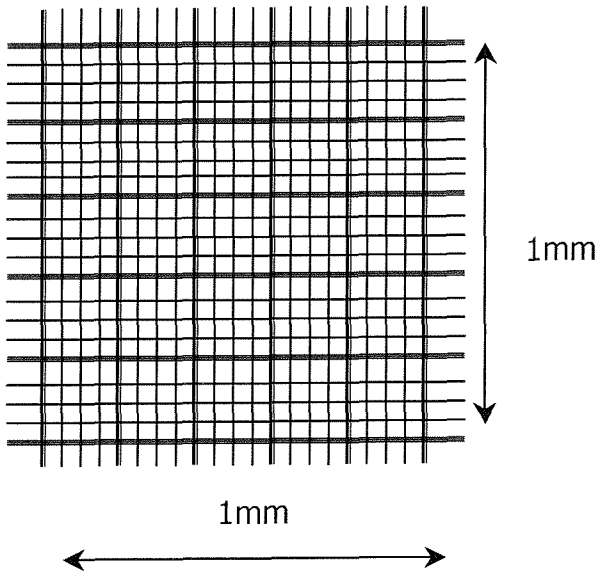

Figure 105. Counting grid on Improved Neubauer Haemacytometer

Protocol 2 Transmission Electron Microscopy

Materials required

Phosphate buffered saline

Glutaraldehyde

Formaldehyde

Piperazine-N,N'-bis[2-ethanesulphonice acid] buffer (PIPES)

Osmium tetroxide

Grade series of ethanols

Acetonitrile

SPURR resin

Saturated uranyl acetate

Reynold's Lead

Equipment Required

Transmission electron microscope (Hitachi H7000)

Copper mounting grids

Fume cupboard

Microtome

Polymerisation oven

Method

1. Wash cell monolayers on culture inserts twice in PBS. While wet, cut from mount while wet with PBS, cut to required size, place in 4ml bijoux of 3% glutaraldehyde / 4% formaldehyde in PIPES buffer fixative
2. **Remainder performed by Ann Farrer**
3. *Allow 1 hour for fixation, then rinse twice for 10mins each in PIPES buffer*
4. *Transfer to post fixative (0.1% osmium tetroxide in PIPES buffer) for 1 hour*
5. *Rinse again twice in PIPES buffer*
6. *Dehydrate through 30%, 50%, 70%, 95%, 100% and 100% ethanol baths, 10mins each up to 95% then 20mins each for 100%*
7. *Place in acetonitrile for 10 mins, then in a 50:50 mixture of acetonitrile and SPURR resin overnight*

8. *Place in resin for 6 hours*
9. *Embed in fresh resin and polymerise at 60°C for 20-24 hours*
10. *Cut ultrathin (80nm) sections on an ultramicrotome*
11. *Mount on copper grids*
12. *Stain with saturated uranyl acetate and Reynold's Lead*
13. *Examine and photograph on transmission electron microscope*

Hazards

- Glutaraldehyde is harmful by inhalation, ingestion and on skin contact: always wear nitrile gloves (glutaraldehyde penetrates latex gloves) and laboratory coat and use in a fume cupboard
- Formaldehyde is toxic by inhalation and ingestion: always wear gloves and laboratory coat and use in a fume cupboard
- Osmium tetroxide is very toxic by inhalation, ingestion and on skin contact: always wear gloves, laboratory coat and safety goggles and use in a fume cupboard
- Ethanol is highly flammable: always keep in screw-top container in flammables chest, avoid naked flames and use with other flammable agents or equipment which causes sparks
- PIPES may be harmful: wear gloves and laboratory coat
- Acetonitrile is harmful by inhalation, ingestion and on skin contact: always wear gloves and laboratory coat and use in a fume cupboard
- Epoxy resin is harmful by inhalation, ingestion and on skin contact: always wear gloves and laboratory coat and use in a fume cupboard
- Uranyl acetate is very toxic by ingestion and inhalation, may cause cumulative effects and is dangerous to the environment: always wear gloves and laboratory coat and use in a fume cupboard, always store waste material for safe disposal
- Reynold's Lead is toxic by inhalation, ingestion, skin contact, and cumulative exposure: always wear gloves and laboratory coat and use in a fume cupboard

Protocol 3 Scanning Electron Microscopy

Materials required

Phosphate buffered saline

Gold-palladium sputter coating

Equipment Required

Fume cupboard

Mounting stubs

Scanning electron microscope (Hitachi S800)

Method

1. See steps 1. to 7. of Protocol 2, then:
8. *Critical point dry by evacuation*
9. *Mount on stub*
10. *Sputter coat with gold palladium for 1-2mins*
11. *Examine and photograph on scanning electron microscope*

Hazards

- Gold palladium is harmful, particularly cumulatively: wear gloves and laboratory coat and use in fume cupboard

Protocol 4 Microprotein Measurement

Materials required

0.01% Bovine serum albumin in H_2O

Bradford reagent (Coomassie blue in phosphoric acid (85%) and methanol)

Equipment Required

96-well microtitre plate

Pipettes

Spectrophotometer

5ml test tubes

Method

1. Gently mix the dye reagent in the bottle
2. Prepare standard solutions as Table 12
3. Prepare cell solutions: add 50µl cell suspension to 1.95ml R.O. H_2O in a bijoux bottle. Sonicate for 10s at 14µm. Make 1:400 and 1:1000 dilutions from sonicated samples
4. Add 100µl standard or protein solutions to each well: see Figure 106.

Table 12. Microprotein assay calibration samples:

Tube No.	0.01% BSA (µl)	H_2O (µl)	Protein (µg/well)
P1	0	1000	0
P2	20	1980	0.1
P3	20	980	0.2
P4	40	960	0.4
P5	60	940	0.6

5. Add 100µl Bradford reagent to each well
6. Leave for 5 mins for full colour to develop
7. Measure absorbance at 620nm (colour stable for 1hr – concentrations measurable and appropriate wavelengths determined Figure 108 and Figure 109)

8. Subtract the absorbance of the appropriate blank from each solution's absorbance
9. Plot the standard curve from the corrected standard absorbances (Figure 107)
10. Determine the protein concentration of each sample from the standard curve
11. Multiply result by dilution factor to determine initial sample protein content

Hazards

- Bradford reagent is corrosive, toxic by contact and inhalation, highly flammable, and should be used with caution: always wear gloves and laboratory coat, avoid sources of ignition. In the event of spillage wear breathing apparatus and rubber gloves and boots, cover with dry lime or soda ash and keep in a closed container until disposal by incineration

	Sample 1			Sample 2						Calibration		
	A	B	C	D	E	F	G	H	I	J	K	L
1	1:40	1:40	1:40	1:40	1:40	1:40				P1	P1	P1
2	1:400	1:400	1:400	1:400	1:400	1:400				P2	P2	P2
3	1:1000	1:1000	1:1000	1:1000	1:1000	1:1000				P3	P3	P3
4										P4	P4	P4
5										P5	P5	P5
6												
7												
8												

Figure 106. Microprotein 96-well microtitre plate layout

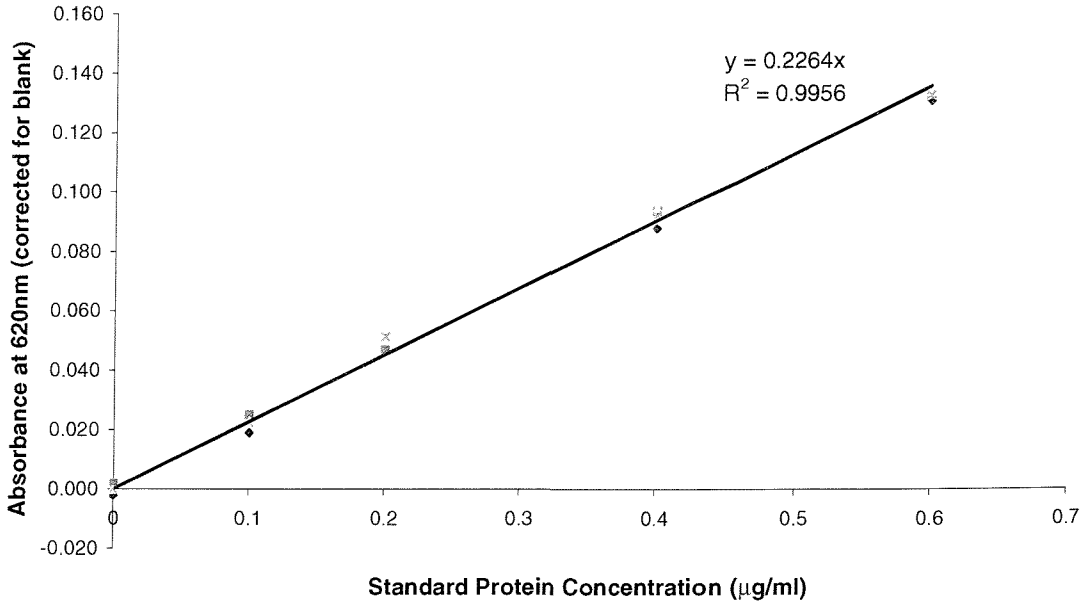

Figure 107. Sample standard curve for microprotein assay. All samples assayed in triplicate.

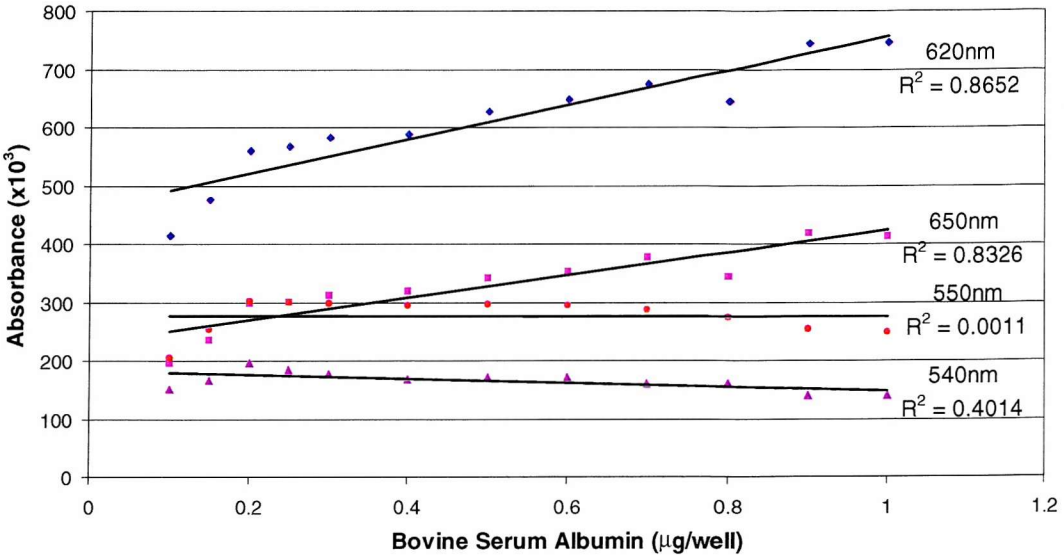

µ

Figure 108. Absorbances of standard protein solutions for different light wavelengths. Absorbance at 620nm gives the greatest discrimination between protein concentrations.

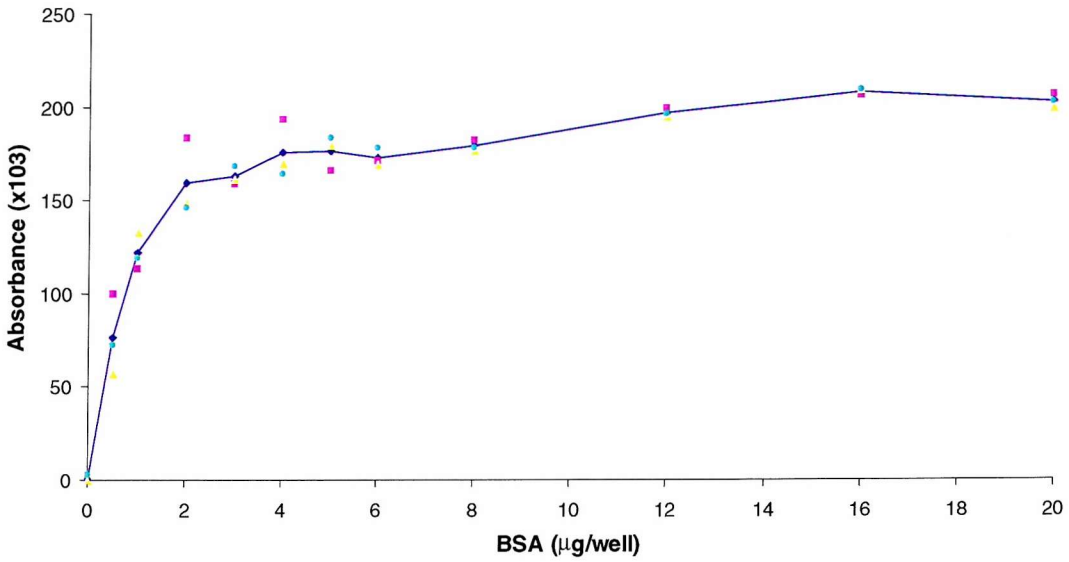

Figure 109. Absorbances of higher protein concentrations. Only protein concentrations below 1µg/well achieve linearity on the standard scale. All samples were subsequently diluted into this range.

Protocol 5 Alkaline Phosphatase Activity Measurement

Materials required

Concentrated hydrochloric acid

Phosphate buffered saline

Reverse-osmosed water

Sigma control enzyme solution 2-E

Sigma kit x

- Alkaline buffer solution (2-amino-2-methyl-1-propanol)
- Stock substrate solution: 100mg capsule into 25ml H_2O (p-Nitrophenyl phosphate – store at –20°C)
- Dilute p-Nitrophenol solution: 0.5ml p-Nitrophenol standard solution diluted to 100ml with 0.02N sodium hydroxide (2:3 dilution of 0.05N NaOH with H_2O)

0.05N sodium hydroxide

Equipment Required

96-well microtitre plate

Pipettes

Spectrophotometer (Titretek MicroScan)

Temperature-controlled water bath

10ml test tubes with stoppers

Method

1. For each sample, label 2 tubes, BLANK and TEST (including control enzyme as a sample)
2. Into BLANK and TEST place 0.25ml 221 Alkaline Buffer Solution and 0.25ml Stock Substrate Solution
3. Place both tubes into 37°C water bath – allow to equilibrate
4. Pipette 0.05ml control (medium for cell sample, PBS for enzyme sample) into BLANK, and 0.05ml sample into TEST, recording exact time, and returning tubes to water bath promptly

5. Set up calibration samples as Table 13. Pipette 300µl of each in triplicate into 96-well microtitre plate as Figure 110.

Table 13. Alkaline phosphatase calibration samples

Tube No.	Dilute p-Nitrophenol solution (µl)	0.02N NaOH (µl)	ALP activity (SU/ml)
A1	0	660	0
A2	60	600	1
A3	180	480	3
A4	360	300	6
A5	600	60	10

6. After exactly 15 mins, add 5ml 0.05N NaOH to each tube, stopper and mix by inversion
7. Remove 200µl aliquots of TEST and BLANK into microtitre plate, as Figure 110.
8. Add 0.1ml concentrated hydrochloric acid to each tube and mix (bleaches out all ALP colour, leaving sample "blank" – affords measurement of and allowance for any non-ALP yellow colour)
9. Remove 200µl aliquots of TEST and BLANK into microtitre plate.
10. Read absorbance of plate at 414nm
11. Plot standard curve of ALP activity against absorbance (see Figure 111)
12. Determine ALP activity of each sample from standard curve
13. Subtract ALP activity in 9 ("Blank" samples) from 7 (Test samples), yielding corrected ALP activity of sample, then control samples from test samples

Hazards

- Risk of infection from human tissue: always wear gloves and laboratory coat, ensure all used cells are disposed of into 10% Virkon disinfectant, clean all used equipment well with water then with 70% ethanol
- Alkaline buffer solution is irritant: wear gloves and laboratory coat
- Stock substrate solution may be harmful: wear gloves and laboratory coat

- p-Nitrophenol is harmful by inhalation, ingestion or skin contact: wear gloves and laboratory coat
- Sodium hydroxide is corrosive: wear gloves and laboratory coat
- Concentrated hydrochloric acid is toxic by skin contact and inhalation: always wear gloves and laboratory coat, decant from contained within fume cupboard, use in well-ventilated area, avoid breathing vapour
- Control enzyme solution may be harmful by contact or inhalation: always wear gloves and laboratory coat
- Risk of electric shock or burns from water bath: ensure all switches and cables are kept away from the water, ensure electrical safety checks are current, ensure the heating element is kept immersed at all times, avoid contact with the heating element

		Sample 1			Sample 2						Calibration		
		A	B	C	D	E	F	G	H	I	J	K	L
Test Samples	1	T1	T1	T1	T2	T2	T2				A1	A1	A1
	2	MB1	MB1	MB1	MB2	MB2	MB2				A2	A2	A2
	3	E1	E1	E1	E2	E2	E2				A3	A3	A3
	4	W1	W1	W1	W2	W2	W2				A4	A4	A4
"Blank" (post-HCl) Samples	5	T1	T1	T1	T2	T2	T2				A5	A5	A5
	6	MB1	MB1	MB1	MB2	MB2	MB2						
	7	E1	E1	E1	E2	E2	E2						
	8	W1	W1	W1	W2	W2	W2						

Figure 110. Alkaline phosphatase 96-well microtitre plate layout

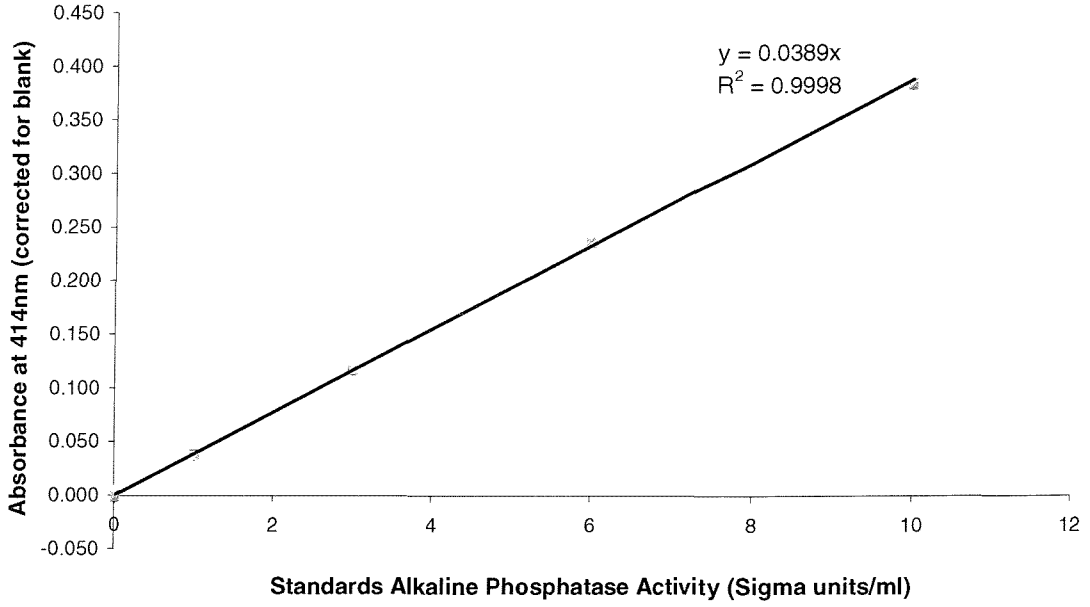

Figure 111. Sample standard curve for alkaline phosphatase activity assay. All samples and blanks assayed in triplicate.

Protocol 6 γ-Glutamyltransferase Activity Measurement

Materials required

Cell suspension(s)

Sigma kit 545

GGT substrate solution: 11ml Trizma buffer (0.1M pH 9.0) solution (at RT) + 1 vial GGT substrate (γ-glutamyl-p-nitroaniline and glycylglycine – cap and shake vigorously for a few seconds. Stand 2-3 mins then shake vigorously again) – stable for 5d at 4°C or 14d at –20°C

Sigma Elevated control enzyme solution: 3ml H_2O into 1 vial. Leave for 3 mins then swirl gently – stable for 3d at 4°C or 1 month at –20°C

Acetic acid solution (10%): 50ml glacial acetic acid → 500ml H_2O – used until infected

Sodium nitrite solution (0.1%): 50mg $NaNO_2$ in 50ml H_2O – stable for 7d at 4°C

Ammonium sulfamate solution – stable for months at 4°C

Naphthylethylenediamine solution: 55mg in 105ml H_2O – stable for months in dark at RT

GGT calibration solution (p-Nitroaniline)

Phosphate buffered saline

Equipment Required

96-well microtitre plate

Spectrophotometer

Temperature controlled water bath

10ml test tubes

Method

1. Add 50µl cell suspension to 150µl PBS. Dilute again to 1:50, 1:100 and 1:200
2. For each sample (and control enzyme) add 0.5ml GGT substrate solution to 2 tubes, labelled TEST & BLANK, and place in water bath

3. Place calibration tubes (see Table 14) in water bath

Table 14. Gamma-glutamyltransferase calibration samples

Tube No.	GGT calibration solution (µl)	Water (µl)	GGT activity (U/ml)
G1	0	500	0
G2	100	400	20
G3	300	200	60
G4	400	100	80
G5	500	0	100

4. Allow to equilibrate at 37°C
5. To TEST add 0.02ml sample. Mix by gently swirling
6. Start timer and incubate all tubes at 37°C for EXACTLY 20 mins
7. (Calibration starts here) Remove from water bath; add 2ml acetic acid solution to all tubes. Mix by gently swirling
8. To BLANK add 0.02ml sample. Mix by gently swirling
9. In timed sequence, add 1ml $NaNO_2$ solution to all tubes. Mix quickly and stand at RT for 3 mins
10. In same timed sequence, add 1ml Ammonium sulfamate solution to all tubes. Mix quickly and wait 3 mins
11. Add 1ml Naphthylethylenediamine solution. Cover and shake vigorously until bubbles rise. Final colour is stable for ≥1 hour
12. Transfer to plate (200µl per well – Figure 112) and read absorbance at 540nm
13. Determine GGT activity from calibration curve (see Figure 113). Subtract activity of BLANK from TEST to obtain activity of sample. Multiply by dilution factor for original activity

Hazards

- Risk of infection from human tissue: always wear gloves and laboratory coat, ensure all used cells are disposed of into 10% Virkon disinfectant, clean all used equipment well with water then with 70% ethanol
- GGT substrate solution may be harmful by contact or inhalation: always wear gloves and laboratory coat. Avoid any dust/vapour when weighing out reagents
- Control enzyme solution may be harmful by contact or inhalation: always wear gloves and laboratory coat Avoid any dust/vapour when weighing out reagents
- Acetic acid is corrosive, flammable and the vapour is irritant: keep away from naked flames and other sources of combustion, store in a stopped jar in the flammables chest, always wear gloves and laboratory coat, make up to 10% by its addition to water – never vice versa – in the fume cupboard
- Sodium nitrite solution is toxic, an oxidiser and likely to ignite flammable materials: always wear gloves and laboratory coat, keep in sealed glass container when not in use
- Ammonium sulphamate solution is toxic by contact or irritation and may cause cancer: always wear gloves and laboratory coat, avoid inhalation of dust/vapour when weighing out reagents
- Naphthylethylenediamine solution is irritant by contact or inhalation: always wear gloves and laboratory coat, avoid inhalation of dust/vapour when weighing out reagents
- Risk of electric shock or burns from water bath: ensure all switches and cables are kept away from the water, ensure electrical safety checks are current, ensure the heating element is kept immersed at all times, avoid contact with the heating element

	Sample 1			Sample 2						Calibration		
	A	B	C	D	E	F	G	H	I	J	K	L
1	1:4	1:4	1:4	1:4	1:4	1:4				G1	G1	G1
2	1:50	1:50	1:50	1:50	1:50	1:50				G2	G2	G2
3	1:100	1:100	1:100	1:100	1:100	1:100				G3	G3	G3
4	1:200	1:200	1:200	1:200	1:200	1:200				G4	G4	G4
5										G5	G5	G5
6												
7												
8												

Figure 112. Gamma-glutamyltransferase 96-well microtitre plate layout

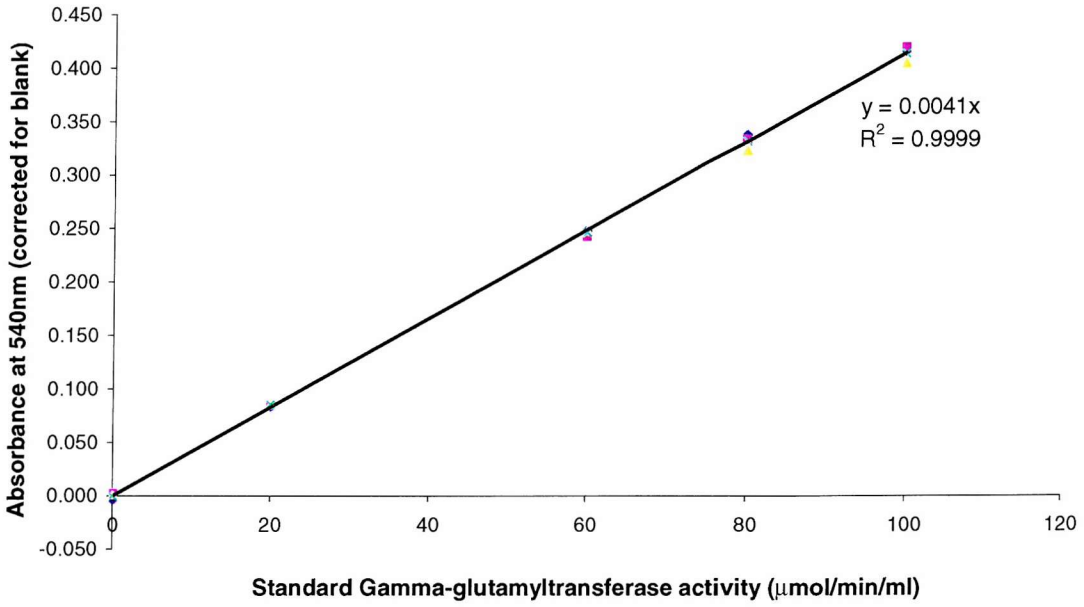

Figure 113. Sample standard curve for gamma-glutamyltransferase activity assay.

All samples assayed in triplicate.

Protocol 7 Indirect Immunofluorescence Staining

Materials required

Anhydrous acetone (filter after use)

Antifade

Bovine serum albumin (1% in TBS)

FITC-conjugated rabbit anti-mouse $F(ab')_2$ (200μg/ml)

Normal Rabbit Serum (neat)

Primary mouse anti-human antibodies (and isotype controls)

Propidium iodide (0.5mg/ml)

Equipment Required

Staining rack

Pipettes

Coplin jar

Glass coverslips

Method

1. **Day 1**:
2. Fix in acetone for 10mins (for cytocentrifuge preparations, immerse in Coplin jar of acetone; for cell culture inserts, cut from mount while wet with PBS, cut to required size, place on slide while wet, allow to air dry on staining rack for at least 30mins, then pipette on sufficient acetone to cover the specimen, taking care to prevent drying of the slide by frequent reapplications), or 4% PFA on staining rack for 4mins, using 2-3 drops per slide (~100μl)
3. For acetone – remove from bath/flick off acetone and air dry for 10mins, for PFA flick off slide well then air dry for 10mins
4. Dilute normal serum (1:20 in TBS)
5. Rehydrate slides with TBS, then flick off
6. Incubate with Normal Serum (~100μl) for 30mins at RT
7. Make up primary antibodies, in 1% BSA
8. Flick off well (not wash) and dry around specimen
9. Incubate with primary antibody (~100μl) at 4°C overnight (in the dark)

10. **Day 2:**
11. Make up FITC-conjugated secondary antibody (in 1% BSA), 20µg/ml with 2.5µg/ml PI, total 100-200µl per specimen
12. Remove slides from cold and wash twice with TBS at RT (with membrane specimens, care is needed to avoid washing away the specimen – holding down the membrane with a pipette tip in one corner is sometimes required)
13. Incubate with secondary antibody with PI in the dark for 30mins at RT
14. Wash with TBS ×1
15. Flick off and dry well around the specimen: avoid drying out the specimen however
16. Mount coverslips with Antifade & seal with nail varnish (Antifade is water soluble and will evaporate, and also does not set so will not hold coverslip in place during microscopy)

17. **Microscope with laser confocal microscope:** see Protocol 9

Hazards

- Propidium iodide is harmful by skin, eye and respiratory contact, with possible risk of irreversible effects: wear gloves and laboratory coat at all times and avoid contact or spillage
- Paraformaldehyde is toxic by contact and inhalation: wear gloves and laboratory coat at all times and avoid contact or spillage
- Acetone is highly flammable: avoid naked flames or storage in anything other than the flammables storage chest
- Acetone is highly volatile, repeated exposure may cause drowsiness or dizziness, vapour is irritant to eyes: use in a well ventilated area, avoid fumes

Protocol 8 Immunofluorescence microscopy

Materials required

Fluorescent-labelled specimen on antifade-mounted coverslip-covered microscope slides

Equipment Required

Zeiss Axioshop 2 – MOT fluorescence microscope

PC attached to microscope running Zeiss KS400 version 3.0 software

Method

1. Turn on microscope and mercury lamp
2. Open software
3. Click on *Image* and *Gallery* buttons on toolbar
4. Click *Acquire* and *Setup*
5. Select FITC-block filter (blue light) on microscope: focus specimen and select appropriate field for FITC microscopy
6. Open shutter on microscope (to enable image acquisition by camera)
7. Click *Live*
8. Set exposure or click *Automatic*
9. Check *Autofocus* box and focus microscope until green focus bar is nearest the highest red line
10. Click *Live* to turn it off
11. Click *Snap*, computer acquires photomicrograph
12. Click *Cancel* once acquisition completed
13. Click on image in gallery, then *Save* button, to save file with .tif extension in appropriate directory
14. Continue from step 3. until completed
15. (To acquire two-colour image, take FITC image, keep same field on microscope, select TRITC-block filter (green light) on microscope in step 4., take picture as steps 5. to 12., then click *Binary* and *Boolean*, ensure correct image numbers (from gallery) are in *Input 1* and *Input 2* windows, click *New output*, check *Function, Or* box, click *Apply* (check output window has correct

appearance) then *OK*. Click on combined image in gallery and *Save* as step 12. Continue from step 3. until all images taken)

Hazards

- Laser light is damaging to sight: always follow standard operating procedure for the fluorescence microscope – never dismantle or use without appropriate safeguards
- Laser light is generated by mercury lamp: mercury vapour is highly toxic – should the lamp blow, evacuate microscopy room immediately

Protocol 9 Laser confocal microscopy

Materials required

Fluorescent-labelled specimen on antifade-mounted coverslip-covered microscope slides

Equipment Required

Leica TCS SP2 laser scanning confocal microscope

PC attached to microscope running Leica Confocal Software version 2.0

Method

1. Turn on PC and microscope / camera / mercury lamp
2. Set laser strength knob to "10-o'clock"
3. Open software – wait for initiation to complete
4. Click *New*
5. Set specimen on stage, pull out beam splitter and select FITC-block filter (blue light). Select appropriate objective, focus specimen and select appropriate field
6. Push in beam splitter and select laser light (number 4)
7. Click *Beam*, double-click *FITC-TRITC* from the menu
8. Ensure *Objective* shows correct one, *8 Bit* is selected, *Expander* is set at *3* for ×10 objective, else *6*, then select *Mode = xyz, Format = 1024×1024, Speed = 400Hz, Scan= Mono*
9. Click *Continuous*, microscope starts scanning
10. Click *Pinhole*, then *AE* and *Airy 1*, *Close*
11. Click *Signal*, then adjust *Gain* and *Offset* to achieve good FITC and TRITC discrimination and minimal / no background
12. Click the little *Series* button, and scan up and down through the section with the *Z-pos* knob, setting *Begin* and *End* positions by checking the small boxes in the *Series* window or clicking on the *Begin* and *End* buttons on the bottom toolbar
13. Click *Stop*
14. Click *Sections* and select the number of sections to scan: maximum is approximately 1 section per 1μm

15. Click *LiA*. This averages x lines and filters noise – *4* is recommended to trade off noise versus speed
16. Click the big *Series* button, microscope scans the specimen in number of sections chosen between start and end depths – images displayed in window
17. While acquiring, click on *LUT* and select *Green* for *Channel 1* and *Red* for *Channel 2*. This ensures saved files are in appropriate colours
18. Images can be overlaid by clicking *RGB*
19. On *Saving* the file, all single images will be saved. To create a composite (red and green) image, particularly one to represent a transmission fluorescence image, click *3D*, then ensure *Maximum projection* is checked
20. To continue, *Close* the file, and return to step 4.

Hazards

- Laser light is damaging to sight: always follow standard operating procedure for the laser confocal microscope – never dismantle or use without appropriate safeguards
- Laser light is generated by mercury lamp: mercury vapour is highly toxic – should the lamp blow, evacuate microscopy room immediately

Protocol 10 Flow Cytometry: General Protocol

Materials required

Cell samples on ice

Equipment Required

Apple Macintosh computer running Cell Quest software attached to flow cytometer

Beckton-Dickinson FACScalibre flow cytometer

Method

1. Switch on FACSCalibur, followed by computer 15 seconds later
2. Remove tube of FACSRinse
3. Fill sheath container ¾ full with FACSFlow
4. Empty waste container
5. Pressurise the sheath fluid container using the Vent Valve
6. Clean the air from the sheath filter by pressing Prime twice
7. Pipette 4ml FACSFlow into a FACS tube. Install and ***RUN*** on ***HI*** for 5 mins
8. Sign in start up information in FACS Users Log

9. Click on *Cell Quest* (from the *Apple Menu*)
10. Press keys *⌘B* (Acquire: Connect to Cytometer)
11. Press keys *⌘1*, *⌘2* then *⌘4* (Cytometer: Detectors/Amps, Threshold, Status)
12. Resize windows *(little square top right)* and position
13. If you have any saved settings, click *Cytometer*, *Instrument Settings*, *[Open]*
14. Open appropriate settings, then click *[Set]* and *[Done]*
15. Load template file for data acquisition: *Close* current file, then click *File*, *Open*, *"Template directory"*, *"Template name"*
16. Click *Acquire, Counters, Parameter Description, [File]*. Change *[Custom Prefix]* to new file name. May need to change/reset *[File Count]*
17. Click *[Folder], "Results directory", [New folder],* type *"Results file name"*, click *[Create]*, then *[Select "Results file name"]*

18. Click *Acquire, Acquisition and Storage, Parameters Saved*, and remove the ones you don't want
19. Consider changing the *[Event Count]*: ensure set to count 10,000 events unless otherwise specified

20. **To test scattergram:**
21. Keep *Setup* ticked ☑ (on *Acquisition Control* window)
22. Ensure *"Status: Ready"* (on *Status* window – machine has to be set to ***RUN*** with sample attached)
23. Click *[Acquire]*
24. Change figures on the Instrument Settings windows until cell scattergram contained within axes (see Figure 114). Click the ⇧⇩ to change slowly, hold the central ✚ then drag the bar which appears to change quickly. Scattergram will contain all cells when there are no dots lined up against the axes. Click *[Pause], [Restart]* to reset display

25. **To test antibody signal:**
26. For FITC-conjugated antibody – adjust FL-1; for Cy5-conjugate, ensure *Four-colour* box is ticked and adjust FL-4. Aim to get all signal within 10^0-10^4, and irrelevant peak $<10^1$ (see Figure 115)
27. Click *[Abort]* when satisfied
28. Click *Instrument Settings, [Save]* to save settings
29. **To sample:**
30. Untick *Setup* ☐
31. (Filename should appear above buttons in same window. Check it's the right one to save into – should be the same one you entered at *[Custom Prefix]* earlier)
32. Change *[P3]* name to Appropriate primary antibody
33. Attach sample to machine (move arm to side, press tube up around probe, move arm back to centre under tube)
34. Click *[Acquire]*
35. Quack/beep will signal end of sampling – remove sample, attach next
36. Return to step 45. until complete

37. When all samples completed, consider saving template file (*Close* file and *Save* when prompted)
38. Press *⌘B* (Disconnect from Cytometer) then *⌘Q* (quit Cell Quest)

39. **Clean Cytometer:**
40. Fill and label 3 FACS tubes with 4ml FACSClean, FACSRinse and dH_2O
41. Install FACSRinse, select [RUN], [HI] & leave sample tube support arm to the side
42. Allow machine to aspirate 2ml
43. Move sample tube support arm to the middle. Continue running for 5 mins
44. Repeat steps 2-4 with FACSClean and dH_2O
45. After 20 secs, select [STANDBY], leave for 5 mins for laser to cool
46. Depressurise the sheath fluid container using the Vent Valve
47. Empty waste container
48. Switch of FACSCalibre
49. Copy data file to ZIP disk [insert disk, find current data file (in "Child Health"), 'drag-and-drop' file to ZIP (should be copied, not moved)]
50. Check ZIP disk (double-click on disk icon etc)
51. Eject ZIP disk ('drag-and-drop' on to "Trash Can")
52. Shut Down computer
53. Sign out shut-down information in FACS Users Log

Hazards

- Laser light is damaging to sight: always follow standard operating procedure for the flow cytometer – never dismantle or use without appropriate safeguards
- Risk of infection from human materials to operator and subsequent users: wear gloves and laboratory coat at all times, add FACSafe to waste container (~1:1 ratio) before disposal, ensure any spillages cleaned up immediately with FACSafe disinfectant, ensure all equipment is thoroughly cleaned after use
- FACSafe (bleach) is caustic: wear gloves and laboratory coat at all times

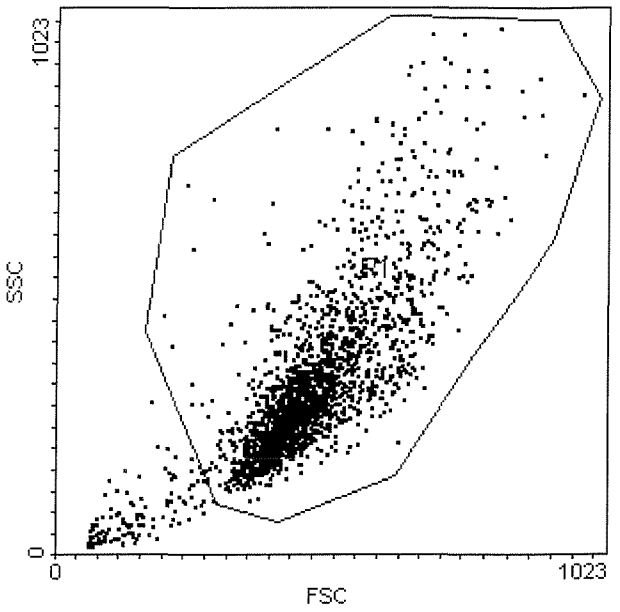

Figure 114: Flow cytometric scattergram of Forward Scatter (FSC) versus Side Scatter (SSC). Forward scatter measures cell size. Side scatter measures cellular granularity. Gate position defined to include all cells and exclude dead cells and fragments – determined by observing effect of gate on antigen expression and by experience.

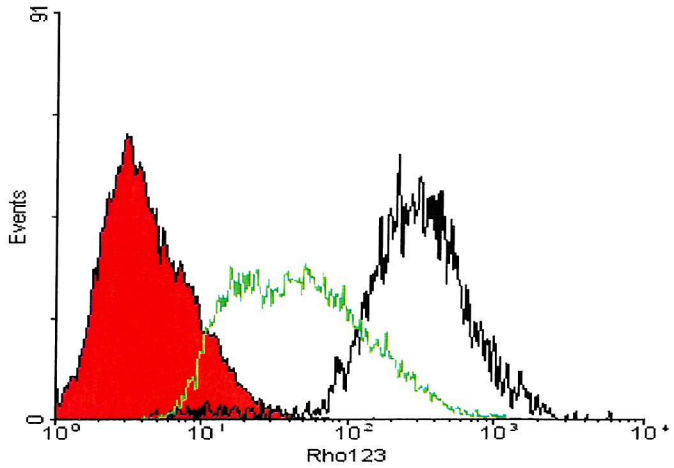

Figure 115. Flow cytometer set-up of FL-1. Photomultiplier settings are adjusted to allow complete inclusion of the positive control peak while keeping negative control signal greater than 10^0 and less than 10^1 (or as near as possible). Filled line = negative control, black line = positive control, green line = sample under investigation.

Protocol 11 Indirect Epitope Detection by Flow Cytometry

Materials required

Cell suspension(s)

Cy5-conjugated goat anti-mouse $F(ab')_2$ (1.4mg/ml)

100% Ethanol

2% Paraformaldehyde

Phosphate buffered saline

Primary mouse anti-human antibodies (and isotype controls)

Wash buffer (PBS / 1% BSA / 0.1% sodium azide [NaN_3])

Equipment Required

Apple Macintosh computer running Cell Quest software attached to flow cytometer

Beckton-Dickinson FACScalibre flow cytometer

12×75mm FACS tubes

Icebox

Pipettes

Refrigerated centrifuge

Method

1. Wash cell suspension in wash buffer at 4°C at 250×*g* for 5mins
2. Resuspend cells in 1ml wash buffer
3. Count cells on haemocytometer (see Protocol 1)
4. Dilute cells further with wash buffer as required – aim ~10^5 cells per sample
5. Add cell suspensions to FACS tubes on ice
6. Spin off medium, resuspend in 100µl of fixative or wash buffer, and incubate for x mins/hours at y temperature (see relevant antibody Tables 10,13,15)
7. Wash in wash buffer (add ~2ml wash buffer, centrifuge at 200×*g* for 5mins, tip off medium – carefully – and flick tube to de-compact pellet)
8. Resuspend in 100µl of 25µg/ml primary antibody solution (in wash buffer)
9. Incubate for appropriate time (see relevant antibody Tables 10,13,15) in the dark at 4°C

10. Wash twice in wash buffer
11. Resuspend in 100µl of secondary antibody solution (in wash buffer)
12. Incubate for 20mins in the dark at 4°C
13. Wash ×1 in wash buffer
14. Wash ×1 in PBS / 0.1% NaN_3 to remove BSA (tends to make cells clump – personal experience)
15. Perform flow cytometry: Protocol 10

Hazards

- Ethanol is highly flammable: always keep in screw-top container in flammables chest, avoid naked flames and use with other flammable agents or equipment which causes sparks
- Paraformaldehyde is harmful by inhalation and skin contact: always wear gloves and laboratory coat, weigh out and dissolve in fume cupboard
- Sodium azide is very toxic, is harmful to the environment, and may create explosive compounds with lead and/or copper: wear gloves and laboratory coat at all times, only use as much as required – do not dispose of down sink unless greatly diluted
- Risk of infection from human materials: wear gloves and laboratory coat at all times, ensure any spillages cleaned up immediately with FACSafe disinfectant, dispose of excess cell suspension into FACSafe, ensure all equipment is thoroughly cleaned after use

Protocol 12 BrdU incorporation by immunofluorescence

Materials required

5-Bromo-2'-deoxy-uridine Labelling and Detection Kit 1 (Boehringer Mannheim)

Bottle 1 Bromodeoxyuridine labelling reagent (BrdU)

Bottle 2 Washing buffer concentrate

Bottle 3 Incubation buffer (Trizma buffer, magnesium chloride, 2-mercaptoethanol)

Bottle 4 Anti-BrdU with nucleases (mouse-anti-BrdU monoclonal antibody containing nucleases, in PBS/glycerine)

Solution 3 Anti-mouse-Ig-fluorescein concentrate

Fixative 70ml 100% Ethanol, made up to 100ml with 50mM glycine

Antifade

Sterile water

Weymouth's Medium

Phosphate Buffered Saline

Equipment required

Pipettes

Staining rack

Method

1. Defrost *Bottles 1-3* – allow about 1 hour
2. Make up *Solution 1* – BrdU labelling medium. Dilute *Bottle 1* 1:1000 with Weymouth's medium (need 10ml)
3. Flick cell culture medium from 8-well culture slide
4. Cover each well with 200µl *Solution 1*
5. Incubate at 37°C for 45mins
6. Make up *Solution 5*. Dilute *Bottle 2* 1:10 with sterile water. Aim ~20ml per slide

7. Remove 8-well inserts (grip the lengthways middle and prise away from slide. Peel off the adhesive gasket from either end). Wash ×3 with *Solution 5*
8. Fix with *Fixative* at –20°C for 20mins
9. Make up *Solution 2* – anti-BrdU working solution. Dilute *Bottle 4* 1:10 with *Bottle 3*. Need 0.4-0.8ml/slide
10. Wash slides ×3 with *Solution 5*
11. Cover with *Solution 2* and incubate at 37°C for 30mins
12. Make up *Solution 4*. – anti-mouse-Ig-fluorescein conjugate. Dilute *Solution 3* 1:10 with PBS (aim same volume as *Solution 2*)
13. Remove slides from incubator and wash again ×3 with *Solution 5*
14. Cover with *Solution 4* and incubate at 37°C for 30mins
15. Remove from incubator and wash finally ×3 with *Solution 5*
16. Mount in Antifade. Seal with nail varnish (Antifade water soluble)
17. **Perform fluorescence microscopy:** see Protocol 8

Hazards

- Ethanol is highly flammable: always keep in screw-top container in flammables chest, avoid naked flames and use with other flammable agents or equipment which causes sparks
- Trizma is irritant: always wear gloves and laboratory coat
- Magnesium chloride is irritant: always wear gloves and laboratory coat
- 2-mercaptoethanol is toxic by skin contact and inhalation, with risk of serious damage to eyes: always wear gloves and laboratory coat, and safety glasses if preparing solutions
- Nucleases should be used with caution: wear gloves and laboratory coat
- Glycine has no hazards data: wear gloves and laboratory coat
- Risk of infection from human materials: wear gloves and laboratory coat at all times, ensure any spillages cleaned up immediately with Virkon disinfectant, ensure all equipment is thoroughly cleaned after use

Protocol 13 Cytocentrifugation

Materials required

Isolated/detached cell suspension

Medium

Equipment Required

APES (3-aminopropyltriethoxysilane)-coated glass microscope slides

Cytocentrifuge (Shandon Cytospin 3)

Pipettes

Method

1. Isolated/detached cell suspension prepared as per General Methods
2. Performed test spin(s) first:
3. Load 2 opposing cytocentrifuge chambers (see Figure 116E)
4. 100µl cell suspension added to each cup
5. Lock rotor lid in place (see Figure 116f)
6. Close and lock centrifuge lid
7. Perform centrifugation at 1000rpm for 5mins
8. Remove chambers, detach slides
9. Briefly air dry slides and examine under microscope
10. Cells should not appear "confluent" on the slide – if density too great, dilute cell suspension with appropriate volume of medium (1:2-4) and perform another test spin
11. Once appropriate cell density achieved, load all cytocentrifuge chambers
12. Cytocentrifuge 12 slides per batch until required number/cell sample exhausted
13. Allow slides to air dry
14. Stain or keep in air at RT until required

15. Remove and discard filter paper inserts
16. Soak plastic inserts in 10% bleach for 5mins, then allow to dry
17. Spray slide holders with 70% ethanol and wipe clean

Hazards

- Risk of injury from spinning materials: always ensure chambers are symmetrically loaded, that rubber seal is in place and not perished, centrifuge rotor lid is securely fastened and centrifuge lid is fastened and locked. Never attempt to open the lid before the rotor has stopped
- Risk of infection from human materials: wear gloves and laboratory coat at all times, ensure any spillages cleaned up immediately with Virkon disinfectant, dispose of excess cell suspension into Virkon, ensure all equipment is thoroughly cleaned after use
- Bleach is caustic: wear gloves and laboratory coat at all times, add bleach to water for dilution – not vice versa, avoid vapour inhalation
- APES is corrosive by skin contact, ingestion or inhalation: wear gloves and laboratory coat at all times

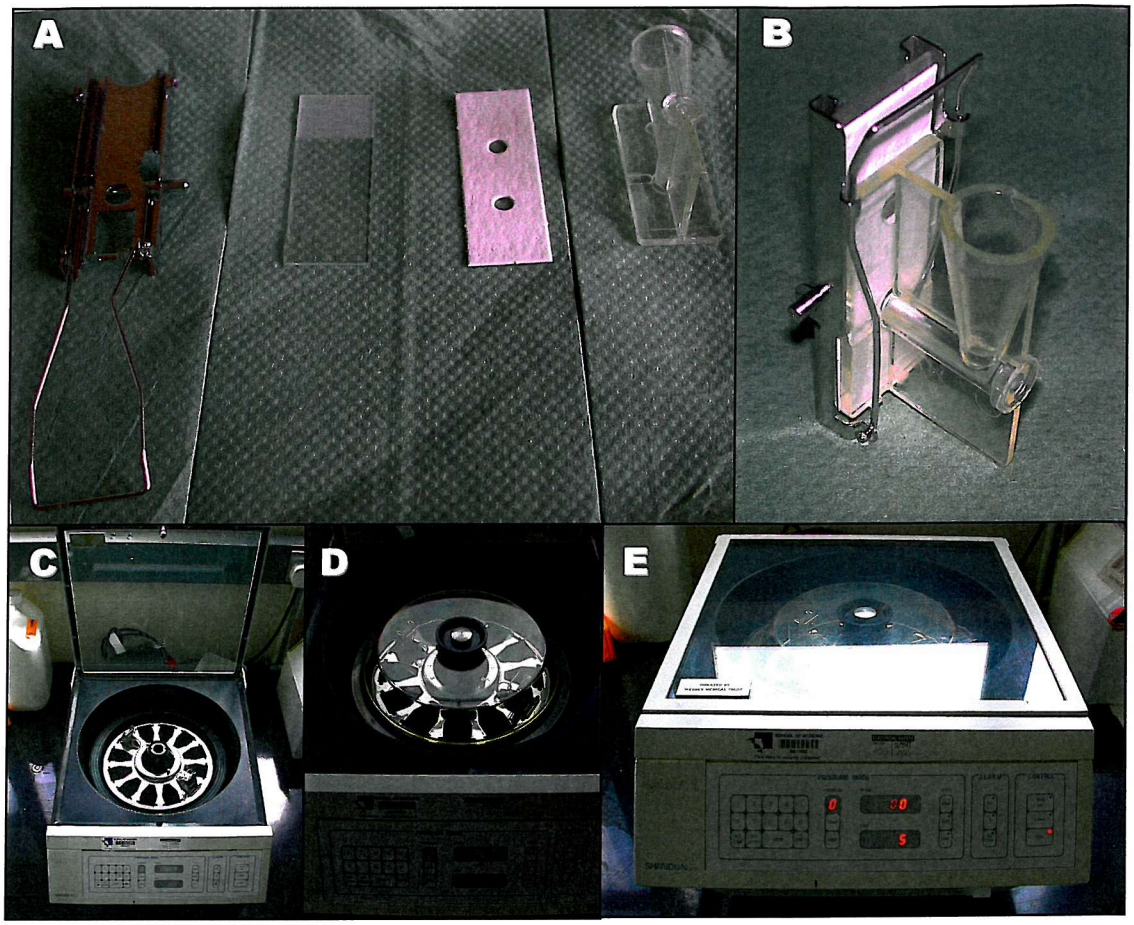

Figure 116: Cytocentrifuge: (A) Individual components of cytocentrifuge chamber showing (left to right) slide holder, microscope slide, filter paper, chamber cup **(B) Complete cytocentrifuge chamber, (C) Symmetrically loaded chambers,** note rubber gasket around rotor **(D) Rotor lid in place, (E) Cytocentrifuge closed, locked and ready for use**

Protocol 14 Cell Cycle Determination by Flow Cytometry

Materials required

Cell suspension(s)

Phosphate buffered saline

Propidium iodide (0.5mg/ml)

Ribonuclease A (RNAse A)

Equipment Required

12×75mm FACS tubes

Icebox

Pipettes

Method

1. Suspend cell sample in 2ml PBS and centrifuge at RT, 250×*g* for 5mins
2. Resuspend pellet in 300µl PBS with 5µg/ml PI + 0.2mg/ml RNAse A (10ml PBS, 50µg PI, 2mg RNAse A)
3. Incubate at room temperature for 30 mins
4. Place on ice
5. Analyse by flow cytometry: see Protocol 10 for machine set-up, use and shut-down, with the following alterations:

18. Ensure FL2-H, -A and -W are checked in *Parameters Saved*

From step 25.

25. **To test PI signal:**
26. *Pause*
27. Open histogram for FL2-H and scattergram of FL2-A vs. FL2-W (*Plots, Histograms/Dot plots*)
28. *Resume/Restart*
29. Adjust FL-2 *Amplification* and *Voltage* to get all FL2-H and the first two FL2-A signal peaks within 10^0-10^4 (see Figure 117)
30. Set gates to include R2 without necrotic cells (Figure 117B)

31. Return to Protocol 10, step 27. when adjustments complete

Hazards

- Laser light is damaging to sight: always follow standard operating procedure for the flow cytometer – never dismantle or use without appropriate safeguards
- Risk of infection from human tissue: always wear gloves and laboratory coat, risk is minimised by use of fixed tissue
- Propidium iodide is harmful by skin, eye and respiratory contact, with possible risk of irreversible effects: wear gloves and laboratory coat at all times and avoid contact or spillage
- Ethanol is highly flammable: always keep in screw-top container in flammables chest, avoid naked flames and use with other flammable agents or equipment which causes sparks
- Ribonuclease should be handled with caution: wear gloves and laboratory coat

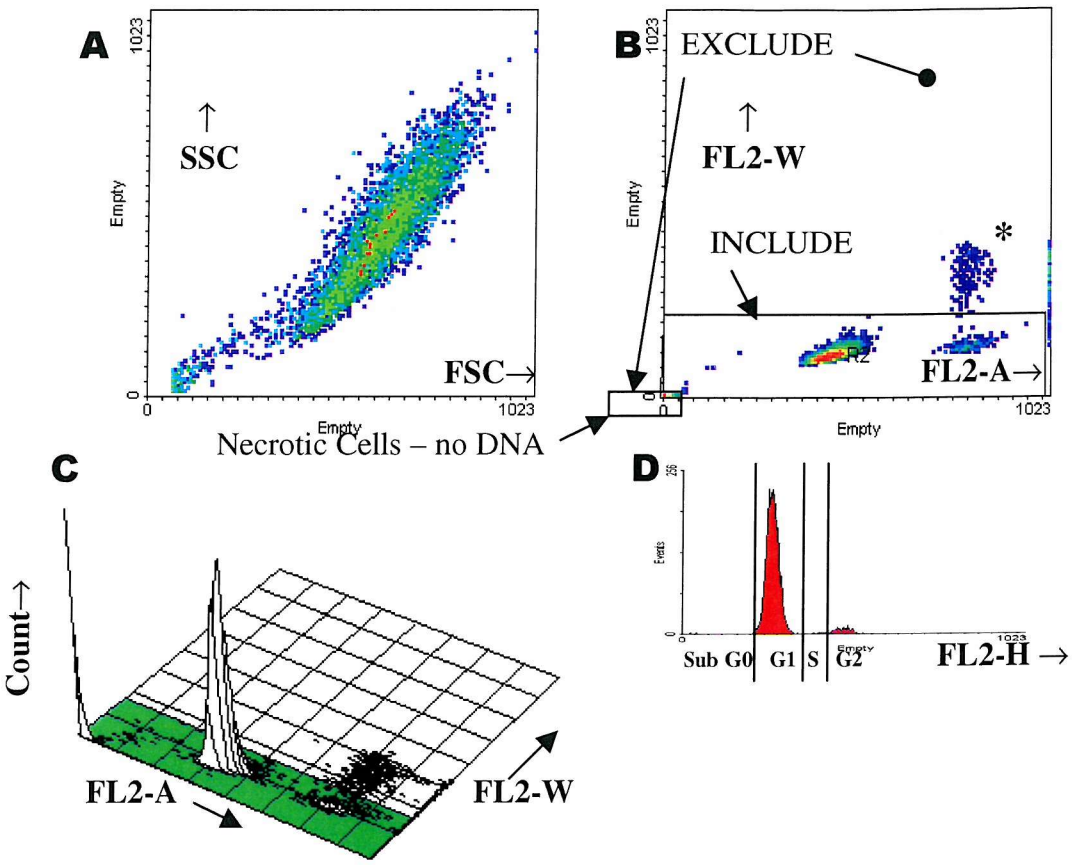

Figure 117. Flow cytometer set-up for cell cycle: (A) scattergram of forward vs. side scatter – not gated, blue = low-density, red = high-density; **(B) scattergram of FL2-A vs. FL2-W** – determining doublets (*) and necrotic cells to be excluded from the analysis; **(C) 3D plot of FL2-A, FL2-W and cell counts** – showing relative proportions of cells in each group; **(D) FL2-H histogram gated to exclude doublets and necrotic cells** (doublets = cells clumped in pairs) – the proportions of cells in cell cycle can be determined by setting markers to include each peak and intervening regions as shown

Protocol 15 Measurement of Cyclosporin A

Materials required

CYCLO-Trac® SP-whole blood, Diasporin Ltd, Wokingham, Berkley, USA

Equipment required

Scintillation tubes

Gamma scintillation counter (Cobra Series Canberra Packard Liquid Scintillation Counting System, Packard, Pangbourne, Berkshire)

Reagents

Cyclosporin A standard (16µg in 1ml 70% aqueous ethanol)

Standard dilutions: 400, 200, 100, 50, 25 and 0ng/ml (diluted in PBS)

^{125}I CYCLO-Trac SP

CYCLO-Trac SP NSB

Anti-CYCLO-Trac SP ImmunoSep

Method

1. **Performed by Janet Albano**
2. *Standard solutions were made serially in PBS.*
3. *Samples were diluted 1:1 in PBS*
4. *All assay reagents were allowed to reach room temperature (20-25°C) before use*
5. *Assay tubes were set up in duplicate as follows:*

a. ***Total count tubes*** *(100µl ^{125}I CYCLO-Trac SP)*

b. ***Non-specific binding tubes (NSB)*** *(50µl PBS, 100µl ^{125}I CYCLO-Trac SP, 1ml thoroughly mixed CYCLO-Trac SP NSB)*

c. ***Standard curve*** *(50µl standard, 100µl ^{125}I CYCLO-Trac SP)*

d. ***Unknown samples*** *(50µl samples, 100µl ^{125}I CYCLO-Trac SP)*

6. *After vigorous mixing, 1ml of Anti-CYCLO-Trac SP ImmunoSep was added to all tubes except Total count and NSB tubes*
7. *All tubes were mixed well, vortexed and incubated at RT for 1hr*
8. *All tubes (except Total counts) were centrifuged at 1600g for 209mins at RT*

9. *Supernatants were aspirated and inverted and carefully blotted to remove any remaining drops of supernatant that remained. This step was completed as quickly as possible*
10. *The precipitate of each tube and the total counts were counted for 1min or 10k using the gamma scintillation counter*
11. *Concentration of cyclosporin A in the samples was calculated by spline analysis*

Hazards

- Cyclosporin A is harmful by skin contact and inhalation, may cause cancer and harm the unborn child, particularly through prolonged exposure: always wear gloves and laboratory coat, perform initial dilution within a fume hood
- PBS – see Appendix 5
- ^{125}I emits ionising radiation: although these experiments use low levels of radioactive isotope, always wear laboratory coat and gloves. Always carry out work within a tray lined with Benchkote®. Monitor area with mini-monitor (Geiger counter) at the end of the experiment. Dispose of isotope according to local policy. Record disposal of isotope.

Protocol 16 Measurement of Lactate Dehydrogenase Activity

Materials required

Lactate Dehydrogenase Kit (Roche Diagnostics, Cat. No. 1 644 793)

Solution 1: Catalyst

Solution 2: Dye solution

Reaction mixture = 250µl solution 1 to 11.25ml solution 2, prepared immediately before use

Equipment required

96-well microtitre plate

Spectrophotometer

Method

1. Refresh culture medium
2. Remove refreshed culture medium at set time
3. Add 200µl per well of culture medium to 96-well plate
4. Add 100µl reaction mixture
5. Incubate at RT for 30mins in the dark
6. Measured absorbance at 490nm
7. Standard curve absorbances measured
8. Concentrations of LDH calculated from standard curve

Hazards

- Risk of infection from human materials: wear gloves and laboratory coat at all times, ensure any spillages cleaned up immediately with Virkon disinfectant, dispose of excess cell suspension into Virkon, ensure all equipment is thoroughly cleaned after use
- Diaphorase is irritant: wear gloves and laboratory coat at all times

Protocol 17 Transcellular passage of Cyclosporin A

Materials required

Half-defined medium (HM)

3ml stopped test tubes

^{125}I-labelled CsA

CsA (100µg/ml)

Equipment required

Pipettes

24-well cell culture plate

3ml test tubes with stoppers

12G hypodermic needle

Method

1. As per General Methods for 6-well plate subculture:
2. Subculture passage 0 cells 1:4 to 8×24-well inserts in HM
3. Leave 2 wells without cells as control wells (see Figure 118)
4. When confluent, change apical medium to 500µl fresh HM, and basal medium to 500µl fresh HM with 270ng/ml CsA and 30ng/ml ^{125}I-CsA, in all 10 wells
5. Incubate at 37°C
6. At each time point – 1, 2, 4, 6, 10 and 25 hour(s) – pipette off apical and basal media and store separately in stopped test tubes for later analysis. Gently rinse cells on membrane with cold PBS, cut membrane from insert using a hypodermic needle and stopper within a separate test tube
7. When all samples collected, measure ^{125}I activity of 1ml of 300ng/ml labelled CsA HM ×2, and each tube, using Protocol 15
8. Remove cells from membranes by incubation with Hanks' buffer, trypsin / EDTA solution then 10%FBS / RPMI as per Cell Detachment, wash with PBS and determine microprotein content as per Protocol 4.
9. Calculate CsA content of well medium; insert medium and cells from individual counts and standards as per Protocol 15.

Hazards

- Risk of infection from human materials: wear gloves and laboratory coat at all times, ensure any spillages cleaned up immediately with Virkon disinfectant, ensure all equipment is thoroughly cleaned after use
- Radiation: although these experiments use low levels of radioactive isotope, always wear laboratory coat and gloves. Always carry out work within a tray lined with Benchkote®. Monitor area with mini-monitor (Geiger counter) at the end of the experiment. Dispose of isotope according to local policy. Record disposal of isotope.

	☑ (1)	☑ (2)	☑ (4)	☐ (2)	
	☑ (6)	☑ (10)	☑ (25)	☐ (25)	

Figure 118. 24-well set-up for transcellular CsA movement protocol. ☑ = inserts with cells, ☐ = inserts without cells, (n) = time of sampling in hours

Protocol 18 P-gp activity and expression by flow cytometry 1

Materials required

Bovine serum albumin

Cy5-conjugated goat anti-mouse $F(ab')_2$ monoclonal antibody

Cyclosporin A (100µg/ml solution in PBS / 0.2% ethanol)

DMEM : F-12 Ham's medium with 2mM L-glutamine

Foetal bovine serum

IgG_{2a} isotype control antibody (mouse anti-rat IgG)

MRK16 mouse anti-human P-gp monoclonal antibody

Phosphate Buffered Saline

Rhodamine 123 (0.5mg/ml solution)

Sodium orthovanadate (100mM solution)

0.02% Trypsin / 0.05% EDTA solution

Wash buffer (PBS / 1% BSA / 0.1% NaN_3)

Weymouth's Medium

Equipment required

Pipettes

Icebox

12×75mm test tubes

Method

1. Detach cells from 6-well membranes as per General Methods: incubating cells with Hank's salt solution and Trypsin / EDTA, wash in Weymouths/10% FBS and resuspend pellet in 250µl wash buffer
2. Count cells on haemocytometer (Protocol 1)
3. Dilute cells further as required – aim same number of cells per sample
4. Spin off medium
5. Add 1ml DMEM : F12-Ham's / 10% FBS with 0.5µg/ml R123 to cell suspensions, mix well and incubate at 37°C for 30mins

Table 15. Tube contents / treatment for P-gp activity / expression flow cytometry

	No CsA					100ng/ml CsA				500ng/ml CsA			
Tube	**1**	**2**	**3**	**4**	**5**	**6**	**7**	**8**	**9**	**10**	**11**	**12**	**13**
Rhodamine	✓	✓	✓	✓	✓	✓	✓	✓	✓	✓	✓	✓	✓
Block				CsA	Van			CsA	Van			CsA	Van
Efflux			✓	✓	✓		✓	✓	✓		✓	✓	✓
MRK16	IgG_{2a}	✓	✓	✓	✓	✓	✓	✓	✓	✓	✓	✓	✓

6. Spin off medium (340×*g* for 5mins at RT – all washes performed at 340×*g*)
7. Resuspend in 100µl of [1,2,6,10] wash buffer and place in dark on ice, else 1ml DMEM:H-F12/10% FBS at 37°C, with [3,7,11] nil else, [4,8,12] 3.0µg/ml CsA, or [5,9,13] 250µM Vanadate (see Table 15 and Figure 119) and incubate at 37°C, for 90mins.
8. Wash in wash buffer at 4°C.
9. Fix in 2% PFA at 4°C for 60mins
10. Rewash in wash buffer
11. Resuspend in 100µl of [1] 25µg/ml IgG_{2a} in wash buffer, or [2-13] 25µl/ml MRK16 in wash buffer
12. Incubate at 4°C for 30mins
13. Wash twice in wash buffer
14. Resuspend in 2.8µg/ml GaM-Cy5 in wash buffer and incubate at 4°C for 20mins
15. Rewash in wash buffer
16. Resuspend in 300µl PBS / 0.1% NaN_3 and place on ice
17. Analyse by flow cytometry: see Protocol 10 for machine set-up, use and shut-down, with the following alterations:

26. Ensure *Four Colour* box is ticked at the bottom of *Detectors/Amps* window

From step 27.

32. **To test R123 signal:**
33. *Pause*

Pages 272-274
missing

Table 16. Tube contents / treatment for P-gp activity / expression flow cytometry

Repeated for Each Cell Group....									
Tube	**1**	**2**	**3**	**4**	**5**	**6**	**7**	**8**	**9**
Rhodamine				Wait then ✓	Wait then ✓+CsA	Wait then ✓+Van	✓	✓	✓
Efflux							✓	✓+CsA	✓+Van
MAb	IgG_{2a}	MRK16							

6. Add 1ml DMEM : F12-Ham's / 10% FBS with 0.5µg/ml R123 to cell suspensions [7-9], mix well and incubate at 37°C for 30mins
7. Spin off medium (250×*g* for 5mins at RT – all washes performed at 250×*g*)
8. Resuspend in 1ml DMEM:F12-Ham's / 10% FBS at 37°C [7], + 3.0µg/ml CsA [8], or 5mM Vanadate [9] (see Table 16 and Figure 121) and incubate at 37°C, for 90mins
9. After [7-9] have incubated for 60mins, add 1ml DMEM : F12-Ham's / 10% FBS with 0.5µg/ml R123 to cell suspensions [4-6], mix well and incubate at 37°C for 30mins
10. Wash all in wash buffer at 4°C.
11. Double-staining is not performed. All flow cytometry is performed at the same time: all R123-exposed cells are kept on ice for the same (short) time before cytometry

12. While tubes [3-9] are incubating, perform MRK16 staining:
13. Fix [1,2] in 2% PFA at 4°C for 60mins
14. Rewash in wash buffer
15. Resuspend in 100µl of 25µg/ml [1] IgG_{2a} in wash buffer, or [2] MRK16 in wash buffer
16. Incubate at 4°C for 30mins
17. Wash twice in wash buffer
18. Resuspend in 2.8µg/ml GaM-Cy5 in wash buffer and incubate at 4°C for 20mins
19. Rewash in wash buffer

20. Resuspend all samples in 300µl PBS / 0.1% NaN_3 and place on ice
21. Analyse by flow cytometry: see Protocol 10 for machine set-up, use and shut-down, with the following alterations:

18. Ensure *Four Colour* box is ticked at the bottom of *Detectors/Amps* window

From step 27.

27. **To test R123 signal:**
28. *Pause*
29. Open histograms for FL2-H and FL4-H (*Plots*, *Histograms*)
30. *Resume/Restart*
31. Set FL-2 *Amplification* and *Voltage* to 400, 1 to standardise R123 signal. Adjust FL4-H *Amplification* and *Voltage* using sample [1] to keep all the control signal peak within 10^0-10^1 (if possible)
32. Return to step 29. in Protocol 10 to perform flow cytometry

Hazards

- Cyclosporin A is harmful by skin contact and inhalation, may cause cancer and harm the unborn child, particularly through prolonged exposure: always wear gloves and laboratory coat, perform initial dilution within a fume hood
- Rhodamine 123 should be used with caution: wear gloves and laboratory coat
- Sodium azide is very toxic, is harmful to the environment, and may create explosive compounds with lead and/or copper: wear gloves and laboratory coat at all times, only use as much as required – do not dispose of down sink unless greatly diluted
- Sodium orthovanadate is harmful by skin contact and inhalation: perform initial solution formulation in a fume hood, wear gloves and laboratory coat at all times

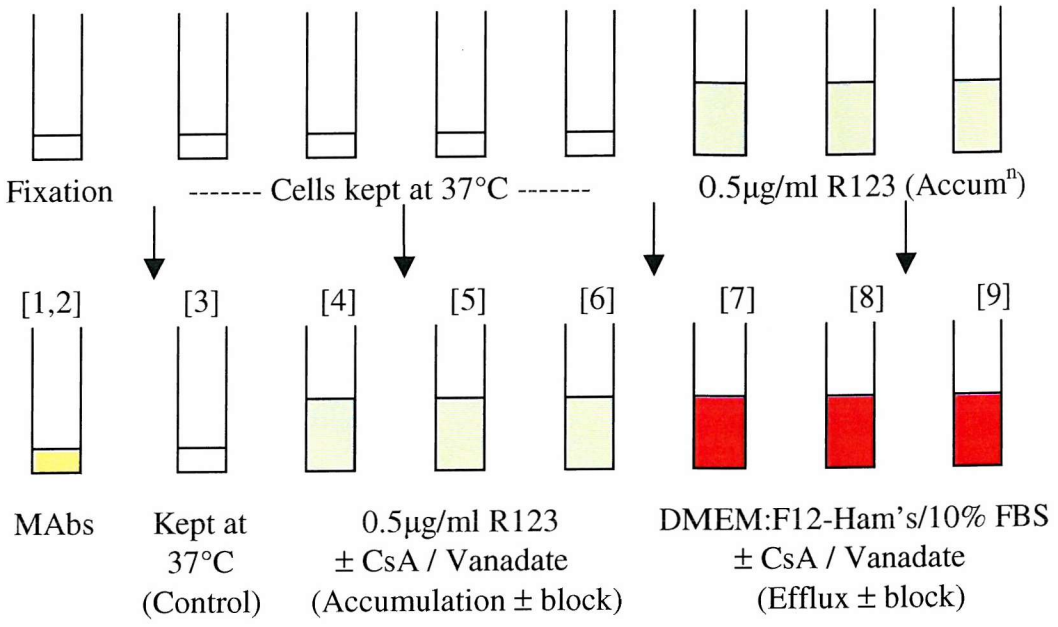

Figure 121. Schematic of experimental protocol for parallel Pgp activity / expression measurement

Protocol 20 Quantification of Immunofluorescence

Materials required

Confocal microscope digital sections (Protocol 9)

Equipment required

Leica SP2 Confocal Laser Scanning Microscope

Zeiss KS400 Image Analysis system

Project specific macros: (i) freehand region density measurements,
(ii) counting of nuclei

Method

1. Obtain confocal microscopy image of section using Protocol 9

2. Use project-specific macro on FITC-stained image (channel 1):
3. Draw freehand around each cell, using the mouse
4. Obtain region specific measurements of the density of the cytoplasm of each cell
5. Density is measured in grey-level values (range 0-255)
6. Results copied to Excel spreadsheet

7. Use second project-specific macro on same PI-counterstained image (channel 2):
8. Set RGB threshold used and convert to a binary image
9. Holes within each detected object are filled automatically by software
10. Any 'non-specific' elements in the background are digitally removed
11. 'Erosion' and 'dilation' procedures used to separate any touching nuclei
12. Overlapping cells and those bisected by the field frame are designated with the mouse and rejected prior to the total count being recorded
13. Results copied to Excel spreadsheet

14. Threshold of 'positive' determined by observation and density measurement
15. Proportions of 'positive' and 'negative' cells calculated from spreadsheet

Glossary

Term	Explanation
4E3	Monoclonal anti-P-gp antibody
Actin	A polarised molecule that constitutes 10-20% of mammalian cells. Fibrils formed of actin (F-actin) form cell cytoskeleton
Antibiotics	Penicillin and Streptomycin (Invitrogen): used in culture medium at the standard concentrations of 100iu/ml and 100mg/ml respectively, or multiples of this (double, half)
Benchkote®	Impermeable coated cardboard for laboratory work-surfaces
C219	Monoclonal anti-P-gp antibody
C494	Monoclonal anti-P-gp antibody
Calcitonin	Calcium-lowering hormone secreted from the thyroid gland
Confluence	The point in cell culture when no gaps are visible in a cell monolayer by phase-contrast microscopy
Cy5	A small, fluorescent organic molecule, typically conjugated to proteins via primary amines. Cy5 is typically excited by the 633 nm line of HeNe laser, and emission is collected at 680 nm.
Cytospin	The preparation of a microscope slide of suspended cells by centrifugation
FK506	Former name for Tacrolimus
Flea	Magnetic stirring bar for use with magnetic stirrer
Fluorochrome	Substance/compound which emits radiation (usually in or near the visual wavelength) when excited by light of specific wavelength
Glutamine	Non-essential amino acid: plays an important role in animal cellular metabolism, particularly in active- or binding-sites
Glycine	Essential amino acid: required for the biosynthesis of nucleic acids as well as of bile acids, porphyrins, creatine phosphate, and other amino acids
Ham's-F12	Nutrient mixture for mammalian cell culture
HB95	Anti-human MHC class I common epitope monoclonal antibody

Term	Explanation
Insulin	Pancreatic hormone required for human cells to utilise glucose
Magnetic stirrer	(Hot)Plate with spinning magnet, to stir (±heat) using flea
MRK16	Monoclonal anti-P-gp antibody, formed in mouse
Mycophenolate mofetil	Immunosuppressant medication used in solid organ transplantation. Prodrug of mycophenolic acid, which reduces lymphocyte activity through effects on purine synthesis.
Paraformaldehyde	Fixative which cross links proteins in tissue with methylene bridges
Passage	The subculture of confluent cells by disruption from the culture surface and plating out at a lower concentration for continued growth
Phalloidin	Specifically binds to actin at the junction between subunits. This is not a site at which many actin-binding proteins bind, thus most of the F-actin in cells is available for phalloidin labelling
Phase contrast microscopy	Contrast-enhancing optical technique which produces high-contrast images of transparent specimens such as living cells
Phaseolus vulgaris	The common annual twining or bushy bean plant grown for its edible seeds or pods [synonym: common bean]
Plating	The application in growth medium of cells to culture surfaces
Polished (water)	Ultra-pure (water with high conductivity – i.e. low solute levels)
PSC833	Non-immunosuppressive cyclosporin D analogue, developed specifically to reverse multidrug resistance by inhibiting P-gp activity
Pyruvate carboxylase	Mitochondrial biotin-dependent carboxylase: catalyses the ATP-dependent carboxylation of pyruvate to form oxaloacetate which may be utilised in the synthesis of glucose, fat, some amino acids or their derivatives and several neurotransmitters
Quench (1)	Inhibit protease activity on a sample by adding protein or diluting the protease significantly

Term	Explanation
Quench (2)	Reduce or inhibit the fluorescence of a fluorochrome by dynamic (quencher blocks excited state), concentration (high concentration of fluorochrome inhibits fluorescence) or static (quencher-fluorochrome combination is non-fluorescent, or quencher removes energy from fluorochrome before emission of light) mechanisms
Rifampicin	Rifamycin antibiotic which inhibits all prokaryotic RNA synthesis
Saponin	Any of various plant glucosides that form soapy lathers when mixed and agitated with water, used in detergents, foaming agents, and emulsifiers
Selenium	Trace element required for removing oxygen free radicals
Sirolimus	An immunosuppressive agent previously known as rapamycin, a macrocyclic lactone produced by Streptomyces hygroscopicus found in the soil of Easter Island. Reduces T-lymphocyte proliferation and signalling through the mTOR pathway
Sodium orthovanadate	Specific inhibitor of protein tyrosine phosphatases, which also traps MgADP in P-gp's nucleotide binding site
Sonication	Applying sound waves to sample, to agitate for stirring or disruption
Spectrophotometry	Detection of coloured substances in solution by extinction of specific wavelengths of transmitted light
SPURR resin	A low-viscosity resin embedding medium for electron microscopy
Subculture	Propagation of cells in culture by removal of growing cells from a culture surface, dilution, then re-plating
T43	Human proximal convoluted tubule membrane antigen (67 and 83% proximal and distal specificity respectively)

Term	Explanation
Tacrolimus	macrolide immunosuppressant with similar immunosuppressant properties and mechanism of action to CsA. Tacrolimus binds to an immunophilin, FKBP (FK506 Binding Protein), which has peptidyl-prolyl isomerase activity, blocks calcineurin mediated T-cell receptor signal transduction and inhibition of IL-2, thereby suppressing T-cell and T-cell-dependent B-cell activation
Triton X-100	A detergent used to permeabilise cells by dissolving lipid portions of cell membranes
Trypan Blue	Blue dye taken up by cytoplasmic proteins of non-viable cells. Taken up slowly by viable cells, so trypan blue exclusion should be performed on freshly exposed cells. Chemical name: 3,3'-([3,3'-Dimethyl(1,1'-biphenyl)-4,4'-diyl]bis(azo))bis-(5-amino-4-hydroxy)-2,7- naphthalenedisulfonic acid, tetra-sodium salt
Trypsin	Proteolytic enzyme, or protease, enzyme which acts to degrade protein by cleaving only the peptide bonds of the amino acids arginine and lysine
UIC-2	Monoclonal anti-P-gp antibody
Vanadate	Salt of vanadic acid
Virkon	Antimicrobial that kills bacteria, fungi and viruses; a blend of peroxygen compounds, surfactant, organic acids, and an inorganic buffer system.

References

(1) Racusen LC, Monteil C, Sgrignoli A, Lucskay M, Marouillat S, Rhim JG et al. Cell lines with extended in vitro growth potential from human renal proximal tubule: characterization, response to inducers, and comparison with established cell lines. J Lab Clin Med 1997; 129(3):318-329.

(2) Bommer J. Prevalence and socio-economic aspects of chronic kidney disease. Nephrol Dial Transplant 2002; 17(90011):8-12.

(3) Keown PA, Stiller CR. Dialysis or transplant: an integrated approach to end-stage kidney disease management. Kidney Int. 24[Suppl Mar], S145-S149. 1988.

(4) Canafax DM, Ascher NL. Cyclosporine immunosuppression. Clin Pharm 1983; 2(6):515-524.

(5) Wenger RM. Pharmacology of cyclosporin (sandimmune). II. Chemistry. Pharmacol Rev 1990; 41(3):243-247.

(6) Billich A, Zocher R. Enzymatic synthesis of cyclosporin A. J Biol Chem 1987; 262(36):17258-17259.

(7) Akagi H, Reynolds A, Hjelm M. Cyclosporin A and its metabolites, distribution in blood and tissues. J Int Med Res 1991; 19(1):1-18.

(8) Kronbach T, Fischer V, Meyer UA. Cyclosporine metabolism in human liver: identification of a cytochrome P-450III gene family as the major cyclosporine-metabolizing enzyme explains interactions of cyclosporine with other drugs. Clin Pharmacol Ther 1988; 43(6):630-635.

(9) Christians U, Schlitt HJ, Bleck JS, Schiebel HM, Kownatzki R, Maurer G et al. Measurement of cyclosporine and 18 metabolites in blood, bile, and urine by high-performance liquid chromatography. Transplant Proc 1988; 20(2 Suppl 2):609-613.

(10) LeGrue SJ, Friedman AW, Kahan BD. Binding of cyclosporine by human lymphocytes and phospholipid vesicles. J Immunol 1983; 131(2):712-718.

(11) Batiuk TD, Pazderka F, Enns J, DeCastro L, Halloran PF. Cyclosporine inhibition of calcineurin activity in human leukocytes in vivo is rapidly reversible. J Clin Invest 1995; 96(3):1254-1260.

(12) Calne RY, White DJ, Evans DB, Thiru S, Henderson RG, Hamilton DV et al. Cyclosporin A in cadaveric organ transplantation. Br Med J (Clin Res Ed) 1981; 282(6268):934-936.

(13) Ferguson RM, Rynasiewicz JJ, Sutherland DE, Simmons RL, Najarian JS. Cyclosporin A in renal transplantation: a prospective randomized trial. Surgery 1982; 92(2):175-182.

(14) Ochiai T, Toma H, Oka T, Takagi H, Kashiwabara H, Ishibashi M et al. A Japanese trial of cyclosporine in living related and cadaveric renal transplantation. Transplant Proc 1985; 17(4):2035-2040.

(15) Pascual M, Swinford RD, Ingelfinger JR, Williams WW, Cosimi AB, Tolkoff-Rubin N. Chronic rejection and chronic cyclosporin toxicity in renal allografts. Immunol Today 1998; 19(11):514-519.

(16) Matas AJ, Almond PS, Moss A, Gillingham KJ, Sibley R, Payne WD et al. Effect of cyclosporine on renal function in kidney transplant recipients: a 12-year follow-up. Clin Transplant 1995; 9(6):450-453.

(17) English J, Evan A, Houghton DC, Bennett WM. Cyclosporine-induced acute renal dysfunction in the rat. Evidence of arteriolar vasoconstriction with preservation of tubular function. Transplantation 1987; 44(1):135-141.

(18) Myers BD. Cyclosporine nephrotoxicity. Kidney Int 1986; 30(6):964-974.

(19) Myers BD, Sibley R, Newton L, Tomlanovich SJ, Boshkos C, Stinson E et al. The long-term course of cyclosporine-associated chronic nephropathy. Kidney Int 1988; 33(2):590-600.

(20) Powles AV, Cook T, Hulme B, Baker BS, Lewis HM, Thomas E et al. Renal function and biopsy findings after 5 years' treatment with low- dose cyclosporin for psoriasis. Br J Dermatol 1993; 128(2):159-165.

(21) Wolf G, Thaiss F, Stahl RA. Cyclosporine stimulates expression of transforming growth factor-beta in renal cells. Possible mechanism of cyclosporines antiproliferative effects. Transplantation 1995; 60(3):237-241.

(22) Verpooten GA, Wybo I, Pattyn VM, Hendrix PG, Giuliano RA, Nouwen EJ et al. Cyclosporine nephrotoxicity: comparative cytochemical study of rat kidney and human allograft biopsies. Clin Nephrol 1986; 25 Suppl 1:S18-S22.

(23) Ellermann J, David H, Marx I, Grunder W, Pfeifer H, Scholz D et al. 31P-NMR spectroscopy and ultrastructural studies on nephrotoxicity of cyclosporine A. Exp Pathol 1987; 32(2):73-79.

(24) Bennett WM, Houghton DC, Buss WC. Cyclosporine-induced renal dysfunction: correlations between cellular events and whole kidney function. J Am Soc Nephrol 1991; 1(11):1212-1219.

(25) Healy E, Dempsey M, Lally C, Ryan MP. Apoptosis and necrosis: mechanisms of cell death induced by cyclosporine A in a renal proximal tubular cell line. Kidney Int 1998; 54(6):1955-1966.

(26) Ortiz A, Lorz C, Catalan M, Ortiz A, Coca S, Egido J. Cyclosporine A induces apoptosis in murine tubular epithelial cells: role of caspases. Kidney Int Suppl 1998; 68:S25-S29.

(27) Amore A, Emancipator SN, Cirina P, Conti G, Ricotti E, Bagheri N et al. Nitric oxide mediates cyclosporine-induced apoptosis in cultured renal cells. Kidney Int 2000; 57(4):1549-1559.

(28) Conti G, Amore A, Cirina P, Gianoglio B, Peruzzi L, Coppo R. Cyclosporin induces apoptosis of renal cells by enhancing nitric oxide synthesis: modulating effect of angiotensin II inhibitors. Transplant Proc 2001; 33(1-2):276-277.

(29) Goldberg H, Ling V, Wong PY, Skorecki K. Reduced cyclosporin accumulation in multidrug-resistant cells. Biochem Biophys Res Commun 1988; 152(2):552-558.

(30) Garcia dM, O'Valle F, Andujar M, Aguilar M, Lucena MA, Lopez-Hidalgo J et al. Relationship between P-glycoprotein expression and cyclosporin A in kidney. An immunohistological and cell culture study. Am J Pathol 1995; 146(2):398-408.

(31) Hull RN, Cherry WR, Weaver GW. The origin and characteristics of a pig kidney cell strain, LLC-PK. In Vitro 1976; 12(10):670-677.

(32) Koyama H, Goodpasture C, Miller MM, Teplitz RL, Riggs AD. Establishment and characterization of a cell line from the American opossum (Didelphys virginiana). In Vitro 1978; 14(3):239-246.

(33) Monteil C, Leclere C, Fillastre JP, Morin JP. Insulin and glucose impact on functional and morphological differentiation of rabbit proximal tubule cells in primary culture. Ren Physiol Biochem 1993; 16(4):212-221.

(34) Madin SH, Darby NB. American Type Culture Collection Catalogue of Strains (vol 2). Rockville: H. Halt; 1975.

(35) Toutain H, Morin JP. Renal proximal tubule cell cultures for studying drug-induced nephrotoxicity and modulation of phenotype expression by medium components. Ren Fail 1992; 14(3):371-383.

(36) Baer PC, Nockher WA, Haase W, Scherberich JE. Isolation of proximal and distal tubule cells from human kidney by immunomagnetic separation. Technical note. Kidney Int 1997; 52(5):1321-1331.

(37) Freshney RI. The Transformed Phenotype. In: Freshney RI, editor. Culture of Animal Cells: A Manual of Basic Technique. 3rd ed. New York: Wiley-Liss; 1994. 231-239.

(38) Nadasdy T, Laszik Z, Blick KE, Johnson LD, Silva FG. Proliferative activity of intrinsic cell populations in the normal human kidney. J Am Soc Nephrol 1994; 4(12):2032-2039.

(39) Ryan MJ, Johnson G, Kirk J, Fuerstenberg SM, Zager RA, Torok-Storb B. HK-2: an immortalized proximal tubule epithelial cell line from normal adult human kidney. Kidney Int 1994; 45(1):48-57.

(40) Racusen LC, Wilson PD, Hartz PA, Fivush BA, Burrow CR. Renal proximal tubular epithelium from patients with nephropathic cystinosis: immortalized cell lines as in vitro model systems. Kidney Int 1995; 48(2):536-543.

(41) Detrisac CJ, Sens MA, Garvin AJ, Spicer SS, Sens DA. Tissue culture of human kidney epithelial cells of proximal tubule origin. Kidney Int 1984; 25(2):383-390.

(42) Horsburgh T, Brown S, Veitch PS, Bell PR. Cell culture of fine-needle aspirates and tru-cut biopsies. Transplant Proc 1988; 20(4):679-680.

(43) Blaehr H. Human renal biopsies as source of cells for glomerular and tubular cell cultures. Scand J Urol Nephrol 1991; 25(4):287-295.

(44) Carr T, Evans P, Campbell S, Bass P, Albano J. Culture of human renal tubular cells: positive selection of kallikrein- containing cells. Immunopharmacology 1999; 44(1-2):161-167.

(45) Xian CJ, Upton Z, Goddard C, Shoubridge CA, McNeil KA, Wallace JC et al. Production of a human epidermal growth factor fusion protein and its degradation in rat gastrointestinal flushings. J Mol Endocrinol 1996; 16(1):89-97.

(46) Altman SA, Randers L, Rao G. Comparison of trypan blue dye exclusion and fluorometric assays for mammalian cell viability determinations. Biotechnol.Prog. 9(6), 671-674. 1993.

(47) Bradford MM. A rapid and sensitive method for the quantitation of microgram quantities of protein utilizing the principle of protein-dye binding. Anal Biochem 1976; 72:248-254.

(48) Chuman L, Fine LG, Cohen AH, Saier MH, Jr. Continuous growth of proximal tubular kidney epithelial cells in hormone-supplemented serum-free medium. J Cell Biol 1982; 94(3):506-510.

(49) Trifillis AL, Regec AL, Trump BF. Isolation, culture and characterization of human renal tubular cells. J Urol 1985; 133(2):324-329.

(50) Ronco P, Antoine M, Baudouin B, Geniteau-Legendre M, Lelongt B, Chatelet F et al. Polarized membrane expression of brush-border hydrolases in primary cultures of kidney proximal tubular cells depends on cell differentiation and is induced by dexamethasone. J Cell Physiol 1990; 145(2):222-237.

(51) Eddy AA. Experimental insights into the tubulointerstitial disease accompanying primary glomerular lesions. J Am Soc Nephrol 1994; 5(6):1273-1287.

(52) Courjault-Gautier F, Chevalier J, Abbou CC, Chopin DK, Toutain HJ. Consecutive use of hormonally defined serum-free media to establish highly differentiated human renal proximal tubule cells in primary culture. J Am Soc Nephrol 1995; 5(11):1949-1963.

(53) Baer PC, Tunn UW, Nunez G, Scherberich JE, Geiger H. Transdifferentiation of distal but not proximal tubular epithelial cells from human kidney in culture. Exp Nephrol 1999; 7(4):306-313.

(54) Gstraunthaler G, Seppi T, Pfaller W. Impact of culture conditions, culture media volumes, and glucose content on metabolic properties of renal epithelial cell cultures. Are renal cells in tissue culture hypoxic? Cell Physiol Biochem 1999; 9(3):150-172.

(55) Sens DA, Detrisac CJ, Sens MA, Rossi MR, Wenger SL, Todd JH. Tissue culture of human renal epithelial cells using a defined serum- free growth formulation. Exp Nephrol 1999; 7(5-6):344-352.

(56) Yeoh G, Douglas A, Brighton V. Long-term culture of fetal rat hepatocytes in media supplemented with fetal calf-serum Ultroser SF or Ultroser G. Biol Cell 1986; 58(1):53-63.

(57) Rolleston WB. Bovine serum: reducing the variables through the use of donor herds. Dev Biol Stand 1999; 99:79-86.

(58) Iwata M, Zager RA. Myoglobin inhibits proliferation of cultured human proximal tubular (HK- 2) cells. Kidney Int 1996; 50(3):796-804.

(59) Zager RA. Calcitriol directly sensitizes renal tubular cells to ATP-depletion- and iron-mediated attack. Am J Pathol 1999; 154(6):1899-1909.

(60) Zimmerhackl LB, Mesa H, Kramer F, Kolmel C, Wiegele G, Brandis M. Tubular toxicity of cyclosporine A and the influence of endothelin-1 in renal cell culture models (LLC-PK1 and MDCK). Pediatr Nephrol 1997; 11(6):778-783.

(61) Mirto H, Henge-Napoli MH, Gibert R, Ansoborlo E, Fournier M, Cambar J. Intracellular behaviour of uranium(VI) on renal epithelial cell in culture (LLC-PK1): influence of uranium speciation. Toxicol Lett 1999; 104(3):249-256.

(62) Regec AL, Trifillis AL, Trump BF. The effect of gentamicin on human renal proximal tubular cells. Toxicol Pathol 1986; 14(2):238-241.

(63) Sens MA, Hennigar GR, Hazen-Martin DJ, Blackburn JG, Sens DA. Cultured human proximal tubule cells as a model for aminoglycoside nephrotoxicity. Ann Clin Lab Sci 1988; 18(3):204-214.

(64) Hazen-Martin DJ, Sens DA, Blackburn JG, Sens MA. Cadmium nephrotoxicity in human proximal tubule cell cultures. In Vitro Cell Dev Biol 1989; 25(9):784-790.

(65) Andersen KJ, Vik H, Eikesdal HP, Christensen EI. Effects of contrast media on renal epithelial cells in culture. Acta Radiol Suppl 1995; 399:213-218.

(66) Baer PC, Gauer S, Hauser IA, Scherberich JE, Geiger H. Effects of mycophenolic acid on human renal proximal and distal tubular cells in vitro. Nephrol Dial Transplant 2000; 15(2):184-190.

(67) Burton CJ, Harper SJ, Bailey E, Feehally J, Harris KP, Walls J. Turnover of human tubular cells exposed to proteins in vivo and in vitro. Kidney Int 2001; 59(2):507-514.

(68) Ignatescu MC, Fodiger M, Kletzmayr J, Bieglmayer C, Horl WH, Sunder-Plassmann G. Is there a role of cyclosporine A on total homocysteine export from human renal proximal tubular epithelial cells? Kidney Int 2001; 59 (Suppl 78):S258-S261.

(69) Medterms.
Quiescent. www medterms com/script/main/art asp?articlekey=10595, 2004.

(70) Rozengurt E. Early signals in the mitogenic response. Science 1986; 234(4773):161-166.

(71) Begg AC, McNally NJ, Shrieve DC, Karcher H. A method to measure the duration of DNA synthesis and the potential doubling time from a single sample. Cytometry 1985; 6(6):620-626.

(72) Ockleford CD, Hsi BL, Wakely J, Badley RA, Whyte A, Faulk WP. Propidium iodide as a nuclear marker in immunofluorescence. I. Use with tissue and cytoskeleton studies. J.Immunol.Methods 43(3), 261-267. 1981.

(73) von Willebrand E, Lautenschlager I, Inkinen K, Lehto VP, Virtanen I, Hayry P. Distribution of the major histocompatibility complex antigens in human and rat kidney. Kidney Int 1985; 27(4):616-621.

(74) Bishop GA, Hall BM, Suranyi MG, Tiller DJ, Horvath JS, Duggin GG. Expression of HLA antigens on renal tubular cells in culture. I. Evidence that mixed lymphocyte culture supernatants and gamma interferon increase both class I and class II HLA antigens. Transplantation 1986; 42(6):671-679.

(75) Gumbiner B. Structure, biochemistry, and assembly of epithelial tight junctions. Am J Physiol 1987; 253(6 Pt 1):C749-C758.

(76) Kreisberg JI, Wilson PD. Renal cell culture. J Electron Microsc Tech 1988; 9(3):235-263.

(77) Aleo MD, Taub ML, Nickerson PA, Kostyniak PJ. Primary cultures of rabbit renal proximal tubule cells: I. Growth and biochemical characteristics. In Vitro Cell Dev Biol 1989; 25(9):776-783.

(78) Tang MJ, Tannen RL. Metabolic substrates alter attachment and differentiated functions of proximal tubule cell culture. J Am Soc Nephrol 1994; 4(11):1908-1911.

(79) Wilson PD, Dillingham MA, Breckon R, Anderson RJ. Defined human renal tubular epithelia in culture: growth, characterization, and hormonal response. Am J Physiol 1985; 248(3 Pt 2):F436-F443.

(80) Bander NH, Finstad CL, Cordon-Cardo C, Ramsawak RD, Vaughan ED, Jr., Whitmore WF, Jr. et al. Analysis of a mouse monoclonal antibody that reacts with a specific region of the human proximal tubule and subsets renal cell carcinomas. Cancer Res 1989; 49(23):6774-6780.

(81) Scherberich JE, Gauhl C, Mondorf W. Biochemical, immunological and ultrastructural studies on brush-border membranes of human kidney. Curr Probl Clin Biochem 1977; 8:85-95.

(82) Helbert MJ, Dauwe SE, De Broe ME. Flow cytometric immunodissection of the human distal tubule and cortical collecting duct system. Kidney Int 2001; 59(2):554-564.

(83) Bessey OA, Lowry OH, Brock MJ. A method for the rapid determination of alkaline phosphatase with five cubic milliliters of serum. J.Biol.Chem. 1946; 164:321.

(84) Szasz G. A kinetic photometric method for serum gamma-glutamyl transpeptidase. Clin Chem 1969; 15(2):124-136.

(85) Bratton AC, Marshall EKJr. A new coupling component for sulphonamide determinations. J.Biol.Chem. 1939; 128:537.

(86) Kulhanek V, Dimov DM. A new useful modification for the determination of gamma- glutamyltranspeptidase activity. Clin Chim Acta 1966; 14(5):619-623.

(87) Stanton RC, Mendrick DL, Rennke HG, Seifter JL. Use of monoclonal antibodies to culture rat proximal tubule cells. Am J Physiol 1986; 251(5 Pt 1):C780-C786.

(88) Fillastre JP, Godin M. Drug-induced nephropathies. In: Dawson AM, Cameron JS, Grunfeld JP, Kerr DNS, Ritz E, Winearls CG, editors. Oxford Textbook of Clinical Nephrology. 2nd ed. Oxford: Oxford University Press; 1998. 2645-2657.

(89) Bashir N, Kuhen K, Taub M. Phospholipids regulate growth and function of MDCK cells in hormonally defined serum free medium. In Vitro Cell Dev Biol 1992; 28A(9-10):663-668.

(90) Hougland AE, Gaush CR, Mayberry WR. Canine kidney cells: III. Neutral lipids, phospholipids and fatty acids of primary canine kidney cells in monolayer culture. Growth 1978; 42(4):427-433.

(91) Ernst F, Hetzel S, Stracke S, Czock D, Vargas G, Lutz MP et al. Renal proximal tubular cell growth and differentiation are differentially modulated by renotropic growth factors and tyrosine kinase inhibitors. Eur J Clin Invest 2001; 31(12):1029-1039.

(92) Pote A, Zwizinski C, Simon EE, Meleg-Smith S, Batuman V. Cytotoxicity of myeloma light chains in cultured human kidney proximal tubule cells. Am.J.Kidney Dis. 36(4), 735-744. 2000.

(93) Wulf E, Deboben A, Bautz FA, Faulstich H, Wieland T. Fluorescent phallotoxin, a tool for the visualization of cellular actin. Proc.Natl.Acad.Sci.U.S.A 76(9), 4498-4502. 1979.

(94) Morel F. Sites of hormone action in the mammalian nephron. Am J Physiol 1981; 240(3):F159-F164.

(95) Fauth C, Chabardes D, Allaz M, Garcia M, Rossier B, Roch-Ramel F et al. Establishment of renal cell lines derived from S2 segments of the proximal tubule. Ren Physiol Biochem 1991; 14(3):128-139.

(96) You Y, Hirsch DJ, Morgunov NS. Functional integrity of proximal tubule cells. Effects of hypoxia and ischemia. J Am Soc Nephrol 1992; 3(4):965-974.

(97) Horibe Y, Hosoya K, Kim KJ, Ogiso T, Lee VH. Polar solute transport across the pigmented rabbit conjunctiva: size dependence and the influence of 8-bromo cyclic adenosine monophosphate. Pharm Res 1997; 14(9):1246-1251.

(98) Dorkoosh FA, Setyaningsih D, Borchard G, Rafiee-Tehrani M, Verhoef JC, Junginger HE. Effects of superporous hydrogels on paracellular drug permeability and cytotoxicity studies in Caco-2 cell monolayers. Int J Pharm 2002; 241(1):35-45.

(99) Chung SD, Alavi N, Livingston D, Hiller S, Taub M. Characterization of primary rabbit kidney cultures that express proximal tubule functions in a hormonally defined medium. J Cell Biol 1982; 95(1):118-126.

(100) Sakhrani LM, Badie-Dezfooly B, Trizna W, Mikhail N, Lowe AG, Taub M et al. Transport and metabolism of glucose by renal proximal tubular cells in primary culture. Am J Physiol 1984; 246(6 Pt 2):F757-F764.

(101) Denker BM, Nigam SK. Molecular structure and assembly of the tight junction. Am J Physiol Renal Physiol 1998; 274(1):F1-F9.

(102) Horibe Y, Hosoya K, Kim KJ, Ogiso T, Lee VH. Polar solute transport across the pigmented rabbit conjunctiva: size dependence and the influence of 8-bromo cyclic adenosine monophosphate. Pharm Res 1997; 14(9):1246-1251.

(103) Dorkoosh FA, Setyaningsih D, Borchard G, Rafiee-Tehrani M, Verhoef JC, Junginger HE. Effects of superporous hydrogels on paracellular drug permeability and cytotoxicity studies in Caco-2 cell monolayers. Int J Pharm 2002; 241(1):35-45.

(104) Chung SD, Alavi N, Livingston D, Hiller S, Taub M. Characterization of primary rabbit kidney cultures that express proximal tubule functions in a hormonally defined medium. J Cell Biol 1982; 95(1):118-126.

(105) Sakhrani LM, Badie-Dezfooly B, Trizna W, Mikhail N, Lowe AG, Taub M et al. Transport and metabolism of glucose by renal proximal tubular cells in primary culture. Am J Physiol 1984; 246(6 Pt 2):F757-F764.

(106) Han HJ, Choi HJ, Park SH. High glucose-induced inhibition of alpha-methyl-D-glucopyranoside uptake is mediated by protein kinase C-dependent activation of arachidonic acid release in primary cultured rabbit renal proximal tubule cells. J Cell Physiol 2000; 183(3):355-363.

(107) Del Moral RG, Olmo A, Aguilar M, O'Valle F. P glycoprotein: a new mechanism to control drug-induced nephrotoxicity. Exp Nephrol 1998; 6(2):89-97.

(108) Thiebaut F, Tsuruo T, Hamada H, Gottesman MM, Pastan I, Willingham MC. Cellular localization of the multidrug-resistance gene product P-glycoprotein in normal human tissues. Proc Natl Acad Sci U S A 1987; 84(21):7735-7738.

(109) Sampaio-Maia B, Gomes R, Soares-Da-Silva P. P-glycoprotein phosphorylation/dephosphorylation and cellular accumulation of L-DOPA in LLC-GA5 Col300 cells. J Auton Pharmacol 1999; 19(3):173-179.

(110) Sugawara I. Expression and functions of P-glycoprotein (mdr1 gene product) in normal and malignant tissues. Acta Pathol Jpn 1990; 40(8):545-553.

(111) Higgins CF. ABC transporters: from microorganisms to man. Annu Rev Cell Biol 1992; 8:67-113.

(112) Lanning CL, Fine RL, Sachs CW, Rao US, Corcoran JJ, Abou-Donia MB. Chlorpyrifos oxon interacts with the mammalian multidrug resistance protein, P-glycoprotein. J Toxicol Environ Health 1996; 47(4):395-407.

(113) Fricker G, Drewe J, Huwyler J, Gutmann H, Beglinger C. Relevance of p-glycoprotein for the enteral absorption of cyclosporin A: in vitro-in vivo correlation. Br J Pharmacol 1996; 118(7):1841-1847.

(114) Ernest S, Rajaraman S, Megyesi J, Bello-Reuss EN. Expression of MDR1 (multidrug resistance) gene and its protein in normal human kidney. Nephron 1997; 77(3):284-289.

(115) Lown KS, Mayo RR, Leichtman AB, Hsiao HL, Turgeon DK, Schmiedlin-Ren P et al. Role of intestinal P-glycoprotein (mdr1) in interpatient variation in the oral bioavailability of cyclosporine. Clin Pharmacol Ther 1997; 62(3):248-260.

(116) Ernest S, Bello-Reuss E. P-glycoprotein functions and substrates: possible roles of MDR1 gene in the kidney. Kidney Int Suppl 1998; 65:S11-S17.

(117) Melk A, Daniel V, Weimer R, Mandelbaum A, Wiesel M, Staehler G et al. P-glycoprotein expression in patients before and after kidney transplantation. Transplant Proc 1999; 31(1-2):299-300.

(118) Soldner A, Christians U, Susanto M, Wacher VJ, Silverman JA, Benet LZ. Grapefruit juice activates P-glycoprotein-mediated drug transport. Pharm Res 1999; 16(4):478-485.

(119) Smit JW, Schinkel AH, Weert B, Meijer DK. Hepatobiliary and intestinal clearance of amphiphilic cationic drugs in mice in which both mdr1a and mdr1b genes have been disrupted. Br J Pharmacol 1998; 124(2):416-424.

(120) Cordon-Cardo C, O'Brien JP, Casals D, Rittman-Grauer L, Biedler JL, Melamed MR et al. Multidrug-resistance gene (P-glycoprotein) is expressed by endothelial cells at blood-brain barrier sites. Proc Natl Acad Sci U S A 1989; 86(2):695-698.

(121) Ushigome F, Takanaga H, Matsuo H, Yanai S, Tsukimori K, Nakano H et al. Human placental transport of vinblastine, vincristine, digoxin and progesterone: contribution of P-glycoprotein. Eur.J.Pharmacol. 2000; 408(1):1-10.

(122) Atkinson DE, Greenwood SL, Sibley CP, Glazier JD, Fairbairn LJ. Role of MDR1 and MRP1 in trophoblast cells; elucidated using retroviral gene transfer. Am J Physiol Cell Physiol 2003; 285(3):C584-C591.

(123) Schinkel AH, Wagenaar E, Mol CA, van Deemter L. P-glycoprotein in the blood-brain barrier of mice influences the brain penetration and pharmacological activity of many drugs. J Clin Invest 1996; 97(11):2517-2524.

(124) Kochi S, Takanaga H, Matsuo H, Naito M, Tsuruo T, Sawada Y. Effect of cyclosporin A or tacrolimus on the function of blood-brain barrier cells. Eur J Pharmacol 1999; 372(3):287-295.

(125) Suzuki H, Sugiyama Y. Role of metabolic enzymes and efflux transporters in the absorption of drugs from the small intestine. Eur J Pharm Sci 2000; 12(1):3-12.

(126) Jones PM, George AM. A new structural model for P-glycoprotein. J Membr Biol 1998; 166(2):133-147.

(127) Ambudkar SV, Dey S, Hrycyna CA, Ramachandra M, Pastan I, Gottesman MM. Biochemical, cellular, and pharmacological aspects of the multidrug transporter. Annu Rev Pharmacol Toxicol 1999; 39:361-398.

(128) Loo TW, Clarke DM. Determining the structure and mechanism of the human multidrug resistance P-glycoprotein using cysteine-scanning mutagenesis and thiol- modification techniques. Biochim Biophys Acta 1999; 1461(2):315-325.

(129) Martin C, Berridge G, Higgins CF, Mistry P, Charlton P, Callaghan R. Communication between multiple drug binding sites on P-glycoprotein. Mol Pharmacol 2000; 58(3):624-632.

(130) Nagy H, Goda K, Arceci R, Cianfriglia M, Mechetner E, Szabo G, Jr. P-Glycoprotein conformational changes detected by antibody competition. Eur J Biochem 2001; 268(8):2416-2420.

(131) Wang EJ, Casciano CN, Clement RP, Johnson WW. Cooperativity in the inhibition of P-glycoprotein-mediated daunorubicin transport: evidence for half-of-the-sites reactivity. Arch Biochem Biophys 2000; 383(1):91-98.

(132) Wang EJ, Casciano CN, Clement RP, Johnson WW. Two transport binding sites of P-glycoprotein are unequal yet contingent: initial rate kinetic analysis by ATP hydrolysis demonstrates intersite dependence. Biochim Biophys Acta 2000; 1481(1):63-74.

(133) Lu L, Leonessa F, Clarke R, Wainer IW. Competitive and allosteric interactions in ligand binding to P- glycoprotein as observed on an immobilized P-glycoprotein liquid chromatographic stationary phase. Mol Pharmacol 2001; 59(1):62-68.

(134) Watanabe T, Kokubu N, Charnick SB, Naito M, Tsuruo T, Cohen D. Interaction of cyclosporin derivatives with the ATPase activity of human P-glycoprotein. Br J Pharmacol 1997; 122(2):241-248.

(135) Hrycyna CA, Airan LE, Germann UA, Ambudkar SV, Pastan I, Gottesman MM. Structural flexibility of the linker region of human P-glycoprotein permits ATP hydrolysis and drug transport. Biochemistry 1998; 37(39):13660-13673.

(136) Hrycyna CA, Ramachandra M, Ambudkar SV, Ko YH, Pedersen PL, Pastan I et al. Mechanism of action of human P-glycoprotein ATPase activity. Photochemical cleavage during a catalytic transition state using orthovanadate reveals cross-talk between the two ATP sites. J Biol Chem 1998; 273(27):16631-16634.

(137) Szabo K, Welker E, Bakos, Muller M, Roninson I, Varadi A et al. Drug-stimulated nucleotide trapping in the human multidrug transporter MDR1. Cooperation of the nucleotide binding domains. J Biol Chem 1998; 273(17):10132-10138.

(138) Berridge G, Walker JA, Callaghan R, Kerr ID. The nucleotide-binding domains of P-glycoprotein. Functional symmetry in the isolated domain demonstrated by N-ethylmaleimide labelling. European Journal of Biochemistry 2003; 270(7):1483-1492.

(139) van Helvoort A, Smith AJ, Sprong H, Fritzsche I, Schinkel AH, Borst P et al. MDR1 P-glycoprotein is a lipid translocase of broad specificity, while MDR3 P-glycoprotein specifically translocates phosphatidylcholine. Cell 1996; 87(3):507-517.

(140) Regev R, Assaraf YG, Eytan GD. Membrane fluidization by ether, other anesthetics, and certain agents abolishes P-glycoprotein ATPase activity and modulates efflux from multidrug-resistant cells. Eur J Biochem 1999; 259(1-2):18-24.

(141) Lu P, Liu R, Sharom FJ. Drug transport by reconstituted P-glycoprotein in proteoliposomes. Effect of substrates and modulators, and dependence on bilayer phase state. Eur J Biochem 2001; 268(6):1687-1697.

(142) Sharom FJ, Liu R, Qu Q, Romsicki Y. Exploring the structure and function of the P-glycoprotein multidrug transporter using fluorescence spectroscopic tools. Semin Cell Dev Biol 2001; 12(3):257-265.

(143) Szakacs G, Ozvegy C, Bakos E., Sarkadi B, Varadi A. Role of glycine-534 and glycine-1179 of human multidrug resistance protein (MDR1) in drug-mediated control of ATP hydrolysis. Biochem J 2001; 356(pt1)):71-75.

(144) Urbatsch IL, Tyndall GA, Tombline G, Senior AE. P-glycoprotein catalytic mechanism. Studies of the ADP-vanadate inhibited state. J Biol Chem 2003; 278(25):23171-23179.

(145) Varadi A, Szakacs G, Bakos E, Sarkadi B. P glycoprotein and the mechanism of multidrug resistance. Novartis Found Symp 2002; 243:54-65.

(146) Qu Q, Chu JW, Sharom FJ. Transition State P-glycoprotein Binds Drugs and Modulators with Unchanged Affinity, Suggesting a Concerted Transport Mechanism. Biochemistry 2003; 42(5):1345-1353.

(147) Loo TW, Clarke DM. Vanadate trapping of nucleotide at the ATP-binding sites of human multidrug resistance P-glycoprotein exposes different residues to the drug-binding site. Proc Natl Acad Sci U S A 2002; 99(6):3511-3516.

(148) Loo TW, Clarke DM. Drug-stimulated ATPase activity of human P-glycoprotein requires movement between transmembrane segments 6 and 12. J Biol Chem 1997; 272(34):20986-20989.

(149) Song J, Melera PW. Further characterization of the sixth transmembrane domain of Pgp1 by site-directed mutagenesis. Cancer Chemother Pharmacol 2001; 48(5):339-346.

(150) Song J, Melera PW. Transmembrane domain (TM) 9 represents a novel site in P-glycoprotein that affects drug resistance and cooperates with TM6 to mediate (125I]iodoarylazidoprazosin labeling. Mol Pharmacol 2001; 60(2):254-261.

(151) Lee JS, Paull K, Alvarez M, Hose C, Monks A, Grever M et al. Rhodamine efflux patterns predict P-glycoprotein substrates in the National Cancer Institute drug screen. Mol Pharmacol 1994; 46(4):627-638.

(152) Dey S, Ramachandra M, Pastan I, Gottesman MM, Ambudkar SV. Evidence for two nonidentical drug-interaction sites in the human P- glycoprotein. Proc Natl Acad Sci U S A 1997; 94(20):10594-10599.

(153) Seelig A. A general pattern for substrate recognition by P-glycoprotein. Eur J Biochem 1998; 251(1-2):252-261.

(154) Shapiro AB, Fox K, Lam P, Ling V. Stimulation of P-glycoprotein-mediated drug transport by prazosin and progesterone. Evidence for a third drug-binding site. Eur J Biochem 1999; 259(3):841-850.

(155) Scala S, Akhmed N, Rao US, Paull K, Lan LB, Dickstein B et al. P-glycoprotein substrates and antagonists cluster into two distinct groups. Mol Pharmacol 1997; 51(6):1024-1033.

(156) Maki N, Hafkemeyer P, Dey S. Allosteric Modulation of Human P-glycoprotein. Inhibition of transport by preventing substrate translocation and dissociation. J Biol Chem 2003; 278(20):18132.

(157) Loo TW, Bartlett MC, Clarke DM. Substrate-induced Conformational Changes in the Transmembrane Segments of Human P-glycoprotein. Direct evidence for the substrate-induced fit mechanism for drug binding. J Biol Chem 2003; 278(16):13603.

(158) Qu Q, Sharom FJ. Proximity of Bound Hoechst 33342 to the ATPase Catalytic Sites Places the Drug Binding Site of P-glycoprotein within the Cytoplasmic Membrane Leaflet. Biochemistry 2002; 41(14):4744-4752.

(159) Loo TW, Bartlett MC, Clarke DM. Permanent activation of the human P-glycoprotein by covalent modification of a residue in the drug-binding Site. J Biol Chem 2003; 278(23);20449-20452.

(160) Seigneuret M, Garnier-Suillerot A. A structural model for the open conformation of the mdr1 P-glycoprotein based on the MsbA crystal structure. J Biol Chem 2003; 278(32):30115-30124.

(161) Rothnie A, Storm J, Campbell J, Linton KJ, Kerr ID, Callaghan R. The topography of transmembrane segment six is altered during the catalytic cycle of P-glycoprotein. J Biol Chem 2004; 279(33):34913-34921.

(162) Demeule M, Laplante A, Murphy GF, Wenger RM, Beliveau R. Identification of the cyclosporin-binding site in P-glycoprotein. Biochemistry 1998; 37(51):18110-18118.

(163) Juliano RL, Ling V. A surface glycoprotein modulating drug permeability in Chinese hamster ovary cell mutants. Biochim Biophys Acta 1976; 455(1):152-162.

(164) Fojo AT, Reuben PM, Whitney PL, Awad WM, Jr. Effect of glycerol on protein acetylation by acetic anhydride. Arch Biochem Biophys 1985; 240(1):43-50.

(165) Su SF, Huang JD. Inhibition of the intestinal digoxin absorption and exsorption by quinidine. Drug Metab Dispos 1996; 24(2):142-147.

(166) Drescher S, Glaeser H, Mürdter T, Hitzl M, Eichelbaum M, Fromm MF. P-glycoprotein-mediated intestinal and biliary digoxin transport in humans. Clin.Pharmacol.Ther. 73(3), 223-231. 2003.

(167) de Lannoy IA, Koren G, Klein J, Charuk J, Silverman M. Cyclosporin and quinidine inhibition of renal digoxin excretion: evidence for luminal secretion of digoxin. Am J Physiol 1992; 263(4 Pt 2):F613-F622.

(168) Schinkel AH. The physiological function of drug-transporting P-glycoproteins. Semin Cancer Biol 1997; 8(3):161-170.

(169) Wang EJ, Casciano CN, Clement RP, Johnson WW. In vitro flow cytometry method to quantitatively assess inhibitors of P- glycoprotein. Drug Metab Dispos 2000; 28(5):522-528.

(170) Urbatsch IL, Sankaran B, Weber J, Senior AE. P-glycoprotein is stably inhibited by vanadate-induced trapping of nucleotide at a single catalytic site. J Biol Chem 1995; 270(33):19383-19390.

(171) Rao US. Drug binding and nucleotide hydrolyzability are essential requirements in the vanadate-induced inhibition of the human P-glycoprotein ATPase. Biochemistry 1998; 37(42):14981-14988.

(172) Goodno CC. Myosin active-site trapping with vanadate ion. Methods Enzymol 1982; 85 Pt B:116-123.

(173) Cantley LC, Jr., Josephson L, Warner R, Yanagisawa M, Lechene C, Guidotti G. Vanadate is a potent (Na,K)-ATPase inhibitor found in ATP derived from muscle. J Biol Chem 1977; 252(21):7421-7423.

(174) Masereeuw R, Moons MM, Russel FG. Rhodamine 123 accumulates extensively in the isolated perfused rat kidney and is secreted by the organic cation system. Eur J Pharmacol 1997; 321(3):315-323.

(175) Ando H, Nishio Y, Ito K, Nakao A, Wang L, Zhao YL et al. Effect of endotoxin on p-glycoprotein-mediated biliary and renal excretion of rhodamine-123 in rats. Antimicrob Agents Chemother 2001; 45(12):3462-3467.

(176) Dudley AJ, Brown CD. Mediation of cimetidine secretion by P-glycoprotein and a novel H(+)- coupled mechanism in cultured renal epithelial monolayers of LLC-PK1 cells. Br J Pharmacol 1996; 117(6):1139-1144.

(177) Vanoye CG, Castro AF, Pourcher T, Reuss L, Altenberg GA. Phosphorylation of P-glycoprotein by PKA and PKC modulates swelling-activated Cl- currents. Am J Physiol 1999; 276(2 Pt 1):C370-C378.

(178) Didziapetris R, Japertas P, Avdeef A, Petrauskas A. Classification analysis of P-glycoprotein substrate specificity. J Drug Target 2003; 11(7):391-406.

(179) Wang RB, Kuo CL, Lien LL, Lien EJ. Structure-activity relationship: analyses of p-glycoprotein substrates and inhibitors. J Clin Pharm Ther 2003; 28(3):203-228.

(180) Wei LY, Roepe PD. Low external pH and osmotic shock increase the expression of human MDR protein. Biochemistry 1994; 33(23):7229-7238.

(181) Laouari D, Yang R, Veau C, Blanke I, Friedlander G. Two apical multidrug transporters, P-gp and MRP2, are differently altered in chronic renal failure. Am J Physiol Renal Physiol 2001; 280(4):F636-F645.

(182) Veau C, Leroy C, Banide H, Auchere D, Tardivel S, Farinotti R et al. Effect of chronic renal failure on the expression and function of rat intestinal P-glycoprotein in drug excretion. Nephrol Dial Transplant 2001; 16(8):1607-1614.

(183) Maitra R, Halpin PA, Karlson KH, Page RL, Paik DY, Leavitt MO et al. Differential effects of mitomycin C and doxorubicin on P-glycoprotein expression. Biochem J 2001; 355(Pt 3):617-624.

(184) Arceci RJ, Stieglitz K, Bras J, Schinkel A, Baas F, Croop J. Monoclonal antibody to an external epitope of the human mdr1 P- glycoprotein. Cancer Res 1993; 53(2):310-317.

(185) Kleinow KM, Doi AM, Smith AA. Distribution and inducibility of P-glycoprotein in the catfish: immunohistochemical detection using the mammalian C-219 monoclonal. Mar Environ Res 2000; 50(1-5):313-317.

(186) van Den Elsen JM, Kuntz DA, Hoedemaeker FJ, Rose DR. Antibody C219 recognizes an alpha-helical epitope on P-glycoprotein. Proc Natl Acad Sci U S A 1999; 96(24):13679-13684.

(187) Rao VV, Anthony DC, Piwnica-Worms D. MDR1 gene-specific monoclonal antibody C494 cross-reacts with pyruvate carboxylase. Cancer Res 1994; 54(6):1536-1541.

(188) Scheper RJ, Bulte JW, Brakkee JG, Quak JJ, van der SE, Balm AJ et al. Monoclonal antibody JSB-1 detects a highly conserved epitope on the P-glycoprotein associated with multi-drug-resistance. Int J Cancer 1988; 42(3):389-394.

(189) Rao VV, Anthony DC, Piwnica-Worms D. Multidrug resistance P-glycoprotein monoclonal antibody JSB-1 crossreacts with pyruvate carboxylase. J Histochem Cytochem 1995; 43(12):1187-1192.

(190) Georges E, Tsuruo T, Ling V. Topology of P-glycoprotein as determined by epitope mapping of MRK-16 monoclonal antibody. J Biol Chem 1993; 268(3):1792-1798.

(191) Zhou Y, Gottesman MM, Pastan I. The extracellular loop between TM5 and TM6 of P-glycoprotein is required for reactivity with monoclonal antibody UIC2. Arch Biochem Biophys 1999; 367(1):74-80.

(192) Lehne G, De Angelis P, Clausen OP, Egeland T, Tsuruo T, Rugstad HE. Binding diversity of antibodies against external and internal epitopes of the multidrug resistance gene product P-glycoprotein. Cytometry 1995; 20(3):228-237.

(193) Georges E, Zhang JT, Ling V. Modulation of ATP and drug binding by monoclonal antibodies against P- glycoprotein. J Cell Physiol 1991; 148(3):479-484.

(194) Efferth T, Volm M. Modulation of P-glycoprotein-mediated multidrug resistance by monoclonal antibodies, immunotoxins or antisense oligodeoxynucleotides in kidney carcinoma and normal kidney cells. Oncology 1993; 50(4):303-308.

(195) Frank M, Denton M, Alexander S, Khoury S, Sayegh M, Briscoe D. Specific MDR1 P-glycoprotein blockade inhibits human alloimmune T cell activation in vitro. J Immunol 2001; 166(4):2451-2459.

(196) Thevenod F, Friedmann JM, Katsen AD, Hauser IA. Up-regulation of multidrug resistance P-glycoprotein via nuclear factor- kappaB activation protects kidney proximal tubule cells from cadmium- and reactive oxygen species-induced apoptosis. J Biol Chem 2000; 275(3):1887-1896.

(197) Bentires-Alj M, Barbu V, Fillet M, Chariot A, Relic B, Jacobs N et al. NF-B transcription factor induces drug resistance through MDR1 expression in cancer cells. Oncogene 2003; 22(1):90-97.

(198) Lee CH, Ling V. Superinduction of P-glycoprotein messenger RNA in vivo in the presence of transcriptional inhibitors. J.Exp.Ther.Oncol. 2003; 3(1):14-26.

(199) Begley GS, Horvath AR, Taylor JC, Higgins CF. Cytoplasmic domains of the transporter associated with antigen processing and P-glycoprotein interact with subunits of the proteasome. Mol Immunol 2005; 42(1):137-141.

(200) Jette L, Beaulieu E, Leclerc JM, Beliveau R. Cyclosporin A treatment induces overexpression of P-glycoprotein in the kidney and other tissues. Am J Physiol 1996; 270(5 Pt 2):F756-F765.

(201) Vickers AE, Alegret M, Meyer E, Smiley S, Guertler J. Hydroxyethyl cyclosporin A induces and decreases P4503A and P- glycoprotein levels in rat liver. Xenobiotica 1996; 26(1):27-39.

(202) Del Moral RG, Andujar M, Ramirez C, Gomez-Morales M, Masseroli M, Aguilar M et al. Chronic cyclosporin A nephrotoxicity, P-glycoprotein overexpression, and relationships with intrarenal angiotensin II deposits. Am J Pathol 1997; 151(6):1705-1714.

(203) Ledoux S, Leroy C, Siegfried G, Prie D, Moullier P, Friedlander G. Overexpression of ecto-5'-nucleotidase promotes P-glycoprotein expression in renal epithelial cells. Kidney Int 1997; 52(4):953-961.

(204) Hauser IA, Koziolek M, Hopfer U, Thevenod F. Therapeutic concentrations of cyclosporine A, but not FK506, increase P- glycoprotein expression in endothelial and renal tubule cells. Kidney Int 1998; 54(4):1139-1149.

(205) Jette L, Murphy GF, Beliveau R. Drug binding to P-glycoprotein is inhibited in normal tissues following SDZ-PSC 833 treatment. Int J Cancer 1998; 76(5):729-737.

(206) Koziolek MJ, Riess R, Geiger H, Thevenod F, Hauser IA. Expression of multidrug resistance P-glycoprotein in kidney allografts from cyclosporine A-treated patients. Kidney Int 2001; 60(1):156-166.

(207) Bai S, Liu J, Lu SK, Brunner LJ. In vivo induction of hepatic p-glycoprotein by cyclosporine in the rat. Res Commun Mol Pathol Pharmacol 2001; 109(1-2):103-114.

(208) Kuo MT, Liu Z, Wei Y, Lin-Lee YC, Tatebe S, Mills GB et al. Induction of human MDR1 gene expression by 2-acetylaminofluorene is mediated by effectors of the phosphoinositide 3-kinase pathway that activate NF-kappaB signaling. Oncogene 2002; 21(13):1945-1954.

(209) Takara K, Tsujimoto M, Ohnishi N, Yokoyama T. Digoxin up-regulates MDR1 in human colon carcinoma Caco-2 cells. Biochem Biophys Res Commun 2002; 292(1):190-194.

(210) Ziemann C, Schafer D, Rudell G, Kahl GF, Hirsch-Ernst KI. The cyclooxygenase system participates in functional mdr1b overexpression in primary rat hepatocyte cultures. Hepatology 2002; 35(3):579-588.

(211) Daoudaki M, Fouzas I, Stapf V, Ekmekcioglu C, Imvrios G, Andoniadis A et al. Cyclosporine A Augments P-Glycoprotein Expression in the Regenerating Rat Liver. Biol.Pharm.Bull. 2003; 26(3):303-307.

(212) Vishnuvardhan D, von Moltke LL, Richert C, Greenblatt DJ. Lopinavir: acute exposure inhibits P-glycoprotein; extended exposure induces P-glycoprotein. AIDS 2003; 17(7):1092-1094.

(213) Hoffmeyer S, Burk O, von Richter O, Arnold HP, Brockmoller J, Johne A et al. Functional polymorphisms of the human multidrug-resistance gene: multiple sequence variations and correlation of one allele with P-glycoprotein expression and activity in vivo. Proc Natl Acad Sci U S A 2000; 97(7):3473-3478.

(214) Murakami T, Yumoto R, Nagai J, Takano M. Factors affecting the expression and function of P-glycoprotein in rats: drug treatments and diseased states. Pharmazie 2002; 57(2):102-107.

(215) Stein U, Lage H, Jordan A, Walther W, Bates SE, Litman T et al. Impact of BCRP/MXR, MRP1 and MDR1/P-Glycoprotein on thermoresistant variants of atypical and classical multidrug resistant cancer cells. Int J Cancer 2002; 97(6):751-760.

(216) Banfield C, Gupta S, Marino M, Lim J, Affrime M. Grapefruit juice reduces the oral bioavailability of fexofenadine but not desloratadine. Clin Pharmacokinet 2002; 41(4):311-318.

(217) Shibata N, Morimoto J, Hoshino N, Minouchi T, Yamaji A. Factors that affect absorption behavior of cyclosporin a in gentamicin- induced acute renal failure in rats. Ren Fail 2000; 22(2):181-194.

(218) Ernst E. St John's Wort supplements endanger the success of organ transplantation. Arch Surg 2002; 137(3):316-319.

(219) Finch CK, Chrisman CR, Baciewicz AM, Self TH. Rifampin and rifabutin drug interactions: an update. Arch Intern Med 2002; 162(9):985-992.

(220) Kemnitz J, Uysal A, Haverich A, Heublein B, Cohnert TR, Stangel W et al. Multidrug resistance in heart transplant patients: a preliminary communication on a possible mechanism of therapy-resistant rejection. J Heart Lung Transplant 1991; 10(2):201-210.

(221) Yousem SA, Sartori D, Sonmez-Alpan E. Multidrug resistance in lung allograft recipients: possible correlation with the development of acute and chronic rejection. J Heart Lung Transplant 1993; 12(1 Pt 1):20-26.

(222) Montano E, Schmitz M, Blaser K, Simon HU. P-glycoprotein expression in circulating blood leukocytes of patients with steroid-resistant asthma. J Investig Allergol Clin Immunol 1996; 6(1):14-21.

(223) Maillefert JF, Jorgensen C, Sany J. Multidrug resistance in rheumatoid arthritis. J Rheumatol 1996; 23(12):2182.

(224) Vanholder R, Glorieux G, de Smet R, Lamiere N. New insights in uremic toxins. Kidney Int. 2003; 63[Suppl 84]:S6-S10.

(225) Kunihara M, Nagai J, Murakami T, Takano M. Renal excretion of rhodamine 123, a P-glycoprotein substrate, in rats with glycerol-induced acute renal failure. J Pharm Pharmacol 1998; 50(10):1161-1165.

(226) Huang ZH, Murakami T, Okochi A, Yumoyo R, Nagai J, Takano M. Expression and function of P-glycoprotein in rats with carbon tetrachloride-induced acute hepatic failure. J Pharm Pharmacol 2001; 53(6):873-881.

(227) Patel VA, Dunn MJ, Sorokin A. Regulation of MDR-1 (P-glycoprotein) by Cyclooxygenase-2. J Biol Chem 2002; 277(41):38915.

(228) Veau C, Faivre L, Tardivel S, Soursac M, Banide H, Lacour B et al. Effect of Interleukin-2 on Intestinal P-glycoprotein Expression and Functionality in Mice. J Pharmacol Exp Ther 2002; 302(2):742.

(229) Belliard A-M, Tardivel S, Farinotti R, Lacour B, Leroy C. Cytokines influence mRNA expression of cytochrome P450 3A4 and MDRI in intestinal cells. J.Pharm.Pharmacol. 2002; 54(8):1103-1109.

(230) Bertilsson PM, Olsson P, Magnusson K-E. Cytokines influence mRNA expression of cytochrome P450 3A4 and MDRI in intestinal cells. J.Pharm.Sci. 2001; 90(5):638-646.

(231) Parasrampuria DA, Lantz MV, Birnbaum JL, Vincenti FG, Benet LZ. Effect of calcineurin inhibitor therapy on P-gp expression and function in lymphocytes of renal transplant patients: a preliminary evaluation. J Clin Pharmacol 2002; 42(3):304-311.

(232) Zanker B, Barth C, Stachowski J, Baldamus CA, Land W. Multidrug resistance gene MDR1 expression: a gene transfection in vitro model and clinical analysis in cyclosporine-treated patients rejecting their renal grafts. Transplant Proc 1997; 29(1-2):1507-1508.

(233) Zacher T, Thiele B, Wassmuth R, Albert FW. Cyclosporine A sensitivity in vitro and P-glycoprotein expression in patients on dialysis and after kidney transplantation. Transpl Immunol 2000; 8(2):147-150.

(234) Gotzl M, Wallner J, Gsur A, Zochbauer S, Kovarik J, Balcke P et al. MDR1 gene expression in lymphocytes of patients with renal transplants. Nephron 1995; 69(3):277-280.

(235) Liu J, Brunner LJ. Chronic cyclosporine administration induces renal P-glycoprotein in rats. Eur J Pharmacol 2001; 418(1-2):127-132.

(236) Myers BD, Ross J, Newton L, Luetscher J, Perlroth M. Cyclosporine-associated chronic nephropathy. N Engl J Med 1984; 311(11):699-705.

(237) Greenberg A, Egel JW, Thompson ME, Hardesty RL, Griffith BP, Bahnson HT et al. Early and late forms of cyclosporine nephrotoxicity: studies in cardiac transplant recipients. Am J Kidney Dis 1987; 9(1):12-22.

(238) Myers BD. What is cyclosporine nephrotoxicity? Transplant Proc 1989; 21(1 Pt 2):1430-1432.

(239) Opelz G. Investigation of the relationship between maintenance dose of cyclosporine and nephrotoxicity or hypertension. Transplant Proc 2001; 33(7-8):3351-3354.

(240) Mahalati K, Belitsky P, Sketris I, West K, Panek R. Neoral monitoring by simplified sparse sampling area under the concentration-time curve: its relationship to acute rejection and cyclosporine nephrotoxicity early after kidney transplantation. Transplantation 1999; 68(1):55-62.

(241) Albano JDM, Harris KR, Digard NJ, Athersmith KV, Sharman VL, Slapak M. Accumulation of Cyclosporine A in Rat Tissues Following Oral Dosing: Relationship to Peak and Trouogh Blood Levels. Transplant.Proc. 1986; 18:1278-1280.

(242) Kumar MS, White AG, Alex G, Antos MS, Philips EM, Abouna GM. Correlation of blood levels and tissue levels of cyclosporine with the histologic features of cyclosporine toxicity. Transplant Proc 1988; 20(2 Suppl 2):407-413.

(243) Hanas E, Tufveson G, Lindgren PG, Sjoberg O, Totterman TH. Concentrations of cyclosporine-A and its metabolites in transplanted human kidney tissue during rejection and stable graft function. Clin.Transplantation 1991; 5:107-111.

(244) Belitsky P, Dunn S, Johnston A, Levy G. Impact of absorption profiling on efficacy and safety of cyclosporin therapy in transplant recipients. Clin Pharmacokinet 2000; 39(2):117-125.

(245) Sebille S, Morjani H, Poullain MG, Manfait M. Effect of S9788, cyclosporin A and verapamil on intracellular distribution of THP-doxorubicin in multidrug-resistant K562 tumor cells, as studied by laser confocal microspectrofluorometry. Anticancer Res 1994; 14(6A):2389-2393.

(246) Ernest S, Bello-Reuss E. Expression and function of P-glycoprotein in a mouse kidney cell line. Am J Physiol 1995; 269(2 Pt 1):C323-C333.

(247) Ayesh S, Lyubimov E, Algour N, Stein WD. Reversal of P-glycoprotein is greatly reduced by the presence of plasma but can be monitored by an ex vivo clinical assay. Anticancer Drugs 1996; 7(6):678-686.

(248) Kawamoto S, Deguchi T, Nezasa S, Yamada S, Okano M, Kawada Y. Detection of low-level expression of P-glycoprotein in ACHN renal adenocarcinoma cells. Jpn J Cancer Res 1996; 87(5):475-479.

(249) Ito T, Yano I, Tanaka K, Inui KI. Transport of quinolone antibacterial drugs by human P-glycoprotein expressed in a kidney epithelial cell line, LLC-PK1. J Pharmacol Exp Ther 1997; 282(2):955-960.

(250) Nooter K, Sonneveld P, Janssen A, Oostrum R, Boersma T, Herweijer H et al. Expression of the mdr3 gene in prolymphocytic leukemia: association with cyclosporin-A-induced increase in drug accumulation. Int J Cancer 1990; 45(4):626-631.

(251) Marques-Santos LF, Harab RC, de Paula EF, Rumjanek VM. The in vivo effect of the administration of resistance-modulating agents on rhodamine 123 distribution in mice thymus and lymph nodes. Cancer Lett 1999; 137(1):99-106.

(252) Lehne G, Rugstad HE. Cytotoxic effect of the cyclosporin PSC 833 in multidrug-resistant leukaemia cells with increased expression of P-glycoprotein. Br J Cancer 1998; 78(5):593-600.

(253) Chiodini B, Bassan R, Barbui T. Apoptosis by anthracyclines at therapeutic concentrations in MDR1+ human leukemic cells. Adv Exp Med Biol 1999; 457:313-324.

(254) Leith CP, Kopecky KJ, Chen IM, Eijdems L, Slovak ML, McConnell TS et al. Frequency and clinical significance of the expression of the multidrug resistance proteins MDR1/P-glycoprotein, MRP1, and LRP in acute myeloid leukemia: a Southwest Oncology Group Study. Blood 1999; 94(3):1086-1099.

(255) Siekierka JJ, Wiederrecht G, Greulich H, Boulton D, Hung SH, Cryan J et al. The cytosolic-binding protein for the immunosuppressant FK-506 is both a ubiquitous and highly conserved peptidyl-prolyl cis-trans isomerase. J Biol Chem 1990; 265(34):21011-21015.

(256) Schmidt U, Dubach UC, Guder WG, Funk B, Paris K. Metabolic patterns in various structures of the rat nephron. The distribution of enzymes of carbohydrate metabolism. Curr Probl Clin Biochem 1975; 4:22-32.

(257) Zager RA. P glycoprotein-mediated cholesterol cycling determines proximal tubular cell viability. Kidney Int 2001; 60(3):944-956.

(258) Bleck JS, Schlitt HJ, Christians U, Thiesemann C, Strohmeyer S, Schottmann R et al. Urinary excretion of ciclosporin and 17 of its metabolites in renal allograft recipients. Pharmacology 1989; 39(3):160-164.

(259) Fleming S, Gibson AA. Proteinase inhibitors in the kidney and its tumours. Histopathology 1986; 10(12):1303-1313.

(260) Franke WW, Schmid E, Osborn M, Weber K. Intermediate-sized filaments of human endothelial cells. J Cell Biol 1979; 81(3):570-580.

(261) Billett EE, Gunn B, Mayer RJ. Characterization of two monoclonal antibodies obtained after immunization with human liver mitochondrial membrane preparations. Biochem J 1984; 221(3):765-776.

(262) Rosati A, Decorti G, Klugmann FB, Candussio L, Granzotto M, Melato M et al. Cytofluorimetric analysis of a renal tubular cell line and its resistant counterpart. Anticancer Res 2000; 20(5B):3403-3410.

(263) van dS, I, Blom-Roosemalen MC, de Boer AG, Breimer DD. Specificity of doxorubicin versus rhodamine-123 in assessing P- glycoprotein functionality in the LLC-PK1, LLC-PK1:MDR1 and Caco-2 cell lines. Eur J Pharm Sci 2000; 11(3):207-214.

(264) Pan BF, Dutt A, Nelson JA. Enhanced transepithelial flux of cimetidine by Madin-Darby canine kidney cells overexpressing human P-glycoprotein. J Pharmacol Exp Ther 1994; 270(1):1-7.

(265) van der Kolk DM, De Vries EG, van Putten WJ, Verdonck LF, Ossenkoppele GJ, Verhoef GE et al. P-glycoprotein and multidrug resistance protein activities in relation to treatment outcome in acute myeloid leukemia. Clin Cancer Res 2000; 6(8):3205-3214.

(266) Brown AS, Hong Y, de Belder A, Beacon H, Beeso J, Sherwood R et al. Megakaryocyte Ploidy and Platelet Changes in Human Diabetes and Atherosclerosis. Arterioscler Thromb Vasc Biol 1997; 17(4):802-807.

(267) Twentyman PR, Rhodes T, Rayner S. A comparison of rhodamine 123 accumulation and efflux in cells with P- glycoprotein-mediated and MRP-associated multidrug resistance phenotypes. Eur J Cancer 1994; 30A(9):1360-1369.

(268) Wang E, Casciano CN, Clement RP, Johnson WW. Cholesterol interaction with the daunorubicin binding site of P- glycoprotein. Biochem Biophys Res Commun 2000; 276(3):909-916.

(269) Rothnie A, Theron D, Soceneantu L, Martin C, Traikia M, Berridge G et al. The importance of cholesterol in maintenance of P-glycoprotein activity and its membrane perturbing influence. Eur Biophys J 2001; 30(6):430-442.

(270) Canitrot Y, Lautier D. [Use of rhodamine 123 for the detection of multidrug resistance]. Bull Cancer 1995; 82(9):687-697.

(271) Hebert MF, Fisher RM, Marsh CL, Dressler D, Bekersky I. Effects of rifampin on tacrolimus pharmacokinetics in healthy volunteers. J Clin Pharmacol 1999; 39(1):91-96.

(272) Romiti N, Tramonti G, Chieli E. Influence of Different Chemicals on MDR-1 P-Glycoprotein Expression and Activity in the HK-2 Proximal Tubular Cell Line. Toxicology and Applied Pharmacology 2002; 183(2):83-91.

(273) Ludescher C, Eisterer W, Hilbe W, Hofmann J, Thaler J. Decreased potency of MDR-modulators under serum conditions determined by a functional assay. Br J Haematol 1995; 91(3):652-657.

(274) Duggin GG, Baxter C, Hall BM, Horvath JS, Tiller DJ. Influence of cyclosporine A (CSA) on intrarenal control of GFR. Clin Nephrol 1986; 25 Suppl 1:S43-S45.

(275) Bates SE, Lee JS, Dickstein B, Spolyar M, Fojo AT. Differential modulation of P-glycoprotein transport by protein kinase inhibition. Biochemistry 1993; 32(35):9156-9164.

(276) Stromskaya TP, Grigorian IA, Ossovskaya VS, Rybalkina EY, Chumakov PM, Kopnin BP. Cell-specific effects of RAS oncogene and protein kinase C agonist TPA on P-glycoprotein function. FEBS Lett 1995; 368(2):373-376.

(277) Masanek U, Stammler G, Volm M. Modulation of multidrug resistance in human ovarian cancer cell lines by inhibition of P-glycoprotein 170 and PKC isoenzymes with antisense oligonucleotides. J Exp Ther Oncol 2002; 2(1):37-41.

(278) Goodfellow HR, Sardini A, Ruetz S, Callaghan R, Gros P, McNaughton PA et al. Protein kinase C-mediated phosphorylation does not regulate drug transport by the human multidrug resistance P-glycoprotein. J Biol Chem 1996; 271(23):13668-13674.

(279) Miller DS, Sussman CR, Renfro JL. Protein kinase C regulation of p-glycoprotein-mediated xenobiotic secretion in renal proximal tubule. Am J Physiol 1998; 275(5 Pt 2):F785-F795.

(280) Masereeuw R, Terlouw SA, Van Aubel RA, Russel FG, Miller DS. Endothelin B receptor-mediated regulation of ATP-driven drug secretion in renal proximal tubule. Mol Pharmacol 2000; 57(1):59-67.

(281) Haug C, Grill C, Schmid-Kotsas A, Gruenert A, Jehle PM. Endothelin release by rabbit proximal tubule cells: modulatory effects of cyclosporine A, tacrolimus, HGF and EGF. Kidney Int 1998; 54(5):1626-1636.

(282) Kon V, Awazu M. Endothelin and cyclosporine nephrotoxicity. Ren Fail 1992; 14(3):345-350.

(283) Murat A, Pellieux C, Brunner HR, Pedrazzini T. Calcineurin Blockade Prevents Cardiac Mitogen-activated Protein Kinase Activation and Hypertrophy in Renovascular Hypertension. J Biol Chem 2000; 275(52):40867-40873.

(284) Lerman L, Textor SC. Pathophysiology of ischemic nephropathy. Urol Clin North Am 2001; 28(4):793-803.

(285) Zhang X, Wang T, Batist G, Tsao MS. Transforming growth factor beta 1 promotes spontaneous transformation of cultured rat liver epithelial cells. Cancer Res 1994; 54(23):6122-6128.

(286) Schluesener HJ, Meyermann R. Spontaneous multidrug transport in human glioma cells is regulated by transforming growth factors type beta. Acta Neuropathol (Berl) 1991; 81(6):641-648.

(287) Mohamed MA, Robertson H, Booth TA, Balupuri S, Gerstenkorn C, Kirby JA et al. Active TGF-β1 expression in kidney transplantation: a comparative study of Cyclosporin-A (CyA) and tacrolimus (FK506). Transpl Int 2000; 13(Suppl 1):S295-S298.

(288) Wolf G. Link between angiotensin II and TGF-beta in the kidney. Miner Electrolyte Metab 1998; 24(2-3):174-180.

(289) Gatlik-Landwojtowicz E, Aanismaa P, Seelig A. The rate of p-glycoprotein activation depends on the metabolic state of the cell. Biochemistry 2004; 43(46):14840-14851.

(290) Asai T, Nakatani T, Tamada S, Kuwabara N, Yamanaka S, Tashiro K et al. Activation of transcription factors AP-1 and NF-kappaB in chronic cyclosporine A nephrotoxicity: role in beneficial effects of magnesium supplementation. Transplantation 2003; 75(7):1040-1044.

(291) Kunz D, Walker G, Eberhardt W, Nitsch D, Pfeilschifter J. Interleukin 1[beta]-Induced Expression of Nitric Oxide Synthase in Rat Renal Mesangial Cells Is Suppressed by Cyclosporin A. Biochemical and Biophysical Research Communications 1995; 216(2):438-446.

(292) Goto M, Masuda S, Saito H, Inui Ki. Decreased expression of P-glycoprotein during differentiation in the human intestinal cell line Caco-2. Biochemical Pharmacology 2003; 66(1):163-170.

(293) Park S, James CD. Lanthionine Synthetase Components C-like 2 Increases Cellular Sensitivity to Adriamycin by Decreasing the Expression of P-Glycoprotein through a Transcription-mediated Mechanism. Cancer Res 2003; 63(3):723-727.

(294) Aggarwal S, Tsuruo T, Gupta S. Altered expression and function of P-glycoprotein (170 kDa), encoded by the MDR 1 gene, in T cell subsets from aging humans. J Clin Immunol 1997; 17(6):448-454.

(295) Ameyaw MM, Regateiro F, Li T, Liu X, Tariq M, Mobarek A et al. MDR1 pharmacogenetics: frequency of the C3435T mutation in exon 26 is significantly influenced by ethnicity. Pharmacogenetics 2001; 11(3):217-21.

(296) Kim RB, Leake BF, Choo EF, Dresser GK, Kubba SV, Schwarz UI et al. Identification of functionally variant MDR1 alleles among European Americans and African Americans. Clin Pharmacol Ther 2001; 70(2):189-199.

(297) Cascorbi I, Gerloff T, Johne A, Meisel C, Hoffmeyer S, Schwab M et al. Frequency of single nucleotide polymorphisms in the P-glycoprotein drug transporter MDR1 gene in white subjects. Clin Pharmacol Ther 2001; 69(3):169-174.

(298) Schaeffeler E, Eichelbaum M, Brinkmann U, Penger A, Asante-Poku S, Zanger UM et al. Frequency of C3435T polymorphism of MDR1 gene in African people. Lancet 2001; 358(9279):383-384.

(299) Jamroziak K, Balcerczak E, Mlynarski W, Mirowski M, Robak T. Distribution of allelic variants of functional C3435T polymorphism of drug transporter MDR1 gene in a sample of Polish population. Pol J Pharmacol 2002; 54(5):495-500.

(300) Bernal ML, Sinues B, Fanlo A, Mayayo E. Frequency distribution of C3435T mutation in exon 26 of the MDR1 gene in a Spanish population. Ther Drug Monit 2003; 25(1):107-111.

(301) Cavaco I, Gil JP, Gil-Berglund E, Ribeiro V. CYP3A4 and MDR1 alleles in a Portuguese population. Clin Chem Lab Med 2003; 41(10):1345-1350.

(302) Hitzl M, Drescher S, van der KH, Schaffeler E, Fischer J, Schwab M et al. The C3435T mutation in the human MDR1 gene is associated with altered efflux of the P-glycoprotein substrate rhodamine 123 from CD56+ natural killer cells. Pharmacogenetics 2001; 11(4):293-298.

(303) Kerb R, Aynacioglu AS, Brockmoller J, Schlagenhaufer R, Bauer S, Szekeres T et al. The predictive value of MDR1, CYP2C9, and CYP2C19 polymorphisms for phenytoin plasma levels. Pharmacogenomics J 2001; 1(3):204-210.

(304) Fellay J, Marzolini C, Meaden ER, Back DJ, Buclin T, Chave JP et al. Response to antiretroviral treatment in HIV-1-infected individuals with allelic variants of the multidrug resistance transporter 1: a pharmacogenetics study. Lancet 2002; 359(9300):30-36.

(305) Illmer T, Schuler US, Thiede C, Schwarz UI, Kim RB, Gotthard S et al. MDR1 gene polymorphisms affect therapy outcome in acute myeloid leukemia patients. Cancer Res 2002; 62(17):4955-4962.

(306) Kurata Y, Ieiri I, Kimura M, Morita T, Irie S, Urae A et al. Role of human MDR1 gene polymorphism in bioavailability and interaction of digoxin, a substrate of P-glycoprotein. Clin Pharmacol Ther 2002; 72(2):209-219.

(307) Meineke I, Freudenthaler S, Hofmann U, Schaeffeler E, Mikus G, Schwab M et al. Pharmacokinetic modelling of morphine, morphine-3-glucuronide and morphine-6-glucuronide in plasma and cerebrospinal fluid of neurosurgical patients after short-term infusion of morphine. Br J Clin Pharmacol 2002; 54(6):592-603.

(308) Roberts RL, Joyce PR, Mulder RT, Begg EJ, Kennedy MA. A common P-glycoprotein polymorphism is associated with nortriptyline-induced postural hypotension in patients treated for major depression. Pharmacogenomics J 2002; 2(3):191-196.

(309) Siegsmund M, Brinkmann U, Schaffeler E, Weirich G, Schwab M, Eichelbaum M et al. Association of the P-glycoprotein transporter MDR1(C3435T) polymorphism with the susceptibility to renal epithelial tumors. J Am Soc Nephrol 2002; 13(7):1847-1854.

(310) Vogelgesang S, Cascorbi I, Schroeder E, Pahnke J, Kroemer HK, Siegmund W et al. Deposition of Alzheimer's beta-amyloid is inversely correlated with P-glycoprotein expression in the brains of elderly non-demented humans. Pharmacogenetics 2002; 12(7):535-541.

(311) Yamauchi A, Ieiri I, Kataoka Y, Tanabe M, Nishizaki T, Oishi R et al. Neurotoxicity induced by tacrolimus after liver transplantation: relation to genetic polymorphisms of the ABCB1 (MDR1) gene. Transplantation 2002; 74(4):571-572.

(312) Zheng H, Webber S, Zeevi A, Schuetz E, Zhang J, Lamba J et al. The MDR1 polymorphisms at exons 21 and 26 predict steroid weaning in pediatric heart transplant patients. Hum Immunol 2002; 63(9):765-770.

(313) Anglicheau D, Verstuyft C, Laurent-Puig P, Becquemont L, Schlageter MH, Cassinat B et al. Association of the multidrug resistance-1 gene single-nucleotide polymorphisms with the tacrolimus dose requirements in renal transplant recipients. J Am Soc Nephrol 2003; 14(7):1889-1896.

(314) Asano T, Takahashi KA, Fujioka M, Inoue S, Okamoto M, Sugioka N et al. ABCB1 C3435T and G2677T/A polymorphism decreased the risk for steroid-induced osteonecrosis of the femoral head after kidney transplantation. Pharmacogenetics 2003; 13(11):675-682.

(315) Brumme ZL, Dong WW, Chan KJ, Hogg RS, Montaner JS, O'Shaughnessy MV et al. Influence of polymorphisms within the CX3CR1 and MDR-1 genes on initial antiretroviral therapy response. AIDS 2003; 17(2):201-208.

(316) Drozdzik M, Bialecka M, Mysliwiec K, Honczarenko K, Stankiewicz J, Sych Z. Polymorphism in the P-glycoprotein drug transporter MDR1 gene: a possible link between environmental and genetic factors in Parkinson's disease. Pharmacogenetics 2003; 13(5):259-263.

(317) Kafka A, Sauer G, Jaeger C, Grundmann R, Kreienberg R, Zeillinger R et al. Polymorphism C3435T of the MDR-1 gene predicts response to preoperative chemotherapy in locally advanced breast cancer. Int J Oncol 2003; 22(5):1117-1121.

(318) Siddiqui A, Kerb R, Weale ME, Brinkmann U, Smith A, Goldstein DB et al. Association of multidrug resistance in epilepsy with a polymorphism in the drug-transporter gene ABCB1. N Engl J Med 2003; 348(15):1442-1448.

(319) Verstuyft C, Schwab M, Schaeffeler E, Kerb R, Brinkmann U, Jaillon P et al. Digoxin pharmacokinetics and MDR1 genetic polymorphisms. Eur J Clin Pharmacol 2003; 58(12):809-812.

(320) Yates CR, Zhang W, Song P, Li S, Gaber AO, Kotb M et al. The effect of CYP3A5 and MDR1 polymorphic expression on cyclosporine oral disposition in renal transplant patients. J Clin Pharmacol 2003; 43(6):555-564.

(321) Zheng H, Webber S, Zeevi A, Schuetz E, Zhang J, Bowman P et al. Tacrolimus dosing in pediatric heart transplant patients is related to CYP3A5 and MDR1 gene polymorphisms. Am J Transplant 2003; 3(4):477-483.

(322) Bonhomme-Faivre L, Devocelle A, Saliba F, Chatled S, Maccario J, Farinotti R et al. MDR-1 C3435T polymorphism influences cyclosporine a dose requirement in liver-transplant recipients. Transplantation 2004; 78(1):21-25.

(323) Singh D, Alexander J, Owen A, Rustom R, Bone M, Hammad A et al. Whole-blood cultures from renal-transplant patients stimulated ex vivo show that the effects of cyclosporine on lymphocyte proliferation are related to P-glycoprotein expression. Transplantation 2004; 77(4):557-561.

(324) Becquemont L, Verstuyft C, Kerb R, Brinkmann U, Lebot M, Jaillon P et al. Effect of grapefruit juice on digoxin pharmacokinetics in humans. Clin Pharmacol Ther 2001; 70(4):311-316.

(325) von AN, Richter M, Grupp C, Ringe B, Oellerich M, Armstrong VW. No influence of the MDR-1 C3435T polymorphism or a CYP3A4 promoter polymorphism (CYP3A4-V allele) on dose-adjusted cyclosporin A trough concentrations or rejection incidence in stable renal transplant recipients. Clin Chem 2001; 47(6):1048-1052.

(326) Calado RT, Falcao RP, Garcia AB, Gabellini SM, Zago MA, Franco RF. Influence of functional MDR1 gene polymorphisms on P-glycoprotein activity in CD34+ hematopoietic stem cells. Haematologica 2002; 87(6):564-568.

(327) Drescher S, Schaeffeler E, Hitzl M, Hofmann U, Schwab M, Brinkmann U et al. MDR1 gene polymorphisms and disposition of the P-glycoprotein substrate fexofenadine. Br J Clin Pharmacol 2002; 53(5):526-534.

(328) Gerloff T, Schaefer M, Johne A, Oselin K, Meisel C, Cascorbi I et al. MDR1 genotypes do not influence the absorption of a single oral dose of 1 mg digoxin in healthy white males. Br J Clin Pharmacol 2002; 54(6):610-616.

(329) Siegmund W, Ludwig K, Giessmann T, Dazert P, Schroeder E, Sperker B et al. The effects of the human MDR1 genotype on the expression of duodenal P-glycoprotein and disposition of the probe drug talinolol. Clin Pharmacol Ther 2002; 72(5):572-583.

(330) De L, V, Mundo E, Trakalo J, Wong GW, Kennedy JL. Investigation of polymorphism in the MDR1 gene and antidepressant-induced mania. Pharmacogenomics J 2003; 3(5):297-299.

(331) Haas DW, Wu H, Li H, Bosch RJ, Lederman MM, Kuritzkes D et al. MDR1 gene polymorphisms and phase 1 viral decay during HIV-1 infection: an adult AIDS Clinical Trials Group study. J Acquir Immune Defic Syndr 2003; 34(3):295-298.

(332) Hesselink DA, van Schaik RH, van dH, I, van der WM, Gregoor PJ, Lindemans J et al. Genetic polymorphisms of the CYP3A4, CYP3A5, and MDR-1 genes and pharmacokinetics of the calcineurin inhibitors cyclosporine and tacrolimus. Clin Pharmacol Ther 2003; 74(3):245-254.

(333) Kuzuya T, Kobayashi T, Moriyama N, Nagasaka T, Yokoyama I, Uchida K et al. Amlodipine, but not MDR1 polymorphisms, alters the pharmacokinetics of cyclosporine A in Japanese kidney transplant recipients. Transplantation 2003; 76(5):865-868.

(334) Morita N, Yasumori T, Nakayama K. Human MDR1 polymorphism: G2677T/A and C3435T have no effect on MDR1 transport activities. Biochem Pharmacol 2003; 65(11):1843-1852.

(335) Nasi M, Borghi V, Pinti M, Bellodi C, Lugli E, Maffei S et al. MDR1 C3435T genetic polymorphism does not influence the response to antiretroviral therapy in drug-naive HIV-positive patients. AIDS 2003; 17(11):1696-1698.

(336) Oselin K, Gerloff T, Mrozikiewicz PM, Pahkla R, Roots I. MDR1 polymorphisms G2677T in exon 21 and C3435T in exon 26 fail to affect rhodamine 123 efflux in peripheral blood lymphocytes. Fundam Clin Pharmacol 2003; 17(4):463-469.

(337) Pauli-Magnus C, Feiner J, Brett C, Lin E, Kroetz DL. No effect of MDR1 C3435T variant on loperamide disposition and central nervous system effects. Clin Pharmacol Ther 2003; 74(5):487-498.

(338) Winzer R, Langmann P, Zilly M, Tollmann F, Schubert J, Klinker H et al. No influence of the P-glycoprotein genotype (MDR1 C3435T) on plasma levels of lopinavir and efavirenz during antiretroviral treatment. Eur J Med Res 2003; 8(12):531-534.

(339) Bleiber G, May M, Suarez C, Martinez R, Marzolini C, Egger M et al. MDR1 genetic polymorphism does not modify either cell permissiveness to HIV-1 or disease progression before treatment. J Infect Dis 2004; 189(4):583-586.

(340) Haufroid V, Mourad M, Van K, V, Wawrzyniak J, De MM, Eddour DC et al. The effect of CYP3A5 and MDR1 (ABCB1) polymorphisms on cyclosporine and tacrolimus dose requirements and trough blood levels in stable renal transplant patients. Pharmacogenetics 2004; 14(3):147-154.

(341) Lilja JJ, Niemi M, Neuvonen PJ. Rifampicin reduces plasma concentrations of celiprolol. Eur J Clin Pharmacol 2004; 59(11):819-824.

(342) Yasui-Furukori N, Mihara K, Takahata T, Suzuki A, Nakagami T, De VR et al. Effects of various factors on steady-state plasma concentrations of risperidone and 9-hydroxyrisperidone: lack of impact of MDR-1 genotypes. Br J Clin Pharmacol 2004; 57(5):569-575.

(343) Johne A, Kopke K, Gerloff T, Mai I, Rietbrock S, Meisel C et al. Modulation of steady-state kinetics of digoxin by haplotypes of the P-glycoprotein MDR1 gene. Clin Pharmacol Ther 2002; 72(5):584-594.

(344) Chowbay B, Cumaraswamy S, Cheung YB, Zhou Q, Lee EJ. Genetic polymorphisms in MDR1 and CYP3A4 genes in Asians and the influence of MDR1 haplotypes on cyclosporin disposition in heart transplant recipients. Pharmacogenetics 2003; 13(2):89-95.

(345) Kroetz DL, Pauli-Magnus C, Hodges LM, Huang CC, Kawamoto M, Johns SJ et al. Sequence diversity and haplotype structure in the human ABCB1 (MDR1, multidrug resistance transporter) gene. Pharmacogenetics 2003; 13(8):481-494.

(346) Marzolini C, Paus E, Buclin T, Kim RB. Polymorphisms in human MDR1 (P-glycoprotein): recent advances and clinical relevance. Clin Pharmacol Ther 2004; 75(1):13-33.

(347) Soranzo N, Cavalleri GL, Weale ME, Wood NW, Depondt C, Marguerie R et al. Identifying candidate causal variants responsible for altered activity of the ABCB1 multidrug resistance gene. Genome Res 2004; 14(7):1333-1344.

(348) Woodahl EL, Ho RJ. The role of MDR1 genetic polymorphisms in interindividual variability in P-glycoprotein expression and function. Curr Drug Metab 2004; 5(1):11-19.